SELECTIVE MANIPULATION OF MICROGLIA USING NON-VIRAL TARGETED DNA DELIVERY

By Josephine Malmevik
Student number: 2051437

SUPERVISORS
Prof. Neil Sims
Dr. Håkan Muyderman

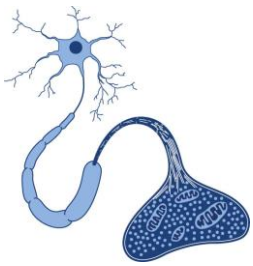

INSTITUTION
Department of Medical Biochemistry,
Flinders Medical Centre,
Flinders University of South Australia

This thesis is submitted in partial fulfillment of the requirements of the award of Doctor of Philosophy at Flinders University of South Australia
December, 2012

TABLE OF CONTENTS

THESIS SUMMARY

Microglia are the resident immunocompetent cells of the central nervous system (CNS) and are integrally involved in the response to disease and injury. There are currently limited approaches to investigate microglial function *in vivo*. Targeted delivery of DNA plasmids via cell surface receptors provides one possible means to selectively modify expression of proteins of interest. The potential of this approach has been demonstrated in previous studies using constructs termed "immunogenes" to selectively transfect neuronal subpopulations. These immunogenes consist of antibodies against a cell surface receptor linked to polycations, which in turn bind the DNA.

The broad aim of the present studies was to test whether immunogenes could be used to manipulate protein expression in microglia. The specific aims were to identify a receptor capable of supporting antibody internalisation into microglia, to generate immunogenes incorporating this antibody and test their capacity to transfect microglia in culture and *in vivo*.

Scavenger receptor class B, type I (SR-BI) was initially identified from published studies as a potential target for delivering DNA to glial cells. Using immunohistochemistry, SR-BI was identified in both astrocytes and microglia in mixed glial cultures. However, no immunolabelling of SR-BI was detected in adult

rat brain, despite the use of several antigen retrieval protocols. Antibodies directed against an external epitope of SR-BI were highly selectively internalised by microglia both in mixed glial cultures and in the adult brain. Uptake was not seen following injection of two other antibodies into the brain, suggesting that internalisation of this antibody either involved SR-BI that was present but not detected by immunohistochemistry, or resulted from interactions with another microglial protein. This result provided evidence of microglia-specific antibody delivery and prompted studies to test the capacity of immunogenes incorporating the SR-BI antibody to transfect microglia.

The initial immunogene was based on constructs used to successfully transfect neurons and contained poly-L-lysine as the polycation. The preparative procedure was subsequently extensively modified to improve immunogene recovery and increase DNA binding. Trials with the final construct resulted in transfection of occasional cells in culture and in the brain as detected from expression of green fluorescent protein encoded by the DNA plasmid. An alternative construct was developed incorporating polyethylenimine as the polycation. This construct produced transfection of both astrocytes and microglia in mixed glial cultures. Transfection efficiencies were much higher than with DNA bound to the polycation alone and similar to that achieved with other non-viral vectors.

More significantly, infusions of the immunogene into the hippocampus resulted in transfection of many cells, extending several millimetres from the infusion site. More than 80 % of transfected cells were immunoreactive for microglial markers. Transfection was not seen with an immunogene incorporating a different antibody or with DNA bound to free polyethylenimine. Transfection was also produced using single intracerebral injections of the SR-BI-based immunogene, albeit in fewer cells. Modifications of the immunogene were tested aimed at promoting release from intracellular vesicles and entry of DNA into the nucleus. These constructs also produced widespread selective transfection, but the modifications did not substantially increase transfection efficiencies.

These studies demonstrate that immunogenes can generate highly targeted transfection of microglia *in vivo* and constitute the first non-viral vector to achieve this outcome. The studies further identify the antibody against SR-BI as a novel carrier to selectively deliver DNA, and potentially other nucleic acids or drugs, to microglia in the brain. Further development of immunogenes or other constructs based on the SR-BI antibody has the potential to provide valuable means for better understanding the functions of microglia in the CNS.

DECLARATION

I declare that this thesis does not incorporate without acknowledgement any material previously submitted for a degree or diploma in any University; and that to the best of my knowledge and belief, it does not contain any material previously published or written by another person except where due reference is made in the text.

Josephine Malmevik, December 2012, Lund, Sweden

PUBLISHED ABSTRACTS ARISING FROM THIS WORK

Malmevik J.M.K., Herbert M.K., Berhanu D.A., Rogers M-L., Nilsson M., Nakanishi Y., Rush R.A., Sims N.R. and Muyderman H. *Scavenger receptor, class B, Type I: Expression in the adult rat brain and implications for receptor-mediated gene delivery.* POS-TUE-127. Australian Neuroscience Society (ANS) Annual Conference, Hobart, TAS, AU, 2008.

Malmevik J.M.K., Rogers M-L., Nilsson M., Nakanishi Y., Rush R.A., Sims N.R. and Muyderman H. *Scavenger receptor, class B, type I; receptor-mediated gene delivery*. Australian Society for Medical Research (ASMR) SA meeting, Adelaide, SA, AU, 2008.

Homkajorn B., Malmevik J., Rogers M-L, Rush R.A., Sims N.R., and Muyderman H., *Mannose receptor-mediated gene delivery into astrocytes*. POS-WED-319. ANS Annual Conference, Canberra, ACT, AU, 2009.

Malmevik J., Rogers M-L., Nilsson M., Nakanishi Y., Rush R.A. Sims N.R. and Muyderman H. *Receptor-mediated gene delivery into microglia via Scavenger*

Receptor, Class B, Type I. POS-MON-228. ANS Annual Conference, Sydney, NSW, AU, 2010.

Malmevik J., Rogers M-L., Nilsson M., Nakanishi Y., Rush R.A., Sims N.R. and Muyderman H. *Targeted gene delivery to microglia via the scavenger receptor, class B, type I*. POS-MON-81. Ozbio Conference, Melbourne, VIC, AU, 2010.

Malmevik J., Rogers M.-L., Nilsson M., Nakanishi Y., Rush R.A. Sims N.R.and Muyderman H. *Highly selective receptor-mediated transfection of microglia* in vivo. Poster no. 515.13. Society for Neuroscience Meeting, San Diego, CA, USA, 2010.

Malmevik J., Atkin J., Walker A. and Muyderman H. *Mutant TDP-43 impairs cytoskeleton organization, response to injury and glutamate transporter expression in astrocytes in primary culture.* ORAL-20-05. ANS Annual Conference, Auckland, NZ, 2011.

Sims N. R., Malmevik J., Rogers M-L., Nilsson M., Nakanishi Y., Rush R. A. and Muyderman H. *Receptor-mediated DNA delivery to modulate gene expression by microglia in adult rat brain*. Poster no. 207.4. Forum of European Neuroscience (FENS), Amsterdam, Netherlands, 2010.

ACKNOWLEDGEMENTS

First of all, I want to thank my supervisors Professor Neil Sims and Dr Håkan Muyderman for providing me with a very interesting project and helping me through my PhD with their expertise, good advice, long meetings and a lot of e-mail correspondence. Other lab members to which I would like to give special mention is Dr Benjaporn (June) Homkajorn, Alison Wadey, Megan Herbert and Wai Ping.

Highly valuable help and input has also been provided by Professor Robert Rush in personal meetings, expert advice and in the progression of the final thesis. Other members of the lab of Professor Robert Rush have also been very helpful in my work, including Dr Mary-Louise Rogers, Dr Degu Abebe and Dr Dusan Matusica. Furthermore, others who have provided assistance throughout my PhD at Flinders University include Professor Greg Barritt, Professor Ian Gibbins, Professor John Powers, Dr Tim Chataway, Dr Michael Michael, Dr Rainer Haberberger, Mrs Angela Binns, Mrs Pat Vilimas and Ms Yvette DeGraaf. All present and many past members of the Centre for Neuroscience at Flinders University also played important parts in my PhD via their support and constructive criticism of my work. I would also like to take the opportunity to thank my examiners Dr Jennifer Pocock and Professor Emilio Badoer for their valuable comments and suggested changes to form the final version of my thesis.

I would also like to underline my gratitude to Professor Michael Nilsson (Gothenburg University, Sweden) for providing the funding used for living expenses and PhD fees, which made it possible to conduct my PhD project in the beautiful country of Australia. Also, the FMC Foundation and the National Health and Research Council have provided financial support that ensured the possibility to conduct all experiments in this project.

On a more personal level, I undoubtedly want to thank my parents Gerth and Eva-Maria for their support throughout not only my PhD, but my whole life, where I have been taught to be persistent and thorough, and at the same time appreciate the good things in life. And to my big sister Terese, I thank you for teaching me how to read when I was very little and inspiring me to follow the path of Science. Without the support of my family, I would definitely not be where I am today.

Particular gratitude is given to my life partner and best friend Micheal, who gave me support especially in the end of my PhD when things were most difficult. Not only do you give me strength in tough times, you also constantly remind me to believe in myself in all aspects of life. Thank you for everything.

To Andrew, my dear friend and fellow musician, I want to give thanks for the priceless support you have given me at any time of day and the notion that we

will be friends forever. Heshan, Kim, Rashelle, Claire, Sarah, Tim, Russell, Curtis, Patrick, Helen, Melissa and others I have come to know via Flinders Living; I thank you for all the memories, good and bad, that we have experienced together in Adelaide. To people closer to home; Helena, Anna F, Brita, Sofia, Oskar, Hoda, Anna J, Annica and Christiane, I thank you for all your 'online' support and wonderful visits during my time in Australia.

Finally, I wish to thank the music in my life, which as a contrast to Science made it easier to go through the long and testing path of my PhD.

ABBREVIATIONS

Abbreviation	Explanation
A_{NNN}	absorbance at *NNN* nm
AAV	adeno-associated virus
AD	Alzheimer's disease
ALS	amyotrophic lateral sclerosis
amyloid-β	amyloid beta
AP	anteroposterior
ATP	adenosine-5'-triphosphate
BBB	blood-brain barrier
BDNF	brain-derived neurotrophic factor
bp / kbp	basepair / kilobasepair(s)
BSA	albumin from bovine serum
BSA/Triton IHC	immunohistochemistry using albumin from bovine serum as blocking agent
CA^N	*Cornu Ammonis N* field of the hippocampus
Ca^{2+}	calcium ion(s)
CD^N	cluster of differentiation molecule *N*
$CD206^{Ab}$	antibody against extracellular domain of CD206 mannose receptor
CHO	chinese hamster ovary
CL^N / CR^N CC^L / CCR^N $CXCL^N$ / $CXCR^N$	chemokine ligand / receptor cysteine-cysteine chemokine ligand / receptor chemokine ligand / receptor with two cysteines separated by one amino acid
Cl^-	chloride ion(s)
CMV	cytomegalovirus
CNS	central nervous system
Cre recombinase	causes recombination recombinase
Da / kDa	dalton(s) / kilodalton(s)
DMEM	Dulbecco's modified Eagle's medium (low glucose)
DNA	deoxyribonucleic acid
DNAse	deoxyribonuclease
DTS	DNA-targeting sequence
DTT	DL-dithiothreitol
DV	dorsoventral
E_N	embryonic day *N*
EDTA	ethylenediaminetetraacetic acid
EMSA	electrophoretic mobility shift assay
FBS	foetal bovine serum
Fc	fragment crystallizable
GDNF	glial-derived neurotrophic factor

Abbreviation	Explanation
GFAP	glial fibrillary acidic protein
GFP	green fluorescent protein
GIBCO H_2O	UltraPure™ DNase/RNase-free distilled water
GM-CSF	granulocyte/macrophage colony-stimulating factor
H^+	hydrogen ion(s)
HA2	hemagglutinin 2
HBSS	Hank's buffered salt solution
HEPES	4-(2-hydroxyethyl)-1-piperazineethanesulfonic acid
HDL	high-density lipoprotein
HSV	herpes simplex virus
Iba1	ionized calcium binding adaptor molecule 1
IFNγ	interferon gamma
IgG	immunoglobulin G
IHC	immunohistochemistry
IL-^{N}	interleukin *N*
L	lateral
LB	Luria-Bertani
LDL	low-density lipoprotein
LPS	lipopolysaccharide
loxP	locus of crossing (x) over P1
Mac-1	macrophage-1 antigen
MCP-1	monocyte, memory T lymphocytes and NK-cell specific chemoattractant
MHC	major histocompatibility complex
mRNA	messenger ribonucleic acid
MS	multiple sclerosis
MWCO	molecular weight cut-off
NaCl	sodium chloride
NFκβ	nuclear factor kappa-light-chain-enhancer of activated B cells
NGF	nerve growth factor
NHS	normal horse serum
NHS/Triton IHC	immunohistochemistry using normal horse serum as blocking agent
NLS	nuclear localisation signal
NO	nitric oxide
NPC	nuclear pore complex
O/N	overnight
P_N	postnatal day *N*
p75^{NTR}	p75 neurotrophin receptor
p75^{NTRAb}	antibody against the extracellular domain of p75^{NTR}
PBS	phosphate-buffered saline
PEI	polyethylenimine
PEST	penicillin-streptomycin
PFA	paraformaldehyde
PI	propidium iodide

Abbreviation	Explanation
pK_a	acid dissocation constant
PLL	poly-L-lysine
RNA	ribonucleic acid
rpm	revolutions per minute
RT	room temperature
SDS	sodium dodecyl sulphate
SDS-PAGE	sodium dodecyl sulfate polyacrylamide gel electrophoresis
siRNA	small interfering RNA
SMPT	sulfosuccinimidyl 6-(α-methyl-α[2-pyridyldithio]-toluamido)hexanoate
SPDP	N-succinimidyl 3-(2-pyridyldithio)propionate
SR-BI	scavenger receptor, class B, type I
$SR\text{-}BI^{Ab}$	antibody against extracellular domain of SR-BI
SV40	simian virus 40
TBE	tris-borate-EDTA
TGF-β	transforming growth factor β
TNF-α	tumour necrosis factor alpha
Traut's reagent	2-iminothiolane hydrochloride
Tris	tris(hydroxymethyl)aminomethane
TrkA	tropomyosin-receptor-kinase A
w/w ratio	weight/weight ratio

LIST OF FIGURES AND TABLES

CHAPTER 1: INTRODUCTION

1.1 The nervous system

The nervous system is a complex communication network, which receives and processes sensory information from the external environment and from the rest of the body. Motor activity is also initiated and controlled in this network. Processing of information within the nervous system accounts for other complex functions including memory and emotions. The nervous system in veterbrates is usually divided into central and peripheral components. The brain, spinal cord and retina constitute the CNS. Cells outside these tissues that are involved in information transfer make up the peripheral nervous system.

Neurons and glia are the two major classes of cells within the nervous system (Figure 1.1). Neuronal cells propagate information via electrical signals along their processes, called dendrites and axons. At synapses, these signals are transduced to neighbouring neurons through intercellular movement of chemicals known as neurotransmitters *(Nag, 2011)*. Initially, glial cells were thought to mainly provide structural support for neurons, and were thus called glia from the Greek word 'gliok'; 'glue' *(Virchow, 1858; Virchow, 1860; Nedergaard et al., 2003; Volterra and Meldolesi, 2005; Nag, 2011; Oberheim et al., 2012)*. This previous idea is partially responsible for the less extensive characterisation of glia. There are now many known functions for glia that are imperative for nervous system function.

Glia are divided into microglia and macroglia, of which the latter consists of

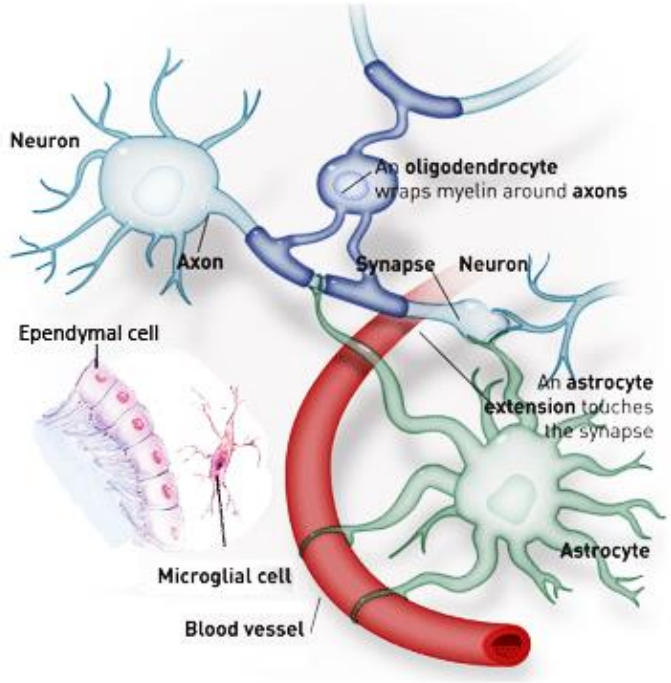

Figure 1.1 Cells of the nervous system. *Modified with permission from Arne Hurty, BayCreative, Inc.*

astrocytes, oligodendrocytes and ependymal cells. The most common glial cell type is the astrocyte, which is involved in a range of functions, including structural support, neurotransmitter buffering and energy supply to neurons and other cells of the CNS *(Kimelberg and Nedergaard, 2010; Nag, 2011)*. Oligodendrocytes produce myelin, a lipid rich substance that ensheaths the axons of neurons resulting in faster propagation of electrical signals *(Emery, 2010)*. Ependymal cells line the fluid-filled cavities of the brain and spinal cord *(Del Bigio, 2010)*. Lastly, microglia constitute the main resident cells of the CNS capable of producing immune responses *(Streit, 2002; Badoer, 2010)*.

The central focus of these studies was to investigate an approach for selectively manipulating gene expression in microglia *in vivo*. As a background for these investigations, section 1.1 provides an introduction to microglia. A shorter overview of astrocytes follows in section 1.2 as these cells were examined together with microglia in some aspects of this work. In addition to the information in these subsequent subchapters, we also refer to additional recent reviews in the area of glial cells and their function *(Chastain et al., 2011; Kettenmann et al., 2011; Kofler and Wiley, 2011; Nag, 2011; Oberheim et al., 2012; Parpura et al., 2012; Ransohoff and Brown, 2012; Kettenmann et al., 2013)*. Section 1.3 discusses established methods used for genetic modification, with an emphasis on vector-based receptor-mediated gene delivery in section 1.4. This is followed by a discussion of the application of established genetic modification methods in studying microglial function (section 1.5). Thereafter

follows a statement of the hypothesis and aims for the work in this thesis (section 1.6).

1.2 Microglia

Microglia constitute the primary innate immunocompetent cell population of the CNS *(Graeber and Streit, 2010)*. This cell type was discovered by Nissl in 1894 due to its proliferating nature in response to injury *(Graeber et al., 1988)*. Subsequently, microglia were extensively characterised by del Rio-Hortega in 1932. He pioneered microglial research by discussing the origin and entry of microglial progenitors in development and by characterising their morphology and dispersion *(del-Rio Hortega, 1932)*. Furthermore, he observed microglial transformation in response to injury upon which these cells had the capacity to migrate, proliferate and remove dying cells from the injured brain *(del-Rio Hortega, 1932)*.

1.2.1 Microglia in development

In contrast to other resident cell types of the CNS, microglia originate from a myeloid monocyte lineage during development *(del-Rio Hortega, 1932; Hickey and Kimura, 1988; Graeber and Streit, 2010; Kofler and Wiley, 2011)*. These microglial precursors distribute throughout the CNS via migration from the yolk sac. Proliferation of these precursors and differentiation of their progeny form the microglial population of the CNS. This is in contrast to other tissue macrophages, which are produced in bone marrow and differentiate via a

different set of transcription factors than the microglial population *(Ginhoux et al., 2010; Saijo and Glass, 2011)*.

Most findings on microglial function have been obtained using animal models, however many of these have been confirmed in human. In the human brain, the first microglial cells are detected from 5.5 weeks of gestation *(Monier et al., 2006; Graeber and Streit, 2010)*. With regards to the rodent brain, migration of external microglial progenitors into the CNS occurs between embryonic day 10 (E_{10}) and E_{19} *(Chan et al., 2007)*. The progenitors initially have a rounded morphology without any processes extended from the cell soma. Microglial cells with this amoeboid morphology are seen in cultures originating from the developing neonatal rat brain, determined using microglial markers such as cluster of differentiation molecule 11 b (CD11b; Figure 1.2a). Amoeboid microglia in the developing rodent start to proliferate as early as E_{15} *(Chan et al., 2007)*. This proliferation reaches its maximum at postnatal day 9 (P_9) and is largely completed by P_{18} *(Dalmau et al., 2003)*. The proliferation of microglia ensures a constant microglial density as the brain volume increases during development *(Dalmau et al., 2003)*.

The rate of newly produced neuronal cells during development reaches hundreds of thousands of cells in minutes *(Schlegelmilch et al., 2011)*. Alongside this neuronal proliferation, an extensive apoptosis of superfluous neurons is evident in the developing CNS *(Buss et al., 2006)*. Some neurons die in a programmed manner as these cells are produced in excess in the developing

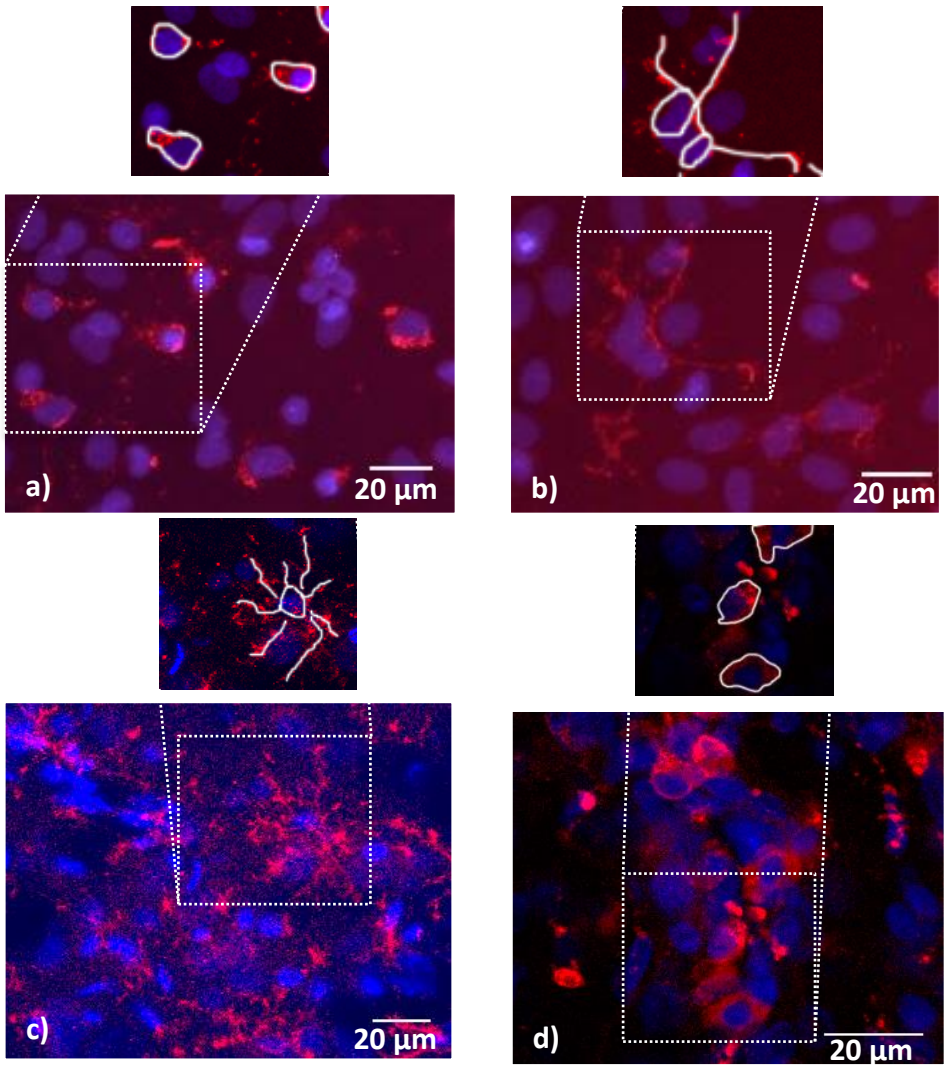

Figure 1.2 Main microglial activation stages in culture and in vivo *in representative images from fluorescence microscopy and confocal microscopy, respectively. CD11b/c-positive (red) microglia displaying amoeboid morphology (a) and ramified morphology (b) in mixed glial cultures derived from developing neonatal rat brain (day 14 in culture; prepared as in section 2.2 and 3.2.2.1). The ramified morphology of a subpopulation of cells in these glial culture, resembles that of healthy resident microglia in the adult rat brain (c). Microglia of the adult rat CNS may revert to an amoeboid state upon activation in disease or upon smaller damage (d). Cultures and brain sections treated with secondary antibodies alone did not display any immunoreactivity. Nuclei were labelled with Hoechst 33258 (blue).*

brain *(Oppenheim, 1991)*. In the later stages of nervous system development, further cell death is thought to correct for erroneous conncections between them *(Oppenheim, 1991)*. Apoptotic neurons in the proliferative zone of the rodent cortex have been detected as early as E_{10} *(Blaschke et al., 1996)*. This apoptosis increases to between 25 and 70 % of neurons until E_{18} *(Blaschke et al., 1996)*. These observations taken together with studies in other mammals have led to an estimate that approximately 50 % of neurons are lost during CNS development *(Cowan et al., 1984; Blaschke et al., 1996; Cepko et al., 1996)*. If these cells do not exhibit apoptotic signals to be removed from the developing brain, abnormal hypercellularity is found in proliferative regions of the mature CNS *(Lindsten et al., 2003)*.

In the healthy developing brain, microglia are known to phagocytose apoptotic neurons *(Ferrer et al., 1990; Marin-Teva et al., 2004; Caldero et al., 2009)* and to be involved in synaptic remodelling of the developing CNS *(Neumann et al., 2009)*. The seminal study by Stevens et al. (2007) linked the neonatal appearance of immature astrocytes to the neuronal expression of complement component 1q (C1q) in the developing mouse retina. As the complement cascade proceeds, C3 accumulates at synapses and flags these for phagocytosis by microglial cells. When astrocytes differentiate from their immature form into mature astrocytes, complement proteins are down-regulated, followed by a lower degree of synaptic pruning. A similar process has been identified in disease, as shown in a model of adult mouse glaucoma. Synaptic pruning by microglia is also present at lower levels in the healthy adult CNS *(Stevens et al., 2007)*.

It has been hypothesised that microglia may act as direct initiators of cell death in some neurons *(Banati et al., 1993; Kofler and Wiley, 2011)*. Pioneers in this field were Frade and Barde (1998), who observed an apoptotic-promoting function of microglia via secretion of nerve growth factor (NGF) in the developing chick retina *(Frade and Barde, 1998)*. Although NGF is known for its neurotrophic abilities *(Cohen, 1960)*, this molecule is also implicated in apoptotic processes in the developing CNS. In later years, Marin-Teva et al. (2004) strengthened the evidence for potential pro-apoptotic effects by microglia *(Marin-Teva et al., 2004)*. Upon selective removal of microglia, they observed increased survival of Purkinje neurons in the developing brain of postnatal mouse *(Marin-Teva et al., 2004)*. The molecular details of this pro-apoptotic effect on Purkinje neurons have not been determined. Tumour necrosis factor alpha (TNF-α), glutamate and nitric oxide (NO) were found not to be initators of this effect *(Marin-Teva et al., 2004)*.

1.2.2 Microglia in the mature CNS

Microglia represent 5-12 % of cells in the healthy mature human and rodent brain *(Lawson et al., 1990; Mittelbronn et al., 2001; Olson et al., 2003; Garman, 2011; Kofler and Wiley, 2011)*. Most of the microglia in the healthy CNS have small cell bodies and numerous fine, branched processes with even smaller, innumerable protrusions *(del-Rio Hortega, 1932; Kettenmann et al., 2011)*. Microglia with these features are commonly referred to as ramified microglia. Resident microglial cells of the adult rat brain with ramified morphology are

shown in Figure 1.2c. In culture, cells also exhibit ramified-like morphologies as shown in mixed glial culture derived from the brain of neonatal rat in Figure 1.2b. However, it is important to note that microglial morphology in these cultures does not fully resemble that of the intact brain.

During development, microglia initially have an amoeboid morphology, but acquire ramified morphologies at the 18th week of gestation of the human brain *(Monier et al., 2006)*. In this stage, microglia do not proliferate. This strongly suggests that the healthy human brain has an established microglial population before birth *(Monier et al., 2006; Kofler and Wiley, 2011)*. A ramified phenotype is induced in the CNS environment through glial expression of anti-inflammatory cytokines, including transforming growth factor β (TGF-β) *(Ramirez et al., 2005)*, a known agent promoting microglial ramification *(Ransohoff and Perry, 2009)*. In addition, the presence of the blood-brain barrier (BBB) in the healthy brain further preserves the ramified microglial phenotype by inhibiting the presence of blood serum constituents that may otherwise affect the properties of the microglial population *(Ransohoff and Perry, 2009; Michalski et al., 2010)*.

Until recently, ramified microglia in the healthy adult brain were thought to be in a resting stage with no evidence of specific functions. However, it is now recognised that these cells are continuously surveying the environment by constantly extending, retracting and rearranging their thin processes and protrusions in any direction within minutes *(Nimmerjahn et al., 2005; Kettenmann et al., 2011; Kofler and Wiley, 2011)*. Contact between neighbouring

microglia is kept to a minimum, through retraction and reformation of processes when these come in contact with each other *(Nimmerjahn et al., 2005)*. Therefore, microglia are found to occupy distinct regions of the brain *(del-Rio Hortega, 1932; Nimmerjahn et al., 2005)*.

The seminal article by Nimmerjahn et al. (2005) further investigated the movement of microglial processes. These investigations demonstrated that the processes of the microglial population survey the entire surrounding extracellular fluid within the territorial domains of these cells every two hours *(Lehmenkühler et al., 1993; Nimmerjahn et al., 2005)*. Due to their ongoing surveillance, these ramified cells are sometimes referred to as 'surveying microglia' *(Hanisch and Kettenmann, 2007; Ransohoff and Perry, 2009; Kofler and Wiley, 2011).*

Although the ramified phenotype is the only established microglial phenotype in the healthy CNS *(Graeber and Streit, 2010)*, different patterns of protein expression have been detected in microglial populations of distinct brain regions *(Hanisch and Kettenmann, 2007)*. Microglia in specific parts of the brain are believed to settle into these expression patterns during CNS development, depending on the microenvironmental cues at their final destination *(Lawson et al., 1990; McCluskey and Lampson, 2000; Davoust et al., 2008; Kettenmann et al., 2011; Kofler and Wiley, 2011)*.

These differences in protein expression patterns in microglia are in part related to the heterogeneous neuronal population of the CNS *(Aloisi, 2001)*. Neurons in different regions of the brain produce distinct neurochemical environments, affecting the phenotype of neighbouring microglia *(Aloisi, 2001; Tynan et al., 2010)*. One established example of proteome differences in microglial cells is TNF-α expression, which is significantly higher in hippocampal microglia compared to other brain regions *(Ren et al., 1999; Hanisch and Kettenmann, 2007)*. Differences between grey and white matter have also been observed. Microglia in white matter in comparison to grey matter, express higher levels of the T cell/transmembrane, Ig and mucin 3 receptor *(Anderson et al., 2007)*. This receptor is involved in the induction of T helper lymphocyte-mediated inflammatory responses. Therefore, it has been suggested that expression level variations of this receptor in grey and white matter may cause differences in immunoregulatory responses in these areas *(Anderson et al., 2007)*.

In addition to these proteomic differences, some microglial cells have minor morphological differences to the general population of resident microglia. For example, perivascular microglia have extended processes that are wrapped around blood venules and arterioles. These perivascular microglia may have important functions in disease, as their location enables quick interaction with foreign molecules and cells entering the CNS from the blood stream during BBB disruption *(Hickey and Kimura, 1988; Kida et al., 1993; Adams et al., 2007)*. The location of perivascular microglia also enhances their ability to present antigens

to infiltrating T lymphocytes in brain pathology, including autoimmune disease *(Hickey and Kimura, 1988; Kida et al., 1993; Adams et al., 2007)*. More information on antigen presentation is presented in section 1.2.4.4.

1.2.3 Microglial stages of activation

Microglia can become activated, upon which they acquire altered morphologies in response to injury, infection and inflammatory agents. Initial stages of activation involve thickening and shortening of microglial protrusions, which are later retracted to the enlarged cell body *(del-Rio Hortega, 1932; Sugama et al., 2007; Tynan et al., 2010)*. These morphological changes occur at rates of 0.5 - 1.5 µm/min according to detailed confocal time-lapse studies in acute rat brain slices *(Stence et al., 2001)*. Upon full or near-to full retraction of these 'surveillance processes' by activated microglia, a new set of 'motility processes' may be rapidly extended and retracted at rates of up to 4 µm/min. These morphological transformations provide microglia with the capacity to move at speeds of up to 118 µm/h *(Stence et al., 2001)*.

With stronger activating stimuli, the microglia progress towards an amoeboid shape (Figure 1.2d) resembling microglia in development and related macrophages in other tissues of the body. These microglia are capable of phagocytosis and extensive proliferation *(del-Rio Hortega, 1932; Tynan et al., 2010; Kettenmann et al., 2011; Szabo and Gulya, 2013)*. As mentioned

previously, the first described microglial cells were detected due to this proliferating nature *(Graeber et al., 1988)*.

Alongside these morphological changes, activated microglia in the CNS have altered gene expression profiles. This involves increased expression of surface proteins including CD11b, major histocompatibility complexes (MHCs), integrins and fragment crystallisable (Fc) receptors. There is also an increased release of molecules including TNF-α, NO, proteases, chemokines, interleukins and prostaglandin synthases such as cyclooxygenase *(Chao et al., 1992; Minghetti and Levi, 1998; Kingham and Pocock, 2001; De Simone et al., 2005; Kettenmann et al., 2011)*. The upregulation of these molecules is involved in the functions of activated microglia, including phagocytosis and interactions with the immune system *(Kettenmann et al., 2011)*.

These expression changes in microglia differ in different brain regions, partly due to pre-existing differences in protein expression between microglial populations of the healthy CNS (see section 1.2.2). For example, microglia have different expression profiles upon cytokine administration in distinct regions of the rat brain, depending on the resident neuronal expression of Substance P and glutamate *(McCluskey and Lampson, 2001)*. The effect of these local neurotransmitters on microglial activation has been shown after intrahippocampal injections of the pro-inflammatory molecule interferon gamma (IFNγ). This injection induced expression of MHC II molecules on microglia. The addition of antagonists against receptors for Substance P or

glutamate attenuated this up-regulation, indicating the role of these neurotransmitters in microglial activation. Also, the addition of Substance P together with IFNγ synergistically up-regulated MHC II to even higher levels than IFNγ alone *(McCluskey and Lampson, 2001)*.

Additional regional microglial profiles are evident in close proximity to blood vessels. Upon disruption of the BBB, perivascular microglia react quickly to stimuli from infiltrating blood. For example, fibrinogen can induce responses via macrophage-1 antigen; Mac-1 *(Adams et al., 2007)*. The binding of fibrinogen to this receptor causes microglial activation and induces microglial secretion of pro-inflammatory molecules *(Adams et al., 2007)*.

Coupled with the constant surveillance of ramified microglia, the quick reaction speed of these cells enables them to act swiftly upon changes in their surroundings *(Kreutzberg, 1996; Stence et al., 2001)*. This has been studied in confocal time-lapse studies of acute rat hippocampal slices *(Stence et al., 2001)*. Within 30 min of preparing this tissue, ramified microglia were seen to retract their processes. These studies also identified microglia in a full amoeboid stage in less than 2 h. Within 12 h, all microglia with the exception of a few cells had an activated morphology *(Stence et al., 2001)*.

This is consistent with studies in the intact brain. Quick responses of microglia in the form of up-regulated microglial markers (including isolectin markers), have been seen as early as 20 min after initiation of a 25 min long forebrain ischemia

(Morioka et al., 1991). Further increase of microglial marker expression was observed up to 24 h. Other studies in the intact diseased CNS have also shown a fully activated microglial response within 24 h, which is significantly faster than the response of other glia, including astrocytes *(Raivich et al., 1999)*.

1.2.3.1 Microglial ramification signals

A microglial cell can transform into both higher and lower stages of activation, initiated by specific molecular signals. Studies in culture have shown that monocytes and microglia seeded on astrocytic monolayers, or grown as pure cultures in astrocyte-conditioned medium, initially have an amoeboid morphology. After seeding, these cells progressively mature into ramified microglia *(Schmidtmayer et al., 1994; Sievers et al., 1994; Kettenmann et al., 2011)*. Initially, microglia in these cultures express many macrophage markers, including CD11b and transient receptor potential cation channel subfamily M member 1. Some of these proteins are down-regulated within a few days. During this time, microglial cells flatten out and extend processes to acquire a more ramified morphology *(Sievers et al., 1994; Wollmer et al., 2001)*. Similar microglial phenotype changes have been reported upon initial seeding of astrocytes and microglia together in mixed primary glial cultures *(Tanaka et al., 1999)*. Initially, this culture type contains a main astrocytic layer, with an amoeboid microglial population growing on top. As the astrocyte monolayer reaches confluence, the progeny of microglial proliferation integrates into this layer and acquires a more ramified morphology. At 7 days in culture, cells start

to display ramified morphologies and this has been shown to increase up to 28 days in mixed glial culture *(Szabo and Gulya, 2013)*. Studies by Tanaka et al. (1999) also showed that the expression of other proteins normally expressed by activated microglia is progressively lowered from the start of these cultures; for example fibronectin, laminin and MHC I.

Cell culture studies have suggested potential microglial ramification signals, including TGF-β, granulocyte/macrophage colony-stimulating factor (GM-CSF) and physiological extracellular levels of adenosine or adenosine-5'-triphosphate (ATP; *Schillling et al., 2001; Wollmer et al., 2001)*. The addition of inhibitory antibodies against TGF-β and GM-CSF has counteracted the promotion of the ramified phenotype by astrocyte-conditioned medium *(Schilling et al., 2001),* indicating that the preservation of a ramified microglial phenotype is influenced by astrocytic release of these factors. It has also been shown that the morphology of microglia in culture is changed after exposure to the bacterial surface molecule lipopolysaccharide (LPS), and that this change can be fully attenuated by the addition of lower levels of ATP or adenosine *(Wollmer et al., 2001)*.

1.2.3.2 Microglial activation signals

In addition to signals promoting development of the ramified stage, there are also many agents that can cause activation of microglia. These activating agents can be classified into 'on'-signals and 'off'-signals *(Biber et al., 2007; Kettenmann*

et al., 2011). On-signals consist of direct triggers of microglial activation, whereas off-signals involve the withdrawal of molecules normally available in the healthy CNS.

On-signals triggering microglial activation can be a) molecules foreign to the organism, b) increased concentrations of intracellular constituents in the extracellular space, c) immunoglobulin-antigen opsonisation complexes, and d) specific molecules released by neighbouring neurons, astrocytes and microglia in response to disease or injury *(Hanisch and Kettenmann, 2007)*.

Examples of foreign molecules inducing microglial activation are viral particles *(Kofler and Wiley, 2011)* and prions *(Le et al., 2001)*, which can be detected by microglial toll-like receptors. Morphological changes in culture and *in vivo* with a lowered number of ramified microglia and an increased number of amoeboid cells, have been used to determine microglial activation, of which many studies use the bacterial agent LPS *(Giulian and Baker, 1986; Glenn et al., 1992; Rosenstiel et al., 2001; Stence et al., 2001; Kauppinen et al., 2008)*.

Another group of on-signals involve the detection of increased extracellular levels of components normally found in the cytoplasm of cells. These components may arise extracellularly after excretion by damaged neurons and other cells of the CNS *(Kaushal and Schlichter, 2008).* One example is the detection of the neurotransmitter glutamate in the extracellular space, when this is not sufficiently cleared by astrocytes *(Ransohoff and Perry, 2009).* This

increased detection of glutamate activates group II metabotropic glutamate receptors on microglia, which induces microglial activation. *(Taylor et al., 2002; Kaushal and Schlichter, 2008).* In addition to glutamate, other neurotransmitters can activate microglia via numerous neurotransmitter receptors. For example, activation of microglial gamma-amino-butyric acid receptors leads to an anti-inflammatory response *(Pocock and Kettenmann, 2007)*. It has further been established that the ramification agent ATP (see last paragraph of section 1.2.3.1) can in excess extracellular amounts from diseased neighbouring neurons provoke microglial activation and movement via purinergic receptors *(Pocock and Kettenmann, 2007; Monif et al., 2009)*. Therefore, the activation stage of microglia is dependent on the levels of ATP present in its environment. In addition to these neurotransmitter receptors, microglia respond in various ways via adrenergic, dopaminergic, cholinergic and opioid receptors (see review in *Pocock and Kettenmann, 2007*)

The third group of microglial activation agents consists of immunoglobulin-antigen complexes involved in opsonisation *(Wilcock et al., 2004)*. In an example related to Alzheimer's disease (AD), transgenic mice that express the amyloid precursor protein were treated with anti-amyloid-beta (amyloid-β) antibodies. This treatment resulted in an up-regulation of microglial receptors for the Fc gamma (Fc-γ) part of antibodies. Thereafter, the antibody treatment enabled opsonisation of amyloid-β protein aggregates in the extracellular space, triggering microglial activation and phagocytosis mediated via Fc-γ receptor stimulation *(Wilcock et al., 2004)*. In the light of the aims of this study, these

phagocytic Fc-γ receptors have been shown to internalise IgG antibodes into microglia of the rat brain *(Aihara et al., 1994)* and in a range of mouse strains *(Hazama et al., 2005)*. However, recent reviews imply that Fc receptor binding causes intracellular signals rather than direct internalisation of its ligands *(Albanesi and Daeron, 2012)*. Furthermore, other reviews demonstrate that internalistaion of antibodies via Fc receptors is the result of opsonisation rather than endocytosis of individual antibodies *(Okun et al., 2010)*. The presence of Fc receptors has also been suggested on astrocytes, oligodendrocytes and neurons, however this has not been studied in as much detail.

The last subgroup of on-signals causing microglial activation entails molecules such as cytokines released by injured/diseased cells of the CNS. Secretion of many chemokines *(Kreutzberg, 1996; Ransohoff and Perry, 2009)* and interleukins *(Kreutzberg, 1996; Kettenmann et al., 2011)* acts as distress signals from neurons and glia to microglia, thereby inducing microglial activation. For example, pronounced secretion of cysteine-cysteine chemokine ligand 21 (CCL21) by distressed neurons has been shown in a rat spinal cord injury model *(Zhao et al., 2007)*. This ligand activates microglia through two of its chemokine receptors; CCR7 and CXCR3 *(Zhao et al., 2007)*. Another chemokine, CCL5, has also been shown to induce microglial activation and NO release subsequent to binding to chemokine receptors CCR1 and CCR5 *(Skuljec et al., 2011)*. In addition to these chemokines, interleukins such as interleukin 4 (IL-4) can induce microglial activation, manifested by up-regulation of phagocytic markers, including CD36 *(Shimizu et al., 2008)*.

As well as these groups of on-signals, microglial activation can be initiated by off-signals. For example, microglia are activated in the absence of the CD200 glycoprotein, which is a protein expressed by neurons and other cells of the healthy CNS *(Webb and Barclay, 1984; Hoek et al., 2000)*. In the healthy brain, the binding of CD200 protein to CD200 receptors on microglia constantly inhibits microglial activation *(Hoek et al., 2000; Kofler and Wiley, 2011)*. Withdrawal of CD200 in the diseased CNS removes this effect and induces activation of microglia *(Hanisch, 2002; Wang et al., 2007b; Kettenmann et al., 2011)*. The CD200 protein is significantly decreased in the ageing rat brain. This decline is associated with, and potentially contributes to, an increased microglial expression of inflammatory molecules including MHC II and IFNγ *(Frank et al., 2006)*. The expression of the microglial CD200 receptor did not change significantly in these studies, indicating that it is not specifically ageing of the microglial population that causes this activation. It has therefore been postulated that decreases in off-signals provide a pro-inflammatory environment in the ageing brain *(Frank et al., 2006)*.

1.2.4 Microglial involvement in brain injury and disease

Activated microglia provide responses that form the first line of defence against injury and disease in the CNS *(Kreutzberg, 1996; Kettenmann et al., 2011; Kofler and Wiley, 2011)*. The responses of these cells are dependent on the nature, duration and complexity of the stimuli triggering activation, and also on their

activation stage at the onset of disease or time of injury *(Gordon, 2003; Hanisch and Kettenmann, 2007; Ransohoff and Perry, 2009)*.

1.2.4.1 Inflammatory responses by microglia

Different microglial responses have been observed in acute disorders compared to chronic CNS diseases *(Ransohoff and Perry, 2009)*. Acute disorders, such as ischemia and traumatic brain injury, involve rapid degeneration of neurons and result in substantial necrosis *(Lucin and Wyss-Coray, 2009; Ransohoff and Perry, 2009)*. This uncontrolled cell death generally intensifies inflammatory responses in the form of proliferation, phagocytosis and increased release of cytokines, mediated by microglia and other glial cells. These inflammatory responses may further exacerbate neuronal loss *(Lucin and Wyss-Coray, 2009; Haselkorn et al., 2010)*. In contrast, chronic diseases are associated with slow neurodegeneration over several years, and generally cause only subtle inflammatory responses in the CNS *(Lucin and Wyss-Coray, 2009)*.

Nonetheless, some chronic diseases involve stronger inflammatory responses, such as those caused by amyloid plaques in AD *(Heneka and O'Banion, 2007; Lee et al., 2010)*, and particularly by myelin in multiple sclerosis (MS; see review by *Chastain et al., 2011*). Similarly to other tissues of the body, inflammatory effects in the CNS consist of automated host responses to injury and disease and are generally beneficial *(Graeber and Streit, 2010)*. However, if inflammatory processes become chronic or if these are directed at self antigens in the CNS, this

process can have detrimental outcomes as seen after excessive cytokine expression and inflammatory cell proliferation *(Denes et al., 2010)*.

MS is an autoimmune disease, involving activated glia that cause chronic inflammation in the CNS. These inflammatory responses in the CNS involve phagocytosis of myelin debris by microglia and the presentation of these constituents as antigens to infiltrating T lymphocytes *(Katz-Levy et al., 2000; Chastain et al., 2011)*. Autoreactive T lymphocytes thereafter cause further inflammatory responses that result in demyelination and degradation of neuronal axons. One contributing factor to the extensive microglial phagocytosis of myelin is the activation of microglia through fibrinogen, as previously mentioned in section 1.2.3 *(Adams et al., 2007)*. Due to their role in phagocytosis and antigen presentation of myelin, microglia have been implicated in the progression of MS *(Adams et al., 2007; Chastain et al., 2011)*.

Glial gene expression and behaviour undergoes major changes under conditions of inflammation. It has been shown that some stimulatory signals may cause an additive effect. Cunningham et al. (2005) put forward a priming hypothesis, where they postulated that an initial activation of microglia may cause a more aggressive microglial profile upon a later insult. In their model of chronic neurodegeneration induced by prion disease, microglial cells caused a more severe inflammatory response to peripheral LPS treatment compared to control animals. Under these conditions, microglia increased expression of IL-1β and TNF-α, promoting neuronal death *(Cunningham et al., 2005).* The hypothesis that

previous priming of microglia exacerbates subsequent responses has gained more support in recent years *(Ferrari and Tarelli, 2011; Machado et al., 2011)*.

1.2.4.2 Neurotrophic role of microglia

Microglia also serve protective roles in the diseased brain through excretion of neurotrophic factors *(Morgan et al., 2004; Bessis et al., 2007; Caldero et al., 2009)*. For example, microglial release of TGF-β has been shown to result in neuronal protection in the adult diseased brain *(Battista et al., 2006)*. Furthermore, a striatal injury model has provided evidence for a similar effect by brain-derived neurotrophic factor (BDNF) and glial cell line-derived neurotrophic factor (GDNF). Upon excretion by microglia and astrocytes, BDNF and GDNF causes sprouting of dopaminergic neurons *(Batchelor et al., 1999)*. In a later study, the same research group has implicated activated microglia in intimate relationships with neurons in the same striatal injury model. In this work, microglia were found to act as 'stepping stones' for axonal sprouting around the wound edge *(Batchelor et al., 2002)*.

1.2.4.3 Phagocytosis and pro-apoptotic effects by microglia

In response to disease and injury, microglia also aid in the internalisation and degradation of whole cells and cell debris *(Wilcock et al., 2004; Napoli and Neumann, 2009)*. Microglia are therefore important for clearing potentially damaging molecules from the extracellular space *(Napoli and Neumann, 2009)*. Phagocytosis of entire cells can be promoted by signals on the plasma

membranes of dying or foreign cells. One prominent example is the detection of translocated phosphatidylserine residues from the inner to the outer leaflet of the cell membrane of dying cells, which is an indicator of caspase-3-mediated apoptosis *(Lauber et al., 2003).* In addition, the binding of microglial purinergic receptors to uridine diphosphate, which is released in response to cellular stress, results in phagocytosis *(Koizumi et al., 2007)*. Also, similarly to other phagocytes of various tissues of the body, microglia express the Mac-1 receptor complex *(Napoli and Neumann, 2009)*. This complex consists of CD11b and CD8 and can mediate phagocytosis of foreign material including opsonised bacteria through the proteolytic fragment of C3b *(Napoli and Neumann, 2009)*.

In contrast to the protective effect of microglia, these cells have also been implicated in promoting neuronal apoptosis *(Floden et al., 2005; Kofler and Wiley, 2011)*. This apoptosis promotion has been observed in cell culture where microglial excretion of TNF-α and glutamate has induced neuronal death via TNF-α and N-methyl-D-aspartate receptors, respectively *(Piani et al., 1991; Floden et al., 2005; Barger et al., 2007)*. Other molecules such as NO *(Chao et al., 1992)* and proteases *(Kingham and Pocock, 2001)* are released by microglia in stressed cell culture models, which may also contribute to neuronal death.

In contrast to the developing brain, debate still remains over the capacity of microglia to promote apoptosis in the adult CNS. In a model of excitotoxic motor neuron death, Caldero et al. (2009) reported that microglial activation and migration towards the site of injury was delayed until appropriate apoptotic

signals were expressed in chick spinal cord. Therefore, they postulated that microglia have no major role in promoting apoptosis, but are largely playing a phagocytic role *(Caldero et al., 2009)*. In conclusion, it has not yet been established whether the same microglial pro-apoptotic effects demonstrated in culture occur in the intact CNS.

1.2.4.4 Antigen presentation by microglia

Constituents derived from phagocytosed cells and cell debris can be used in antigen presentation to the innate immune system. It has been established that microglia constitute the main antigen-presenting cell population of the CNS *(Chastain et al., 2011)*. This microglial antigen presentation was identified in an early study of experimental allergic encephalomyelitis by Hickey and Kimura (1988). They found that microglia expressed various monocyte/macrophage/dendritic proteins involved in antigen presentation *(Hickey and Kimura, 1988)*, which is primarily conveyed by MHCs. As mentioned previously, MHC II up-regulation has been detected on microglia when activated with pro-inflammatory cytokines (section 1.2.3). MHC II has also been seen to increase with age (see the end of section 1.2.3.2), in autoimmune disease and as a result of viral infection *(Chastain et al., 2011)*. These MHC complexes together with co-stimulatory signals including CD40, bind foreign antigens and present these to infiltrating cells from the blood - T lymphocytes and T helper lymphocytes *(Aloisi et al., 1998; Chastain et al., 2011)*. Presentation of these antigens causes T lymphocyte proliferation, mediates immune responses

involving T helper cells *(Aloisi et al., 1998)* and provides protection against infectious diseases, among others. In contrast to other antigen-presenting cells such as those in lymph node, microglial activation of T lymphocytes has in one culture study been shown to induce subsequent apoptosis of the lymphocytes *(Ford et al., 1996)*. This apoptosis suggests that microglia may play a role in the regulation of T lymphocyte responses in the CNS *(Ford et al., 1996)*. As previously mentioned, microglia thereby play pertinent roles in the progression of MS (see section 1.2.4.1).

1.2.5 Microglial turnover in response to injury and disease

There is a limited number of studies investigating the life span of microglia in the healthy CNS and the mechanisms through which microglial numbers are kept constant in the healthy and diseased brain *(Ransohoff and Perry, 2009)*. The general turnover of microglia in the healthy CNS is believed to be a slow process *(Lawson et al., 1992)* and the life span of microglia stands out in comparison to other members of the same myeloid lineage. Monocytes in blood have a life span of 8 - 70 h *(Soulet and Rivest, 2008)*. In contrast, microglia are believed to reside in the brain parenchyma from years to a whole life time *(Sievers et al., 1994; Kofler and Wiley, 2011)*. For example, perivascular microglia have been shown to function in the healthy CNS for at least two years in rat, spanning most of its life *(Kida et al., 1993; Bechmann et al., 2001; Kofler and Wiley, 2011)*.

The number of microglia is clearly increased in areas of brain injury and neurodegeneration. This has been established for many neuropathological models, such as facial nerve axotomy in rat *(Graeber et al., 1988)*, a mouse model of amyotrophic lateral sclerosis; ALS *(Solomon et al., 2006)* and excitotoxin treatment of the chick spinal cord *(Caldero et al., 2009)*. This increase in cell number can result from local microglial proliferation, migration from neighbouring brain regions and potentially from the entry of microglial presursors from the circulation.

It has been hypothesized that cells acting as precursors for microglia may circulate in the blood, adhere to blood capillaries of the CNS and enter the brain through specific infiltration of individual cells to increase microglial numbers *(Zhang et al., 2007a)*. Monocytes are known to populate other tissues as macrophages *(van Furth and Cohn, 1968; Geissmann et al., 2010)*. With regards to infiltration into the CNS, this has mostly been based on studies in which the BBB has been compromised *(Kofler and Wiley, 2011)*. Migrating cells have also been reported in neuropathological models with an intact BBB, such as in demyelination induced in the corpus callosum using cuprizone *(McMahon et al., 2002).*

Infiltration of progenitors may be further stimulated by chemokines released by activated microglia within the CNS *(Zhang et al., 2007a)*. Examples of key migration signals involved in this process are CL2 *(Kofler and Wiley, 2011)* and MCP-1 (abbreviation for *monocyte, memory T lymphocytes and NK-cell specific*

chemoattractant; Zhang et al., 2007). As previously mentioned, it has been suggested that microglial release of cytokines is more extensive in acute disorders in comparison to chronic diseases. This secretion could potentially cause more recruitment of blood monocytes and other immune cells into the CNS *(Lucin and Wyss-Coray, 2009)*. These newly migrated blood-derived cells are said to initially have a different phenotype compared to resident microglia. Due to the different proportions of resident and blood-derived microglia in chronic and acute disorders, the macrophage/microglial population may give rise to different immune responses *(Lucin and Wyss-Coray, 2009)*.

After infiltration, migrated cell progenitors have been proposed to proliferate and differentiate into resident microglia inside the CNS parenchyma, similarly to that which occurs in the developing CNS *(Zhang et al., 2007a; Soulet and Rivest, 2008)*. Tissue macrophages that have recently infiltrated the CNS, have been shown to acquire a more microglia-like profile, and resident microglia acquire a more activated, amoeboid morphology in response to the disease or injury *(Lucin and Wyss-Coray, 2009; Kettenmann et al., 2011)*. Difficulties persist in distinguishing these infiltrated progenitors from previous resident microglia of the CNS. This has partially been overcome by transplanting bone marrow in which the microglial progenitors express green fluorescent protein (GFP; *Furuya et al., 2003*). In this model, exogenous microglial progenitors are found to infiltrate the CNS even in the adult diseased brain *(Kettenmann et al., 2011)*.

However, in essentially all bone marrow transplantations used to study the infiltration of microglial progenitors, the bone marrow recipient is prepared through whole-body irradiation to kill its endogenous progenitors *(Furuya et al., 2003; Mildner et al., 2007)*. This means that the transplantations involve a) a non-physiological amount of stem cells circulating in the blood, b) irradiation damage to the BBB enabling infiltration and c) activation of resident CNS microglia and astrocytes due to the irradiation *(Mildner et al., 2007; Ransohoff and Perry, 2009)*.

To address this issue, Ajami et al. (2007) studied conditions in which requirements for irradiation and bone marrow transplantation had been abolished. In these studies, mice were surgically joined in pairs to allow for a shared blood circulation. One of these mice expressed GFP in all hematopoietic cells, including potential progenitors for microglia. When analysing the brain of the other, wild-type mouse, no microglial cells were found to express GFP. Even upon axotomy of the facial nerve (outside the CNS) and in a model of ALS on this wild-type mouse, no GFP-positive progenitor cells were found to infiltrate the brain. Some GFP-positive / Iba1-positive macrophages were however found to have infiltrated the liver. As injection of exogenous bone marrow was necessary to induce infiltration by progenitors into the brain, this study demonstrates that infiltration of progenitors from the blood is not a common event in the healthy CNS nor upon two neuropathological models. They therefore present strong evidence that microglial proliferation sustains the microglial population throughout life *(Ajami et al., 2007)*. This coincides with recent understanding

that microglia stems from a different progenitor in comparison to other tissue macrophages *(Ginhoux et al., 2010; Saijo and Glass, 2011)*.

In some instances, microglial numbers may be reduced. One such instance has been observed after 'over-actvation' of these cells. For example, after exposure to high concentrations of LPS, excessive activation of microglia was followed by caspase-3-mediated apoptosis of these cells in primary cultures *(Liu et al., 2001).* Another mediator of microglial activation, as found in a culture model of AD, is chromogranin A, which can also lead to microglial apoptosis via overexpression of caspase-1, leading to cell death via a different apoptotic pathway *(Kingham et al., 1999)*. It has thus been postulated that microglia undergo cell death as a safety mechanism to limit their potential to kill neighbouring neurons and other cells after excessive microglial activation *(Liu et al., 2001; Polazzi and Contestabile, 2006)*. However, there are contradicting results to the caspase-mediated apoptosis mechanisms. For example, Calderò et al. (2009) could not detect a similar caspase-3 expression by dying microglia in LPS over-activation studies of the chick embryo *in vivo*. They therefore proposed a non-apoptotic process of microglial death upon over-activation that requires further study *(Caldero et al., 2009)*.

1.2.6 Microglial markers

A range of microglial markers have been used to identify microglia and assess their activation stages. Most microglial markers found commercially have lower

immunoreactivity in ramified microglia than in cells of activated stages *(Saura, 2007; Kofler and Wiley, 2011)*, causing detection difficulties in the healthy CNS *(Matsumoto et al., 2007; Garman, 2011)*. There is also no established microglial marker that does not label for peripheral macrophages *(Graeber and Streit, 2010)*. CD11b is expressed by microglia *(Robinson et al., 1986)*, where it is one of the components of the Mac-1 heterodimeric receptor *(Napoli and Neumann, 2009)*. Monocytes, macrophages, dendritic cells, neutrophils and granulocytes also express CD11b. However, microglia constitute the only native cell type of the healthy CNS expressing the CD11b protein *(Robinson et al., 1986)*. Upon traumatic injury, the potential infiltration of macrophages *(Robinson et al., 1986; Tanaka et al., 2003)* and neutrophils *(Matsumoto et al., 2007)* causes labelling difficulties using CD11b. Morphological distinctions can be made between microglia and neutrophils due to the polymorph nuclei of the latter *(Matsumoto et al., 2007)*. However, difficulties remain in distinguishing microglia from macrophages that may potentially infiltrate the brain after certain invasive injuries.

Griffonia simplicifolia isolectin B4 is another marker for microglia with an unknown binding site *(Kettenmann et al., 2011)*. Isolectin B4 had initially been used to label proliferating glia of the CNS, however it is now generally accepted that it can be used to detect microglia of any activation stage *(Streit and Kreutzberg, 1987, Monif et al., 2009)*.

Iba1 is another established microglial marker *(Imai et al., 1996; Kettenmann et al., 2011)*. Similarly to CD11b immunolabelling *(Frau et al., 2011),* Iba1 immunolabelling *(Ito et al., 1998; Imai and Kohsaka, 2002; Tynan et al., 2010)* shows increased numbers of immunoreactive cells upon activation. Each activated microglial cell also displays increased immunolabelling intensities of these markers in neuropathological models *in vivo*. Hence, an activated microglial cell can be identified due to a more intense labelling of certain microglial markers, and by looking at distinct morphological changes (see section 1.2.3) including larger cell bodies and fewer, shorter and thicker processes *(del-Rio Hortega, 1932; Kettenmann et al., 2011)*.

Upon microglial activation, increased expression of microglial markers Iba1 and CD11b is accompanied by the increased expression of several other proteins involved in immune responses *(Kettenmann et al., 2011).* Many of these proteins are expressed in other tissues by cells of the same myeloid lineage. One example is CD68 (also known as ED1), which can be found on lysosomal membranes in phagocytic microglia *(Hickey and Kimura, 1988; Flaris et al., 1993; Garman, 2011)*. As phagocytosis is not featured in all stages of microglial activation, CD68 labelling cannot be used to detect microglia of all activated stages. In the detection of activated microglia, it is therefore recommended to combine immunolabelling using such markers with morphological studies *(Graeber and Streit, 2010)*.

1.2.7 Microglia in cell culture

Cells grown in culture are widely used to study many different cell types. These can be either immortalised cell lines or primary cultures. Cell lines can be produced a) by direct extraction from a live tumour *(Zhou et al., 2011)*, b) by inducing random mutagenesis, c) by introducing expression of proteins such as telomerase or viral proteins that provide immortality *(Olson et al., 2003)* or d) through fusion with cancer cell lines to form hybridomas *(Tomita and Tsumoto, 2011)*.

Cell lines available to date have provided clues to the function of microglia, especially in activated stages *(Franco et al., 2006)*. Although immortalised microglial cell lines have been useful in the study of specific proteins and conditions, they have striking differences in comparison to microglia *in vivo (Franco et al., 2006; De Vries and Boullerne, 2010; Graeber and Streit, 2010)*. Microglial cell lines express aberrant levels of many proteins, constantly proliferate and do not fully differentiate into mature, ramified microglia as in the healthy CNS *(De Vries and Boullerne, 2010)*. For instance, a constant up-regulation of CD38 has been reported in the N9 microglial cell line *(Franco et al., 2006)*. CD38 is normally only expressed upon activation and is therefore indicative of properties not found in microglia in the healthy CNS environment.

Primary microglial cultures better mimic aspects of cellular function in the CNS. One established method for preparation of pure microglial cultures is the mild trypsinisation method. Such cultures are achieved by slowly peeling off the

astrocytic layer from mixed glial cultures using low concentrations of trypsin, leaving predominantly microglia on the culture plate *(Saura et al., 2003)*. This method provides microglial cultures with prolonged survival in comparison to other methods. Another commonly used method for preparation of pure microglial cultures utilises mixed glial cultures that contain both microglia and astrocytes, and detaches microglial cells growing on top of the latter through shaking *(Persson et al., 2005)*. These detached cells are thereafter seeded in new cell culture plates to achieve pure microglial cultures. A more recently adapted microglial purification method involves the use of silica-based density gradients. This protocol is not preceded by the production of mixed glial cultures. Instead, this involves homogenization of entire rodent adult brain tissue, followed by the separation of different cell types in a layer formed between 70 and 35 % Percoll™. The cells are thereafter cultivated in astrocyte-conditioned medium to further inhibit microglial activation after plating *(Hooper et al., 2005)*.

Innumerable studies of primary microglia in pure culture, and together with astrocytes in mixed glial cultures, have contributed substantially to understanding microglial function. When isolated from the neonatal brain, a mixture of ramified microglia and microglia of higher activation stages (see Figure 3.3) can be detected *(Tanaka et al., 1999; Kalla et al., 2003)*. This provides an avenue for analysis of microglial function at various stages of activation. However, there are also some limitations for primary microglial cultures, as these can be costly and time consuming to maintain and generally contain low numbers of microglia *(Horvath et al., 2008)*. As for all studies in cell culture,

these cells are removed from the CNS environment and have little to no interaction with other cell types, depending on the preparation method and growth medium. In addition, any of these three culture preparations are generally used within 24 h in culture due to the increased activation of these cells in the absence of astrocytes and other cell types *(Hooper et al., 2005; Labuzek et al., 2010; Welser-Alves et al., 2011; Hooper et al., 2012; Szabo and Gulya, 2013)*, providing a short time for experiments.

1.3 Astrocytes

Another glial cell type, with a very different functional profile to microglia is the astrocyte. An astrocytic cell has five to eight major processes, which gives it a stellate appearance under some immunolabelling conditions. The major processes are extended by countless smaller processes, giving them an overall 'bushy' appearance when all processes are visible *(Bushong et al., 2002; Nedergaard et al., 2003; Nag, 2011)*.

Astrocytes are distributed throughout the grey and white matter of the CNS *(Nedergaard et al., 2003; Nag, 2011)* and can be divided into at least two anatomically and functionally different subpopulations. In general, the white matter contains mainly fibrous astrocytes, whereas the grey matter such as the cerebral cortex consists of mostly protoplasmic astrocytes *(Miller and Raff, 1984; Nag, 2011).* Protoplasmic astrocytes are organised in domains by occupying designated areas with little overlap with neighbouring astrocytes *(Chang Ling*

and Stone, 1991; Nag, 2011). Within these domains, protoplasmic astrocytes form numerous connections with neighbouring glia, neurons and blood vessels without interfering with the domains of other neighbouring astrocytes.

Protoplasmic astrocytes are known to express a lower amount of some cytoskeletal proteins than their fibrous counterparts *(Miller and Raff, 1984)*. Fibrous astrocytes, which have a high abundance of fibrils, have straighter and less branched processes, which interact extensively with each other *(Oberheim et al., 2009; Nag, 2011)*. These fibrous astrocytes also have larger cell bodies and a decreased amount of fine bulbous processes *(Oberheim et al., 2009)*. As the majority of these cells are situated in white matter where there is a lack of synaptic connections, they are believed to facilitate more structural support than information processing, in contrast to protoplasmic astrocytes *(Oberheim et al., 2009; Nag, 2011)*.

One of the cytoskeletal proteins with varying expression in astrocytic subtypes is glial fibrillary acidic protein (GFAP). In the CNS, GFAP forms intermediate filaments specifically in astrocytes *(Eng et al., 1971; Lee et al., 2006)* and is therefore a commonly used astrocytic marker *(Miller and Raff, 1984; Su et al., 2004)*. However, GFAP is not found in the tiny protrusions of astrocytic processes and only covers approximately 13 % of the astrocytic cell volume as determined in the hippocampus *(Bushong et al., 2002)*.

In addition, evidence has emerged for hetereogeneity of GFAP expression within the astrocytic population *(Miller and Raff, 1984; Bushong et al., 2002)*. One example is the CA1 layer of the hippocampus, where GFAP is undetected in 20 % of astrocytes *(Walz and Wuttke, 1999)*. These regional differences have been proposed to relate to differences in functional demands, such as the need for potassium buffering *(Holthoff and Witte, 2000)*. Also, some populations of GFAP-negative astrocytes have been postulated to be mature astrocytes *(Stichel et al., 1991)* or even 'passive' astrocytes *(Bushong et al., 2002)*.

The heterogeneity in GFAP expression limits the use of this marker to identify the entire astrocytic population. Other markers have been used to detect a larger proportion of astrocytes. For example, S100 calcium binding protein beta is widely expressed in astrocytes but also in oligodendrocyte progenitors and microglia *(Steiner et al., 2011)*. Therefore, GFAP constitutes the only established astrocyte-specific marker in the CNS.

1.3.1 Astrocytes in the healthy CNS

1.3.1.1 Astrocytic function

Astrocytes play important roles in various functions of the CNS, including structural support, metabolic support, uptake of neurotransmitters and the provision of transmitter precursors to neurons. An intricate part of their multifaceted functions is their ability to form glial networks *(Brightman and Reese, 1969; Dermietzel et al., 1991; Orthmann-Murphy et al., 2008)*. This

astrocytic syncytium is built up by gap junctions along the astrocytic processes, which are particularly concentrated at the endfeet of the latter. These gap junctions allow for intercellular exchange of low-molecular weight molecules between adjacent astrocytes *(Brightman and Reese, 1969; Orthmann-Murphy et al., 2008)*. Glial networks are believed to play a part in CNS function, which have been implicated in a) long range calcium signalling *(Orthmann-Murphy et al., 2008)*, b) the contribution of buffering of extracellular potassium by spreading this after uptake *(Dermietzel et al., 1991; Nordin et al., 2005; Orthmann-Murphy et al., 2008)*, c) distributing glutathione that can be used as an antioxidant also by other cell types *(Kaur et al., 2007)*, d) and allowing for the diffusion of glucose to provide metabolic support for neurons throughout the CNS *(Nordin et al., 2005)*.

Astrocytes also form close connections to neurons and clear neurotransmitters from the synaptic cleft. Their function is important for the regulation of synaptic activity through calcium ion (Ca^{2+}) signalling *(Perea et al., 2009)*. One prominent example of astrocytic clearing is that of glutamate which is internalised into astrocytes via excitatory amino-acid transporters *(Danbolt, 2001)*. After conversion of glucose to glutamine in astrocytes, this is shuttled back to neurons for reconversion to glutamate or use in other metabolic processes *(Kimelberg and Nedergaard, 2010)*.

Results have also been presented for the notion that glucose internalised by astrocytes is transformed into lactate before transfer to neurons *(Pellerin and Magistretti, 1994; Laughton et al., 2007)*. However, this lactate shuttling from astrocytes to neurons still remains controversial, especially with regards to *in vivo* studies *(Nedergaard et al., 2003; Kimelberg and Nedergaard, 2010)*.

Astrocytes also contribute to neuronal protection against toxicity. In the CNS, astrocytes release high levels of the antioxidant glutathione. Extracellularly, this glutathione is broken down into glutathione precursors, which can be taken up by neurons and used for glutathione synthesis in these cells *(Aschner, 2000; Dringen et al., 2000; Kaur et al., 2007; Backos et al., 2012)*. Glutathione has the capacity to counteract reactive oxygen species, thereby limiting the exposure of these damaging molecules to neurons *(Dringen et al., 2000; Kaur et al., 2007)*. The higher expression of glutathione in astrocytes compared to neurons is considered essential for neuronal protection, which has been exemplified in a model of ischemia *(Kaur et al., 2007)*.

The astrocytic population is also implicated in the modulation of BBB formation *(Moody, 2006; Nag, 2011)*. This barrier is built up of tight junctions between endothelial cells in blood vessels. These tight junctions make it essentially impossible for water-soluble ions and molecules to translocate between the blood and CNS in the absence of specific transporters in the endothelial cell membranes. The BBB thereby constitutes the first obstruction for external

toxins, pathogens *(Moody, 2006)* and reactive oxygen species from entering the CNS *(Schroeter et al., 1999)*.

In culture, the astrocytic influence of the BBB has been studied by exposing endothelial cells in culture to astrocyte-conditioned medium *(Prat et al., 2001)*. The presence of astrocyte-released factors has been shown to influence the proximity of endothelial cells to each other, causing decreased permeability of molecules such as albumin *(Prat et al., 2001)*. This finding points towards a promoting role by astrocytes in the regulation of the BBB. Moreover, transport of specific molecules through the BBB is subject to astrocytic regulation *(Nedergaard et al., 2003)*. The enclosing of blood vessels by astrocytic endfeet make astrocytes key holders to the CNS supply of molecules, including glucose *(Moody, 2006; Iadecola and Nedergaard, 2007)*.

The close connection to the CNS blood vasculature has also implicated astrocytes in the regulation of vascular tone *(Zonta et al., 2003; Iadecola and Nedergaard, 2007)*. Increased blood flow has been linked to a neuron-to-astrocyte-linked mechanism. Neuronal activity via the release of neurotransmitters such as glutamate can trigger astrocytic responses via glutamate receptors. This astrocytic activation induces Ca^{2+} oscillations. In turn, these oscillations stimulate release of prostaglandins from astrocytic endfeet. This conversion relaxes blood vessels and increases blood flow, which has been shown in rat cortical slices. *In*

vivo, it has also been demonstrated that specific blockage of glutamate receptors prevents Ca^{2+} oscillations and reduces blood flow *(Zonta et al., 2003)*.

1.3.1.2 Phylogenetic advance of glial cells

The importance of astrocytes is further suggested by changes seen in the quantity and size of these cells throughout evolution. Glial numbers are clearly increased when comparing brain composition in animals of increasing complexity. In the majority of these studies, the number of glia is based on the number of astrocytes and oligodendrocytes *(Sherwood et al., 2006)*.

One of the simplest organisms used to investigate nervous system function - *Caenorhabditis elegans* - constitutes an early example of low glial abundance where the total number of glial cells are outnumbered by neurons in a 1 : 6 ratio *(Sulston et al., 1983; Nedergaard et al., 2003)*. A higher glial abundance is seen in rat, where the ratio of astrocyte : neuron ranges from 1 : 1.3 up to 1 : 2.5 *(Bass et al., 1971; Nedergaard et al., 2003)*. In the prefrontal cortex of higher mammals such as anthropoid primates, this ratio ranges from 1 : 2.17 to 1.22 : 1 *(Sherwood et al., 2006)*. Further increase is evident in the human temporal lobe, which includes the hippocampus, where astrocytes outnumber neurons in a 1.4 : 1 ratio *(Bass et al., 1971; Nedergaard et al., 2003)*. In the human prefrontal cortex, this ratio reaches 1.65 : 1 *(Sherwood et al., 2006)*.

In addition to increased numbers of glia, the size of astrocytes and the amount of extended processes have been found to increase along the branching of the phylogenetic tree. Compared to rodents, human neocortical astrocytes possess 2.6-fold larger diameters and extend 10-fold more processes *(Oberheim et al., 2009)*.

Increases in cell body size, population size and number of extended processes of the glial population have been linked to the increasing complexity of the CNS *(Nedergaard et al., 2003)*. It is now believed that the expansion of the astrocytic population of higher eukaryotes is an adaption to increased CNS metabolic demand and/or synaptic complexity *(Nedergaard et al., 2003; Oberheim et al., 2009; Araque and Navarrete, 2010; Sofroniew and Vinters, 2010; Porto-Pazos et al., 2011)*.

1.3.2 Astrocytic involvement in brain injury and disease

In brain injury and disease, the housekeeping functions of astrocytes including structural support and neurotransmitter buffering still play an important part. Also, preceded by microglial responses, progressive changes in gene expression and cellular phenotype of astrocytes occur in the response to CNS pathology *(Sofroniew and Vinters, 2010)*. This process is referred to as astrocytic activation or astrogliosis *(Sofroniew, 2009)*.

Astrocytic activation is universally manifested by increased expression of GFAP *(Eng et al., 1971; Volterra and Meldolesi, 2005; Li et al., 2008)*. This has been detected in pathologies including ischemia, epilepsy, excitotoxic insults and mechanical brain injury *(Floyd et al., 2004; Badoer, 2010)*. In ischemia, increased GFAP expression is evident after a minimum of 4 h, and generally reaches its maximum at 24 - 48 h after the onset of ischemia *(Petito et al., 1990; Morioka et al., 1991; Shannon et al., 2007)*. Increased expression of GFAP is also accompanied by apparent hypertrophy of cells with enlargement of the major processes.

Mild to moderate astrogliosis is generally caused by minor, non-penetrative injuries and diseases. In these pathologies, astrocytic numbers are kept at similar levels and GFAP is moderately up-regulated. These mild to moderate stages of gliosis often resolve, allowing astrocytes to return to their original state of normal astrocytic function in the healthy CNS *(Sofroniew and Vinters, 2010)*. In contrast, severe gliosis caused by various penetrating traumas and invasive infections involves a higher degree of hypertrophy, proliferation and further activation of astrocytes. This results in an even higher intensity of astrocytic marker protein expression *(Sofroniew and Vinters, 2010)*.

In severe gliosis, the CNS is subject to tissue reorganisation, which causes functional deficits of cells in the CNS, including astrocytes. For instance, protective astrocytic functions such as glutamate uptake and potassium buffering are impaired. Furthermore, hypertrophy, increased cellular activation

and proliferation causes physical overlaps within the protoplasmic astrocytic population and the disruption of their distinct, isolated domains *(Sofroniew and Vinters, 2010)*.

The tissue reorganisation in severe gliosis is prominent around the area of injury or disease, where there is a formation of a dense glial scar consisting of numerous glial cells, and secreted proteoglycans from astrocytes. Glial scars have been shown to prevent the spreading of mechanical damage, inflammatory molecules and the infiltration of non-CNS cells in brain pathology *(Silver and Miller, 2004; Voskuhl et al., 2009; Sofroniew and Vinters, 2010)*. On the other hand, the glial scar also forms a barrier that inhibits regeneration of neuronal connections *(Silver and Miller, 2004; Sofroniew and Vinters, 2010)*. Astrocytes also secrete pro-inflammatory agents such as IL-1, IL-6 and TNF-α, which affects the involvement of the immune system, including microglia *(Lee et al., 2010)*.

Overall, astrocytic responses to injury and disease are mixed with positive and negative outcomes. Astrocytic influence on increased neuronal viability and decreased spreading of injury, is accompanied by severe gliosis with the release of potentially damaging cytokines and glial scarring that may inhibit new formation of neuronal synapses.

1.4 Genetic modification

Many questions still remain on the function of glial cells in the healthy and diseased CNS. New and advanced tools are required to study glia in the intact brain in order to fully understand their function in the healthy CNS and in many neurodegenerative disorders *(Kofler and Wiley, 2011)*. Genetic modification is a widely used approach to study the function of specific proteins and specific cell types in the healthy or diseased animal. In addition, many prevalent human diseases today are caused by genetic abnormalities or at least have a genetic component *(Polazzi and Monti, 2010)*. These disorders can also be investigated by introducing genes of interest through techniques of genetic modification.

Genetic modification can be achieved on either DNA or messenger RNA (mRNA) level. The nucleic acid used for this purpose is chosen depending on whether the genetic modification should be permanent or transient *(Zou et al., 2010)*. On a DNA level, genetic modification can be either permanent or transient, depending on whether the introduced nucleic acid sequence is inserted into the host genome or kept as an extra-chromosomal unit. Permanent genetic modification has been used to produce numerous genetically modified animals and immortalised cell lines.

Transient genetic modification is also a common approach and can be performed at a DNA or RNA level. Different durations and timing of maximum expression is achieved with DNA compared to RNA. For example, in primary cortical neurons,

transgenes were expressed 7 h after the start of DNA transfection and continued with a high intensity up to 36 - 48 h post transfection start *(Zou et al., 2010)*. In contrast, similar conditions using RNA resulted in quicker expression of the transgene. Transgene expression was evident within 1 h of exposure with maximum intensities at 5 - 7 h after RNA exposure *(Zou et al., 2010)*. In comparison to RNA, not only does transfection on a DNA level give prolonged expression, but also generally leads to higher total amount of gene product *(Zou et al., 2010)*.

The aim of this work was to evaluate an approach to genetically modify microglia in the intact brain on a DNA level. Subsequent sections provide a general overview of genetic modification emphasising particularly approaches to produce transient modification. The section concludes with a short review of the use of these techniques for investigating microglia.

1.4.1 Permanent genetic modification

Permanent genetic modification involves the use of DNA to manipulate gene expression in a long-term manner. An early approach for genetic modification involved the introduction of modifications into cells at the start of embryonic development. This approach results in changes throughout all stages of development and has provided invaluable evidence on the effects of aberrant levels and/or function of specific proteins. These models are especially powerful for the study of hereditary disorders where a mutation is permanently present in

the host genome. However, conventional genetic modification may cause lethality *(Tsai et al., 1994; Guan et al., 2010)*, tissue/organ loss *(Wurst et al., 1994; Nagy and Rossant, 1996)*, accompanying development of pathology *(Rigotti et al., 1997b; Holm et al., 2002)* and/or compensatory mechanisms by proteins with similar function *(Schulte-Herbruggen et al., 2008)*.

The use of conditional genetic modifications that allow for time-dependent and/or tissue-specific expression has been widely used to address some of the shortcomings seen after conventional permanent modifications of gene expression *(Tsien et al., 1996)*. Time-specific conditional gene knockouts allow for normal development of the animal, and the ability to control the initiation of gene knockout or mutation. A tissue-specific conditional gene knockout involves the alteration/addition of a gene in a specific tissue or organ.

One well-established system for conditional gene knockouts is the Cre/loxP system that was pioneered by Sauer and Henderson (1988). Cre (abbreviation for *causes recombination*) recombinase is an enzyme capable of specifically swapping fragments with identical flanking loxP *(*abbreviation for *locus of crossing (x) over P1)* sites between two different DNA sequences *(Sauer and Henderson, 1988; Nagy et al., 2009)*. This allows Cre recombinase to selectively remove or add sequences between loxP sites through site-specific recombination in specific parts of the genome *(Sauer and Henderson, 1988)*. The

Cre/loxP system has been used to specifically remove stop sequences flanked by loxP sites by adding Cre recombinase, either through injection of this enzyme or by mating with Cre recombinant transgenic animals. Upon excision of this sequence by Cre recombinase, a cell or tissue-specific promoter can be used to induce the expression of a gene of interest in a certain cell type or tissue. These promoters are found upstream of a gene, and are responsible for the regulation of the latter.

A different approach using this technique involves the positioning of the cell-specific promoter in front of Cre recombinase. This method has been used in regions of the CNS such as the *Cornu Ammonis* 1 (CA1) field of the hippocampus, producing transgenic animals where only hippocampal neurons express this enzyme *(Tsien et al., 1996)*. There are some limitations in the use of conditional gene knockouts such as the possibility of inserts into multiple Cre and/or loxP sites of the same animal, and with a wrong orientation *(Nagy et al., 2009)*. Not only can this affect the expression of the gene of interest, but also cause chromosomal instability and a flawed animal phenotype *(Nagy et al., 2009)*.

Permanent genetic modification on a DNA level has also been widely used in immortalised cell lines to resemble aspects of various diseases. In comparison with wild-type counterparts, these cell lines have been used to determine protein and/or cellular function. The use of cell lines may be more efficient with

regards to time, cost and ways of manipulation, which usually makes it easier to address specific functions. However, they do not allow for assessment of complex interactions that are present *in vivo* and often have aberrant phenotypes, partially due to their immortalisation and removal from the natural CNS environment. Therefore, cell culture models are highly valuable in certain applications, while genetically modified animals may address other questions than are possible with the use of cultured cell lines.

1.4.2 Transient genetic modification

An alternative method to permanent genetic modification is to investigate the properties of different cell types and tissues on a background of normal development. Through transient genetic modification, DNA or RNA is used to manipulate gene expression in a short-term manner. Generally, vectors for transient genetic modification on a DNA level are maintained extra-chromosomally in their target cells where they use the transcriptional machinery of the host *(Glover and Hames, 1995)*. This method also has high potential for application in the treatment of injuries and diseases with onset at adult ages as the gene of interest can be introduced in an animal at any age.

Transient genetic modification commonly involves the use of a double-stranded DNA type which is normally circular and naturally found in bacteria. This plasmid DNA is present as a mixture of different structural forms with predominantly supercoiled structures when put in aqueous solutions *(Robertson et al., 2006)*.

The intertwined structure of supercoiled DNA is formed in the presence of the gyrase enzyme in most bacteria *(Gellert et al., 1976; Kalkbrenner et al., 2009)*. Supercoiled DNA represents the natural topology of plasmid DNA molecules *(Fishman and Patterson, 1996)*.

Due to their structure, supercoiled plasmid DNA diffuse quicker throughout the cytoplasm than linear DNA of equivalent length *(Robertson et al., 2006)*. A motility of 4.11 x 10^{-8} cm^2/s has been calculated for a supercoiled plasmid DNA of 3.7 kilobases (kb) compared to the equivalent speed of 2.82 x 10^{-8} cm^2/s for linear DNA of the same size *(Fishman and Patterson, 1996)*. Thus, supercoiled plasmid DNA is more mobile than most linear DNA and also non-supercoiled plasmids. The higher diffusibility further enhances the delivery of the DNA to its final destination for transcription; the nucleus *(Hsu and Uludag, 2008)*. Furthermore, plasmid DNA is less susceptible to intracellular degradation than linear DNA equivalents *(Hsu and Uludag, 2008)*. These characteristics enable plasmid DNA to produce higher levels of transfection than linear equivalents *(Cohen et al., 1973; Chen et al., 2001; Hsu and Uludag, 2008)*. Plasmids have therefore been used extensively for transient genetic modification.

Plasmid DNA and other nucleic acid structures can be tailored for specific applications through the insertion of genes of interest or the introduction of specific promoters. This is achieved through the use of restriction enzymes

(Cohen et al., 1973; Klein et al., 1998). Initially, these enzymes were mainly derived from bacteria where they help to protect against virus infection. These days, restriction enzymes are used to recognise and cleave DNA at specific nucleic acid sequences *(Kessler and Manta, 1990)*. A commonly used promoter inserted into many commercially available plasmids is the cytomegalovirus (CMV) promoter *(Thomsen et al., 1984; Choi et al., 2007)*; a strong promoter that can result in high expression levels of the gene of interest especially in mammalian cells *(Pasleau et al., 1985)*. In the nervous system, with no specific targeting agents, this promoter enhances expression predominantly in neurons *(McCown et al., 1996)*. As a proof of function, reporter genes including GFP are often used to visualise the delivery of nucleic acids.

1.4.2.1 Mechanical and chemical transfection

There are different methods of delivering nucleic acids into cells, of which some involve the forcing of this material through mechanical and/or chemical methods. Examples of mechanical methods suitable for mammalian cells include hydrodynamic pressure, microinjection and electroporation. Hydrodynamic pressure involves the injection of high volumes of plasmid DNA that force these molecules into the surrounding tissue, and has been successfully used in for example muscle cells *(Glover et al., 2005)*. DNA has also been microinjected directly into the cell cytosol *(Glover et al., 2005)*.

One mechanical method with high applicability especially *in vitro* is electroporation. This technique involves electric currents that in the presence of certain chemical agents open up pores in cell membranes for delivery of nucleic acids into the cytosol *(Gresch et al., 2004)*. Nucleofection is an improved *in vitro* version of electroporation allowing the delivery of nucleic acids directly to the nucleus by also opening up nuclear pores *(Gresch et al., 2004)*. This method offers a feasible method for gene delivery to cell lines of both neuronal and glial origin *(Schnoor et al., 2009)*. In addition, nucleofection has resulted in increased transfection capacities in post-mitotic cells such as those of primary cultures *(Gresch et al., 2004)*. Nucleofection of primary neurons *(Gresch et al., 2004)* and astrocytes *(Muyderman et al., 2010)* has resulted in transfection efficiencies of up to approximately 70 % and 90 %, respectively. Electroporation methods have also been utilised in the intact developing CNS *in ovo (Muramatsu et al., 1997)*, *exo utero (Akamatsu et al., 1999)*, *in utero (Tabata and Nakajima, 2001)*, and even postnatally in the brain of the neonatal animal *(Boutin et al., 2008)* and the adult animal *(Tanaka et al., 2000; Wang et al., 2007a)*. Electroporation in the CNS of an adult animal generally results in gene expression of a population of cells mainly idenfied as neurons, with a few exceptions of astrocytes and microglia *(Vry et al., 2010)*.

Drawbacks of mechanical methods such as eletroporation include the obvious mechanical damage and gliosis along the needle tract of the electroporation instrument. Significant damage has also been observed in experimental animals

treated with this method, which has been manifested in motor spasms and breathing difficulties *(Vry et al., 2010)*. In addition, the opening of pores in plasma membranes causes toxicity as determined by cell death and tissue damage. This also results in the direct recruitment of inflammatory cells *(De Vry et al., 2010)*. Together with the majority of other established mechanical methods, electroporation is mainly suitable for *in vitro* research. *In vivo*, electroporation also generally produce low transfection efficiencies.

1.4.2.2 Endocytosis of DNA and other macromolecules

In contrast to mechanical methods, the use of endogenous cellular mechanisms such as endocytosis to deliver DNA and other macromolecules is a less invasive option *(Shimizu et al., 1996)*. Endocytosis comprises the encapsulation of extracellular molecules by a portion of the plasma cell membrane and the formation of an intracellular vesicle that buds off inside the cell *(Ziello et al., 2010)*. A variety of eukaryotic cells have demonstrated uptake of various macromolecules such as plasmid DNA molecules. This non-specific internalisation has been demonstrated in culture *(Stacey et al., 1996)* and *in vivo (Wolff et al., 1990; Zauner et al., 1998; Sloane et al., 2009)* and occurs via non-specific phagocytosis (by macrophage-related cells such as microglia) or its non-macrophage equivalent (macro)pinocytosis. Most mammalian cells are capable of this pinocytosis, which involves a similar non-specific mechanism for uptake of protein, DNA and other particles from the extracellular space *(Ziello et al., 2010)*.

A third subtype of endocytosis comprises receptor-mediated endocytosis. This process involves the restricted uptake of molecules through specific binding to corresponding receptors *(Ziello et al., 2010)*. Ligands bound to specific receptors are subsequently internalised by endocytosis of the intact receptor-ligand complex.

Receptor-mediated endocytosis can be clathrin-dependent, caveolae-dependent or independent of either *(Frick et al., 2007; Ziello et al., 2010; Zhao et al., 2011)*. Clathrin-dependent receptor-mediated endocytosis has been studied in most detail. In this subtype of endocytosis, specific receptor-ligand complexes accumulate in clathrin-coated pits of the plasma membrane, induce internalisation and the formation of intracellular clathrin-coated vesicles. These vesicles enter a pathway involving endosomes and lysosomes *(Ziello et al., 2010)*.

Some mechanisms of receptor-mediated endocytosis do not require receptor-ligand binding for initiation of internalisation *(Krangel, 1987; San Jose and Alarcon, 1999; Yu et al., 2000; Mahmutefendic et al., 2007)*. This has been demonstrated as a common feature in clathrin-mediated endocytosis, where ligands do not elicit internalisation but spontaneously enter the cell when the receptor is internalised if they are bound to the receptor at the time of this event. In all mechanisms of receptor-mediated endocytosis, including this constitutive internalisation *(Yu et al., 2000; Thomsen et al., 2002)*, receptor

ligands are specifically internalised, resulting in increased intracellular concentrations. This characteristic provides a useful means of gene delivery by targeting specific receptors.

Caveolae-dependent endocytosis involves similar uptake of macromolecules. Although not as well described as clathrin-dependent endocytosis, this process involves the internalisation of receptor-ligand complexes within structures called caveolae *(Ziello et al., 2010)*. These caveolae are rounded invaginations of the plasma membrane *(Lajoie and Nabi, 2010; Ziello et al., 2010)* and generally allow for a less frequent internalisation with slower speed than that initiated in clathrin-coated pits *(Thomsen et al., 2002; Nichols, 2003)*. Caveolae are often linked to membrane rafts which are approximately 10 - 200 nm *(Pike, 2006)* and sometimes referred to as lipid rafts *(Lajoie and Nabi, 2010; Ziello et al., 2010)*. These rafts are abundant in (glyco)sphingolipids and cholesterol, and become larger in the presence of increased extracellular concentrations of the latter *(Pike, 2006)*. Membrane rafts are found in most cell types *(Lajoie and Nabi, 2010)* and provide locations for protein/lipid trafficking, cellular signalling and the entry of some viruses and toxins *(Pike, 2006)*. The intracellular pathway of cargo delivered via caveolae has not been fully determined. Initially, these vesicles have neutral pH and have been suggested to later fuse with endosomes, entering the endosomal/lysosomal pathway *(Sharma et al., 2003; Kiss, 2012)*.

Figure 1.3 Ligand internalisation via clathrin and caveolin-mediated pathways and subsequent intracellular movement *(see figure text on next page)*

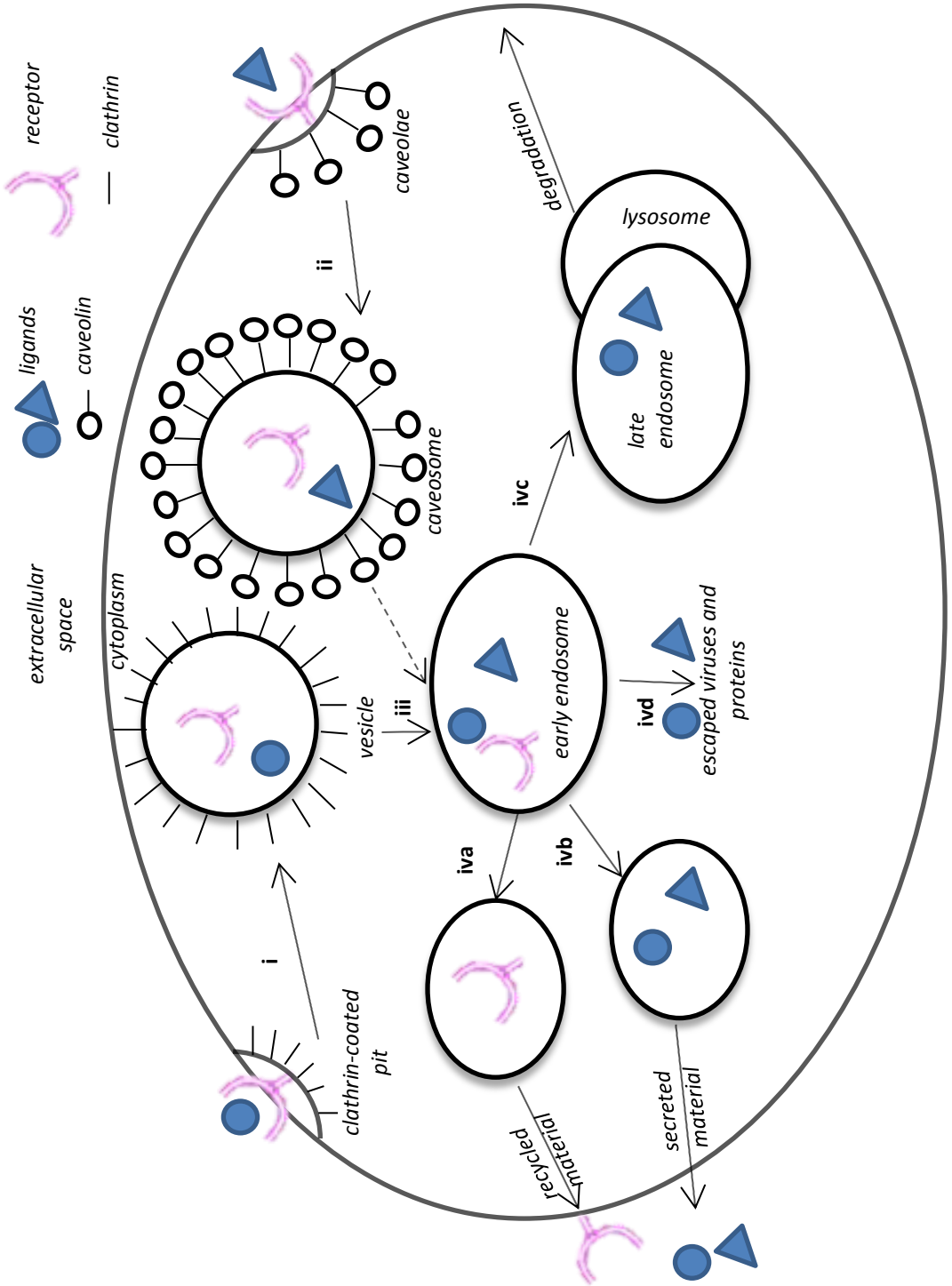

Figure 1.3 Ligand internalisation via clathrin and caveolin-mediated pathways and subsequent intracellular movement *(see previous page). Receptor-mediated endocytosis occurs at receptors situated on the cell membrane, which may be surrounded by for example clathrin or caveolin. Protein-coated vesicles bud off from the plasma membrane, forming endocytic carriers that can fuse with early endosomes (i; for clathrin-mediated pathways) or form caveosomes (ii; for caveolae-mediated pathways). Caveosomes initially have neutral pH and may fuse with endosomes at a later stage as represented by the dotted arrow (Nichols, 2003; Laude and Prior, 2004). Endosomes can transport material back to the cell surface where material is recycled (iva) or secreted to the extracellular space (ivb). The endosomes can also become acidified through energy-dependent uptake of protons, leading to the formation of late endosomes (ivc). As the late endosome fuses with lysosomes, the content of these vesicles is degraded. Alternatively, some viruses and proteins with an intracellular destination can escape this degradation pathway (ivd) and enter the cytoplasm. Adapted from Ziello et al. (2010).*

After internalisation (see Figure 1.3), endocytosed particles follow a sorting process to be either recycled to the plasma membrane, secreted into the extracellular space, passed on into mildly acidic and hydrolytic late endosomes or caveosomes, or in rare instances released into the cytosol *(Ziello et al., 2010)*. In general, naked nucleic acids such as plasmid DNA internalised through non-specific endocytosis are passed onto intracellular vesicles where nucleic acids are quickly degraded. Therefore, DNA requires release from the hydrolytic environment of these vesicles to result in genetic modification *(Seternes et al., 2002)*.

1.4.3 Viral genetic modification

Early studies on genetic modification focussed on the possibility of a viral protective element for nucleic acids. This viral element would harbour a strong potential to guide DNA into the cell, and thereafter safely to the nucleus by escaping the proteolytic environment of cellular organelles. Natural viruses are enveloped packets of plasmid-like DNA or RNA that require host cells in order to proliferate *(Alberts et al., 2008)*. These particles have therefore developed ways of entering eukaryotic cells via endocytosis *(Suh et al., 2001; Askjaer et al., 2002)*. When inside the cell, viruses can escape degradation in acidic vesicles and reach the nucleus by expressing various peptides with capacities to escape intracellular vesicles and/or to translocate to the nucleus. Certain viruses are capable of entering the nucleus and inserting themselves into the host genome, thereby enabling permanent transduction *(Yi et al., 2011)*. Other viruses can be

used as extra-chromosomal DNA sources for transient expression *(Schneider et al., 1997; Lim et al., 2010)*.

Viral gene delivery still constitutes the most commonly used method to express specific proteins in mammalian cells *in vivo*. Among others, the wide range of viral vectors includes retroviruses (including lentiviruses), herpes simplex viruses (HSVs), adenoviruses and adeno-associated viruses (AAVs). Differences within these families with respect to expression of capsid proteins have led to the classification of distinct serotypes *(Wu et al., 2006; Vandenberghe et al., 2009)*. As capsid proteins allow a virus to enter cells through distinct receptors, these serotypes have varying capacities to transduce separate cell populations *(Vandenberghe et al., 2009)*. This cellular tropism is utilised in genetic modification experiments by choosing a virus from a certain family and with an appropriate serotype. In addition to cellular tropism, other factors considered for the purpose of viral gene delivery include genomic nucleic acid type, gene carrying capacity, the capacity to integrate into the host genome and levels of immunogenicity.

1.4.3.1 Retroviral vectors

One of the viral vectors initially used for genetic modification was based on polyoma pseudovirus. This retroviral vector transfected mouse and human embryonic cells in culture *(Qasba and Aposhian, 1971)*. Retroviruses are single-

stranded RNA viruses, which after undergoing conversion into double-stranded DNA can integrate into its host genome *(Yi et al., 2011)*. This integration was initially considered random, however many retroviruses have preference for promoter and enhancer regions *(Yi et al., 2011)*. Retroviruses were used in early clinical trials of viral genetic modificatoin, of which lentiviral vectors have been frequently used for this purpose *(Yi et al., 2011)*. Lentiviruses can optimally carry genes up to 6 - 9 kbp and have the capacity to transduce both mitotic and post-mitotic cells *(Lim et al., 2010)*.

1.4.3.2 Herpes simplex viral vectors

A virus with a higher carrying capacity than most other viruses is HSV, which allow for the integration of up to 150 kb exogenous double-stranded DNA *(Manfredsson and Mandel, 2010; White et al., 2011)*. Harbouring oncolytic capacity, HSV has been used in tumour treatments of organs including the CNS *(Lim et al., 2010)*. The cytotoxicity of this virus has been minimised through the removal of most of its genome, producing replication-deficient amplicon vectors *(Lim et al., 2010)*.

1.4.3.3 Adenoviral vectors

Another family of double-stranded DNA viruses is the adenoviruses. Adenoviral vectors, with capacity of up to 37 kb of double-stranded DNA, can achieve high levels of gene expression in cells of the CNS. Different recombinant subtypes

exist, where genes that are normally transcribed early in the viral infection cycle have been removed *(Lim et al., 2010)*.

1.4.3.4 Adeno-associated viral vectors

Currently, the most commonly used viral vectors are based on AAVs *(Manfredsson and Mandel, 2010)*. Recombinant vectors from these single-stranded DNA viruses can harbour transgenes and/or promoters of up to 6 kb. When used for transduction, the only remaining viral elements of the recombinant virus consist of inverted terminal repeats at each end of the viral genome. These structures are required for appropriate packaging of the viral vector *(Manfredsson and Mandel, 2010)*.

A helper virus, such as adenovirus or HSV, was previously required for the capacity to infect cells. However, advances in the production of AAVs have removed this requirement *(Lim et al., 2010)*. After translocating to the nucleus, the native virus may integrate into a specific location of the host genome, in contrast to the recombinant virus that remains as an extra-chromosomal unit in the nucleus *(Lim et al., 2010)*. AAV serotype 2 (AAV2) constitutes one of the most commonly used AAV vectors *(Lim et al., 2010; Rahim et al., 2011a)* and results in transduction of cells in the nervous system, with a more limited expression in the CNS in comparison to the PNS (Figure 1.4). In addition to their widespread transduction, the use of AAV vectors generally results in lower

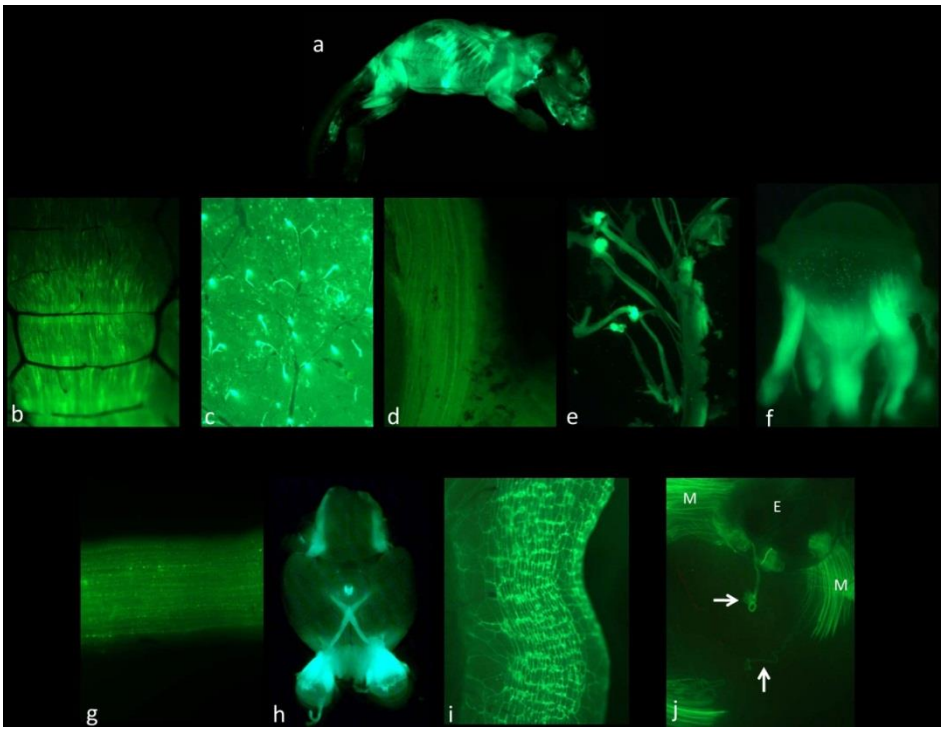

Figure 1.4 Example of viral transduction in the nervous system *one month after AAV serotype 2 / 9 injections* in utero *for foetal mice (a-g) and) intravenously of neonatal mice (h-j). These pictures show GFP expression (green) at the surface of the cerebellum (b) and the cerebrum (c), in the spinal cord (d), and dorsal root ganglia (e), in the eye (f), optic nerve (g) and optic chiasma (h), in the myenteric plexus along the surface of the gut (i) and in nerves (j; arrows) which innervate muscles (M) of the ear (E). Note the widespread transduction of the nervous system achieved using AAV transduction, and the much weaker GFP expression in other parts of the brain than in the cerebellum and optic chiasm (h). Courtesy of Dr Simon Waddington, Gene Transfer Technology Group, Institute for Women's Health, University College London (Rahim et al., 2011a). Copyright permission from FASEB journal was obtained 21 / 12 / 2011.*

immunogenicity than that of adenoviral vectors, broadening the use of AAV vectors in viral gene delivery *(Zaiss et al., 2002)*.

1.4.3.5 Cellular tropism in the CNS

As previously mentioned, virus serotypes have varying capacity to transduce different cell types. For instance, AAV1, AAV5 *(Hutson et al., 2011)* and HSV *(Lim et al., 2010)* exhibit cellular tropism for neurons in the CNS. In addition, oligodendrocytes have been targeted using AAV8 vectors *(Hutson et al., 2011)*.

Furthermore, different cell types of an organism are transduced depending on the age of the animal. For example, mouse embryos transduced using AAV2/9 pseudovectors mainly result in neuronal expression of the reporter gene, as few or no astrocytes are available. In contrast, in the neonatal animal, although both neurons and astrocytes are available for transduction, the majority of transduced cells with this serotype have been identified as protoplasmic astrocytes *(Rahim et al., 2011a)*.

One potential explanation for the observed transduction shift from neurons to astrocytes is the larger proportion of mitotic neurons in the mouse embryo compared to the neonatal animal. Disruption of the nuclear membrane during mitosis allows easier access of DNA to the nucleus (as discussed further in section 1.4.6.3) potentially accounting for the higher transduction in early

embryogenesis. The increased presence of new, immature astrocytes in the neonatal animal would similarly account for the higher transduction capacity of this cell type in the neonate.

Also, there are some viral vectors with the capacity to transduce a range of cell types in the intact CNS. One example is helper-dependent adenoviral vectors, which transfect neurons and glia with equal efficiency *(Manfredsson and Mandel, 2010)*.

1.4.3.6 Drawbacks of viral vectors

In recent years, the use of viral gene delivery has had a high impact on our understanding of cell function in the healthy and diseased CNS. The vast majority of studies have focussed on the neuronal population, which in general is more extensively transduced compared to other cell types. Although viral vectors result in high transduction efficiencies in these cells, the use of these vectors have been impeded by some disadvantages. Genes encoding for viral capsid proteins limit insert sizes into viral vectors *(Zauner et al., 1998; Choi et al., 1999)*. Furthermore, viruses that can integrate into the host genome can potentially cause oncogenicity *(Fox and Littlefield 1971; Suh, Chung et al. 2001)*. One example is that of human deficiency virus, whose origin and potential oncogenicity still raise safety concerns *(Yi et al., 2011)*. On the other hand, the inability to integrate into the host genome can be a limitation as this shortens

the duration of transgene expression, as exemplified by the use of HSV vectors *(Manfredsson and Mandel, 2010)*.

Most importantly, immunological effects complicate the use of viral vectors in the treatment of disease in mammalian models and human trials *(Askjaer et al., 2002; Bhat and Fan, 2002; Fabre and Collins, 2006; Thaci et al., 2011)*. All tested adenoviral vectors have resulted in immunogenicity in human trials even after the removal of essentially the whole viral genome. This immunogenic response is due to the remaining packaging peptides and proteins that are required for appropriate internalisation into target cells *(Manfredsson and Mandel, 2010)*.

Although viruses have been modified to be non-replicating and/or non-disease-inducing, intrinsic protective mechanisms against adenoviruses and other commonly used viral vectors are already initiated at the attachment of viruses to the surface of the cell via integrins and other cell surface receptors *(Bhat and Fan, 2002; Thaci et al., 2011)*. Even after endocytosis of the viral particles, the intracellular pathway of the virus is sensed by toll-like receptors in the endosomal/lysosomal pathway, cytoplasm and nucleus. These stimuli initiate subsequent interferon production and other inflammatory responses that can have detrimental effects upon the host *(Thaci et al., 2011)*.

In numerous clinical trials, viral vectors have induced illness, and even the death of patients. The initial use of retroviral vectors for human trials met a critical turning point when the treatment of the genetic disorder X-linked severe combined immunodeficiency resulted in four cases of T-cell leukaemia, with the death of one of these patients *(Gaspar et al., 2004)*. Another human fatality has been reported due to the use of adenoviral vectors, where acute inflammatory responses caused the death of an 18-year-old patient with ornithine transcarbamylase deficiency *(Raper et al., 2003)*. AAVs are showing most promise for extrapolation to humans due to their lower immunogenicity, but have so far not reached high enough efficiencies for therapeutic use.

1.4.4 Non-viral vector-based genetic modification

Non-viral genetic modification options have been developed alongside the more efficient viral vectors, partially due to the drawbacks of the latter, including limited insert sizes, potential oncogenicity and immunogenicity. One group of non-viral methods are mechanical, including electroporation (see section 1.4.2.1). Another promising group of non-viral methods are vector-based techniques, which provide safer genetic modification as these generally involve less invasive procedures than mechanical methods *(Glover et al., 2005)*. Similarly to viruses, vector-based methods use endogenous mechanisms including endocytosis to enter cells. In many non-viral gene delivery studies, DNA is delivered complexed with substances including liposomes, polycations or dendrimers *(Glover et al., 2005)*.

1.4.4.1 Liposomes

The lipofection technique involves synthetic phospholipid vesicles called liposomes. These bilayer vesicles are formed by hydrophobic groups of the lipid. In an aqueous environment, amine groups of the lipids face the inside of the vesicle, and these amine groups can to bind certain drugs or nucleic acids *(Glover et al., 2005; Kodama et al., 2006)*. For a long time, liposomes have been known to fuse with biological membranes, and were therefore thought to enter cells through fusion with the plasma membrane *(Park et al., 1995; Ziello et al., 2010; Marsden et al., 2011)*. It is now generally accepted that liposome complexes internalise through endocytosis *(Pichon et al., 2010; Pollock et al., 2010)*. Indeed, liposomes have been co-labelled with endosomal/lysosomal markers *(Kodama et al., 2006; Pichon et al., 2010)*.

After internalisation, these liposomes cause fusion of the endosomal membrane, after which they can deliver their contents to the cytosol *(Kodama et al., 2006; Pichon et al., 2010)*. This fusion has been proposed to involve flipping of phospholipids in the endosomal membrane from facing the cytosol to the intraendosomal compartment. The subsequent membrane destabilisation releases the DNA carried by the liposome into the cytosol *(Hoekstra et al., 2007; Douglas, 2008)*. Liposomes have been widely used in culture *(Zhang et al., 2006)* and in explant cultures *(Bauer et al., 2006)*.

1.4.4.2 Polycations

Polycations provide another vector-based non-viral method of genetic modification. Some polycations have been associated with increased endosomal/lysosomal release compared to liposomes. As the name implies, polycations are positively charged molecules. These molecules are able to spontaneously compact negatively charged nucleic acids, including DNA *(Wagner and Kloeckner, 2006)*. This forms a complex with the capacity to escort DNA through a barrier such as the plasma membrane *(Suh et al., 2001)*. Polycations can, similarly to many pathogens, bind to integrin and syndecan (proteoglycan) receptors on the cell surface and subsequently be engulfed into the cell through endocytosis *(Kopatz et al., 2004)*. The size of particles strongly affects this internalisation. Endocytosis is favoured for particle sizes of < 200 nm via clathrin-mediated pathways *(Rejman et al., 2004; Germershaus et al., 2006)*. However, particles < 500 nm in size can be internalised via caveolae *(Rejman et al., 2004)*.

Histones are natural examples of polycations. These are proteins of approximately 20 kilodalton (kDa) with strong DNA-binding properites involved in the chromatin structure of nuclear DNA *(Déas et al., 2002; Fabre and Collins, 2006)*. Natural histones and derivatives of these have been used to deliver nucleic acids to cell lines *(Balicki et al., 2000)* and to cells *in vivo (Déas et al., 2002)*. The positively charged amino acids lysine and arginine constitute 20 - 30 % of the histone structure *(Fabre and Collins, 2006)*. Synthetic polycations have been based on this feature, producing agents such as poly-L-

lysine; PLL *(Chiou et al., 1994; Suh et al., 2001; Barati et al., 2006)* and polyethylenimine; PEI *(Boussif et al., 1995; Boeckle et al., 2004; Xiong et al., 2007)*.

PLL was one of the initially used synthetic polycations for genetic modification *(Wagner and Kloeckner, 2006)*. This polycation contains a long chain of positively charged lysine residues and can electrostatically bind and protect DNA from the external environment at physiological pH *(Barati et al., 2006; Wagner and Kloeckner, 2006; Hsu and Uludag, 2008)*. PLL-DNA complexes possess high surface positive charge (called zeta potential) and may therefore interact with negatively charged cell surfaces, at which they can be internalised via endocytosis *(Wagner and Kloeckner, 2006; Choi et al., 2007)*. This polycation has been successfully used *in vivo* to deliver DNA to organs such as liver *(Perales et al., 1994)* and lung *(Ziady et al., 1999)*. The most limiting step in the use of this polycation is its restricted escape from the endosomal/lysosomal pathway *(Wagner and Kloeckner, 2006)*.

Another polycation which has received a lot of attention is PEI. In some studies, this has been more successful than PLL in transfecting both cells in culture and in the intact animal *(Boussif et al., 1995; Xiong et al., 2007; Deng et al., 2011)*. This group of polycations can be found in numerous shapes and sizes and accommodates the transfection of various cell types. PEI consists of ethylenimine residue chains and can enter cells through non-specific endocytosis

after adhesion to syndecans and other transmembrane heparin proteoglycans *(Kopatz et al., 2004)*.

Each polycation is characterised by a specific acid dissocation constant (pK_a). In an environment with a pH more basic than their pK_a value, the acid-base groups of these polycations are uncharged. With a lower pK_a than other polycations, PEI has a stronger buffering capacity at physiological pH. This characteristic enables PEI to escape the endosomal/lysosomal pathway through exerting a powerful proton sponge effect, which is more thoroughly described in section 1.4.6.1 *(Sonawane et al., 2003; Harada et al., 2006)*. The widely used PEI with a high molecular weight of 25 kDa has a superior transfection efficiency over lower molecular weight PEI *(Xiong et al., 2007)*. Branching may also affect the pK_a of the PEI, and can therefore affect its transfection capacity. Linear PEIs contain only primary amines, and branched forms of PEI contain primary, secondary and tertiary amines *(Breunig et al., 2008)*. Higher transfection efficiencies have been demonstrated using both increased linearity *(Feng et al., 2008)* and increased branching of PEI *(Breunig et al., 2008)* in separate studies.

1.4.4.3 Dendrimers

Dendrimers constitute a more recently developed vector-based non-viral vector for genetic modification *(Posadas et al., 2010)*. These complexes are globular, and consist of a branched network organised in several layers called generations, extending from a central core *(Tsai and Imae, 2011)*. The branches consist of

multiple repeat units with more than one junction. At the outermost ends of these branches, terminal functional groups enable DNA or drug compaction *(Posadas et al., 2010; Tsai and Imae, 2011)*. Presumably through endocytosis, dendrimers enter cells *(Kodama et al., 2006; Posadas et al., 2010)*, where they have been shown to have high capacity to escape endosomes/lysosomes. This escape is possible due to the buffering capacity of amines situated deeper in the dendrimer structure *(Kodama et al., 2006)*.

The use of polyamidoamine dendrimers with the addition of arginine has resulted in up to 40 % transfection of cultured primary neurons *(Kim et al., 2006)*. This high transfection capacity in primary cultures is enhanced by the intricate structure of dendrimers that enables the passing of cellular barriers. However, even low concentrations of these molecules result in cytotoxicity, which complicates their use in the intact animal. This has been demonstrated in erythrocytes *in vivo (Juliano, 2006; Posadas et al., 2010)*. Furthermore, one study has shown that dendrimers with strong capacity to transfect neurons in culture unfortunately results in low efficiencies *in vivo* with respect to the delivery of small interfering RNAs (siRNAs; *Posadas et al., 2010)*.

1.4.5 Cell specificity

Early trials of genetically modifying a single cell population required cell isolation, *in vitro* modification and replacement of these cells *in vivo,* similarly to

transplantations conducted in more recent times *(Selkirk et al., 2002)*. The tedious and invasive nature of this method has motivated the development of a system with the capacity to modify protein expression in only one cell type or a subpopulation of cells in an intact animal. Viral and non-viral vectors are generally non-targeted and can be used to transfect many cell types and populations. One exception is the demonstrated cellular tropism exhibited by specific viral serotypes.

Another approach to confine gene expression to a certain cell type is the use of cell-specific promoters. Transduction efficiencies in early viral gene delivery trials were improved by exchanging the commonly used CMV promoter for mammalian promoters only activated in a single cell type *(Klein et al., 1998; Bockstael et al., 2008)*.

Highly active cell-specific promoters not only offer cell specificity, but may also result in higher and prolonged transfection efficiencies *(Klein et al., 1998; Paterna et al., 2000)*. For example, astrocytes and microglia have previously been targeted successfully using enhanced versions of the GFAP promoter *(Brenner et al., 1994; Bradford et al., 2009; Xu et al., 2010)* and a promoter for the macrophage protein F4/80 *(Cucchiarini et al., 2003)*, respectively. In addition, the neuron-specific enolase promoter has conveyed neuronal expression of the reporter gene up to 3 months after transfection, compared to the CMV

promoter driven vector which usually maintains gene expression up to 3 weeks *(Klein et al., 1998)*.

The shorter expression period using CMV promoters is most likely caused by intrinsic mechanisms of the host cell involving excessive methylation of the delivered nucleic acid *(Klein et al., 1998; Rahim et al., 2011a)*. Furthermore, lower levels of transcription factors such as nuclear factor kappa-light-chain-enhancer of activated B cells (NFκβ) have been shown to affect silencing of exogenous promoters such as the CMV promoter *(Paterna et al., 2000)*. As NFκβ is expressed at lower levels in some cell types, this may cause lower transfection efficiencies when using a CMV promoter in a non-viral vector. Stimulation of NFκβ expression in these cells through exposure to LPS or other viral agents has resulted in increased expression levels. Therefore, it has been postulated that the presence of this transcription factor is crucial for sustained expression of a reporter gene under the influence of the CMV promoter *(Löser et al., 1998)*.

Using cell-specific promoters does not influence the initial delivery of the nucleic acid sequence into target cells. A more efficient way of limiting gene expression to one specific cell population is to control the delivery of the genetic modification vector. Cell-specific delivery will increase the amount of vector available for the cell type of interest *(Kircheis et al., 1997)*. This specificity also

reduces unfavourable effects in non-target cell types and tissues *(Ogris et al., 1999; Zeng et al., 2007)*.

Therefore, another possible approach for cell-specific delivery is to use a cell surface molecule - a receptor - to facilitate endocytosis of the vector. This receptor-mediated endocytosis can be achieved by binding one of the ligands of the receptor to a DNA carrier *(Fabre and Collins 2006)*. By choosing a ligand targeted against the extracellular domain of a receptor that is only expressed by one specific cell population, receptor-mediated gene delivery becomes specific to these cells. To be effective, internalisation of the ligand and bound nucleic acids must be achieved together with the receptor after ligand binding. Also, the target receptor should as far as possible be chosen to produce little if any modification of cell properties upon ligand binding *(Barati et al., 2006)*.

Ligands used for this purpose include viral proteins *(Kumar et al., 2007)*, growth factors *(Zeng et al., 2007)*, carbohydrates (Choi et al., 1999), and antibodies *(Berhanu and Rush, 2008)*. The range of potential ligands allows for targeting of any cell type *(Wagner and Kloeckner, 2006)*. Also, this approach has the capacity to deliver not only nucleic acids but many different types of molecules, including toxins and therapeutic drugs.

Earlier studies using receptor-mediated delivery focused particularly on delivering toxins to tumour cells as an avenue to treat cancer *(Thorpe et al., 1987; Shimizu et al., 1996; Omelyanenko et al., 2003; Germershaus et al., 2006; Yip et al., 2007)*. Transferrin constitutes one example ligand used for this purpose. This protein transports iron via receptor-mediated delivery into a range of cell types which require iron for cellular metabolism *(Schmidt et al., 1986; Zhang et al., 2004)*. The transferrin receptor is also expressed at higher levels in proliferative cells and has therefore been widely used as a target in anti-cancer treatments *(Kircheis et al., 2001)*.

1.4.6 Intracellular pathway of vector-based methods

1.4.6.1 Release from the endosomal/lysosomal pathway

After delivery to its target cell through endocytosis, the gene delivery complex enters the endosomal/lysosomal/cavoesomal pathway *(Mellman, 1996)*. It has been postulated that a portion of caveolae-dependent endocytosed particles is delivered to the endoplasmic reticulum and the Golgi apparatus *(Nichols, 2003; Laude and Prior, 2004)*. The extent of which internalised cargo merges with the endosomal/lysosomal pathway has not been fully determined.

Some chemical bonds are degraded inside cells and are therefore advantageous in the structures of biodegradable delivery vectors *(Saito et al., 2003; Zhang and*

Vinogradov, 2010). One of these bonds is the disulphide bond, which is therefore commonly used to bind a ligand to a drug or DNA carrier. This bond is stable in the extracellular environment, however is degraded in the reducing environment of the intracellular space, resulting in the release of the drug or DNA-carrying moiety from the ligand *(Gosselin et al., 2002; Saito et al., 2003; Schaffert and Wagner, 2008)*. This technology has previously been used in cancer drugs such as Mylotarg, which contained an antibody bound to a cytotoxic drug via a reversible disulphide bond *(Saito et al., 2003)*.

With regards to genetic modification, release of the DNA-carrier from intracellular vesicles and delivery to the cytosol *(Mellman, 1996)* is necessary for the DNA to reach its final destination; the nucleus *(Young et al., 2003)*. The most prominent disadvantage in constructs incorporating PLL is the low capacity of these vectors to escape such vesicles *(Curiel et al., 1991)*. With further decreasing pH, late endosomes mature and fuse into lysosomes, where remaining endocytosed particles are subject to degradation *(Ziello et al., 2010)*. Therefore, further modifications are needed to increase endosomal/lysosomal release of DNA from these vesicles to result in transfection *(Ogris et al., 1998; Zauner et al., 1998; Ziello et al., 2010)*.

Release from endosomal/lysosomal pathways has been induced in culture by using thermal sensitive cationic polymer nanocapsules as a transfection agent

(Lee et al., 2008). By lowering the temperature from normal physiological temperatures (37˚C) after transfection, the natural swelling of these nanocapsules (up to four times the original volume) induces disruption of the endosomal/lysosomal membrane *(Lee et al., 2008)*. This method is however not applicable *in vivo* as temperatures down to 15°C may be required for successful delivery.

Another approach to endosomal/lysosomal release is through chemical induction via the addition of lysosomotropic agents *(Zauner et al., 1998; Barati et al., 2002; Blanchard et al., 2006)*. One example is chloroquine, a weak base that accumulates in acidic vesicles and increases their internal pH *(Zauner et al., 1998).* This increased pH inhibits hydrolytic enzymes with the capacity to degrade nucleic acids *(Luthman and Magnusson, 1983; Zauner et al., 1998)*. The accumulation of chloroquine causes swelling and destabilisation of the vesicle, enabling the release of its contents into the cytosol. Thus, lysosomotropic agents are capable of increasing gene delivery and expression where endosomal/lysosomal release is a limiting step *(Luthman and Magnusson, 1983; Zauner et al., 1998).*

The polycation PEI triggers a similar method of release from acidic compartments, for which different mechanisms have been postulated. One potential mechanism is via a postulated proton sponge potential *(Ogris et al.,*

1998; Wagner, 2004). Upon acidification, polycations such as PEI are protonated by the surplus hydrogen ions; H^+ *(Boussif et al., 1995; Cho et al., 2003; Sonawane et al., 2003; Fabre and Collins, 2006)*. In the gradually acidic endosome/lysosome compartments, this proton buffering causes further influx of hydrogen and accompanying chloride ions (Cl^-). As the H^+ ions are continuously absorbed by polycations in this buffering range, the subsequent accumulation of Cl^- triggers osmotic swelling, and leads to the rupture of and eventual release from the acidic compartment *(Ogris et al., 1998; Sonawane et al., 2003; Wagner, 2004; Fabre and Collins, 2006)*. In contrast to PLL with a pK_a of 10.5 *(Yu et al., 2007)*, PEIs possess a stronger buffering capacity with their lower pK_a values, ranging from 7 - 9, depending on linearity/branching *(Deng et al., 2011)*. However, at physiological pH, where a proportion of the amines on PEI are not ionised, the lower pK_a of this polycation causes a less positive charge, and thereby results in a decreased DNA-binding capacity in comparison to PLL *(Harada et al., 2006)*.

Other hypotheses than the proton sponge theory have been proposed regarding the release of PEI complexes from the endosomal/lysosomal pathway. A study using several cell lines indicated that PEI complexes may be trapped inside vesicles until these reach sufficiently low acidic pH *(Forrest and Pack, 2002)*. It was also suggested that the release of PEI in acidic lysosomes rather than in early endosomes provided a better location for these molecules to reach the nucleus and cause transgene expression.

Destabilisation of intracellular membranes may also be enhanced through the addition of membrane-lytic peptides in the gene delivery construct *(Howard, 2009)*. As mentioned previously (section 1.4.3), many viruses have developed a capacity to escape these intracellular vesicles by expressing certain peptides and proteins. The envelope glycoprotein peptide gp41 of human immunodeficiency virus HIV consists of α-helical structures with the capacity to form pores in membranes and thereby increase endosomal/lysosomal release of viral elements *(Kwon et al., 2008b; Howard, 2009)*. Another established peptide for gene delivery to the cytosol is the hemagglutinin 2 (HA2) peptide derived from the amino-terminal region of influenza virus *(Skehel and Waterfield, 1975)*. This peptide has the capacity to form similar pores in endosomes/lysosomes, which causes solubilisation of the endosomal/lysosomal membrane and results in leakage of up to 90 % of vesicle contents into the cytosol *(Wharton et al., 1988)*. Transfection efficiencies have been increased using additions of peptides with this characteristic, particularly for PLL-based vectors *(Plank et al., 1992; Midoux et al., 1993; Navarro-Quiroga et al., 2002)*.

1.4.6.2 Cytoplasmic trafficking

After release into the cytosol, DNA is required to reach the nucleus and enter the transcriptional machinery of the host. This remains one of the most limiting steps in non-viral genetic modification where the delivered nucleic acid is DNA *(Zabner et al., 1995; Askjaer et al., 2002)*. The limitations of cytoplasmic trafficking are evident when looking at transfection efficiencies after direct

injections of DNA into different intracellular compartments. Injections of plasmid DNA into the nucleus of different cell lines results in the transfection of 50 % of these cells. In contrast, equivalent injections into the cytosol rarely lead to transfection of more than 0.01 % of cells *(Zabner et al., 1995)*. One way to avoid the limiting step of nuclear translocation would be to deliver RNA, which would not require nuclear translocation. However, as mentioned previously, DNA-based vectors may be more beneficial for an application that requires expression which is longer than a few hours.

For vector-based gene delivery, there is contradictory evidence whether or not DNA remains bound to its DNA carrier after endosomal/lysosomal release *(Rogers and Rush, 2012)*. Polycations and other nanoparticles have been hypothesized to release their DNA cargo into the cytosol *(Bieber et al., 2002; Feng et al., 2006)*. In contrast, high-molecular weight polycations, including 25 kDa PEI *(Farrell et al., 2007)* and 800 kDa PEI *(Bieber et al., 2002)*, have been detected inside the nucleus. This finding could however be a manifestation of a dying cell, where the PEI complex can diffuse passively into the disintegrating nucleus and result in transgene expression in cells before cell death occurs *(Bieber et al., 2002)*.

The release of DNA from its DNA carrier prior to nuclear translocation would require the movement of free DNA in the cytosol to reach the nucleus. It has

been shown that the movement of linear, unbound DNA in the cytosol of cell lines is lower than equivalent movements in water, probably due to molecular crowding *(Lukacs et al., 2000)* by the cytoskeleton and other cytosolic components. As previously mentioned in section 1.4.2, circular plasmid DNA diffuses quicker than linear equivalents in aqueous environments such as the cytosol. However, the cytosolic residence time for any DNA structure can be long and DNA may diffuse slowly around the cytosol for hours before reaching the nucleus. This puts the DNA at high risk of degradation. In general, any DNA injected directly into the cytosol is completely degraded within 24 h *(Pollard et al., 2001)*.

Peptides have been added to DNA in order to increase their mobility in the cytosol *(Kwon et al., 2008a)* and thereby reduce cytosolic residence time. Some of these modifications have been based on viral peptides that take advantage of the dynein transport system within the cell. For example, adenoviruses produce peptides that by binding to dynein allow them to be transported towards the nucleus of the cell *(Bergen and Pun, 2007)*. By incorporating a peptide able to bind dynein, DNA would potentially be more efficiently transported to the nucleus.

1.4.6.3 Nuclear translocation

DNA reaches the nuclear envelope as a separate molecule, protected by a DNA carrier and/or guided through the cytosol towards the nucleus using viral-derived peptides. At this point, the DNA is required to enter the nucleus under highly restricted conditions through the nuclear membrane. Nuclear translocation is more straight-forward during mitosis *(Dean et al., 1999; Askjaer et al., 2002; Zhang and Vinogradov, 2010)*. In a dividing cell, temporary disintegration of its nuclear membrane allows for DNA to passively diffuse into the nucleus *(Dean et al., 1999; Askjaer et al., 2002)*. However, the majority of cells in the adult CNS are postmitotic and non-proliferating, in contrast to most cells in cell lines or cells originating from the neonatal brain *(Zanta et al., 1999)*. DNA translocation to the nucleus is therefore less frequent in the adult animal and enhancing this process would be especially beneficial for *in vivo* genetic modification.

Molecular trafficking between the cytoplasm and nucleus in the post-mitotic state occurs through nuclear pore complexes (NPCs) which are scattered over the nuclear envelope *(Franke et al., 1981)*. NPCs were initially linked to osmotic swelling of the nucleus in the 1930s *(Churney, 1942)*. Evidence subsequently emerged implicating NPCs in semi permeable transport into the nucleus in the 1950s *(Harding and Feldherr, 1959)*. It is now known that smaller molecules; < 90 Å ~ 9 nm *(Paine and Feldherr, 1972; Zanta et al., 1999)*, < 40-60 kDa

(Hagstrom et al., 1997)), such as many RNAs and DNA-binding proteins have the capacity to diffuse through the NPCs of a post-mitotic cell.

However, NPCs have been reported as gatekeepers for larger molecules - up to at least 25 nm *(Gerace, 1992; Stewart, 1992)* and 40 nm, as determined in yeast *(Vandenbroucke et al., 2007)*. The size of these pores limits nuclear translocation by macromolecules, including larger DNA sequences. For the majority of these larger macromolecules with a nuclear destination, the NPCs host an active, energy-dependent transport from the cytoplasm to the nucleus *(Zanta et al., 1999; Collins et al., 2007)*. After recognition of nuclear localisation signals (NLSs) on proteins and peptides in the cytoplasm, importins shuttle molecules into the nucleus via NPCs *(Zanta et al., 1999; Talsma et al., 2006)*. Upon binding an NLS, importin α forms a ternary complex with importin β, ready for transport into the nucleus *(Hagstrom et al., 1997; Zanta et al., 1999)*. Importin β enables docking of this complex to a nuclear pore. Cargo delivery is thereafter finalised in the nucleus through release from the importin complex by Ras-related nuclear protein guanosine tri phosphatase *(Hagstrom et al., 1997)*.

The NLS transport mechanism is used by many DNA viruses to assemble into mature viral particles inside the nucleus *(Ishii et al., 1996; Groppo et al., 2011)*. Enhancement of nuclear import using these NLS signals has therefore been utilised in genetic modification *(Sebestyen et al., 1998; Chan and Jans, 2001;*

Groppo et al., 2011). The first established synthetic NLS was derived from simian virus 40 (SV40) large T antigen; a peptide consisting of mostly basic amino acids *(Kalderon et al., 1984)*. This SV40 large T antigen NLS *(Eguchi et al., 2005)*, together with the NLS of the Vp1 structural protein from the same virus *(Ishii et al., 1996; Navarro-Quiroga et al., 2002)* and other sequences with similar motifs *(Collins et al., 2007)* have been widely used to enhance nuclear translocation in applications of genetic modification. The basic property, and thereby cationic property, of NLS peptides enables some DNA compaction, but not enough for them to protect and deliver DNA *per se* through barriers such as the plasma membrane *(Collins et al., 2007)*.

Addition of NLS signals has not only increased the expression of the gene of interest, but has also increased the rate of this expression. For example, genetic modification using a linear DNA fragment capped with an NLS peptide has resulted in maximum expression after 12 h, compared to 24 h without the NLS peptide, further identifying nuclear translocation as a limiting step *(Zanta et al., 1999)*. The amount of NLS added to DNA for successful genetic modification needs to be addressed. Insufficient amounts of NLS peptides would lead to an inadequate signal for nuclear translocation. On the other hand, higher NLS concentrations have been suggested to impair nuclear transport *(Sebestyen et al., 1998)*.

1.5 Requirements for non-viral vector-based receptor-mediated genetic modification

In summary, to successfully achieve genetic modification in eukaryotic cells using vector-based receptor-mediated genetic modification, the DNA sequence of interest is required to pass the plasma membrane, escape potentially acidic vesicles, enter the cytosol and reach the nucleus *(Zauner et al., 1998)*.

Therefore, successful transient genetic modification vectors are required to:

- ✓ have capacity to hold the nucleic acid sequence of interest
- ✓ neutralise the negative charge of the nucleic acid sequence and condense this to a size capable of entering cells
- ✓ bind to a receptor on the outside of a cell (for cell specificity) and/or be internalised inside the cell through endocytosis with few, or preferably no downstream effects
- ✓ escape the endosomal/lysosomal/caveosomal pathway and enter the cytosol
- ✓ have mobility within the cytosol
- ✓ ensure delivery of nucleic acid sequence to the nucleus (for DNA)

In addition, for *in vivo* purposes, the genetic modification vector is required to:

- ✓ be of a size capable of diffusing in the extracellular space
- ✓ withstand the environment of blood (if injected intravenously) and/or other bodily fluids
- ✓ avoid immunological responses or toxicity
- ✓ be biodegradable

(Zauner et al., 1998; Wagner and Kloeckner, 2006)

1.6 Genetic modification of microglia

1.6.1 Bone marrow transplants for the study of microglial function

Compared to other cell types, there are a limited number of studies using genetic modification to specifically investigate the function of microglia *(Balcaitis et al., 2005)*. One method indirectly using microglia for therapeutic use is that of healthy exogenous bone marrow transplants into a diseased host. For example, this method has been used to inhibit disease progression and prolong survival in an ALS model. The majority of bone marrow-derived cells found in the CNS of these studies co-labelled with microglial marker Iba1 and were either ramified or amoeboid. This observation has led to the study of microglial therapeutic function through the use of bone marrow-derived cells in brain injury and disease *(Ohnishi et al., 2009)*.

Genetic modification of these progenitor cells prior to bone marrow transplantation has been used to study microglial function. For example, cytokine receptor gene knockouts have been used to study the function of microglia deficient in these receptors *(Guo et al., 2004)*. In addition, therapeutic proteins have been over-expressed in stem cell-derived microglia to recover normal levels of these proteins in diseased animal models *(Biffi et al., 2004)*.

1.6.2 Gene knockout studies on microglial function

Microglia have also been genetically manipulated in the intact animal. Gene knockout models have been produced to study microglial function in the absence of key proteins *(Das et al., 2003; Lambertsen et al., 2009)*. Microglial function has been studied using gene knockouts of specific receptors such as CCR5 *(Gamo et al., 2008)*, CX3CR1 receptor *(Cardona et al., 2006),* type 1 interferon α/β receptor *(Prinz et al., 2008)*, Fc-γ receptor *(Das et al., 2003)* TNF receptors *(Quintana et al., 2005; Lambertsen et al., 2009)*, purinergic receptor $P2Y_{12}R$ *(Haynes et al., 2006; Tozaki-Saitoh et al., 2008)* and TNF-α protein *(Syed et al., 2007)*.

In these gene knockouts, microglia have been studied with respect to interleukin levels *(Quintana et al., 2005; Prinz et al., 2008)*, regulation of receptors involved in the recruitment of immune system cells *(Syed et al., 2007)*, gliosis *(Quintana et al., 2005)*, process movement and migration *(Haynes et al., 2006; Tozaki-*

Saitoh et al., 2008), neuropathic pain *(Tozaki-Saitoh et al., 2008)* amyloid-β phagocytosis *(Das et al., 2003)*, neuronal degeneration *(Cardona et al., 2006; Gamo et al., 2008; Prinz et al., 2008)* and neuroprotection *(Lambertsen et al., 2009)*. These factors have been studied in models such as nerve-injured hypoglossal nuclei *(Gamo et al., 2008)*, cortical cryolesions *(Quintana et al., 2005)*, excess ATP stimuli *(Haynes et al., 2006)* and experimental allergic encephalomyelitis *(Prinz et al., 2008)*. Microglial knock-out studies have provided clues on neuropathologies including viral infections *(Syed et al., 2007)*, Parkinson's disease *(Cardona et al., 2006)*, AD *(Das et al., 2003)*, ALS *(Cardona et al., 2006)*, autoimmune disease *(Prinz et al., 2008)*, cerebral ischemia *(Lambertsen et al., 2009)* and tactile allodynia *(Tozaki-Saitoh et al., 2008)*.

1.6.3 Viral genetic modification of microglia

Viral transduction of microglia and related cells has also been used to study cellular function, however with limited success *(Balcaitis et al., 2005)*. The few studies on viral transduction of microglia have partially been hindered due to the low amount of integrins on the surface of these cells. Low levels of integrins inhibit attachment and entry of viruses, as has been shown for adenoviruses *(Huang et al., 1995)*. Lentiviruses have resulted in higher transduction efficiencies; up to 50 % in primary microglia *(Balcaitis et al., 2005)*. In addition, a more glia-targeted transduction profile has been observed *in vivo* using HSV 1. Infusions of this virus resulted in transduction of glial cells in the corpus callosum, out of which between 25 and 40 % were identified as microglia with an

activated phenotype *(White et al., 2011)*. To date, no virus serotype has been identified that selectively transduces the microglial population.

The first successful selective genetic modification of microglia in culture and *in vivo* was reported by Cucchiarini et al. (2003). Up to 25 % of rat primary microglial cultures were transduced using an AAV5 vector. Furthermore, *in vivo* expression using this vector was cell-specific using microglia-related promoters. The promoter derived from the macrophage-specific protein F4/80 was superior to CD68 and CD11b promoters in achieving microglial expression of the reporter gene *(Cucchiarini et al., 2003)*. Striatal injection of this F4/80 vector resulted in reporter gene expression by ramified microglial cells up to 3 weeks after injection. Pre-activation of the microglia with IFNγ did not alter observed transduction efficiencies *(Cucchiarini et al., 2003)*.

A common feature of viral transduction is the increased expression of pro-inflammatory mediators such as cytokines in microglial cultures *(Bhat and Fan, 2002)* and *in vivo (Polazzi and Monti, 2010)*. Although Cucchiarini et al. (2003), Rahim et al. (2011) and others using viral vectors in the CNS report the absence of any significant inflammatory effects, a majority of trials with any target tissue in human patients have resulted in detrimental effects in patients due to immunogenicity. Pharmacological treatments have only partially attenuated

inflammatory responses by microglia and potentially infiltrating cells after viral transduction in the CNS *(Polazzi and Monti, 2010)*.

1.6.4 Non-viral genetic modification of microglia

As for viral vectors, there are few reports using non-viral approaches to genetically modify microglial function. Primary microglia have been nucleofected with efficiencies of up to a maximum of 10 % *(Aravalli et al., 2008)*. The low number of additional studies using nucleofection to investigate microglial function does not report specific transfection efficiencies. However, key proteins such as interleukins *(Aravalli et al., 2008)* and chemokine receptors *(Li et al., 2006)* have been over-expressed using this technique in culture and have produced functional changes. In addition to the application of electroporation, vector-based liposomes have been used to transfect microglia, with transfection efficiencies rarely exceeding more than 20 % in microglial cell lines and in primary glial cultures *(Wiesenhofer and Humpel, 2000; Jana et al., 2001; Mitrasinovic et al., 2001)*. To our knowledge, non-viral genetic modification of microglia has not been been utilised *in vivo*. Hence, more advanced gene therapy is required to provide a better approach for the purpose of microglial genetic modification *(Polazzi and Monti, 2010; Kofler and Wiley, 2011)*.

1.7 Hypothesis and aims

Genetic modification of a specific cell population is a highly valuable tool in order to study cell function in the healthy and diseased brain. The only approach reported so far which can selectively target microglia in the brain uses AAV vectors and a microglia-specific promoter. This technique has not been widely adopted in subsequent investigations. A potential alternative approach was suggested by the successful targeting of neuronal subpopulations in the brain in studies by the research group of Professor Robert Rush which used the combination of an antibody targeting unit with that of a polycation carrying nucleic acids. This immunoporter had the capacity to deliver nucleic acids to neurons specifically *(Berhanu and Rush, 2008)*. These investigations opened up the possibility of using a similar approach to target microglia in the CNS. We investigated the following hypothesis and specific aims.

Hypothesis: Expression of specific proteins can be selectively modified in microglia using plasmid DNA linked to an antibody directed against a cell surface receptor.

As further described in Chapter 3, scavenger receptor, class B, type I (SR-BI) was initially considered as a potential candidate for delivery of DNA bound to an immunoporter to astrocytes in the brain, based on studies in adult mice *(Husemann and Silverstein, 2001)* and the known properties of this receptor (see

section 3.1.2.1). After further investigations, the antibody was shown to target microglia in primary glial culture and in the adult rat brain.

Aim 1a) To evaluate the distribution of SR-BI in glial cells in culture and in rat brain (see Chapter 3)

Aim 1b) To test whether an antibody directed against the extracellular domain of this receptor is internalised by cells expressing SR-BI (see Chapter 3)

Based on these initial investigations, the following aims were subsequently pursued:

Aim 2) To generate immunoporters consisting of polycations covalently linked to an antibody against SR-BI (see Chapter 4)

Aim 3) To test whether immunogenes comprising plasmid DNA bound to SR-BI-based immunoporters, can transfect microglia and/or astrocytes in culture and in the brain (see Chapter 4 and 5)

Aim 4) To test whether transfection by the SR-BI-based immunogene can be improved through modifications aimed at promoting endosomal release and/or nuclear targeting (see Chapter 5)

CHAPTER 2: GENERAL MATERIALS

2.1 Materials

Table 2.1 through 2.3 provide summaries of project-specific equipment (Table 2.1), chemicals and reagents (Table 2.2), and the supply companies for these materials (Table 2.3).

2.2 Animals

In this work, neonatal Sprague Dawley rat pups (P_1 - P_3) were used for preparation of primary glial cultures. Adult Sprague Dawley rats (250 - 350 g) were used for injections and infusions of antibodies and transfection constructs. All rats were purchased from the University of Adelaide Animal Facility or were bred in-house from the same stock in the Flinders University School of Medicine Animal Facility. Animal experimentation was approved by the Flinders University Animal Welfare Committee (Approval number 686/08).

2.3 Antibodies

Primary antibodies used in this work (see more information in Table 2.4) included microglial markers mouse anti-CD11b/c (1 : 100 in culture; 1 : 200 *in vivo*; Invitrogen Co.), rabbit anti-CD11b (1 : 200; Novus Biologicals LLC), isolectin $B4^{647}$ fluorophore conjugate (1 : 200; Invitrogen Co.) and the marker for activated microglia mouse anti-CD68 (1 : 100; AbD Serotec). The astrocytic markers used were mouse anti-GFAP (1 : 250; Sigma-Aldrich Co.) and rabbit anti-GFAP (1 : 250; Sigma-Aldrich Co.). Other markers included the stem cell marker mouse anti-A2B5 (1 : 1000; Abcam), the neuronal marker mouse anti-neuronal

nuclei (NeuN; 1 : 500; Millipore) and the glial progenitor mouse anti-nerve glial antigen 2 (NG2) marker (1 : 200; Millipore). GFP immunoreactivity was detected using a rabbit anti-Aequorea Victoria GFP antibody (1 : 250; anti-GFP; Invitrogen Co.) in culture and *in vivo*.

These primary antibodies were detected using anti-mouse/rabbit secondary antibodies excited at 488 nm (Alexa Fluor^{TM} 488 *highly crossadsorbed*; Alexa Fluor^{488}; Invitrogen Co.) and/or 647 nm (Alexa Fluor^{TM} 647 *highly crossadsorbed*; Alexa Fluor^{647}; Invitrogen Co.). Nuclei were labelled with Hoechst 33258 (Invitrogen Co.). Cultured cells and brain tissue only exposed to secondary antibodies were included as controls to rule out non-specific binding.

Table 2.1 Materials and equipment

Description	**Company**
6-well cell culture plate	Greiner Bio-one International AG
24-well cell culture plate	Greiner Bio-one International AG
29 gauge dental needles - Kendall Monoject *(for intracerebral injections)*	Tyco Healthcare (UK), Ltd.
96-well cell culture microplate *(polystyrene)*	Greiner Bio-one International AG
Alzet brain infusion kit 2	Durect Co.
Alzet 1004 osmotic pump	Durect Co.
BX50 Fluorescence microscope	Olympus Co.
Cell culture flasks (T25, T75, T175)	Greiner Bio-one International AG
Confocal microscope (TCS SP5)	Leica Microsystems GmbH
Coverslips (22 x 40 mm; for brain sections)	Gerhard Menzel Glasbearbeitungswerk GmbH & Co. KG
Coverslips (circular, 12 mm radius; for 24-well culture plates)	Gerhard Menzel Glasbearbeitungswerk GmbH & Co. KG
Cryostat (CM180)	Leica Microsystems GmbH
Cryostat blades (Sec35, low profile)	Microm

Table 2.1 Materials and equipment, continued

Description	Company
Digital multi-channel pipette 10 - 200 µl	Labnet International, Inc.
Freezone 6 Freezedry system	Labconco Co.
GeneGenius Gel Imaging System and Software	Synoptics Ltd.
Glass microscope slides (ground edges 90˚ frosted end)	Gerhard Menzel Glasbearbeitungswerk GmbH & Co. KG
Glass syringe (for pump injection)	Hamilton Company
Haemocytometer (Improved Neubauer Bright-line Double Ruling Counting chamber)	Brand GmbH + CO KG
Hi-trap SP HP cation exchange column	GE Healthcare
Inoculation loops	Copan Diagnostics, Inc.
IX71 (for cultures without coverslips)	Olympus Co.
Mini horizontal gel system + gel tray + polycarbonate dual-sided comb	GeneWorks Pty. Ltd.
Microbalance C-31	Cahn instruments, Inc.
Microperpex Peristaltic pump 2132 (for Protein G column)	LKB
Microsep™ centrifugal device (1kDa MWCO)	Pall Life Sciences Co.
Microtest plate (96-well, flat- bottom)	Sarstedt AG & Co.
NanoDrop™ 8000 multi-sample micro-volume UV-Vis Spectrophotometer	Thermo Fischer Scientific, Ltd.
Nucleofector II	Lonza Group, Ltd.
NuPAGE® Novex 4 - 12% Bis-Tris Gel	Invitrogen Co.
Orbital shaker	Edwards Instruments Co.
PD10 desalting columns	GE Healthcare
pH test strips, pH 0 - 14 and 4.5 - 10.0	Sigma-Aldrich Co.
Polypropylene column *(for Protein G separation)*	Bio-rad Laboratories, Inc.
sp200i syringe pump	World Precision Instruments
Spreader bar	Techno Plas, Pty. Ltd.
Stereotaxic frame	David Kopf Instruments
Steritop-GV filter unit (500 ml, 0.22 µm)	Millipore
UV-3000 Spectrophotometer (Dual wave length / double beam recording spectrophotometer)	Shimadzu Co.
Victor X4 2030 multilabel plate reader	PerkinElmer, Inc.
Vivaspin® concentrators (4ml) 5kDa MWCO and 100 kDa MWCO	Sartorius Stedim Biotech S.A.
Water bath	Ratek Instruments, Pty. Ltd.
XCell SureLock® Mini-Cell and XCell II™ Blot Module Kit CE Markgel system	Invitrogen Co.

Table 2.2 Chemicals and reagents

Description	Company
2-iminothiolane hydrochloride (Traut's reagent)	Pierce Biotechnology Inc.
Acetic acid	Sigma-Aldrich Co.
Agarose	Sigma-Aldrich Co.
Albumin from bovine serum, fatty acid-free (BSA)	Sigma-Aldrich Co.
Blue loading dye	New England Biolabs, Inc.
Boric acid	Sigma-Aldrich Co.
Bovine gamma globulin	Sigma-Aldrich Co.
Brilliant blue (R 250)	Sigma-Aldrich Co.
Bromophenol blue	Sigma-Aldrich Co.
Calcein-acetoxymethyl (Calcein-AM; *1 mg⁄mL solution in anhydrous DMSO*)	Invitrogen Co.
Calcium chloride	Ajax Finechem, Pty. Ltd.
DC Protein Assay reagents	Bio-rad Laboratories, Inc.
Dimethylsulfoxide (DMSO)	ACE Chemical Company
DL-dithiothreitol (DTT)	Sigma-Aldrich Co.
Dulbecco's modified Eagle's medium - low glucose (DMEM)	Sigma-Aldrich Co.
Eosin B	Sigma-Aldrich Co.
Ethidium bromide	Sigma-Aldrich Co.
Ethylenediaminetetraacetic acid (EDTA)	Sigma-Aldrich Co.
Foetal bovine serum (FBS)	Invitrogen Co.
Glycerol	Sigma-Aldrich Co.
Glycine	Sigma-Aldrich Co.
gWizGFP *(plasmid DNA)*	Aldevron
Hemagglutinin 2 (HA2) peptide *(custom-ordered)*	Auspep, Pty. Ltd.
HEPES *(powder)*	Sigma-Aldrich Co.
HEPES *(solution)*	Invitrogen Co.
Hoechst 33258	Invitrogen Co.
Hypoxanthine thymidine supplement (HT supplement)	Invitrogen Co.
Isopentane	Chem-Supply, Pty. Ltd.
Jet acrylic powder (cross-linked, self curing)	Lang dental Manufacturing Company, Inc.
Kanamycin (disulfate salt from *Streptomyces kanamyceticus*)	Sigma-Aldrich Co.
L-cysteine	Sigma-Aldrich Co.
LB broth (powder)	Sigma-Aldrich Co.
Lethabarb	Virbac Animal Health
Lipopolysaccharide (LPS)	Sigma-Aldrich Co.
Magnesium chloride	Sigma-Aldrich Co.
Magnesium sulphate	Ajax Finechem, Pty. Ltd.

Table 2.2 Chemicals and reagents, continued

Description	Company
Marcain local anaesthesia (Bupivacaine injection BP, PolyAmp DuoFit ampoules, sterile AstraZeneca Theatre Pack, sterile, isotonic anaesthesia for injection)	AstraZeneca AB
Methanol	Sigma-Aldrich Co.
Monopotassium phosphate	Ajax Finechem, Pty. Ltd.
Mouse IgG	Sigma-Aldrich Co.
Nail polish (Cutex 60 seconds supershine 210 clear)	Cutex
Normal horse serum (NHS; heat-inactivated)	Invitrogen Co.
NOVEX Sharp pre-stained protein markers	Invitrogen Co.
N-succinimidyl 3-(2-pyridyldithio)propionate (SPDP)	Sigma-Aldrich Co.
Nuclear localisation signal (NLS) peptide	Auspep, Pty. Ltd.
OneShot TOP10 chemically competent E.coli (incl SOC medium)	Invitrogen Co.
Optimal cutting temperature medium	Sakura Finetech, Inc.
paraformaldehyde (PFA)	Sigma-Aldrich Co.
penicillin-streptomycin (PEST)	Invitrogen Co.
Pentobarbital sodium salt	Sigma-Aldrich Co.
Phosphate buffered saline (PBS; powder bags)	Sigma-Aldrich Co.
Polyethylenimine (PEI)	Sigma-Aldrich Co.
Poly-L-lysine (PLL)	Sigma-Aldrich Co.
Potassium chloride	Sigma-Aldrich Co.
Propidium iodide (PI)	Sigma-Aldrich Co.
Protein G agarose (fast flow)	Millipore
Qiagen Gigaprep kit	Qiagen N.V.
Qiagen spin Miniprep kit	Qiagen N.V.
Rat astrocyte nucleofector kit	Lonza Group, Ltd.
Roswell Park Memorial Institute media 1640 (RPMI)	Invitrogen Co.
Select agar	Sigma-Aldrich Co.
Self-cure acrylic repair material	Dentsply International Ltd.
Sephadex G-25	Sigma-Aldrich Co.
Slowfade Gold antifade reagent	Invitrogen Co.
Sodium acetate	Ajax Finechem, Pty. Ltd.
Sodium azide	Sigma-Aldrich Co.
Sodium bicarbonate	Sigma-Aldrich Co.
Sodium chloride (NaCl)	Sigma-Aldrich Co.
Sodium citrate	Sigma-Aldrich Co.
Sodium dodecyl sulfate (SDS)	Sigma-Aldrich Co.
Sodium nitrite	Sigma-Aldrich Co.
Sucrose	Sigma-Aldrich Co.

Table 2.2 Chemicals and reagents, continued

Description	Company
Sulfosuccinimidyl 6-(α-methyl-α[2-pyridyldithio]-toluamido)hexanoate (Sulfo-LC-SMPT)	Pierce Biotechnology Inc.
Supercoiled DNA ladder	Invitrogen Co.
Supercoiled DNA ladder	Promega Co.
Tris(hydroxymethyl)aminomethan (Tris)	Sigma-Aldrich Co.
Tris-hydrochloric acid	Ajax Finechem, Pty. Ltd.
Triton X-100 (for molecular biology)	Sigma-Aldrich Co.
Trypsin-ethylenediaminetetraacetic acid (trypsin-EDTA)	Sigma-Aldrich Co.
Trypsin-ethylenediaminetetraacetic acid (trypsin-EDTA) - 0.25 % phenol red	Invitrogen Co.
Tween 20	Sigma-Aldrich Co.
UltraPure™ DNase/RNase-free distilled water (GIBCO H2O)	Invitrogen Co.
Water for irrigation	Baxter International, Inc.

Table 2.3 Information on materials and chemical suppliers

Company	Location
AbD Serotec	Kidlington, UK
Abacam	Cambridge, UK
ACE Chemical Company	Camden Park, SA, Australia
Ajax Finechem, Pty. Ltd.	Taren Point, NSW, Australia
Aldevron	Fargo, ND, USA
Asahi Techno Glass Co.	Singapore, Singapore
AstraZeneca AB	Södertälje, Sweden
Auspep, Pty. Ltd.	Tullmarine, VIC, Australia
Baxter International, Inc.	Deerfield, IL, USA
Beckman Coulter, Inc.	Brea, CA, USA
Bio-rad Laboratories, Inc.	Hercules, CA, USA
Brand GmbH + Co. KG	Wertheim, Germany
Cahn instruments, Inc.	Cerritos, CA, USA
Canon, Inc.	Tokyo, Japan
Chem-Supply, Pty. Ltd.	Gillman, SA, Australia
Copan Diagnostics, Inc.	Murrieta, CA, USA
Cutex	London, UK
David Kopf Instruments	Tujunga, CA, USA
Dentsply International Ltd. (DeTrey Division)	York, PA, USA
Durect Co.	Cupertino, CA, USA
Edwards Instruments Co.	Narellan, NSW, Australia
GE Healthcare	Waukesha, WI, USA
GeneWorks Pty. Ltd.	Hindmarsh, SA, Australia
Gerhard Menzel Glasbearbeitungswerk GmbH & Co. KG	Braunschweig, Germany
Greiner Bio-one International AG	Kremsmuenster, Austria
Hamilton Company	Reno, NV, USA
Invitrogen Co.	Carlsbad, CA, USA
Labconco Co.	Kansas City, MO, USA
Lang dental Manufacturing Company, Inc.	Wheeling, IL, USA
Leica Microsystems GmbH	Wetzlar, Germany
LKB	Bromma, Sweden
Lonza Group, Ltd.	Basel, Switzerland
Microm *(now Thermo Scientific)*	Walldorf, Germany
Millipore	Billerica, MA, USA
New England Biolabs, Inc.	Ipswich, MA, USA
Novus Biologicals LLC	Littleton, CO, USA
Olympus Co.	Tokyo, Japan
Pall Life SciencesCo.	Port Washington, NY, USA
PerkinElmer, Inc.	Waltham, MA, USA
Pfizer Pty Ltd.	Perth, WA, Australia
Pierce Biotechnology, Inc.	Rockford, IL, USA
Promega	Madison, WI, USA
Qiagen N.V.	Venlo, The Netherlands
Ratek Instruments, Pty. Ltd.	Boronia, VIC, Australia
Sakura Finetech, Inc.	Torrance, CA, USA
Santa Cruz Biotechnology, Inc.	Santa Cruz, CA, USA
Sarstedt AG & Co.	Nümbrecht, Germany
Sartorius Stedim Biotech S.A.	Aubagne Cedex, France
Shimadzu Co.	Kyoto, Japan
Sigma-Aldrich Co.	St. Louis, MO, USA
Synoptics, Ltd.	Cambridge, UK
Techno Plas, Pty. Ltd.	St Marys, SA, Australia
Thermo Fischer Scientific, Ltd.	Wilmington, DE, USA
Tyco Healthcare (UK) Ltd.	Hampshire, Northern Ireland
Virbac Animal Health	Regents Park, NSW, Australia
World Precision Instruments	Sarasota, FL, USA

Table 2.4 Antibodies and cellular markers

Host species	anti-	Abbreviaton	Description	Catalogue #	Company
mouse	anti-mouse/ rat/ chicken/ human	A2B5	A2B5 stem cell marker	AB53521	Abcam
goat	anti-mouse	IgG	Alexa Fluor™ 488 *highly crossadsorbed*	A11029	Invitrogen Co.
goat	anti-mouse	IgG	Alexa Fluor™ 647 *highly crossadsorbed*	A21236	Invitrogen Co.
goat	anti-rabbit	IgG	Alexa Fluor™ 488 *highly crossadsorbed*	A11034	Invitrogen Co.
goat	anti-rabbit	IgG	Alexa Fluor™ 647 *highly crossadsorbed*	A21245	Invitrogen Co.
rabbit	anti-bovine/ rat/ mouse/ human	CD11b	cluster of differentiation molecule 11b	NB110-89474	Novus Biologicals LLC
mouse	anti-rat	CD11b/c	cluster of differentiation molecule 11b/c	MR6200	Invitrogen Co.
mouse	anti-rat	CD68	cluster of differentiation molecule 68	MCA341 GA	AbD Serotec
mouse	anti-rat/ pig/ human	GFAP	glial fibrillary acidic protein	G6171	Sigma-Aldrich Co.
rabbit	anti-rat/human	GFAP	glial fibrillary acidic protein	G9269	Sigma-Aldrich Co.
rabbit	anti-Aequorea victoria	GFP	green fluorescent protein	A11122	Invitrogen Co.
-	-	Isolectin B4	isolectin GS-IB4 from *Griffonia simplicifolia*, Alexa Fluor™ 647 conjugate	I32450	Invitrogen Co.
mouse	anti-rat	CD206	mannose receptor CD206	16109	Beckman Coulter, Inc.
mouse	anti-avian/ chicken/ ferret/ human/ mouse/ pig/ rat/ salamander	NeuN	neuronal nuclei	MAB377	Millipore
rabbit	anti-human/ mouse/ rat/ monkey	NG2	NG2 chondroitin sulfate proteoglycan	AB5320	Millipore
rabbit	anti-human/mouse/rat	Nrf2	Nuclear factor erythroid 2-related factor	sc-722	Santa Cruz

Table 2.4 Antibodies and cellular markers, continued

Host species	anti-	Abbreviaton	Description	Catalogue #	Company
rabbit	anti-human/ mouse/ rat	SR-BI	scavenger receptor, class B, type I	NB400-104	Novus Biologicals LLC
mouse	anti-rat	SR-BI	scavenger receptor, class B, type I	-	(kindly provided by Professor Yoshi Nakanishi)
mouse	-	X63	IgG with no identified antigen	-	(kindly provided by Professor Robert Rush)

CHAPTER 3: SR-BI EXPRESSION AND ANTIBODY INTERNALISATION IN RAT BRAIN AND GLIAL CELL CULTURES

3.1 Introduction

3.1.1 Receptor-mediated gene delivery

Transient expression or knockdown of specific proteins *in vivo* provides a powerful approach to investigate normal cellular function and disease pathways. The function of specific cell populations have previously been studied in selected tissues using genetic modification, however there is no established method which selectively delivers nucleic acids to separate glial populations of the CNS. Instead, the few selective glial genetic modification studies in the past have restricted transgene expression to cell populations using cell-specific promoters, as previously discussed in section 1.4 - 1.6 *(Brenner et al., 1994; Cucchiarini et al., 2003; Bradford et al., 2009; Xu et al., 2010; Rahim et al., 2011b)*.

A promising approach to genetically modify a specific cell population involves the restricted delivery of DNA to these cells using cell surface receptors. By using a ligand such as an antibody, this receptor-mediated transfection technique has been used to target cholinergic neurons in rat forebrain *(Berhanu and Rush, 2008)* and other populations of the CNS (see Chapter 4). These studies led us to investigate whether receptor-mediated gene delivery could be used to transiently modify protein expression in glial cells.

The development of constructs for receptor-mediated transfection requires the identification of a cell surface receptor with the potential to bind and internalise ligands (such as antibodies) bound to nucleic acids. As further described in the following sections, SR-BI was initially considered as a potential candidate for delivery to astrocytes in the brain, based on studies in adult mice *(Husemann and Silverstein, 2001)* and the known properties of this receptor (see section 3.1.2.1). Rats were chosen for our investigations because of their widespread use in other studies involving intracerebral injections and also due to the potential for future investigations using well-characterised models of acute brain disorders such as stroke and trauma. The expression and properties of SR-BI have not been investigated in rat brain. Thus, the aims of the studies presented in this chapter were to:

a) investigate the expression of SR-BI in adult rat brain and in glial cells in culture originating from neonatal rat
b) test the capacity of an antibody targeted against the external domain of SR-BI to be internalised by glial cells in culture and *in vivo*
c) test for changes in microglial activation in response to treatment

In contrast to our initial predictions, antibodies targeted against the extracellular part of SR-BI were not internalised by astrocytes. Rather, they selectively targeted microglia in the adult rat brain. This microglial targeting could potentially be used to selectively deliver nucleic acids using antibodies directed against SR-BI.

3.1.2 Scavenger receptors

In the late 1970's, advances in the investigation of cholesterol metabolism led to the identification of receptors on macrophages that were able to internalise circulating low-density lipoproteins (LDL). It was shown that LDL was internalised to a larger extent into macrophages after modification of this lipoprotein by oxidation and acetylation *(Krieger and Herz, 1994; Krieger, 1999)*. Furthermore, this internalisation was not subject to feedback inhibition in response to increasing intracellular concentrations of cholesterol, unlike LDL uptake via LDL receptors in cells of other tissues *(Krieger, 1999)*. The group of macrophage receptors for modified lipoproteins (by for example oxidation and acetylation) were given the collective name scavenger receptors *(Goldstein et al., 1979a)*.

Today, the scavenger receptor family comprises a range of receptors based on their capacity to internalise modified LDL *(Stephen et al., 2010)*. A range of additional ligands have been identified, including high-density lipoprotein (HDL) and other lipoproteins, polyanions, lysine-modified proteins *(Goldstein et al., 1979b)*, pathogens; including *Neisseria meningitidis (Pluddemann et al., 2006)*, apoptotic cells and amyloid-β *(Wyss-Coray et al., 2003)*.

Scavenger receptors on macrophages play an important role in the removal of proteins and lipoproteins which have been modified during normal cellular activity, and also in the uptake of cell debris in damaged tissues *(Murao et al., 1997; Krieger, 1999)*. These receptors also accommodate for the internalisation of cholesterol into biological membranes of cells in many tissues *(Krieger, 1999;*

Husemann et al., 2002). Furthermore, internalisation of cholesterol via these receptors is important in cells of steroidogenic tissues for hormone production *(Krieger, 1999; Husemann et al., 2002)*.

Prominent examples of scavenger receptors include CD36, CD68, CD163, CD206 mannose receptor, CXCL16, dectin-1, galectin-3, LDL receptor-1, macrophage receptor with collagenous structure, SR-A and SR-BI. These members of the scavenger receptor family are structurally diverse. However, the receptors have been divided into classes which share similar structural domains *(Stephen et al., 2010)*.

3.1.2.1 SR-BI

SR-BI is a glycoprotein of 509 amino acids with a weight of 57 kDa *(Dao Thi et al., 2011)*. Originally named 'CLA-1' by Calvo and Vega (1993), this receptor contains two trans-membrane domains, a large extracellular loop structure and two short cytoplasmic tails at each end *(Calvo and Vega, 1993; Acton et al., 1996; Krieger, 2001)*. Figure 3.1 shows a simplified diagram of SR-BI with the number of amino acids at the different parts of the receptor and with marked cysteines which form a number of disulphide bonds in the receptor structure.

Like other members of the scavenger receptor family, SR-BI has a wide range of mainly lipid-based ligands *(Acton et al., 1994; Feng et al., 2009)*. SR-BI was the first receptor to be linked with high-affinity binding of HDL and subsequent

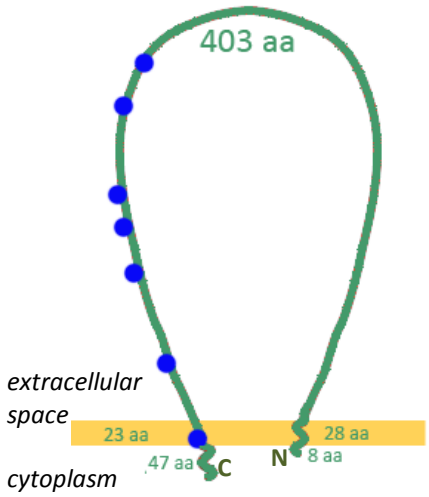

Figure 3.1 General structure of SR-BI*; a loop structure with two cytoplasmic ends. The number of amino acids (aa) are presented on parts of the structure. A few disulphide links exist between the cysteine residues (blue circles) of this receptor. Adapted from (Krieger, 2001; Rhainds et al., 2004).*

uptake of lipids *(Rigotti et al., 1996; Feng et al., 2009)*. Due to its localisation in the plasma membrane and its internalisation of various lipoproteins in a range of tissues, SR-BI was proposed in early studies to serve crucial functions in a variety of cell types of the healthy organism *(Calvo and Vega, 1993)*. As previously mentioned for scavenger receptors, cholesterol internalisation through SR-BI is also strongly linked to hormone production in steroidogenic tissues *(Cai et al., 2008)*. Furthermore, SR-BI expression in liver allows for internalisation of excess cholesterol via HDL from peripheral tissues. This process is called reverse cholesterol transport. After internalisation into liver cells, this cholesterol can be excreted as bile acid *(Glomset, 1968; Rigotti et al., 1997a; Krieger, 1999; Kocher et al., 2003; Lewis and Rader, 2005; Ji et al., 2011)*.

Similarly to several other scavenger receptors, SR-BI has been found on the surface of monocytes, macrophages and Kupffer cells in the liver *(Murao et al., 1997; Fluiter et al., 1998; Buechler et al., 1999; Hirano et al., 1999; Husemann et al., 2001; Manzano-Leon et al., 2006)*. SR-BI is also highly expressed in the adrenal gland, ovary *(Landschulz et al., 1996)* and other steroidogenic tissues *(Feng et al., 2009)*. Fibroblast cell lines *(Acton et al., 1994)* and endothelial cells in culture *(Seetharam et al., 2006)* have also been found to express this receptor.

SR-BI has also been detected in cells of the CNS. In cultures originating from the brain of neonatal rat, this receptor is expressed by microglia *(Alarcon et al., 2005; Zhang et al., 2006)* and astrocytes *(Alarcon et al., 2005)*. This receptor has been reported in microglia in cultures prepared from neonatal brain and in

astrocytes in adult mouse and human brain *(Husemann and Silverstein, 2001; Husemann et al., 2002)*. On the basis of this observation and unpublished findings from neonatal mice (discussed in *Husemann et al., 2002*), a developmental shift in expression of SR-BI in glia has been proposed *(Husemann and Silverstein, 2001; Husemann et al., 2002)*. It remains unknown whether a similar developmental shift is present in other species, including rat. A summary of glial SR-BI expression in neonatal cell cultures and in the adult CNS of mouse, rat and/or human is presented in Table 3.1.

Table 3.1 Summary of SR-BI expression in human, mouse and rat

Species	Culture/ tissue	SR-BI expression by		Reference
		Astrocytes	Microglia	
Human	Adult brain	+	-	*(Husemann and Silverstein, 2001)*
Mouse	Culture from neonatal brain	?	+	*(Husemann and Silverstein, 2001)*
Mouse	Adult brain	+	-	*(Husemann and Silverstein, 2001)*
Rat	Culture from neonatal brain	+	+	*(Alarcon et al., 2005)* *(Zhang et al., 2006)*
Rat	Adult brain	?	?	

The specific function of SR-BI in cells of the CNS has not been determined. With regards to astrocytes, studies in culture indicate that SR-BI is involved in

intercellular exchange of cholesterol via HDL *(Husemann et al., 2002)*. SR-BI has also been implicated in the internalisation and degradation of amyloid-β by astrocytes, as demonstrated in glial culture *(Husemann et al., 2001; Alarcon et al., 2005)*.

Roles of SR-BI in microglia may be suggested based on studies in other members of the same myeloid lineage. In macrophages and monocytes, SR-BI is involved in clearing of modified lipoproteins, phospholipids and apoptotic cells, as demonstrated *in vitro (Murao et al., 1997)*. Internalisation of cholesterol through this receptor on macrophages is not regulated by intracellular cholesterol (as mentioned previously). This may result in unregulated uptake of modified lipoproteins and accumulation of cholesterol in these cells, which has been linked to the formation of foam cells - known key players in atherogenesis *(Krieger, 1999; Julve et al., 2011; Norata et al., 2011)*. This is in contrast to liver, where expression of this receptor is increased upon the depletion of cellular cholesterol pools *(Wang et al., 1996; Krieger, 2001; Dong et al., 2011)*.

Little is known about the regulation of SR-BI expression in the brain. However, it has been suggested in other tissues that SR-BI expression levels are regulated by a variety of hormones and inflammatory molecules. In cells of the adrenal gland, SR-BI expression has been shown to increase upon exposure to adrenocorticotropic hormone *(Rigotti et al., 1996)*. SR-BI expression and stability is also regulated by oestrogen, as demonstrated *in vivo (Landschulz et al., 1996)*. Furthermore, lowered SR-BI expression in cultured macrophages has been

observed after exposure to the pro-inflammatory cytokines TNF-α and IFNγ *(Buechler et al., 1999)*. It has also been shown in culture and in the adult apolipoprotein E gene knockout mouse that nuclear peroxisome proliferator-activated receptor activation regulates the expression of SR-BI in mouse macrophages *(Chinetti et al., 2000)*.

With regards to cellular localisation, SR-BI has been found in tiny clustered invaginations of the plasma membrane *(Krieger, 1999)*. Different mechanisms have been hypothesised for SR-BI ligand binding and internalisation. It has been suggested that the high affinity SR-BI ligand HDL remains bound to SR-BI in the extracellular space, where it releases its cholesterol cargo directly to the plasma membrane *(Seo et al., 2002; Connelly et al., 2003; Hu et al., 2010)*. This mechanism has been named the selective cholesteryl ester uptake pathway *(Hu et al., 2010)*. The majority of HDL cholesterol (70 - 80 %) bound to SR-BI is thought to be quickly hydrolysed in a metabolically active plasma membrane pool. The remaining 20 - 30 % of HDL cholesteryl esters is believed to stay intact and to be delivered to other parts of the cell, including internal membranes *(Connelly et al., 2003)*. Other findings have indicated that essentially all HDL cholesteryl esters are initially internalised and thereafter transported to internal membranes prior to hydrolysis in the plasma membrane *(Uittenbogaard et al., 2002)*.

Many studies also suggest that SR-BI mediates the internalisation of the entire HDL molecule *(Silver et al., 2001; Dao Thi et al., 2011)*. Subsequent to this

internalisation, it has been suggested that HDL remains bound to SR-BI and releases a portion (or all) of its carried lipids into the formed intracellular compartment. Thereafter, lipid-depleted HDL bound to SR-BI is recycled to the plasma membrane where HDL is released to the extracellular space. This mechanism is termed retroendocytosis and has been suggested to be the internalisation pathway for HDL via SR-BI, as demonstrated in human hepatoma HepG2 cells, in chinese hamster ovary (CHO) cells expressing SR-BI and in macrophages in culture *(Silver et al., 2001; Rhainds et al., 2004)*.

The postulated retroendocytosis of HDL via SR-BI is distinct from that of LDL via the LDL receptor, which enters the endosomal/lysosomal pathway *(Valacchi et al., 2011)*. However, retroendocytosis of HDL has similarities to that of transferrin *(Schmidt et al., 1986; Rogers and Rush, 2012)*, which through receptor-mediated endocytosis delivers iron ions to cells expressing the transferrin receptor.

As a third alternative, it has also been suggested that SR-BI ligands similarly to transferrin enter the traditional endosomal/lysosomal pathway after internalisation. HDL exposure to SR-BI-expressing COS-7 cells and to hepatocellular carcinoma HepG2 cells in culture, resulted in 45 % and 15 % internalisation, respectively *(Sun et al., 2006)*. In addition, oxidised LDL which has even higher affinity for SR-BI has been shown to be internalised and degraded by SR-BI-expressing CHO cells *(Gillotte-Taylor et al., 2001)*. Another observation in CHO cell cultures expressing SR-BI is that these cells internalise and degrade

albumin from bovine serum (BSA) with advanced glycation end-products *(Ohgami et al., 2001)*. Similar internalisation without degradation has also been suggested for the SR-BI ligand maleylated BSA by HepG2 cells expressing SR-BI *(Rhainds et al., 1999)*. More evidence suggesting that SR-BI ligands are internalised via traditional receptor-mediated endocytosis include studies where internalised SR-BI has been co-labelled with clathrin *(Dao Thi et al., 2011)*. Internalised SR-BI has also been co-labelled with caveolin-1 *(Krieger, 1999; Balazs et al., 2004)*, implicating SR-BI in caveolae *(Babitt et al., 1997; Dao Thi et al., 2011)* and lipid rafts *(Rhainds et al., 2004; Dao Thi et al., 2011)*.

One reason for the conflicting results regarding SR-BI ligand internalisation through classical endocytosis or retroendocytosis versus the selective cholesteryl ester uptake pathway could be that different ligands may evoke different responses when bound to SR-BI. It has been shown that the nature of the ligand can affect whether SR-BI remains on the cell surface or if it is internalised with the ligand upon binding. This has been demonstrated in SR-BI-expressing CHO cells, where the amount of this receptor was studied on the cell surface after exposure to different ligands *(Zhang et al., 2007b)*. Pharmacological inhibition of the recycling of this receptor after internalisation enabled the measurement of internalised SR-BI after exposure to the ligands HDL and acetylated LDL *(Zhang et al., 2007b)*. Therefore, the amount of SR-BI at the cell surface at the end of the experiment corresponded to the amount of SR-BI from the start of the experiment that had not been internalised although ligands had bound to the receptor. When exposed to acetylated LDL, SR-BI expression on the plasma

membrane was significantly decreased within 60 min, whereas this remained at similar levels after the exposure to HDL *(Zhang et al., 2007b)*. This suggests that the binding of different lipoproteins may result in specific forms of internalisation via SR-BI; modified (acetylated) LDL may enter the endosomal/lysosomal pathway, whereas HDL does not.

Because of the solid evidence that ligands could be internalised via SR-BI and in some instances had the capacity to escape degradation within the cell *(Rhainds and Brissette, 2004)*, this receptor offered a potentially attractive system to deliver DNA to cells. To initially assess this potential, the distribution of this receptor and internalisation of an antibody targeting an extracellular domain was investigated in the brain and in glial cell cultures.

3.2 Materials and methods

3.2.1 Antibody preparation and characterisation

3.2.1.1 SR-BI hybridoma cell line preparation and growth

An antibody recognising the extracellular domain of SR-BI was used to investigate internalisation into cells in culture and *in vivo*. This antibody is subsequently abbreviated as $SR\text{-}BI^{Ab}$ and was isolated from a mouse hybridoma cell line (clone 3D12). This cell line was kindly provided by Professor Yoshinobu Nakanishi, Pharmaceutical Chemistry and Biology, Kanazawa University, Japan

(Nakagawa et al., 2004; Osada et al., 2006). These cells were always grown in a humidified atmosphere of 5 % CO_2 in air at 37°C.

SR-BI hybridoma cells were grown in culture flasks (T25, T75, T175; Greiner Bio-one International AG) containing Roswell Park Memorial Institute media 1640 (RPMI; Invitrogen Co.), supplemented with 10 % v/v foetal bovine serum (FBS; Invitrogen Co.) / 1 % v/v penicillin-streptomycin (PEST; Invitrogen Co) / 1 % v/v hypoxanthine thymidine supplement (HT supplement; Invitrogen Co.). Passaging of cells and harvesting of supernatant was performed when the cultures reached confluence. Conditioned medium containing SR-BI^{Ab} was poured out of all flasks, centrifuged for 5 min at 300*g* (Sigma Laboratory centrifuge 6K15) and supernatant stored at -20°C until further use. After the removal of the conditioned medium, cells in one culture flask was covered in 1 : 10 trypsin-ethylenediaminetetraacetic acid (trypsin-EDTA; Sigma-Aldrich Co.) in phosphate-buffered saline (PBS; at final use comprising 0.01 M phosphate / 0.14 M sodium chloride (NaCl) / 2.7 mM potassium chloride, pH 7.4; Sigma-Aldrich Co.). This was exchanged for another lot of trypsin-EDTA / PBS at 37°C for a maximum of 5 min. Cells were gently dislodged and transferred to a 50 ml tube. This tube was filled with FBS / PEST / HT supplement / RPMI and centrifuged for 5 min at 90*g*. Supernatant was removed and cells resuspended in 6 ml of medium. Cells were re-plated into six new cell culture flasks. When the cultures reached confluence, conditioned medium was extracted from all flasks (as described at the start of this paragraph) and one flask was used for the next passage.

3.2.1.2 SR-BI^{Ab} preparation from SR-BI hybridoma conditioned medium

A polypropylene column (Bio-rad Laboratories, Inc.) containing Protein G agarose (3 ml packed volume; fast flow; Millipore) was washed with 1.5 ml/min PBS for 30 min, followed by 0.1 M glycine (Sigma-Aldrich Co.) / PBS (pH 2.7) for 20 min, and an additional 30 min PBS wash using a Microperpex Peristaltic pump (2132; LKB). SR-BI^{Ab} - conditioned medium was thawed to room temperature (RT) in a water bath (Ratek Instruments, Pty. Ltd.) and sterile-filtered through a 0.22 µm Steritop-GV filter unit (500 ml; Millipore) using vacuum suction. Conditioned medium was run through the column at a rate of 1.5 ml/min at 4°C and the eluate was continuously reintroduced to the same column in order to pass it through 4 times.

After another PBS wash at 1.5 ml/min for 30 min, IgG antibody was eluted in 20 x 1 ml fractions using 0.1 M glycine / PBS (pH 2.7). Fractions containing IgG were identified using absorbance measurements at 280 nm (A_{280}) in a UV-3000 spectrophotometer (Shimadzu Co.). These fractions were mixed and the pH of the mixture was adjusted to 7.4 using 2 M tris(hydroxymethyl)aminomethane (Tris; Sigma-Aldrich Co.) and measured using pH test strips (Sigma-Aldrich Co.). The total antibody mixture was added to a Vivaspin® concentrator (122 x 17 mm, membrane area 2.0 cm^2, 4 ml; 100 kDa molecular weight cut-off - MWCO; Sartorius Stedim Biotech S.A.) in aliquots of 4 ml and concentrated after each addition by centrifugation at 3680*g*. The remaining 1 ml sample following the final centrifugation of this material was diluted to 4 ml using PLL or PEI immunoporter reaction buffers (IRB1 or IRB2, see details in 4.2.1 or 4.2.2,

respectively) and the volume was again reduced to 1 ml by centrifugation through the Vivaspin® concentrator. This process was repeated twice more, with the residual volume in the final centrifugation step giving an antibody concentration of between 2 and 3 mg/ml. The final concentration was measured at A_{280} in a NanoDrop™ 8000 multi-sample micro-volume UV-vis spectrophotometer (Thermo Fischer Scientific, Ltd.; following the instructions of the supplier), after which the antibody was freeze-dried in the Freezone 6 Freezedry system (Labconco Co.) and stored at -20 °C up until one year after preparation.

3.2.1.3 Antibody analysis in SDS-PAGE

The final antibody fraction was analysed using sodium dodecyl sulfate polyacrylamide gel electrophoresis (SDS-PAGE) on a NuPAGE® Novex 4 - 12% Bis-Tris Gel (1.0 mm, 12 well; Invitrogen Co.). Samples (3.5 µg) were diluted in a total volume of 20 µl sample buffer (pH 6.8) containing final concentrations of 62.5 mM Tris-hydrochloric acid (Ajax Finechem, Pty. Ltd.) / 10 % w/v glycerol (Sigma-Aldrich Co.) / 0.7 mM SDS (Sigma-Aldrich Co.) / 0.1 % v/v bromophenol blue (Sigma-Aldrich Co.) with or without 1 mM DL-dithiothreitol (DTT; Sigma-Aldrich Co.) as reducing agent. Bovine gamma globulin (Sigma-Aldrich Co.) was used as a control. A lane adjacent to the samples was loaded with 10 µl NOVEX Sharp pre-stained protein markers (Invitrogen Co.). Gels were run for 60 min run at 200 V, 100 mA in an XCell SureLock® Mini-Cell and XCell II™ Blot Module Kit CE Markgel system (Invitrogen Co.). Thereafter, samples were visualised in the gel

using Brilliant Blue staining (R 250; Sigma-Aldrich Co.) for 60 min and three washes (10 min) in a 10 % v/v methanol (Sigma-Aldrich Co.) / 3.75 % v/v acetic acid (Sigma-Aldrich Co.) destaining solution. Images of the gels were captured using a Digital Ixus 70 camera (Canon).

3.2.2 Studies of glial cells in culture

3.2.2.1 Cell culture preparation and growth

Culture experiments were conducted using primary mixed glial cultures and microglial cultures. Primary mixed glial cultures were prepared as previously described *(Hansson, 1988; Nilsson et al., 1991; Muyderman et al., 2010)* and summarised as follows. The brains of P_1 - P_3 Sprague Dawley rat pups were removed and the cerebral cortices dissected and cleaned of meninges. This tissue was passed through a mesh nylon net (80 µm) into Dulbecco's modified Eagle's medium - low glucose (DMEM; Sigma-Aldrich Co.) supplemented with 10 % v/v FBS and 1 % v/v PEST. Cells were seeded into 6-, 24- or 96-well tissue culture plates with or without coverslips (circular, 12 mm radius; Gerhard Menzel Glasbearbeitungswerk GmbH & Co. KG). Medium was renewed after 3 days of cultivation, and thereafter three times per week. These cells were grown to confluence (14 - 17 days) at a humidified atmosphere of 5 % CO_2 in air at 37°C before experimental use. Primary glial cells were grown in the FBS / PEST / DMEM glial growth medium at all times, unless otherwise stated.

Microglial cultures were prepared via a mild trypsinisation method *(Saura et al., 2003)*. The conditioned medium from 24-well cell culture plates (Greiner Bio-one International AG) of 21-day old mixed glial cultures was removed, centrifuged at 300*g* and the supernatant kept in a cell incubator at 37°C / 5 % CO_2 until the end of the protocol. Cells attached to the culture wells were treated with 750 µl serum-free DMEM for 30 min (at 37°C / 5 % CO_2). After this pre-treatment, cultures were incubated for 30 min in 450 µl 0.0625 % v/v trypsin-EDTA (diluted from 0.25 % phenol-red; Invitrogen Co., using 1 : 1 v/v DMEM / HBSS). The HBSS (140 mM NaCl, 5.4 mM potassium chloride, 0.64 mM monopotassium phosphate, 3.0 mM sodium bicarbonate, 5.5 mM glucose, 1.0 mM EDTA, 20 mM HEPES; Sigma-Aldrich Co.) did not contain magnesium sulphate, magnesium chloride or calcium chloride. After a few minutes of exposure to this low concentration of trypsin, a cell layer consisting mostly of astrocytes slowly detached, leaving a microglial layer adhered to the wells. This process was monitored using phase contrast microscopy. Small numbers of remaining adherent astrocytes were removed using gentle pipetting with the trypsin-EDTA / DMEM / HBSS solution. Addition of 450 µl 1 : 1 v/v DMEM / HBSS, was followed by incubation for 10 min in 750 µl FBS / PEST / DMEM to stop trypsinisation. Microglial culture preparation was finalised by exchanging this FBS / PEST / DMEM with 750 µl of the conditioned medium which had been obtained at the start of this purification protocol.

3.2.2.2 IHC in culture

In this chapter, immunohistochemistry (IHC) in cell culture was performed with BSA (Sigma-Aldrich Co.) as blocking agent. This procedure is subsequently referred to as BSA/Triton IHC. Cells in culture wells were quickly washed in PBS, fixed in 4 % w/v paraformaldehyde (PFA; Sigma-Aldrich Co.) / PBS (pH 7.4) at 4°C for 10 min, followed by three PBS washes for 5 min each. Blocking and permeabilisation was performed in 1 % w/v BSA / 0.2 % v/v Triton X-100 (Sigma-Aldrich Co.) / PBS (pH 7.4) for 45 min. Cells were incubated for 60 min in primary antibodies diluted in 1 % BSA / 0.2 % Triton X-100 / PBS, followed by 45 min incubation in secondary antibodies diluted in the same buffer. PBS washes (3 x 5 min) separated the antibody incubations and also completed the IHC. When cells were grown on coverslips, these coverslips were mounted onto glass microscope slides (Gerhard Menzel Glasbearbeitungswerk GmbH & Co. KG) with SlowFade Gold antifade reagent (Invitrogen Co.) and sealed with nail polish (Cutex).

Astrocytes and microglia were identified by their immunoreactivity for GFAP and CD11b/c markers, respectively. Expression of SR-BI was determined in mixed glial cultures and in microglial cultures using BSA/Triton IHC with a rabbit polyclonal anti-SR-BI antibody (1 : 200; Novus Biologicals LLC) and co-labelling with cellular markers (see section 2.3).

3.2.2.3 Assessment of microglial activation in culture

The capacity of treatments to influence the activation stage of microglia was assessed from changes in cell morphology, similar to approaches adopted in previous studies *(Giulian and Baker, 1986; Glenn et al., 1992; Rosenstiel et al., 2001; Stence et al., 2001; Kauppinen et al., 2008)*. Microglial cells positive for CD11b/c were assigned to one of three categories based on morphology (see Figure 3.3): a) ramified, b) non-amoeboid activated and c) amoeboid activated cells. Cells with at least two processes longer than 25 µm were classified as ramified *(Kauppinen et al., 2008)*. The minimum length criteria for processes was included to assist with separating ramified cells from those bearing shorter processes associated with motility (see section 1.2.3). Amoeboid activated microglia were defined as round cells without any processes. Cells not meeting either criteria were assigned to the non-amoeboid activated category. The total number of microglia and proportion of each morphological criteria in the microglial population was calculated from four separate random images (one from each quadrant of the culture well; captured using a low magnification objective; 10x) obtained for each of three replicate wells.

3.2.2.4 Internalisation of IgG antibodies in culture

The capacity of cells in mixed glial cultures to internalise SR-BI^{Ab} was tested in culture. The CD206 mannose receptor IgG (CD206^{Ab}; Beckman-Coulter, Inc.) had previously been shown to be internalised by both astrocytes and microglia in

mixed glial culture (B. Homkajorn, PhD thesis), and was included as a positive control in these experiments.

Confluent (14 - 17 days old) live mixed glial cultures grown on 12 mm-coverslips in 24-well plates were exposed to 67 µg/ml antibody (200 µl) diluted in DMEM (without FBS/PEST). The duration of this exposure was 3 h (for SR-BI^{Ab} and CD206^{Ab}) or 6 h (only for SR-BI^{Ab}). Live microglial cultures were exposed to the same treatment the day after microglial purification from confluent mixed glial cultures (see section 3.2.2.1). After fixation and IHC (BSA/Triton IHC, see section 3.2.2.2), the presence of antibodies in the cytoplasm was determined through the use of anti-mouse secondary antibody Alexa Fluor^{488}. Randomly chosen images (six per well in each of three replicate wells) were used to quantify internalisation after each treatment (captured using a low magnification objective; 20x). Cells internalising the antibodies were identified by immunolabelling with either the microglial marker isolectin B4^{647} or the astrocytic marker rabbit anti-GFAP.

To further test for specificity for SR-BI^{Ab}, internalisation was similarly assessed in confocal microscopy following separate incubations with 100 µg/ml SR-BI^{Ab}, GFAP IgG (Sigma-Aldrich Co.) or a mixed IgG preparation from mice (Sigma Aldrich Co.).

3.2.3 Studies of glial cells in vivo

3.2.3.1 Intracerebral injections

Internalisation of SR-BI^{Ab}, CD206^{Ab}, an antibody against intracellular nuclear factor erythroid 2-related factor (Nrf2^{Ab}) and an antibody for which no antigen has been identified (X63^{Ab}) was determined through intracerebral injections into the hippocampus (3 µl into CA3*; anteroposterior (AP) -2.12, lateral (L) -1.5, dorsoventral (DV) -4.0)* of adult Sprague Dawley rats (300 g; *n = 3* per group).

These rats were anaesthetised using intraperitoneal injections of pentobarbital sodium salt (50 mg/ml; approximately 15 mg per rat; Sigma-Aldrich Co.). After anaesthetisation, rats were placed in a stereotaxic frame (David Kopf Instruments) and the top of the skull shaved with a razor. The scalp was sterilised using 70 % ethanol, and local anaesthesia (Marcain^{TM}; AstraZeneca AB) was injected subcutaneously over the incision site. A scalpel was used to open the scalp and the skull was cleaned using scalpel and cotton buds.

Bregma was located using a 29 gauge dental needle (Tyco Healthcare (UK), Ltd.) and the stereotaxic frame used to identify the site for injection. A hole with a diameter of approximately 2 mm was drilled through the skull using a manual bone drill. Single injections (8 µg in 3 µl) of each antibody were performed using the needle connected via a catheter to a glass syringe (10 µl; Hamilton

Company). The contents of the syringe were dispensed using an sp200i syringe pump (World Precision Instruments) at a rate of 0.2 µl/min.

After the injection, the needle was left in the injection site for an additional 5 min to minimise leakage. To finalise surgery, the hole in the skull was covered with bone wax and the scalp was closed using suture. Local anaesthesia was applied on top of the wound and rats were monitored closely until awakening.

3.2.3.2 Brain preparation and sectioning

Rats were euthanized 3 h after intracerebral injections, using intraperitoneal injections of 1 ml Lethabarb (pentabarbitone sodium; Virbac animal health). When pinching of back paws did not evoke reflexes, rats were intracardially perfused with 300 ml 145 mM sodium nitrite / 10 mM sodium phosphate (pH 7.4), followed by 300 ml 4 % PFA / PBS (pH 7.4). Animals were decapitated, brains removed from skulls and post-fixed for two days at 4°C in 4 % PFA / PBS. Subsequently, excess water was removed by leaving the brain in 30 % sucrose dissolved in deionised water (Sigma-Aldrich Co.) for two days at 4°C.

Cerebellum and brain stem were removed and the two cerebral hemispheres separated. Each hemisphere was placed in a plastic mould containing optimal cutting temperature medium (Sakura Finetech, Inc.). This plastic mould was placed in a metal mould containing isopentane (Chem-supply, Pty. Ltd.) and was held just above the surface of liquid nitrogen until the brain was completely

frozen. Brain tissue was placed for at least 2 h at -20°C prior to cutting into 50 µm horizontal sections using Sec35 cryostat blades (Microm) at -20°C in a cryostat (CM180; Leica Microsystems GmbH). Free-floating sections were stored in 0.02 % w/v sodium azide (Sigma-Aldrich Co.) / PBS (pH 7.4) in 24-well plates (Greiner Bio-one International AG) at 4°C.

3.2.3.3 IHC in vivo

Another BSA/Triton IHC protocol was used for brain tissue. Selected adult rat horizontal brain sections were washed overnight (O/N) in PBS at 4°C, followed by two more PBS washes (generally 10 min for brain tissue, unless otherwise stated). These sections were blocked and permeabilised at RT for 24 h in 3 % w/v BSA / 0.2 % v/v Triton X-100 / PBS (pH 7.4). Sections were incubated in primary antibody diluted in the same buffer for 24 h. After three PBS washes, sections were incubated for 3 h in secondary antibody, also diluted in 3 % BSA / 0.2 % Triton X-100 / PBS. Brain sections were washed three times in PBS before mounted onto glass microscope slides with coverslips (22 x 40 mm; Gerhard Menzel Glasbearbeitungswerk GmbH & Co. KG) using SlowFade Gold antifade reagent and sealing with nail polish.

A collection of antigen retrieval protocols, as described below, were tested for their capacity to promote detection of SR-BI immunoreactivity in the brain:

a) Sodium citrate antigen retrieval was performed as follows: After PBS washes (3 x 5 min), brain sections were incubated for 30 min in pre-heated (80°C) sodium citrate buffer (10 mM; pH 8.5; Sigma-Aldrich Co.). When the temperature had returned to RT, sections were washed again in PBS (3 x 5 min) and incubated in a blocking solution containing 1 % w/v BSA / 0.3 % v/v Triton X-100 / PBS (pH 7.4), after which the BSA/Triton IHC was followed from the primary antibody step.

b) The antigen retrieval protocol in (a) was also tested with a similar sodium citrate buffer with the addition of 2 mM EDTA / 0.05 % v/v Tween 20 (Sigma-Aldrich Co.; pH 6.2).

c) An SDS protocol was also tested for antigen retrieval purposes: After washing in PBS (3 x 5 min), sections were incubated in 1 % w/v SDS / PBS (pH 7.4) for 5 min at RT. After washing in PBS (3 x 5 min) to remove SDS, sections followed the BSA/Triton IHC protocol from the blocking and permeabilisation step.

d) Lastly, a dimethylsulfoxide (DMSO) method was used for antigen retrieval: Sections were incubated in 1 % v/v DMSO (ACE Chemical Company) diluted in either PBS or 10 mM Tris. After washes in PBS (3 x 20 min), sections were incubated in 0.5 % v/v Triton X-100 / PBS (pH 7.4; 3 x 10 min). This antigen retrieval was finalised using 3 x 20 min washes in PBS and was continued with the BSA/Triton IHC protocol from the blocking and permeabilisation step.

Horizontal brain sections from animals injected with antibodies were analysed for antibody internalisation using Alexa Fluor^{488} (BSA/Triton IHC; see earlier in this section). The presence of internalised antibody was determined together with immunolabelling for the microglial markers rabbit anti-CD11b and isolectin B4^{647}, and for the astrocytic marker rabbit anti-GFAP.

3.2.4 Microscopy

Images of brain tissue sections and cells grown on coverslips were captured using a BX50 fluorescence microscope (Olympus Co.) and/or a confocal microscope (TCS SP5; Leica Microsystems GmbH). Single optical plane images were acquired using confocal microscopy and three-dimensional reconstructions of individual cells were created by assembling successive focal planes (separated by 2 μm). These reconstructions were used to detect intracellular immunoreactivity enclosing the nucleus of cells.

3.2.5 Statistical analysis

Random images were used for analysis of the proportion of microglia and astrocytes in culture, for the proportion of various activation stages of microglia and for the internalisation of antibodies into microglia (see further description in sections 3.2.2.3 and 3.2.2.4). Quantitative results from microscopy analysis are presented as mean +/- standard deviation. A one-way analysis of variance (one-way ANOVA) was used to calculate differences in internalisation after 3 h

exposure to SR-BI^{Ab}, GFAP and a mixed IgG portion at 100 µg/ml in mixed glial cultures. A two-way ANOVA was used to analyse for significant changes in SR-BI^{Ab} internalisation after either 3 h or 6 h exposure in microglial or mixed glial cultures. Significance was determined with p values < 0.05.

3.3 Results

3.3.1 Characterisation of glial cultures

Mixed glial cultures contained 13 ± 3 % of microglia, based on immunoreactivity for CD11b/c respectively (*n = 3*; Figure 3.2). As the vast majority of cells in these cultures were positive for GFAP, 87 ± 3 % were astrocytes. In the microglial cultures, 88 ± 13 % of cells were immunoreactive for CD11b (*n = 3*; Figure 3.3).

As discussed in 3.2.2.3, microglia in mixed glial cultures were categorised according to their morphology into one of three groups that have previously been associated with different degrees of activation *(Giulian and Baker, 1986; Glenn et al., 1992; Rosenstiel et al., 2001; Stence et al., 2001; Kauppinen et al., 2008)*. Microglia with a distinct ramified morphology accounted for 20 ± 2 % of the total number of cells (*n = 3*). A clear amoeboid activated morphology was seen in 35 ± 16 % of microglia and the remaining cells had morphologies that were assigned to the non-amoeboid activated morphology group (*n = 3*).

Figure 3.2 Astrocytes and microglia in mixed glial culture *(see figure text on next page)*

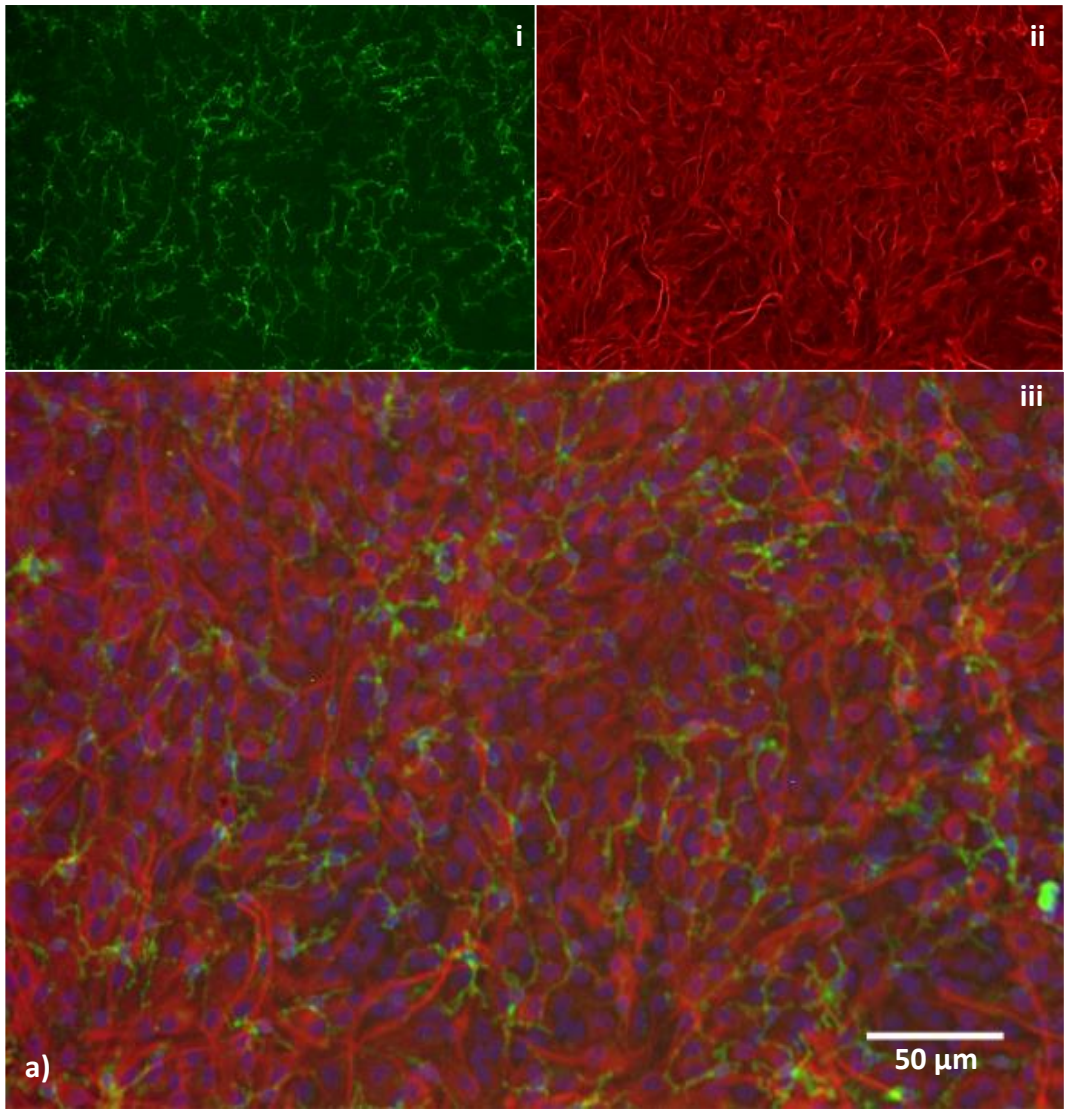

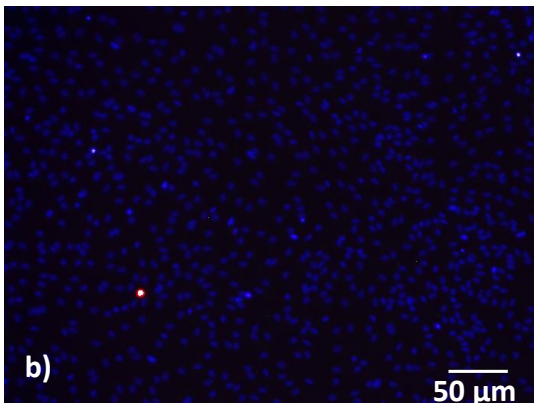

Figure 3.2 Astrocytes and microglia in mixed glial culture *in a) a representative image using fluorescence microscopy in one of three independent experiments. The microglial marker mouse anti-CD11b/c (green in panel a-i) and the astrocytic marker rabbit anti-GFAP (red in panel a-ii) immunolabelling in a merged image (panel a-iii) shows the distribution of these cell types in mixed glial cultures. Cultures treated with secondary antibodies alone did not display any immunoreactivity (b). Nuclei were labelled in a-iii and b with Hoechst 33258 (blue).*

Figure 3.3 Microglial cultures contain microglia of different activation stages

(see figure text on next page)

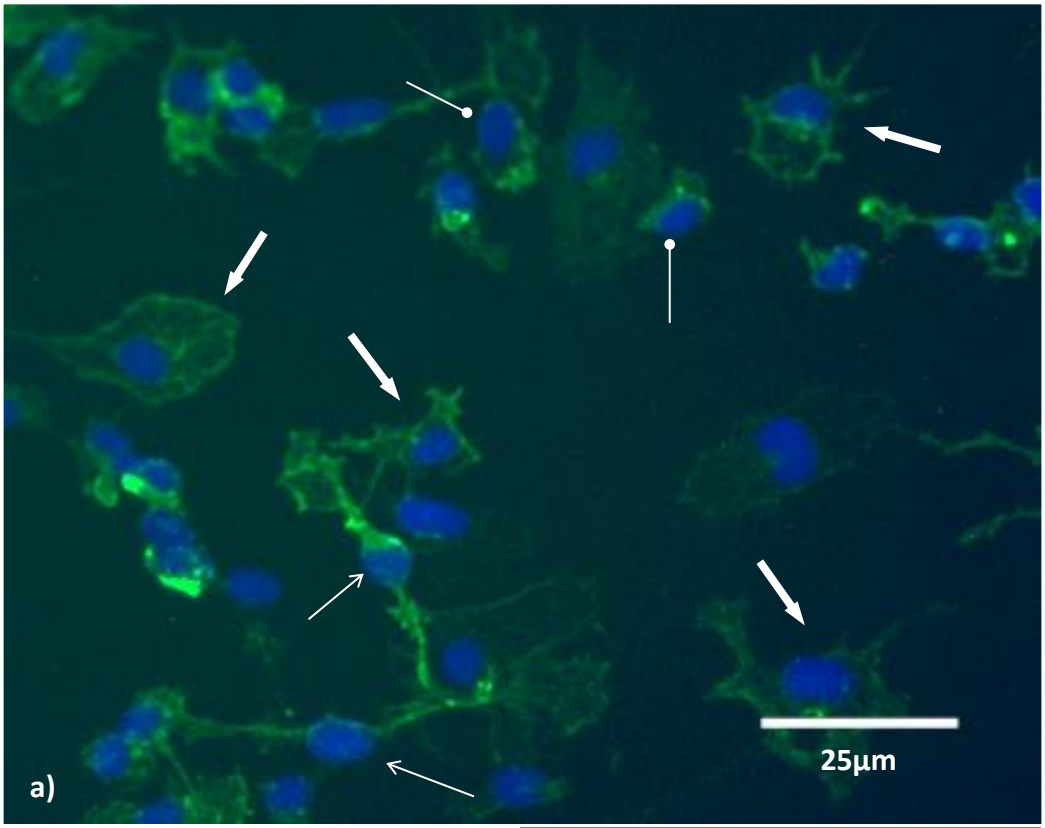

Figure 3.3 Microglial cultures contain microglia of different activation stages *(see previous page) as demonstrated using a) CD11b/c immunolabelling (green) in a representative image from one of three independent experiments. Open arrow = ramified cell, block arrow = activated non-amoeboid cell and oval arrow = activated amoeboid cell. See further explanation of morphologies in Figure 1.2. Nuclei were labelled with Hoechst 33258 (blue). Cultures treated with secondary antibodies alone did not display any immunoreactivity (b).*

3.3.2 SR-BI expression in glial cultures

In mixed glial cultures, essentially all cells were immunoreactive for SR-BI (*n = 3*; Figure 3.4). Labelling intensities were variable, with stronger fluorescence observed in microglia compared to astrocytes. The expression of this receptor was also found in essentially all cells in microglial cultures (*n = 3*; Figure 3.5). Expression of SR-BI was detected in the cell body and processes of all cells in both culture types. Fluorescence intensities were similar for ramified and non-ramified microglia.

3.3.3 Internalisation of antibodies into glial cells in culture

After purification of SR-BI^{Ab} from the hybridoma cell line, an SDS-PAGE demonstrated that the antibody had a molecular weight of approximately 150 kDa (Figure 3.6; *n = 3*), which was the same as for bovine gamma globulin. No degradation products were detected. Exposure of this SR-BI^{Ab} in mixed glial cultures and microglial cultures resulted in its detection in a large proportion of microglial cells after 3 h and 6 h (Figure 3.7). In mixed glial culture, the internalisation of the SR-BI^{Ab} was restricted to microglial cells and was detected in 44 ± 8 % of this population at 3 h, with no significant difference at 6 h ($p > 0.05$; two-way ANOVA, *n = 3* per group). Also, a large proportion (58 ± 10 %) of microglia in pure microglial cultures internalised the SR-BI^{Ab} after 3 h exposure and at similar levels after 6 h exposure. Representative images from 3 h treatment in mixed glial cultures and microglial cultures are shown in Figure 3.8 and Figure 3.9, respectively. Internalisation of the CD206^{Ab} in mixed glial cultures

Figure 3.4 Expression of SR-BI in mixed glial cultures *(see figure text on next page)*

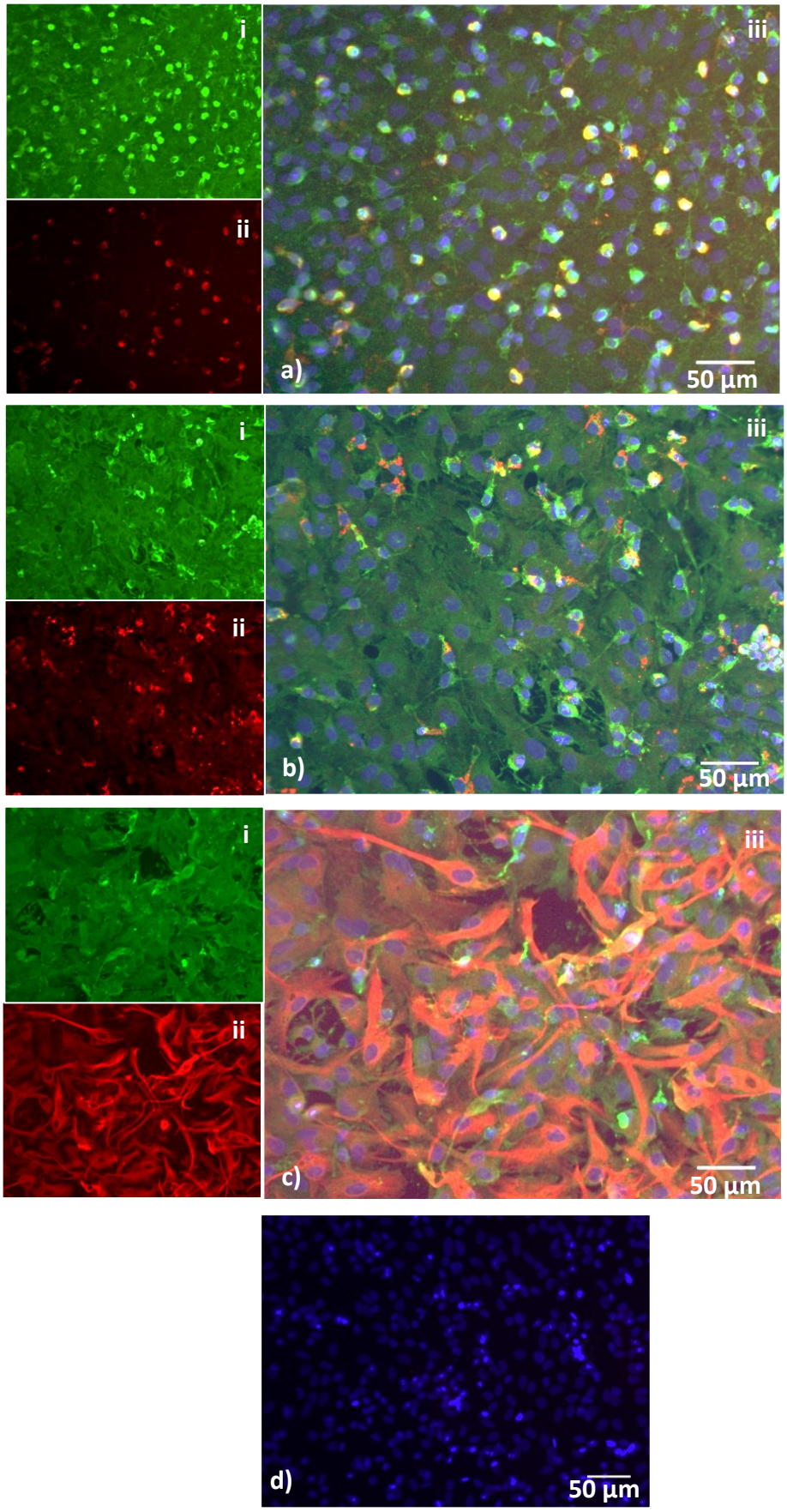

Figure 3.4 Expression of SR-BI in mixed glial cultures *(see previous page) in representative images using fluorescence microscopy from one of three independent experiments. Note that essentially all microglia and astrocytes in these cultures express SR-BI (green in panels i of a-c), as determined using the microglial marker CD11b/c (red in panel a-ii), the marker for activated microglia CD68 (red in panel b-ii) and the astrocytic marker GFAP (red in panel c-ii). Merged images (panels iii of a-c) are shown for each immunolabelling. Cultures treated with secondary antibodies alone did not display any immunoreactivity (d). Nuclei were labelled with Hoechst 33258 (blue) in a-iii, b-iii, c-iii and d.*

Figure 3.5 Expression of SR-BI in microglial cultures *(see figure text on next page)*

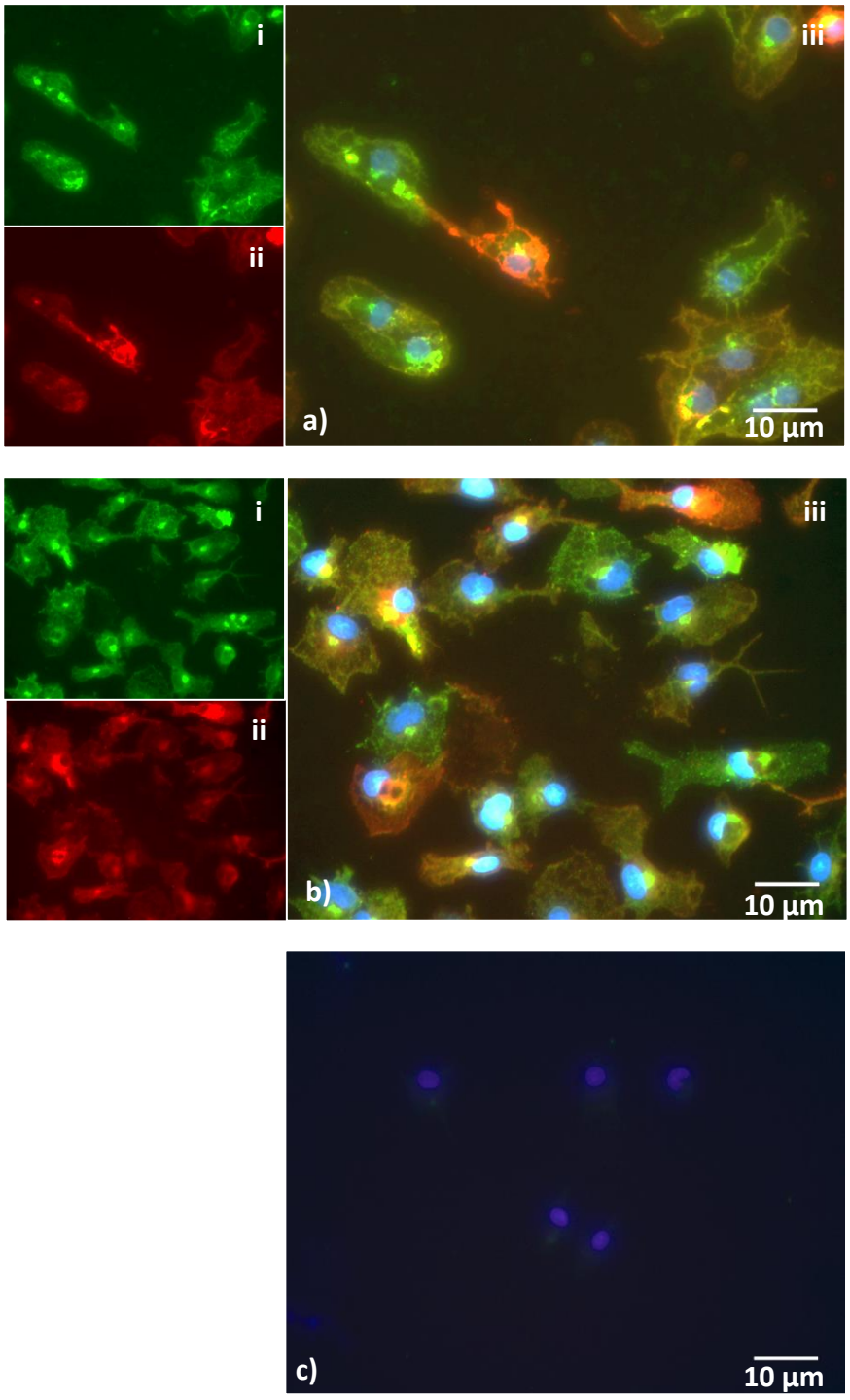

Figure 3.5 Expression of SR-BI in microglial cultures *(see previous page) as shown in representative images using fluorescence microscopy from one of three independent experiments. SR-BI expression (green in panels i of a and b) co-labelled with the microglial markers CD11b/c (red in panel a-ii) and isolectin B4^{647} labelling (red in panel b-ii), as shown in merged images (panels iii of a and b). Essentially all microglia were immunoreactive for SR-BI, independent of activation stage. Cultures treated with secondary antibodies alone did not display any immunoreactivity (c). Nuclei were labelled with Hoechst 33258 (blue).*

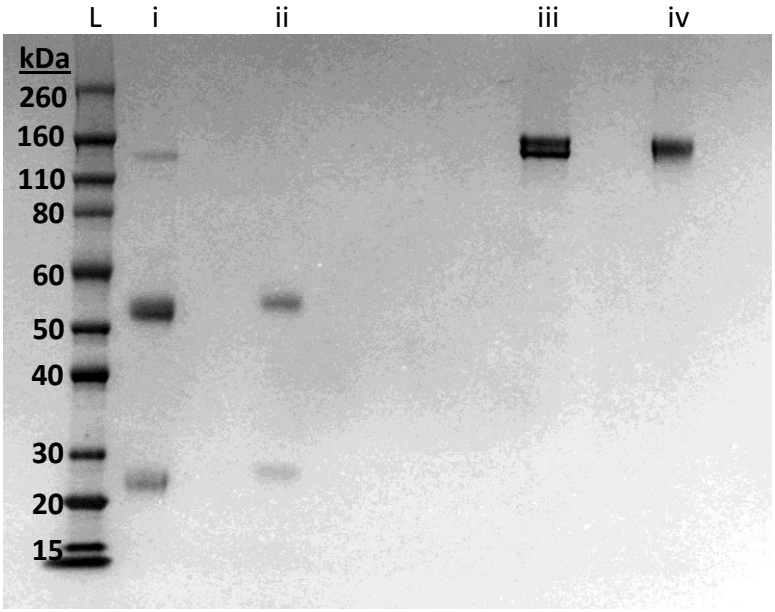

Figure 3.6 SDS-PAGE analysis of SR-BI^{Ab} *(representative image from one of thirteen independent experiments) with non-reduced SR-BI^{Ab} (iii) and the same antibody reduced using an excess of DTT to heavy-chain and light-chain residues (i). Reduced (ii) and non-reduced (iv) bovine gamma globulin were used as controls. Samples were run next to a NOVEX Sharp pre-stained protein marker with marked sizes in kDa (L) The weakly staining band at approximately 140 kDa in lane i was most likely non-reduced IgG.*

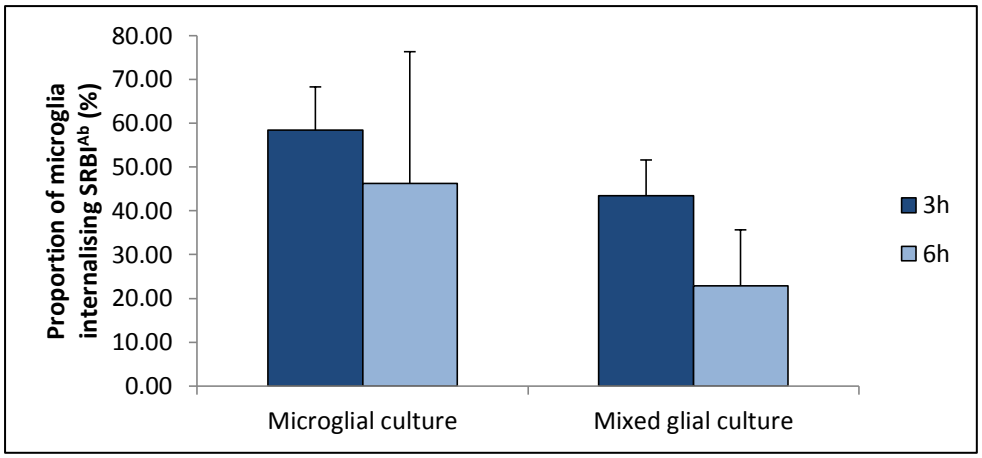

Figure 3.7 Proportion of isolectin B4^{647}-positive microglia with intracellular localisation of SR-BI^{Ab} *in microglial cultures and in mixed glial cultures 3 h and 6 h after the start of exposure. Data are presented as mean + SD. No statistically significant difference was found between culture types or between the two time points ($p > 0.05$, two-way ANOVA, $n = 3$). From this data, we conclude that a large proportion of SR-BI expressing cells, however not all cells, internalised the SR-BI^{Ab}.*

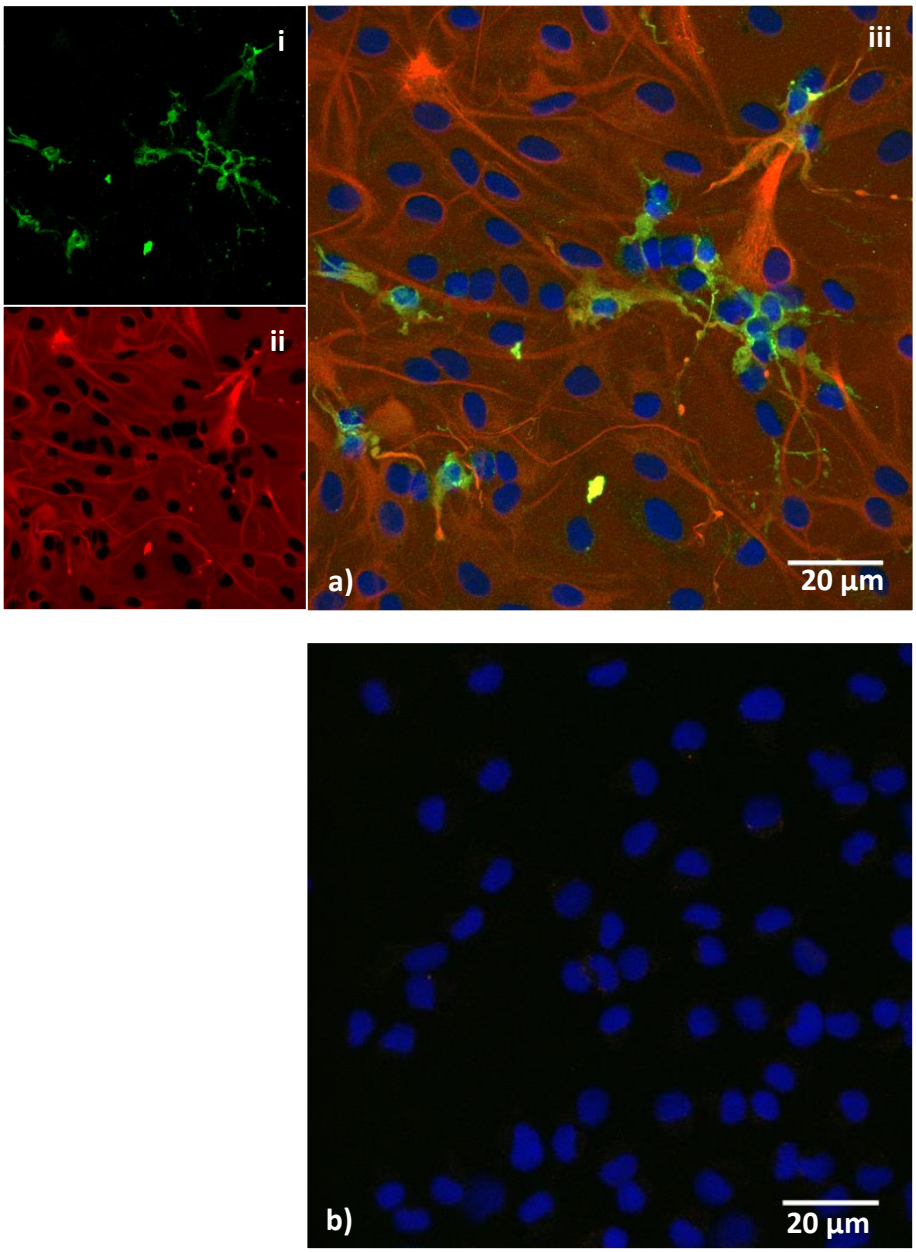

Figure 3.8 SR-BI^{Ab} internalisation in mixed glial cultures *after 3 h exposure to SR-BI^{Ab} (67 µg/ml), as demonstrated by images from confocal microscopy(in one of three independent experiments. SR-BI^{Ab} (green in panel a-i) was not detected in cells labelling for the astrocytic marker rabbit GFAP (red in panel a-ii), as seen in the merged image (panel a-iii). Cells incubated in culture medium without SR-BI^{Ab} and exposed to secondary antibodies alone displayed no immunoreactivity (b). Nuclei were labelled with Hoechst 33258 (blue).*

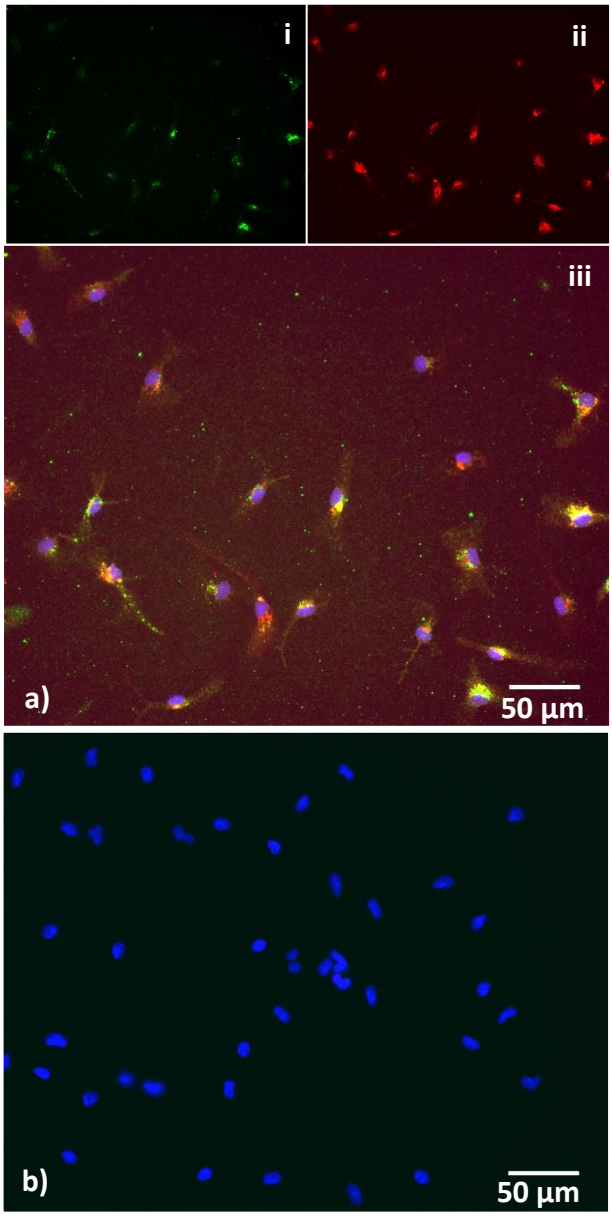

Figure 3.9 SR-BI^{Ab} internalisation in microglial cultures *after 3 h exposure to SR-BI^{Ab} (67 µg/ml), as demonstrated using fluorescence microscopy in one of three independent experiments. SR-BI^{Ab} (green in panel a-i) was detected in cells labelling for the microglial marker isolectin B4^{647} (red in panel a-ii), as shown in the merged image (panel a-iii). Cells incubated in culture medium without SR-BI^{Ab} and exposed to secondary antibodies alone displayed no immunoreactivity (b). Nuclei were labelled with Hoechst 33258 (blue).*

was detected in both astrocytes and microglia (Figure 3.10), similarly to previous results from our research group (B. Homkajorn, PhD thesis).

To further test for specificity of uptake of the SR-BI^{Ab}, this internalisation was compared in a separate study to that achieved using an antibody directed at the intracellular astrocytic protein GFAP and to a mixed IgG fraction from mouse. The use of confocal microscopy identified all three antibodies inside microglial cells in culture after 3 h exposures at concentrations of 100 µg/ml (Figure 3.11; *n = 3* per group). Internalisation levels were 58 ± 4.5 %, 42 ± 8 % and 51 ± 6 % for SR-BI^{Ab}, GFAP and for the mixed IgG fraction, respectively. There was no significant difference between the groups for this internalisation (one-way ANOVA). This suggested that internalisation of SR-BI^{Ab} may be possible through other mechanisms than via SR-BI. We did not detect any obvious changes in total cell number, glial marker expression or morphology after the exposure to any antibody used in this work.

3.3.4 SR-BI expression and internalisation of SR-BI^{Ab} in the adult rat brain

IHC using the antibody that had successfully immunolabelled SR-BI in glial cell cultures did not reveal any immunoreactivity in fixed sections of rat brain when tested under our standard conditions. There was also no immunoreactivity detected when four different antigen retrieval procedures were incorporated into the IHC protocol. Immunoreactivity for the cellular markers CD11b/c and

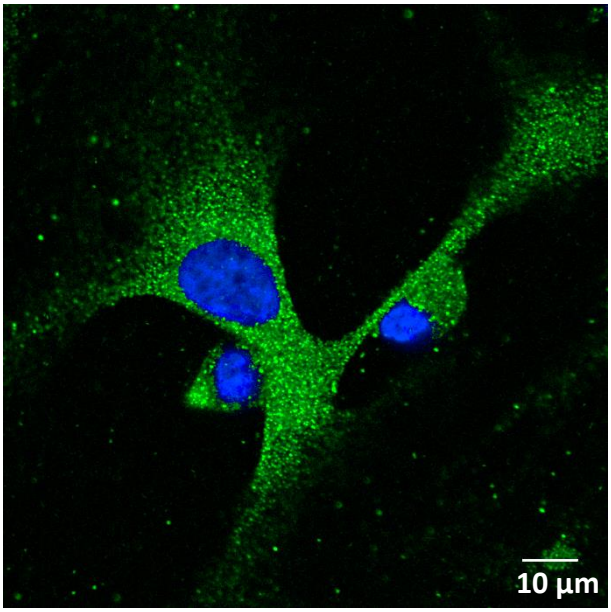

Figure 3.10 Internalisation of CD206^{Ab} in mixed glial cultures *as demonstrated in a representative image where CD206^{Ab} (green) is detected in three cells using confocal microscopy in one of three independent experiments. Cultures treated with secondary antibody alone did not display any immunoreactivity. Nuclei were labelled with Hoechst 33258 (blue).*

Figure 3.11 Detection of antibodies in the cytoplasm of cells in glial cultures

(see figure text on the following page)

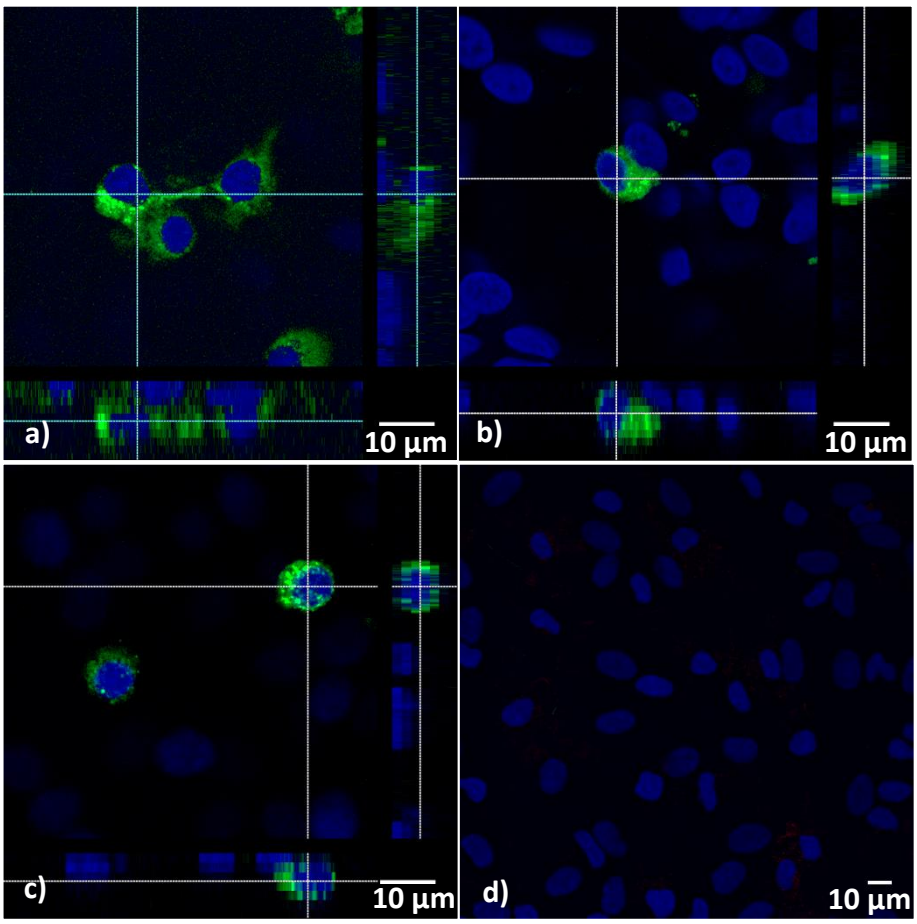

Figure 3.11 Detection of antibodies in the cytoplasm of cells in glial cultures *(see previous page). Confocal microscopy was used to determine whether exposure to specific antibodies in separate mixed glial cultures caused internalisation. Immunoreactivity detected in the same plane as the nuclei was taken as evidence for intracellular localisation of the antibody. Cultures were exposed to antibodies against SR-BI (a), GFAP (b) or to a mouse IgG antibody with no known cellular target (c), all separately at concentrations of 100 µg/ml for 3 h. Internalised antibodies were detected in fixed cultures using Alexa Flour^{488} (green). Nuclei were labelled with Hoechst 33258 (blue). A 3D representation of cells (a-c) was created by assembling stacks of 2D images obtained from successive focal planes with 2 µm intervals. The middle part of each picture shows the maximum projection of the superimposed 2D images while the smaller images below and to the right of these maximum projections show the stacks obtained perpendicular to the focal plane. As shown in these images, antibodies were found in the same plane as the nuclei, indicating that all antibodies resulted in cellular internalisation. Cells exposed to secondary antibodies alone did not display any immunoreactivity (d). These images are representative of those obtained in three independent experiments.*

GFAP was readily detected under the standard conditions and following each of the antigen retrieval protocols.

Due to uptake of the SR-BI^{Ab} and other antibodies selectively by microglia in culture, the possibility of similar uptake in the brain was tested. Intrahippocampal injections of the SR-BI^{Ab} resulted in internalisation into CD11b/c-positive microglia around the injection site (*n = 3*; Figure 3.12). In the vicinity of injection, a large majority of the cells were internalising the antibody. Internalisation of this antibody was not seen in any cells with neuronal morphology or in any cell expressing GFAP. In contrast to the specific uptake of the SR-BI^{Ab} into microglia, injections of the CD206^{Ab} resulted in internalisation by both microglia and astrocytes, with a predominant detection in the latter (*n = 3*; Figure 3.13). Also, injections of two other antibodies, Nrf2^{Ab} and X63^{Ab}, did not result in internalisation into microglial cells or any other cell type (*n = 3* per group; Figure 3.14).

After all antibody injections, activation of microglia was seen in a small area around the injection site, as demonstrated by accumulation of microglial cells with intensive CD11b/c immunoreactivity and morphological changes. Internalisation of SR-BI^{Ab} and CD206^{Ab} was observed in cells beyond this area.

Figure 3.12 Internalisation of SR-BI^{Ab} in adult rat hippocampus *(see figure text on the following page)*

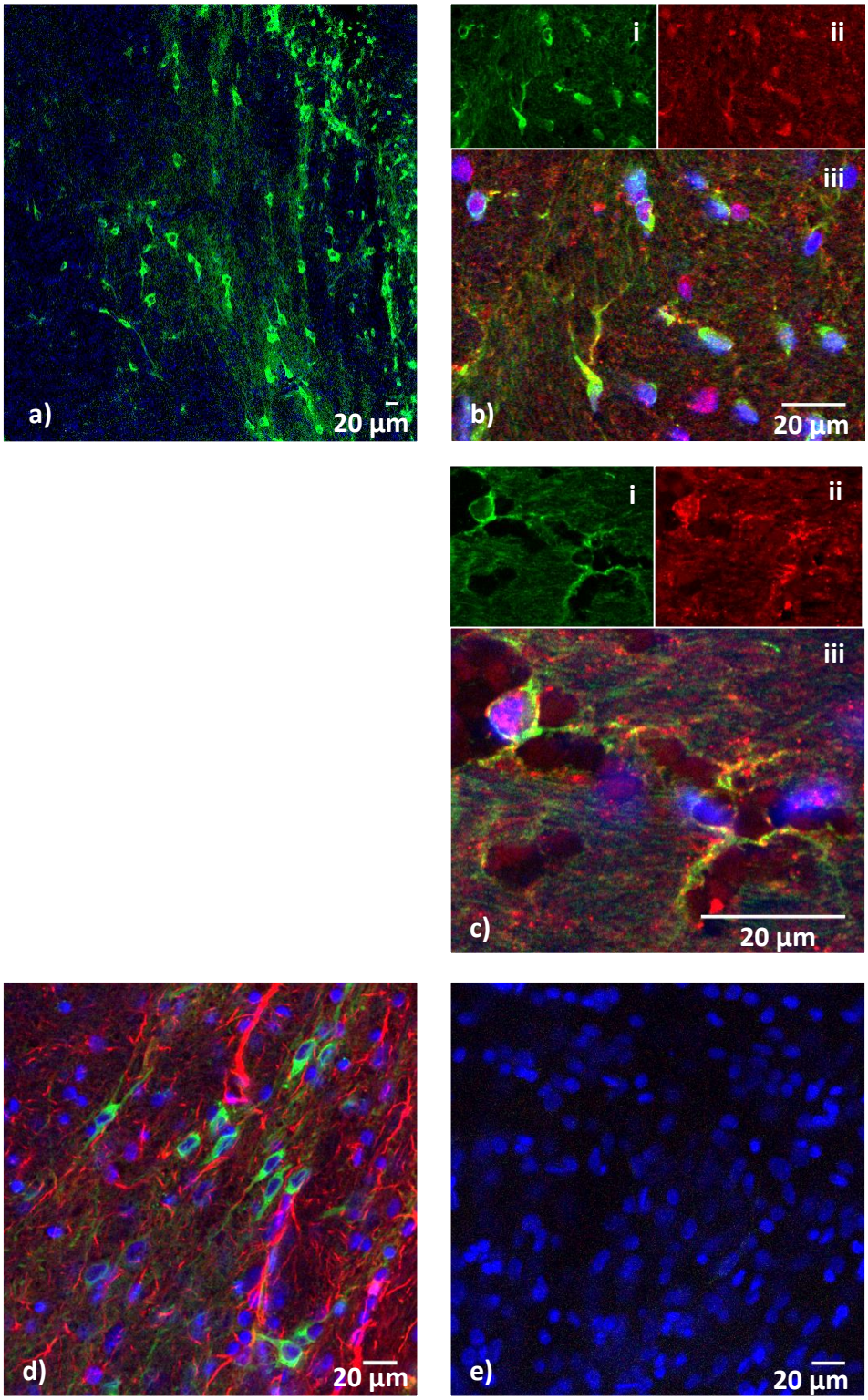

Figure 3.12 Internalisation of SR-BI^{Ab} in adult rat hippocampus *(see previous page) at 3 h after single injections (8 µg in 3 µl), as shown in representative images from confocal microscopy in one of three independent experiments. Immunoreactivity for the SR-BI^{Ab} (green in panel a, b-l, c-i and d) was exclusive for cells labelling for the microglial marker CD11b (red in panel b-ii and c-ii) in a range of activation stages (as determined through morphological observations). The injected SR-BI^{Ab} was not detected in GFAP-positive astrocytes (red in panel d) or in cells with neuronal morphology. No immunoreactivity was found in injected brains when no secondary antibodies were added (e). Furthermore, brain sections located outside the reach of the antibody injections that were exposed to secondary antibodies alone displayed no immunoreactivity. Nuclei were labelled with Hoechst 33258 (blue).*

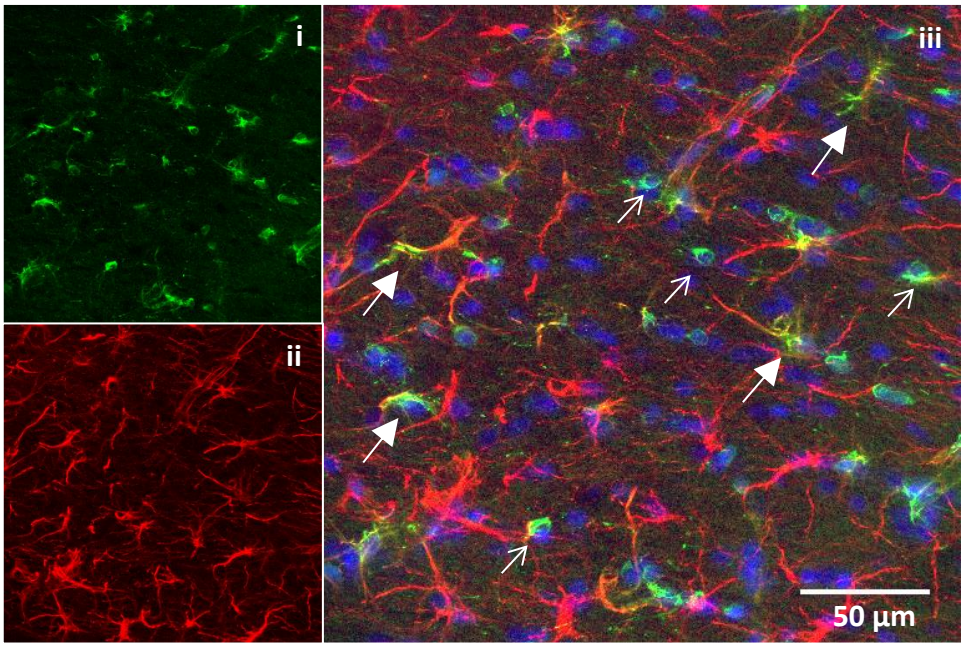

Figure 3.13 Internalisation of CD206^{Ab} in adult rat hippocampus *in a representative image using confocal microscopy from one of three independent experiments. CD206^{Ab} (green in panel i) co-labelled with the astrocytic marker GFAP (red in panel ii), as shown in the merged image (large block arrows in panel iii). Cells with microglial morphology also displayed internalisation of this antibody (small open arrows in panel iii). Brain sections located outside the reach of the antibody injections that were exposed to secondary antibodies alone displayed no immunoreactivity (see Figure 3.12e). Nuclei were labelled with Hoechst 33258 (blue).*

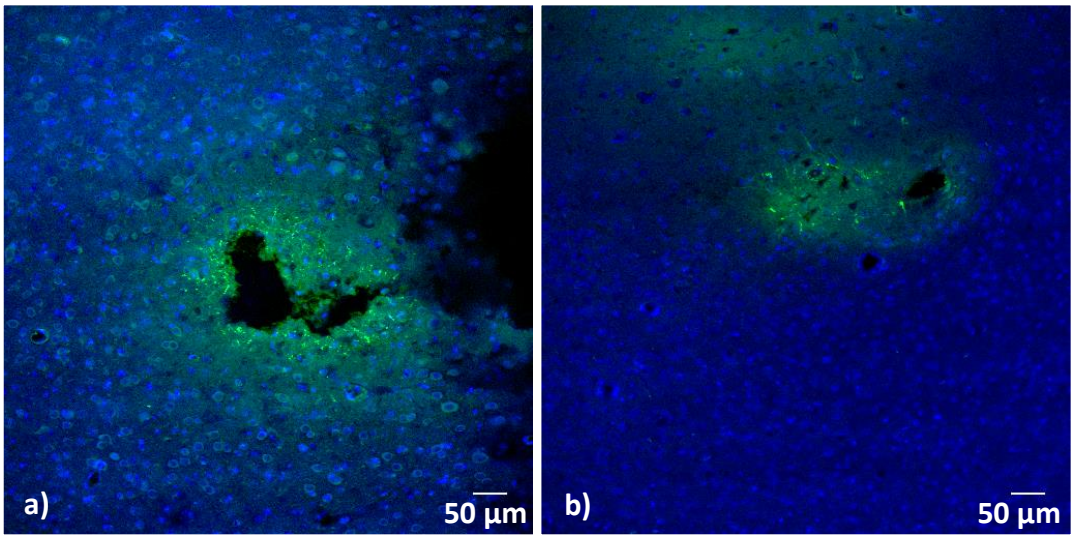

Figure 3.14 Lack of internalisation of antibodies without extracellular targets *3 h after single injections (8 µg in 3 µl), as shown in representative images from confocal microscopy in one of three independent experiments. No immunoreactivity was seen for Nrf2^{Ab} (green in a) which has an intracellular target, or for X63^{Ab} for which no antigen has been identified (green in b). Furthermore, brain sections located outside the reach of the antibody injections that were exposed to secondary antibodies alone displayed no immunoreactivity (see figure 3.12e). Nuclei were labelled with Hoechst 33258 (blue).*

3.4 Discussion

These studies assessed the expression of SR-BI in rat brain and in primary glial cultures from rat and tested the ability of glial cells in culture and *in vivo* to internalise an antibody directed against an extracellular epitope of this receptor.

The finding of most interest for our further investigations on targeted delivery of DNA in the brain was that selective cellular uptake of the SR-BI^{Ab} was seen following injections into the adult rat hippocampus. Internalisation of SR-BI^{Ab} was almost fully restricted to microglia, based on co-labelling with CD11b/c. Internalisation was not seen using other antibody preparations with an intracellular target or without an identified antigen, indicating that uptake most likely required specific interactions between SR-BI and the SR-BI^{Ab}.

Internalisation of the SR-BI^{Ab} by microglia, but not astrocytes, was also seen in mixed glial cultures. However, other antibodies and a mixed IgG preparation were also internalised by the microglia suggesting that, at least in part, the uptake of the SR-BI^{Ab} in these cells in culture may have involved a mechanism that did not depend on specific properties of SR-BI^{Ab}. This process could involve other parts of the immunoglobulin or be due to a relatively non-selective uptake of a wide range of material from the extracellular space (for example via phagocytosis/pinocytosis).

In primary cultures prepared from neonatal rat brains, SR-BI was detected using immunolabelling in both microglia and astrocytes, consistent with previous reports *(Alarcon et al., 2005; Zhang et al., 2006)*. In contrast to the findings in culture, no immunoreactivity for SR-BI was detected in any cells in adult rat brain when assessed using either our standard conditions for brain IHC or several approaches to promote antigen retrieval. The lack of detectable expression in microglia in adult brain, despite expression in cells in primary cell cultures, is consistent with findings in mice *(Husemann and Silverstein, 2001)*. However, in both adult mouse and human brain, SR-BI expression was observed in astrocytes *(Husemann and Silverstein, 2001)*. Thus, the lack of detectable expression in astrocytes of adult rat brain suggests a possible difference between species. Additional approaches such as assessment of gene expression using *in situ* hybridisation, would be needed to further evaluate this apparent difference between species.

Both in the rat brain tissue and in primary cell cultures, there were marked differences between the cells showing internalisation of the SR-BI^{Ab} and the pattern of expression of SR-BI that was detected using immunolabelling. Possible explanations for this mismatch and the mechanisms involved in antibody internalisation are further considered in the following sections.

3.4.1 SR-BI expression and SR-BI^{Ab} internalisation in culture

As microglia were found to internalise a range of IgGs in mixed glial cultures, the most likely explanation for differences seen in SR-BI^{Ab} internalisation in astrocytes and microglia in culture, is that this does not occur via SR-BI. However, we cannot exclude the fact that at least some of the SR-BI^{Ab} uptake involved specific interactions with SR-BI. If so, this would indicate differences in cellular handling of this receptor between astrocytes and microglia. One possible explanation is that the extent of internalisation into astrocytes was below the sensitivity for detection using secondary antibodies.

As discussed in section 3.1.2.1, binding of a ligand to SR-BI may lead to different responses depending on the cell involved and, in some instances, on the nature of the ligand. For example, the delivery of cholesterol from HDL in many cells requires binding of the HDL to SR-BI, but cholesterol transfer occurs without internalisation of either the receptor or the ligand *(Connelly et al., 2003; Hu et al., 2010)*. An alternative process known as retroendocytosis may also operate for the delivery of HDL cholesterol and potentially other ligands *(Rhainds et al., 1999; Gillotte-Taylor et al., 2001; Ohgami et al., 2001; Rhainds and Brissette, 2004)*. This involves transient uptake of the receptor-HDL complex with subsequent extraction of the cholesterol and return of the cholesterol-depleted HDL to the cell surface. In addition, other SR-BI ligands have been co-localised with clathrin or caveolin-1 or shown to be processed via endosomes and

lysosomes. These findings indicate the likely involvement of SR-BI in receptor-mediated endocytosis under some conditions.

The role of SR-BI in astrocytes and microglia and the cellular responses following ligand binding are not well understood. In astrocytes, SR-BI has been proposed to contribute to HDL-mediated exchange of cholesterol similarly to what has been seen in tissues other than the brain *(Husemann and Silverstein, 2001)*. In these tissues, SR-BI plays an important role in lipid incorporation into the plasma membranes and also in the clearance of plasma cholesterol *(Husemann et al., 2002)*.

In contrast to astrocytes, the SR-BI^{Ab} was internalised into microglial cells similarly to what has been found with regards to other ligands of SR-BI *(Wishart and Mackinnon, 1990; Acton et al., 1996; Calvo et al., 1997; Parathath et al., 2004; Zhang et al., 2006; Brandenburg et al., 2007; Ji et al., 2011)*. The function of SR-BI in microglia has not been studied in detail. However, in cultures containing other cells of the monocyte/macrophage lineage, SR-BI has been shown to be more involved in the removal of its ligands, rather than incorporation of these ligands into the plasma membrane *(Murao et al., 1997)*. Also, as previously mentioned, internalisation of SR-BI ligands into cells of the monocyte/macrophage lineage is not regulated to the same extent as in other cells, causing a high influx of SR-BI ligands into cells of this lineage *(Krieger,*

1999). Thus, the lack of internalisation of SR-BI^{Ab} despite the presence of the receptor in astrocytes in culture might reflect roles for this receptor that require ligand binding but not subsequent internalisation.

In our studies, we observed a higher intensity of SR-BI expression in microglia than in astrocytes of mixed glial culture. This may indicate that there is a higher expression level of this receptor in microglia that could contribute to differences in uptake of SR-BI^{Ab}. However, differences in morphology and/or distribution of the receptor on the cell surface are other factors more likely to contribute to these variations in intensity *(Marzolo et al., 2000)*. Furthermore, as SR-BI should still be available to some extent on the cell surface of astrocytes, some degree of antibody internalisation would have been expected also in astrocytes.

There is however a possibility that SR-BI is found mainly intracellularly in astrocytes, which has been shown in studies of other receptors, including the mannose receptor. This receptor is expressed at similar levels in both astrocytes and microglia *(Burudi et al., 1999)*. However, when cells are exposed to horseradish peroxidase (HRP; a ligand to the mannose receptor), a lower amount of HRP is detected in astrocytes compared to microglia. This study also showed that the internalisation rate of HRP was slower in astrocytes than in microglia, and reached a plateau 2 h after the start of exposure. In contrast, the internalisation rate of HRP into microglia was increasing at least up to 4 h after

the start of cell treatment. The difference in internalisation rate in these studies was attributed to the observation that a higher proportion of the mannose receptor was found intracellularly in astrocytes compared to membrane-bound *(Burudi et al., 1999)*. This variability between astrocytes and microglia in receptor localisation could potentially also be attributed to SR-BI.

Other receptors expressed by both astrocytes and microglia have been shown to result in different intracellular signals after binding the same ligands. One example is demonstrated by responses after exposure to prion proteins, where this has produced higher levels of cyclic adenosine monophosphate activation and phosphorylated extracellular-signal-regulated kinases in astrocytic cultures in comparison to microglial cultures *(Brandenburg et al., 2007)*. Another example of differential responses to the same stimuli between astrocytes and microglia is that observed after agonist binding to TLR7 and TLR9. This binding has been demonstrated to produce a larger set of cytokines in microglia compared to astrocytes *(Butchi et al., 2010)*. These examples constitute evidence that some receptors expressed by both microglia and astrocytes can respond differently to the same stimuli in the two cell types.

The internalisation of SR-BI^{Ab} into microglia is similar to that of other receptors expressed by both astrocytes and microglia in culture *(Burudi et al., 1999; Brandenburg et al., 2007)*. One example is the formyl-peptide-receptor-like-1, through which prion proteins have been shown to initiate internalisation of

similar levels of this receptor into microglia and astrocytes, as determined in an enzyme-linked immunosorbent assay *(Brandenburg et al., 2007)*. This study exemplifies the commonly found difference in the number of cells expressing a receptor to those internalising a ligand to this receptor. The discrepancy is similar to our study where essentially all cells expressed SR-BI, but only 40 - 60 % internalised the SR-BI^{Ab}.

As previously mentioned, it has been suggested that microglia may internalise IgG antibodies and IgG antibody aggregates after stimulation of Fc-γ receptors *(Aihara et al., 1994; Wilcock et al., 2004; Hazama et al., 2005; Okun et al., 2010)*. Microglia express all types of Fc receptors, whereas only a few receptors of this family have been detected in astrocytes and other cells of the nervous system *(Okun et al., 2010)*. However, internalisation via these receptors normally occurs due to aggregation of antibodies, which may have been occurring under the conditions used for the tests in culture with relatively high concentrations of antibody. In the healthy brain, Fc-γ receptors are only expressed at low levels in microglia and astrocytes and have been detected mostly in cells with activated morphologies in culture *(Vedeler et al., 1994; Okun et al., 2010)*. Fc-γ receptors are therefore generally expressed by activated cells.

In this study, we demonstrated the internalisation of SR-BI^{Ab} into microglia of various activation stages in culture and *in vivo*, also indicating that this was not

linked to activity. The method used in ths work to determine microglial activation stages was based on cellular morphology. It is important to mention that there are other, more widely used markers of activation that are based on the expression of different proteins, including cyclooxygenase 2, NO and TNF-α (see section 1.2.3).

In summary, as microglia stem from the same myeloid linage as monocytes/macrophages, the extensive internalisation via SR-BI into cells of this lineage may explain the detection of SR-BI^{Ab} in microglia. After internalisation into these cells, SR-BI ligands may enter a traditional endocytic or a retroendocytic pathway. The function of SR-BI in astrocytes may involve the mere delivery of the cargo, rather than the ligand itself, similarly to the selective cholesteryl ester uptake mechanism. This could explain the lack of detected SR-BI^{Ab} inside astrocytic cells in our studies.

3.4.2 SR-BI expression and SR-BI^{Ab} internalisation in adult rat brain

In contrast to mixed glial cultures, the SR-BI^{Ab} was most likely internalised via specific mechanisms into microglia of the adult rat brain. This was supported by injections of an antibody with an intracellular target (Nrf2^{Ab}) and an antibody for which no antigen has been identified (X63^{Ab}), which did not result in internalisation into any cell type.

Also, other IgG antibodies targeted at cell-specific receptors have been injected into the rodent brain. For example, an IgG antibody targeted against a low affinity NGF receptor in the plasma membrane has been used to target cholinergic neurons in rat brain through intraventricular injections *(Book et al., 1992; Gu et al., 2000; Browne et al., 2001)*. Another example is an IgG antibody against p75 neurotrophin receptor ($p75^{NTRAb}$), which has been used to target basal forebrain neurons *(Berhanu and Rush, 2008)*. These studies do not report any microglial internalisation of the specific IgG antibodies that would indicate non-specific internalisation into microglia. This is in contrast to our studies in culture, where microglial cells had the capacity to internalise other IgG antibodies than $SR\text{-}BI^{Ab}$. However, these cells generally reach more activated stages and do not reflect the natural environment of the healthy CNS.

Thus, work presented in this chapter and in other *in vivo* studies point towards the lack of non-specific uptake of IgG antibodies by microglia *in vivo* and supports the view that the $SR\text{-}BI^{Ab}$ is internalised selectively by microglia in the adult rat brain.

Internalisation of $SR\text{-}BI^{Ab}$ into microglia of the adult rat brain was in contrast to the lack of immunoreactivity for SR-BI in this tissue. No immunoreactivity for this receptor was found in any cell type in the adult rat brain, although an extensive range of protocols was used in order to achieve immunolabelling. In preliminary

studies, SR-BI had been detected in liver and testis, however we were unable to obtain any such staining in the adult rat brain. All other cellular markers successfully labelled their antigens in the adult rat brain.

These results suggest that there is no SR-BI expression in adult rat brain, in contrast to the findings of SR-BI in cultures derived from neonatal rat. We might assume that SR-BI expression in our primary cultures reflects that of the neonatal rat brain, however we do acknowledge that immunohistochemistry has not been conducted in this tissue. Under the assumption that the primary cultures truly reflect that of the neonatal brain, SR-BI expression in this tissue in comparison to that of the adult may indicate a developmental shift of SR-BI expression in both astrocytes and microglia of the rat brain. A similar developmental shift has been found for SR-BI in microglia of the adult rat brain of mouse *(Husemann and Silverstein, 2001)*. As the SR-BI antibody used in IHC worked in culture and numerous antigen retrievals were unable to improve SR-BI immunolabelling *in vivo*, it is not likely that the lack of astrocytic SR-BI expression in the adult rat brain is due to difficulties in IHC. However, we cannot eliminate the possibility that SR-BI is expressed on some cells of the adult rat brain, but in a modified form and/or that the antigenic site is inaccessible in this tissue using available antibodies and antigen retrieval techniques.

The apparent difference in SR-BI detection in the adult brain when comparing this work and that of Husemann et al. (2001) is consistent with other variations in receptors identified on glial cells in rat compared to mouse. For example, astrocytes in mouse and rat express different subunits of the sodium-potassium-ATPase when grown in culture from newborn animals *(Peng et al., 1998)*. Another example of differences in other aspects of glia between the two species is the recruitment of microglia in the CNS of injured adult mouse compared to rat, where the latter results in little to no transformation of infiltrated cells into microglial resident cells *(Lambertsen et al., 2011)*. Furthermore, neonatal culture from brain of mouse and rat also differ with respect to glial proliferation, intermediary filament expression and morphological changes in response to scratch wound models *(Puschmann et al., 2010)*.

Reasons for the mismatch of SR-BI^{Ab} internalisation into microglia without any SR-BI immunoreactivity achieved in IHC may be that a) the uptake of SR-BI^{Ab} into microglia occurred through processes that did not require binding to a specific receptor (similarly as described in culture, section 3.4.1), or b) SR-BI is present on microglia, but the antigenic site is hidden or modified, and cannot be detected using IHC in fixed brain. The use of different antibodies for detecting SR-BI by IHC and for the internalisation analysis could have contributed to the apparent mismatch. Thus, modifications affecting binding of the polyclonal antibody used for SR-BI IHC targeted at the intracellular part of the receptor might not have affected internalisation by the monoclonal antibody directed against an

extracellular part of the receptor in live cells. The antibody targeted at the extracellular part of the receptor (used in internalisation studies) had previously been shown to be unsuitable for IHC in fixed tissue (in brain, liver and testis) and in cell culture in preliminary studies.

However, as mentioned in the start of this section, the results presented in this work strongly demonstrate that an antibody against SR-BI can be used to target specifically microglia of the adult rat brain. A large majority of the cells in the vicinity of the injection internalised the antibody. As it would require substantial and complicated three-dimensional analysis of numerous sections, a quantitiative investigation of this internalisation was not performed.

3.4.3 Concluding remarks

We have demonstrated a potential method to target microglial cells in the adult rat brain. The data suggest that the SR-BI^{Ab} has the potential to be used for delivery of cargo selectively to the microglial population of the adult rat brain. This opens possibilities to obtain further knowledge on microglial function.

CHAPTER 4: SR-BI^{AB}

IMMUNOPORTERS AS TOOLS FOR TRANSFECTION OF GLIAL CELLS

4.1 Introduction

There are no established methods which offer targeted, transient gene delivery specifically to microglia *in vivo* (as previously discussed in section 1.6). A viral transduction in conjunction with cell-specific promoters has shown the potential to selectively transduce microglia in the intact brain *(Cucchiarini et al., 2003)*. However, this approach still involves the delivery of DNA to several cell populations of the brain. Furthermore, it has not been widely adopted by other investigators.

Novel non-viral methods have been used to target specific cell populations, involving the use of cell surface receptors. In the previous chapter, we demonstrated the selective internalisation of SR-BI^{Ab} into microglia of the intact rat brain. This chapter builds on these findings to test whether immunoporters based on the SR-BI^{Ab} can be used to selectively transfect microglia.

4.1.1 Transfection using immunoporters

An immunoporter is formed from an antibody covalently linked to a polycation. The antibody provides cellular targeting and the polycation provides the capacity to bind a nucleic acid sequence of interest. These immunoporters, and also similar constructs where smaller peptides are used rather than a whole antibody, have been used to achieve receptor-mediated gene delivery in a range of cell types *(Shimizu et al., 1996; Navarro-Quiroga et al., 2002; Barati et al.,*

2006; Zeng et al., 2007; Berhanu and Rush, 2008; Duan et al., 2008). After the binding of nucleic acids to an immunoporter, an immunogene is formed. This immunogene has the capacity to enter cells via receptor-mediated endocytosis and deliver the bound nucleic acid into cells. Constructs in which DNA bound to a polycation is linked to antibodies directed against cell surface receptors were initially termed immunogenes *(Shimizu et al., 1996)*. These constructs have continued to be identified using this term in subsequent studies by other research groups *(Berhanu and Rush, 2008)* and we have adopted the same terminology. The word immunogene has also been used as a term in DNA vaccination therapy but has a different meaning in that context *(Nakamura et al., 1994)*.

The immunogene approach has previously been utilised to target neurons in the CNS and in brain-derived cells in culture *(Barati et al., 2006; Berhanu and Rush, 2008)*. In these studies, a monoclonal antibody against p75^{NTR}, a receptor expressed by predominantly neurons, has been used in the construction of a p75^{NTRAb} - PLL immunoporter. This construct had the capacity to deliver plasmid DNA coding for GDNF. The mechanism through which this was delivered was retrograde transport from nerve terminals of motor neurons in the periphery, to some of these cells in the spinal cord *(Barati et al., 2006)*. After injection of this construct into the hindlimb of neonatal rat, GDNF expression had a prophylactic effect on damage induced by sciatic nerve axotomy *(Barati et al., 2006)*. In the adult rat, GDNF expression after p75^{NTRAb} - PLL delivery had the capacity to

protect against motor neuron death subsequent to axotomy of either the sciatic nerve or the hypoglossal nerve *(Barati et al., 2006)*.

Immunoporters targeting the same p75^{NTR} have been used to deliver plasmids producing siRNA against tropomyosin-receptor-kinase A (TrkA) to forebrain neurons. Intraventricular osmotic pump infusions of a similar p75^{NTRAb} - PLL complex with a few improvements to enhance transfection, resulted in decreased neuronal TrkA receptor expression. This was manifested in lower spatial learning and memory capacity in Morris water navigation task *(Berhanu and Rush, 2008)*.

Immunoporters have also been used in tumour treatments, including one construct targeting G250 receptors in renal cell carcinoma *(Duan et al., 2008)*. However, the use of these constructs is to our knowledge unexplored in tumours of the brain. Other constructs containing antibody derivatives have been used to act as targeting units in immunoporters, predominantly in cell lines *(Chen et al., 1998b; Merdan et al., 2003; Germershaus et al., 2006)*. For example, derivatives of an antibody against epidermal growth factor receptor have been used to initiate receptor-mediated endocytosis of this moiety bound to PLL *(Chen et al., 1998b)*.

Additional versions of non-viral vectors with similar mechanism as immunoporters have been based on smaller peptides. For example, a recombinant peptide composed of a nerve growth factor loop 4 hairpin motif and a 10 lysine DNA-binding-binding moiety has been used to deliver plasmid DNA to cells expressing the TrkA receptor in culture *(Zeng et al., 2007)*. The addition of a PEI moiety that partially compacted the DNA, improved the transfection capacity of this construct. This demonstrated the advantage of ensuring DNA delivery using this polycation. Another example is the selective targeting and subsequent transfection of dopamine neurons in the substantia nigra of the adult brain *(Navarro-Quiroga et al., 2002)*. In this study, neurotensin was used to initiate internalisation via the neurotensin receptor. After injection of a neurotensin-PLL construct, reporter gene expression was observed in substantia nigra from 48 h up to 60 days after transfection *(Navarro-Quiroga et al., 2002)*.

Non-viral constructs such as immunoporters could potentially be used to achieve gene delivery and modify protein expression specifically in microglia. Hence, the specific aims of these studies were:

a) to develop procedures for preparing SR-BI^{Ab} - based immunoporters
b) to test whether glial cells can be transfected by SR-BI^{Ab}-based immunogenes in culture and in the adult rat brain
c) to analyse for potential effects on cell properties by immunogenes in glial culture, including microglial activation.

4.1.2 Construction of immunoporters

Two types of SR-BI^{Ab} - based immunoporters were produced incorporating either PLL or PEI as polycation. These two polycations have the capacity to bind nucleic acids and have been widely used for transfection purposes (see section 1.4.4.2). PLL contains a long chain of positively charged lysine residues and PEI consists of ethylenimine residues *(Kopatz et al., 2004; Barati et al., 2006; Hsu and Uludag, 2008)*. Both PLL and PEI have the capacity to be internalised via non-specific endocytosis *(Kopatz et al., 2004; Wagner and Kloeckner, 2006; Choi et al., 2007)*.

With regards to the use in immunogenes and similar transfection methods where other mechanisms are responsible for internalisation, PLL has been used due to its capacity to carry DNA and protect it from the external environment *(Wu and Wu, 1987; Perales et al., 1994; Ziady et al., 1999; Navarro-Quiroga et al., 2002; Barati et al., 2006; Wagner and Kloeckner, 2006; Choi et al., 2007; Hsu and Uludag, 2008)*. PEI has also been shown to have a much better capacity to escape intracellular vesicles and its use has increased over the years in similar constructs *(Boussif et al., 1995; Sonawane et al., 2003; Kopatz et al., 2004; Harada et al., 2006; Wagner and Kloeckner, 2006; Xiong et al., 2007; Breunig et al., 2008; Feng et al., 2008; Deng et al., 2011)*.

The methods for preparing the immunogenes used in this work were initially derived from protocols used by our collaborators to modify gene expression in

neurons *(Berhanu and Rush, 2008)*. These constructs are generally believed to follow certain intracellular pathways after classical receptor-mediated endocytosis, which are illustrated in Figure 4.1. Based on the selective internalisation of SR-BI^{Ab} into microglia in culture and in the adult rat brain, we investigated the possibility to produce an immunogene from this antibody that would selectively target microglia.

Combination of a polycation with a targeting moiety such as an antibody to form an immunoporter can be achieved through the use of chemical cross-linking. Different functional groups on these polyamines may be targeted, including sulfhydryl groups (thiols), carbonyls, carbohydrates and carboxylic acids *(Mattson et al., 1993)*. The binding of two (or more) moieties using cross-linkers is said to be a process of conjugation, and the end product is called a conjugate.

Sulfhydryl groups are often used to conjugate polyamines as they provide a linker that is readily disrupted by acidification in intracellular vesicles *(Gosselin et al., 2002; Saito et al., 2003; Schaffert and Wagner, 2008)*. This enables the separation of a targeting moiety and a DNA-carrying moiety for enhanced escape from these intracellular compartments (see section 1.4.6.1).

Traut's reagent (classical name for *2-iminothiolane hydrochloride*) is a water-soluble cyclic thioimidate cross-linker capable of incorporating sulfhydryl groups

Figure 4.1 General view of potential intracellular pathway for internalised immunogenes *(see figure text on next page)*

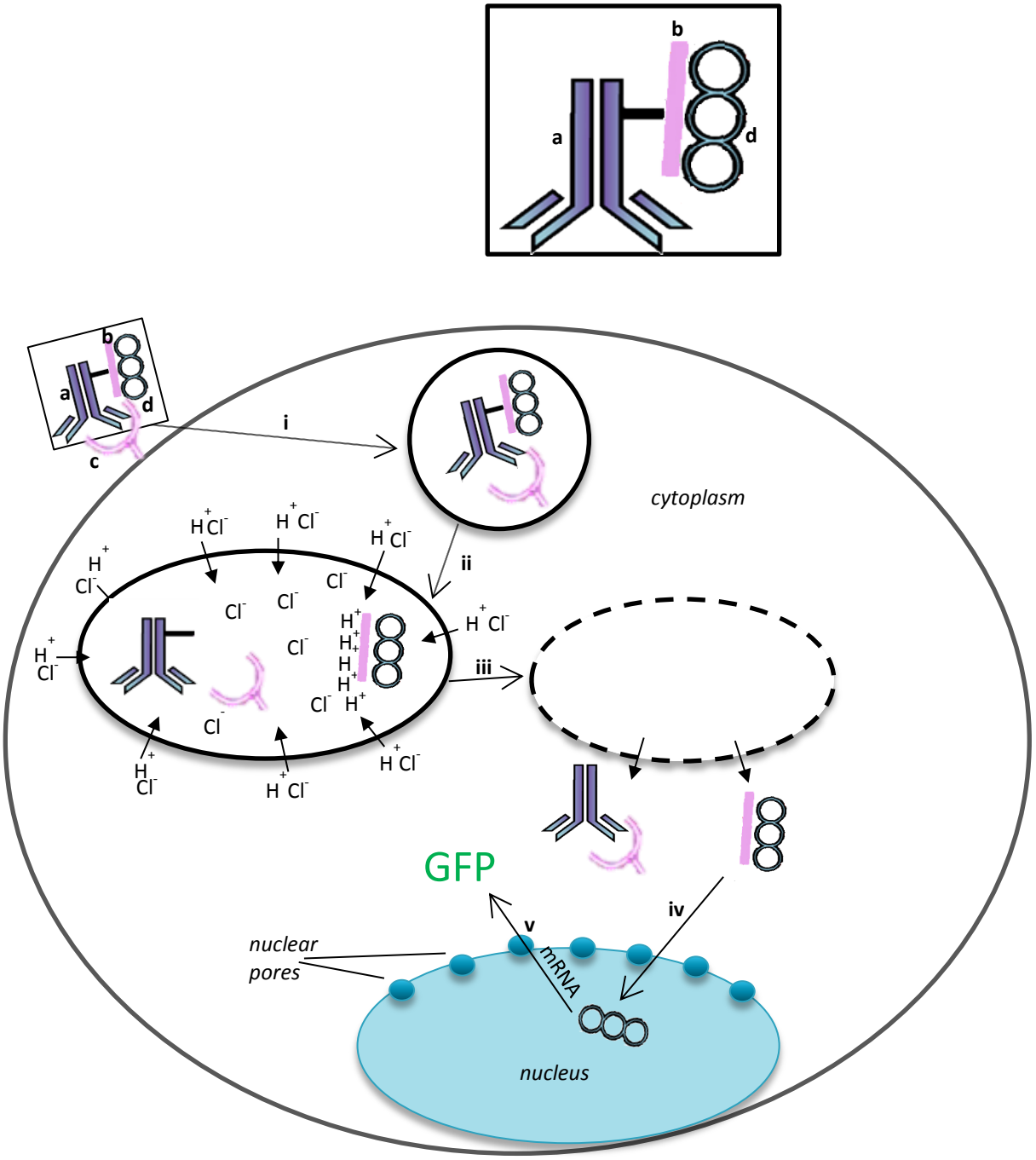

Figure 4.1 General view of potential intracellular pathway for internalised immunogenes *(see previous page). The key components of an immunogene (framed) consist of an antibody (a) cross-linked with a polycation (b) with the capacity to bind DNA (d). This figure also explains parts of the proposed mechanism behind receptor-mediated gene delivery using immunogenes. The antibody (a) moiety guides the internalisation (i) of the construct into the cell, via a cell-specific receptor (c). After this, the construct enter the endosomal/lysosomal pathway or caveosomal pathway (ii), depending on the nature of the receptor (c) through which the construct is internalised. As mentioned previously, it has been suggested that caveosomes later merge with the endosomal/lysosomal pathway. In a classical endosomal/lysosomal pathway, the intracellular vesicle is subjected to decreasing pH through the influx H^+. When the polycation (b) is PEI, it has the capacity to absorb these hydrogen ions. This leads to intravesicular accumulation of Cl^- accompanying the H^+ during the continued ion influx. This accumulation increases the osmolarity of the vesicle, causes water absorption and eventually ruptures this vesicle (iii), releasing its contents into the cytoplasm. For polycations including PLL that lack this buffering capacity at acidic pH, release from vesicles occurs via an unknown mechanism. After release into the cytoplasm, the DNA (d) is transported into the nucleus (iv) where the gene of interest is transcribed to mRNA, and translated into a protein, such as GFP (v). Nuclear translocation is achieved via nuclear pores, which allow for passive diffusion of smaller molecules, or via active transport of larger molecules in the presence of nuclear localisation signals.*

on primary amines *(Thorpe et al., 1987; Mattson et al., 1993)*. Sulfosuccinimidyl6-(α-methyl-α[2-pyridyldithio]-toluamido)hexanoate (Sulfo-SMPT; abbreviated from hereon as SMPT) and N-succinimidyl 3-(2-pyridyldithio)propionate (SPDP) are examples of heterobifunctional N-hydroxysuccinimide-ester pyridyl disulphide cross-linkers *(Mattson et al., 1993)*. When SMPT or SPDP are reacted with primary amines, this introduces a disulphide bond *(Thorpe et al., 1987)*. This can be reduced into a sulfhydryl *(Carlsson et al., 1978)* using for example DTT and used as a target for a second agent containing a sulfhydryl group to link two components together.

4.1.3 Analysis of immunoporters

After binding an antibody to a polycation, the capacity of this immunoporter to carry DNA can be determined in an electrophoretic mobility shift assay (EMSA). This assay is based on the reduction in electrophoretic mobility of DNA upon binding other macromolecules *(Lane et al., 1992)*. The positive charges of the polycation moiety neutralise the negative charge of the DNA and allow for compaction of the latter. This neutralisation obstructs the movement of DNA through the gel towards the anode *(Chen et al., 1994)* and inhibits detection of the DNA in the gel (using for example ethidium bromide). Full charge neutralisation of the DNA by an immunoporter inhibits its entry into the gel and restricts the detection of DNA to the loading area of the gel. Another factor influencing retardation of the DNA in a more subtle manner is the large size of the polycation/immunoporter/peptides as these bind to the DNA. Based on

these mechanisms, EMSAs can be used to measure the DNA-binding capacity of an immunoporter and estimate its potential to deliver DNA to cells.

4.2 Materials and methods

4.2.1 Construction of SR-BI^{Ab} - PLL immunoporter

In this work, PLL was initially investigated as a potential DNA-carrier for non-viral delivery of DNA. Our initial SR-BI^{Ab} - PLL immunoporter protocol (see Appendix 1) was based on previous work of the collaborating research group of Professor Robert Rush *(Berhanu and Rush, 2008)*. After modifications, the following detailed protocol (illustrated in Figure 4.2 alongside that of the final SR-BI^{Ab} - PEI immunoporter protocol) was used to construct the final SR-BI^{Ab} - PLL immunoporter. A p75^{NTRAb} - based immunoporter was also produced to test alongside the SR-BI^{Ab} - PLL protocol.

IRB1 containing 0.15 M NaCl / 0.02 M EDTA / 0.1 M sodium phosphate (Sigma-Aldrich Co.; pH 7.4) was prepared. Sterile-filtration and degassing through a 0.22 µm Steritop-GV filter unit for 30 min was followed by nitrogen gas (N_2) flushing for 30 min to reduce the potential for oxidation in later reactions.

SR-BI^{Ab} (3 mg) previously purified and freeze-dried in IRB1 (as described in section 3.2.1) was reconstituted in UltraPure™ DNase/RNase-free distilled water (GIBCO H_2O; Invitrogen Co.). The antibody was mixed with SMPT (Pierce

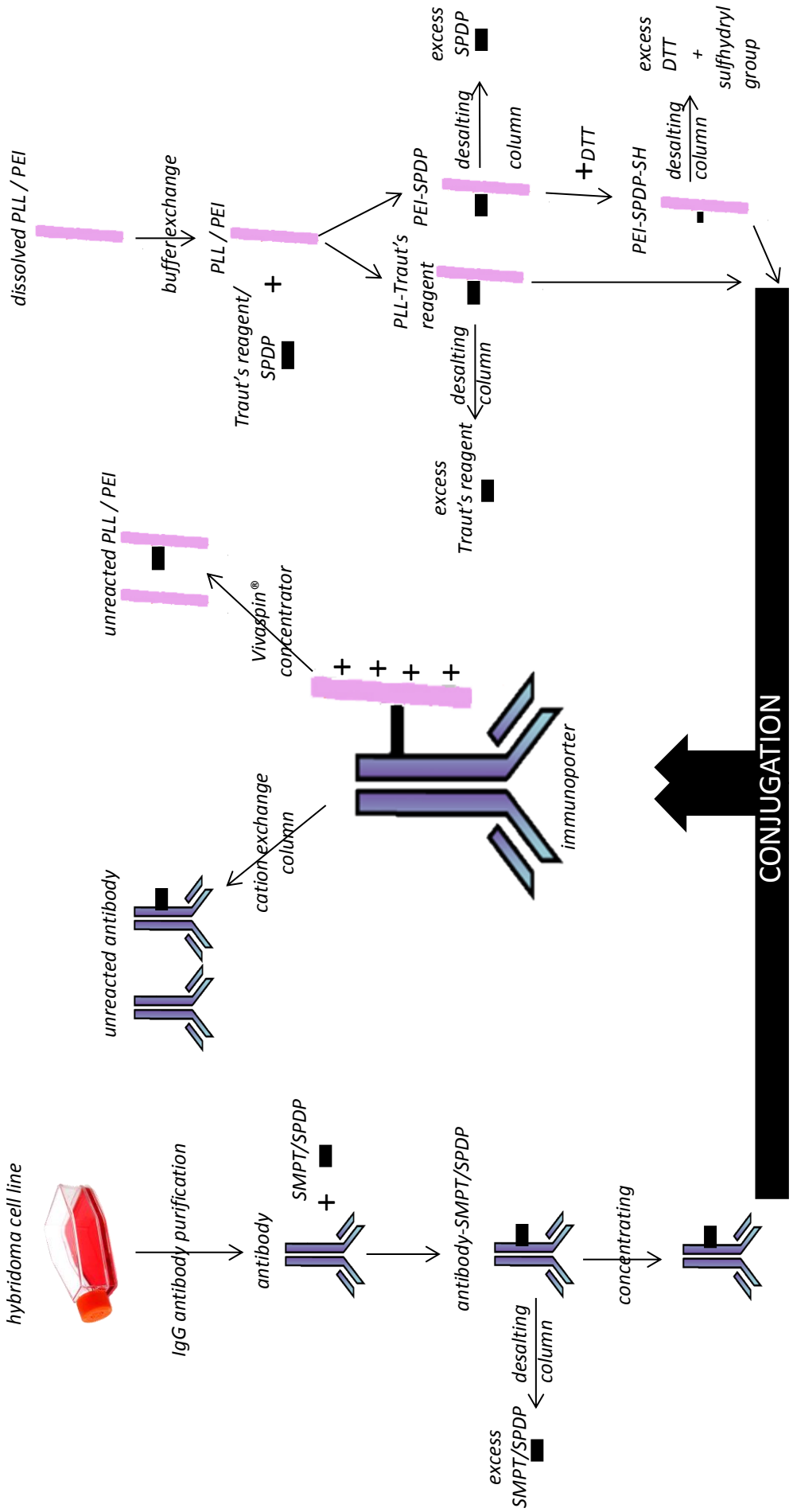

Figure 4.2 Schematic representation of immunoporter constructions based on PLL and PEI *(see figure text on next page)*

Figure 4.2 Schematic representation of immunoporter constructions based on PLL and PEI *(see previous page). For PLL, this polycation was prepared in IRB1, reacted with Traut's reagent and separated from the excess of the latter. With regards to the immunoporter based on PEI, this polycation was prepared in IRB2 and reacted with SPDP. Excess reagent was removed and PEI-SPDP was reduced using DTT to give PEI-SPDP-SH. Alongside PEI/PLL preparations, IgG antibody was purified from a hybridoma cell line and reacted with SMPT (for later conjugation with PLL) or SPDP (for later conjugation with PEI). After removal of excess reagent, antibody-SMPT and antibody-SPDP was conjugated with PLL-Traut's reagent and PEI-SPDP-SH, respectively, to form positively charged immunoporters. These antibody-PLL and antibody-PEI conjugates were purified from excess free antibody using a cation exchange column and from excess PEI/PLL using a spin concentrator.*

Biotechnology, Inc.; 75 µl of 2.5 mg/ml stock in GIBCO H_2O) in a 1 : 5 SR-BI^{Ab} : SMPT molar ratio. SMPT was added in 15 aliquots to the SR-BI^{Ab} to minimise precipitation and constituted 5 % of the total reaction volume. The mixture was degassed for 10 min, flushed with N_2 for 10 min and incubated O/N at 4°C with shaking (80 revolutions per minute (rpm); orbital shaker; Edwards Instruments Co.).

The next day, Traut's reagent (Pierce Biotechnology, Inc.; 91.6 µl of 2 mg/ml stock in IRB1) was added to PLL (Sigma-Aldrich Co.; 824.4 µl of 50 mg/ml in IRB1) in a 1 : 20 molar ratio of PLL : Traut's reagent. Traut's reagent constituted 10 % of the total reaction volume. The mixture was degassed for 10 min, flushed with N_2 for 10 min and thereafter incubated for 30 min at RT with shaking (80 rpm). This reaction mixture was added to a Sephadex G-25 column (9 ml packed volume; Sigma-Aldrich Co.) and 1 ml fractions were collected using IRB1. Fractions containing PLL were determined using a non-quantitative colorimetric assay based on Eosin B *(Waheed et al., 2000)*. Samples (50 µl) of each fraction were diluted in 50 µl GIBCO H_2O. After the addition of 1 ml 0.012 % w/v Eosin B (Sigma-Aldrich Co.), the presence of PLL was determined based on a colour change from red to pink (Figure 4.3).

SR-BI^{Ab} - SMPT product from the O/N incubation was added to another Sephadex G-25 column. The presence of SR-BI^{Ab} protein was detected in 1 ml fractions from the eluate at A_{280} in a UV-3000 spectrophotometer. Fractions containing SR-BI^{Ab} - SMPT were mixed with PLL - Traut's fractions (see above) and

Figure 4.3 PLL detection using Eosin B assay. *After elution from a Sephadex G-25 column using IRB1, PLL content was detected in samples from 1 ml fractions using 0.012 % Eosin B, as shown in a representative image. The fourth fraction from the camera contains PLL which is visualised as a pink colour compared to the red colour of all other fractions.*

concentrated to 1 ml (2 mg/ml) using a Vivaspin® concentrator (5 kDa MWCO; Sartorius Stedim Biotech S.A.; 122 x 17 mm, membrane area 2.0 cm^2; 4 ml) at 2000*g*. This mixture (1 ml) was diluted to 4 ml using IRB1 and the volume was again reduced to 1 ml by centrifugation through the Vivaspin® concentrator. The process was repeated twice more, with the final centrifugation step being used to produce a final volume of 1.5 ml. The concentrated mixture was incubated O/N at 4˚C. This mixture containing SR-BI^{Ab} - PLL conjugates was exposed to 0.02 M L-cysteine (Sigma-Aldrich Co.; 150 µl of 0.2 M stock) for 2 h at RT to block un-reacted sulfhydryl groups on the SR-BI^{Ab}.

Finally, the buffer in which the conjugate had been prepared was exchanged for 0.15 M NaCl / 50 mM 4-(2-hydroxyethyl)-1-piperazineethanesulfonic acid (HEPES; Invitrogen Co.; pH 7.9) using a Vivaspin® concentrator (5 kDa MWCO) at 2000*g*, as described above.

A Hi-trap SP HP cation exchange column (1 ml; 0.7 x 2.5 cm; GE Healthcare) was washed in 4 ml GIBCO H_2O and thereafter in 4 ml 0.15 M NaCl / 50 mM HEPES (pH 7.9), using a 3 ml syringe connected with the provided column adapter. Buffer containing 1 M NaCl / 50 mM HEPES (pH 7.3; 4 ml) was added to the column, followed by the addition of 4 ml 0.15 M NaCl / 50 mM HEPES (pH 7.9). The mixture containing SR-BI^{Ab} - PLL immunoporter was added to the column and the eluate was reintroduced twice more to this column to enhance binding of the conjugate. The resin was washed with 4 ml 0.15 M NaCl / 50 mM HEPES and SR-BI^{Ab} - PLL was thereafter eluted in 1 ml fractions using 50 mM HEPES with

increasing NaCl concentration; 1 M, 2 M and 3 M (4 ml of each; all pH 7.3). Antibody concentrations in all 1 ml fractions of the eluates were determined using A_{280} measurements in a UV-3000 spectrophotometer. Fractions eluted using 2 M NaCl / 50 mM HEPES containing SR-BI^{Ab} were mixed and the concentration measured again. The buffer of the immunoporter was exchanged for 0.15 M NaCl / 50 mM HEPES (pH 7.9) in a Vivaspin® concentrator (5 kDa MWCO) at 2000*g*, as described above for SR-BI^{Ab}-SPDP. The mixture was concentrated to contain between 0.5 and 1 mg/ml SR-BI^{Ab}, as appropriate for subsequent investigations. The immunoporter concentration was calculated based on A_{280} in a UV-3000 spectrophotometer. This immunoporter was freeze-dried in 20 µg aliquots and stored at -20°C up until one year after preparation.

The cation exchange column was washed in 4 ml 1 M NaCl / 50 mM HEPES, followed by 4 ml 0.15 M NaCl / 50 mM HEPES. Before storage, the column was washed in 4 ml filtered GIBCO H_2O and thereafter in 4 ml 0.2 M sodium acetate (Ajax Finechem, Pty. Ltd.) / 20 % v/v ethanol.

4.2.1.1 Analysis of SR-BI^{Ab} - PLL immunoporter construction in an SDS-PAGE

Samples (3.5 µg) of unmodified SR-BI^{Ab}, and from the final solution containing SR-BI^{Ab} - PLL immunoporter were analysed using SDS-PAGE (as described in section 3.2.1.3) to assess charge based on entry into the gel.

4.2.2 Construction of SR-BI^{Ab} - PEI immunoporter

Initial trials of the construction of SR-BI^{Ab} - PEI immunoporter followed a protocol which was currently under investigation by the research group of Professor Robert Rush using the p75^{NTRAb} (see Appendix 2; M-L. Rogers, unpublished protocol). Based on initial experiments, this protocol was modified to improve its use with the SR-BI^{Ab} (see section 4.3.3). The final SR-BI^{Ab} - PEI immunoporter construction protocol is described in detail as follows (illustrated in Figure 4.2 alongside that of the final SR-BI^{Ab} - PLL immunoporter protocol). A p75^{NTRAb} - based immunoporter was also produced to test alongside the SR-BI^{Ab} - PEI protocol.

IRB2 containing 0.25 M NaCl / 20 mM HEPES (pH 7.9) was used for essentially all steps in the SR-BI^{Ab} - PEI immunoporter protocol. All buffers were sterile-filtered through a 0.22 µm Steritop-GV filter unit.

To prepare a working solution of PEI in IRB2, branched PEI of 25 kDa (Sigma-Aldrich Co.; 1 g) was initially dissolved in 10 ml sterile water (water for irrigation; Baxter International, Inc.) on a stirring plate. This solution was adjusted to pH 7.0 using hydrochloric acid (Ajax Finechem, Pty. Ltd.). A PD10 desalting column (GE Healthcare; 8.3 ml Sephadex G-25 column) was pre-washed in 25 ml IRB2. After sterile-filtration, 1.7 ml of PEI solution (pH 7.0) was added to this PD10 column. PEI was eluted using IRB2 and collected in 5 x 1 ml fractions. These fractions were examined for the presence of PEI through a colour change from

transparent to blue using DC protein assay reagents (Bio-rad Laboratories, Inc.): In separate wells of a microtest plate (96-well; flat-bottom; Sarstedt AG & Co.), a sample (5 µl) from each fraction was mixed with 25 µl of Reagent A, followed by 200 µl of Reagent B, using a digital multi-channel pipette (10-200 µl; Labnet International Inc.). The presence of PEI was assessed qualitatively based on the appearance of a blue colour after 1 minute.

Fractions containing PEI were mixed. The PEI content of this mixture was determined in a quantitative DC protein assay by comparison to a standard curve prepared from aliquots of solutions containing 0.05, 0.1, 0.2, 0.4, 0.8 and 1 mg/ml PEI. Replicates (8; each 5 µl) of the sample containing the mixed fractions (1 : 100 dilution) and of each standard were separately mixed with Reagent A and B in microtest plates, as described above. After 15 min, wells were analysed for A_{750} in a Victor X4 2030 multilabel plate reader (PerkinElmer, Inc.). PEI was stored O/N at 4°C.

The next day, a 10 mM SPDP stock was prepared by adding 100 % ethanol to SPDP (Sigma-Aldrich Co.) and dissolving this by shaking the mixture in the dark at 60 rpm for 30 min. PEI (25 mg; 1 µmole) from the previous day was incubated with 1.97 µmoles of SPDP (197 µl of 10 mM stock) for 1 h at RT with shaking (60 rpm). PEI-SPDP mix was added to a PD10 desalting column, after which IRB2 was added, and the eluate collected in 1 ml fractions. Fractions containing PEI-SPDP based on DC protein assay reagents (as determined from the visible colour change described in the previous paragraph) were mixed and an excess of

DTT was added to this mixture (150 µl of a 20 mg/ml DTT solution). After 1 h incubation at RT with shaking (60 rpm), the PEI-SPDP-DTT mixture was added to the same PD10 desalting column (which in the mean-time had been washed with 25 ml IRB2 and kept hydrated) and eluted in 1 ml fractions using IRB2. The fractions where PEI was present (from the visible colour change, as previously described) were mixed and concentration was measured in a quantitative assay (at A_{750} in the Victor X4 2030 multilabel plate reader, as described in the previous paragraph). The resulting PEI-SPDP-SH was stored at 4°C until the SR-BI^{Ab}-SPDP preparations were finalised (see below).

SR-BI^{Ab} (3 mg) had previously been purified and freeze-dried in IRB2 as described in section 3.2.1. On the same day as PEI was reacted with SPDP, freeze-dried SR-BI^{Ab} (3 mg) was reconstituted in GIBCO H_2O and incubated with 11 nmoles SPDP (1.1 µl of 10 mM stock) for 2 h at RT with shaking (60 rpm). The resulting SR-BI^{Ab}-SPDP was added to a PD10 desalting column and 1 ml fractions collected from the eluate using IRB2. Fractions containing SR-BI^{Ab}-SPDP were identified at A_{280} in a UV-3000 spectrophotometer. These SR-BI^{Ab} -SPDP fractions were mixed and concentrated to 1 ml using centrifugations at 3680*g* in a Vivaspin® concentrator (100 kDa MWCO). The concentration of the remaining solution in the Vivaspin® concentrator was determined at A_{280} in a NanoDrop™ 8000 multi-sample micro-volume UV-vis spectrophotometer. EDTA was added to the SR-BI^{Ab}-SPDP mixture at a final concentration of 1 mM. Thereafter, a portion of the freshly prepared PEI-SPDP-SH was added to the full amount of SR-BI^{Ab}-SPDP mixture in a 1.38 : 1 SR-BI^{Ab} : PEI molar ratio (0.23 : 1 SR-BI^{Ab} : PEI weight/weight

(w/w) ratio). This conjugation mixture was incubated for 24 h at RT with shaking (60 rpm).

The following day, SR-BI^{Ab}-SPDP / PEI-SPDP-SH mixture was added to a PD10 desalting column and eluted in 1 ml fractions using IRB2. Fractions containing SR-BI^{Ab}, as determined by A_{280} in a UV-3000 spectrophotometer, were mixed. The concentration of this mixture was again determined at A_{280} in a UV-3000 spectrophotometer.

A Hi-trap SP HP cation exchange column was washed with 4 ml 0.5 M NaCl / 20 mM HEPES (pH 7.3). Thereafter, 4 ml 1 M NaCl / 20 mM HEPES (pH 7.3) was added to the column, followed by another 4 ml 0.5 M NaCl / 20 mM HEPES. SR-BI^{Ab}-SPDP / PEI-SPDP-SH mixture was added to the cation exchange column. Eluate was reintroduced twice more to the column to enhance binding of the SR-BI^{Ab} - PEI conjugate. The cation exchange column was washed with 4 ml 0.5 M NaCl / 20 mM HEPES. Bound constructs were thereafter eluted in 1 ml fractions using 20 mM HEPES with increasing NaCl concentration; 1.0 M, 1.75 M and 3.0 M (4 ml of each; all pH 7.3). SR-BI^{Ab} concentrations were measured in all eluted fractions at A_{280} using a UV-3000 spectrophotometer. Fractions eluted with 3 M NaCl that contained SR-BI^{Ab} were mixed and protein concentration measured again (based on A_{280} in a UV-3000 spectrophotometer). The solution was concentrated to 1 ml using centrifugations at 3680*g* in a Vivaspin® concentrator (100 kDa MWCO). Dilution to 4 ml using 20 mM HEPES (pH 7.3) was followed by the reduction of the volume to 1 ml through centrifugation in the

Vivaspin® concentrator. This process was repeated twice more. Thereafter, the solution was diluted to 4 ml using 0.15 M NaCl / 20 mM HEPES (pH 7.3), and the volume was again reduced to 1 ml by centrifugation through the Vivaspin® concentrator. This process was repeated twice more, in which the last centrifugation aimed to contain between 0.1 and 0.5 mg/ml SR-BI^{Ab}. The final immunoporter concentration was measured at A_{280} using a NanoDrop™ 8000 multi-sample micro-volume UV-vis spectrophotometer. The immunoporter was freeze-dried in aliquots and stored at -20°C until use.

Before storage, the cation exchange column was washed in 4 ml 0.5 M NaCl / 20 mM HEPES, thereafter in 4 ml filtered GIBCO H_2O and lastly in 4 ml 0.2 M sodium acetate / 20 % v/v ethanol.

4.2.3 Plasmid DNA purification and analysis

All transfections in this work were performed using the high expression GFP plasmid gWizGFP (Aldevron) of 5757 base pairs (bps). Under the influence of a CMV promoter, this plasmid is engineered to result in high levels of GFP expression in mammalian cells, which can be detected using fluorescence microscopy (excitation / emission; 470 - 480 nm / 510 nm). The gWizGFP plasmid map is presented in Figure 4.4.

Bacterial transformation of this plasmid was followed by purification from the resulting kanamycin-resistant bacterial cultures using Qiagen kits (Qiagen N.V.),

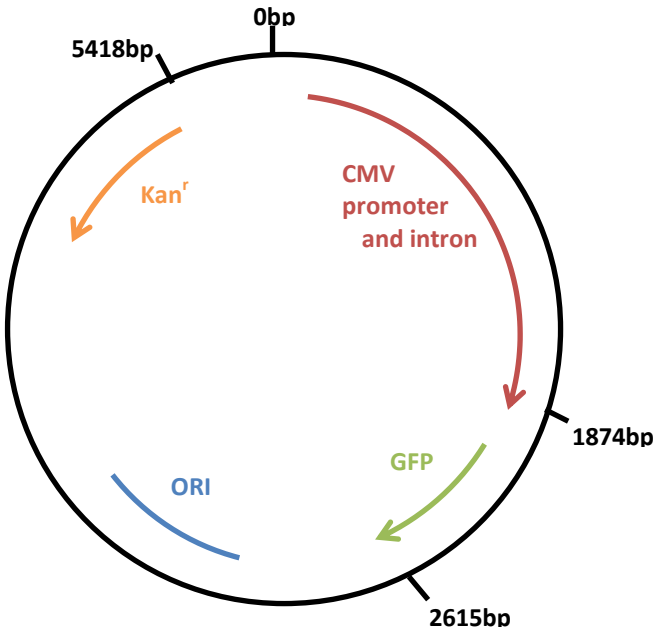

Figure 4.4 Map of gWiZGFP high expression plasmid *obtained from Aldevron. This contains the location and orientation of the CMV promoter and intron, the GFP reporter gene, origin of replication (ORI) and kanamycin resistance (Kan^r).*

as follows: Autoclaved Luria-Bertani (LB) broth at a concentration of 20 g/l (Sigma-Aldrich Co.) was used to grow bacterial cultures. LB broth containing 15 g/l select agar (Sigma-Aldrich Co.) with the addition of 50 μg/ml kanamycin (Sigma-Aldrich Co.) was used to produce kanamycin-selective agar plates. *Escherichia coli* competent cells (OneShot TOP10 chemically competent *E.coli*; Invitrogen Co.) were transformed with the gWizGFP plasmid through 30 min heat-shock at 42°C. This was followed by the addition of super optimal broth with catabolite repression medium (included in the OneShot TOP 10 chemically competent cell kit) and 1 h incubation with shaking (300 rpm) and heating at 37°C (Ratek Instruments, Pty. Ltd.). Plating (using spreader bars; Techno Plas, Pty. Ltd.) of these transformed bacteria on kanamycin-selective culture dishes was followed by incubation O/N at 37°C.

Surviving bacterial colonies were replated on a new set of kanamycin-selective plates and incubated O/N to verify transformation. Sub-culturing of single colonies in 5 ml LB Broth with 50 μg/ml kanamycin at 37°C for 16 h with shaking (300 rpm) was followed by plasmid purification using Qiagen spin Miniprep kit (Qiagen N.V.; following the recommendations of the supplier). Purified plasmid DNA was eluted in 30 μl GIBCO H_2O. Concentration was calculated based on A_{260} using a NanoDrop™ 8000 multi-sample micro-volume UV-vis spectrophotometer.

Plasmid DNA samples (300 ng) were mixed with a blue loading dye (New England Biolabs, Inc.), diluted to 10 µl in GIBCO H_2O and analysed on a 0.8 % w/v agarose gel prepared in 0.09 M boric acid / 2.6 mM EDTA / 0.09 M Tris (pH 8.3; TBE buffer) containing 0.5 µg/ml ethidium bromide (Sigma-Aldrich Co.). Agarose gel electrophoreses were run in a mini horizontal gel box system (GeneWorks, Pty. Ltd.), visualised by GeneGenius Gel Imaging System and Software (Synoptics, Ltd.) in TBE buffer with 0.5 µg/ml ethidium bromide and captured by the GeneSnap 6.04.00 software (Synoptics, Ltd.). One lane of the gel was loaded with one of two supercoiled DNA ladders, one from Invitrogen Co. containing DNA with the following lengths in bps: 2067, 2972, 3990, 5012, 6030, 7045, 8066, 10102, 12138, 14174, 16210, and one from Promega Co. containing DNA with the following lengths in bps: 2000, 3000, 4000, 5000, 6000, 7000, 8000, 9000, 10000. The DNA ladder produced by electrophoresis provided a comparison for estimation of DNA size.

After verification in gel electrophoresis of the gWizGFP plasmid prepared using the Qiagen spin Miniprep kit, gWizGFP-producing bacteria (0.7 ml) originating from one single colony grown for 16 h in the presence of kanamycin, was mixed with autoclaved 50 % w/v glycerol (0.3 ml; Sigma-Aldrich Co.) and stored until further use at -80°C. Frozen bacteria were retrieved using inoculation loops (Copan Diagnostics, Inc.) from these stocks, applied to kanamycin-selective LB agar plates and incubated at 37°C O/N. The Qiagen Gigaprep kit (Qiagen N.V.; following the recommendations of the supplier) was used for large-scale

production of the plasmid. Purified plasmid DNA was dissolved in GIBCO H_2O at a final concentration of 6 - 7 µg/µl.

4.2.4 EMSAs and immunogene formation for transfection purposes

Positively charged SR-BI^{Ab} - PLL and SR-BI^{Ab} - PEI immunoporters were mixed separately at neutral pH with negatively charged gWizGFP plasmid DNA to form SR-BI^{Ab} - PLL and SR-BI^{Ab} - PEI immunogenes, respectively. DNA-carrying capacities of immunoporters were analysed by studying DNA binding and retardation in EMSAs. The mobility and band intensity of DNA previously mixed with immunogenes and subjected to electrophoresis was compared with that of plasmid DNA alone. A supercoiled ladder was used to provide an estimation of DNA size. Plasmid DNA (400 ng in 4 µl) was added to a range of immunoporter amounts (stock concentration 100 ng/µl) and incubated for 30 min at RT. All mixtures had a final plasmid DNA concentration of 40 ng/µl. Samples were mixed with 1 µl blue loading dye and analysed using gel electrophoresis, as previously described in section 4.2.3.

To prepare immunogenes for transfection in culture and *in vivo*, immunoporters were mixed with a slight excess of the gWizGFP plasmid DNA; at a 1 : 3 SR-BI^{Ab} : DNA w/w ratio. The use of an excess of DNA to immunoporter had previously been shown to increase immunoporter transfection in culture *(Shimizu et al., 1996)*.

4.2.5 Transfection of glial cells in culture

4.2.5.1 Testing of gWizGFP plasmid DNA using nucleofection in mixed glial cultures

The capacity of the gWizGFP plasmid to produce GFP expression after nucleofection in primary glial cells was assessed using a rat astrocyte nucleofector kit. Mixed glial cultures (14 - 17 days old) in 6-well plates were quickly washed in PBS and trypsinised in pre-heated trypsin-EDTA / PBS (pH 7.4) for 2 min. Trypsin solution was removed and cells were collected in FBS / PEST / DMEM growth medium. Cell concentration was calculated using a haemocytometer (Brand GmbH + CO KG) and 5 x 10^6 cells were dispensed into 15 ml tubes used for subsequent nucleofection.

The cell suspensions were centrifuged at 90*g* for 5 min in a Sigma Laboratory Centrifuge 6K15 (Sigma-Aldrich Co.). The supernatant was removed, each pellet resuspended in 100 µl rat astrocyte Nucleofector kit solution (Lonza Group, Ltd.) and mixed with 10 µg gWizGFP or with GIBCO H_2O of the same volume (1.5 - 1.8 µl). These cell mixtures were separately transferred to Nucleofector cuvettes and exposed to Nucleofector program T-020 of the Nucleofector II apparatus (Lonza Group, Ltd.). The mixture containing nucleofected cells was diluted in FBS / PEST / DMEM. Cells were thereafter re-plated onto 24-well plate wells with coverslips at 150 000 cells per well in a total volume of 300 µl.

At 72 h after the start of incubation at 37°C, cells were quickly washed in PBS and fixed in 4 % PFA. This fixation was followed by IHC (BSA/Triton IHC; see section 3.2.2.2) with a rabbit anti-GFP antibody (Invitrogen Co.) and the astrocytic marker mouse anti-GFAP (1 : 250). Fluorescent immunolabelling was achieved using subsequent incubation in anti-rabbit Alexa Fluor^{488} and anti-mouse Alexa Fluor^{647} secondary antibodies. GFP and GFAP immunoreactivity was analysed using fluorescence microscopy.

4.2.5.2 Transfection by immunogenes in culture

For transfection in culture, immunogenes were mixed with DMEM to constitute a maximum of 10 % v/v of the culture medium (for SR-BI^{Ab} - PLL immunoporters) or (for SR-BI^{Ab} - PEI immunoporters) at a 1 : 1 v/v ratio with an adjusted double-strength HBSS buffer which resulted in a solution with a final composition of 115 mM sodium chloride, 5.4 mM potassium, 0.4 mM magnesium sulphate, 0.4 mM magnesium chloride, 1.3 mM calcium chloride, 0.6 mM monopotassium phosphate, 25 mM sodium bicarbonate, 5.5 mM glucose, 20 mM HEPES (pH 7.4).

Cell cultures were treated with immunogenes up to 24 h in 24-well or 96-well cell culture plates (Greiner Bio-one International AG) containing cells in mixed glial cultures grown for 14 to 17 days. PLL - DNA or PEI - DNA complexes and DNA alone (in the same concentration as in the treatment with the highest concentration of polycation/immunoporter) were tested for transfection capacity alongside immunogenes.

The SR-BI^{Ab} - PEI immunogene produced using the final modified protocol was tested at 1 µg and 5 µg in triplicate wells of 96-well plates (based on SR-BI^{Ab} protein at A_{280}; containing 6 µg/ml and 29 µg/ml, respectively). As the results from SR-BI^{Ab} - PEI immunogene treatments in 96-well plates reported in this thesis were all performed in a constant volume, we will for simplification purposes primarily state the amount in µg added per well. Vehicle control (the adjusted HBSS buffer) and 1 µg, 2.5 µg and 5 µg PEI - DNA per well (6, 14 and 29 µg/ml, respectively; based on PEI content using DC protein assay at A_{750}) were also included in triplicates. After 6 h exposure to the final SR-BI^{Ab} - PEI immunogene, media was exchanged for DMEM/FBS/PEST and cells were monitored up to 172 h. For the majority of analysis presented in this work, cells in culture were fixed using 4 % PFA at either 24 h or 72 h after the start of exposure.

BSA/Triton IHC was used for cells treated with PLL immunogenes (see section 3.2.2.2) and a protocol involving the use of normal horse serum (NHS; Invitrogen Co.) as blocking agent for cultures exposed to PEI immunogenes. The latter IHC protocol is subsequently referred to as NHS/Triton IHC and was performed as described in section 3.2.2.2 except that blocking and permeabilisation was performed separately by initially blocking 60 min in 10 % v/v NHS / PBS (pH 7.4) and thereafter permeabilising cells for 20 min in 0.5 % v/v Triton X-100 / PBS (pH 7.4). Also, all antibodies were diluted in 2 % v/v NHS / 0.2 % v/v Triton X-100

/ PBS (pH 7.4). GFP immunoreactivity was studied using rabbit anti-GFP primary antibody and Alexa Fluor^{488} secondary antibody.

Cells expressing GFP and/or cell-specific markers were identified using fluorescence microscopy. The proportion of Hoechst 33258-positive cells expressing GFP was determined from analysis of one random image captured from within each of four quadrants in each well using a low magnification objective (10x). A single mean value was calculated from three identically treated wells for each treatment condition for every independent experiment. Either all of the GFP-positive cells in triplicate wells or (when there were large numbers of GFP-positive cells) at least 10 randomly selected GFP-positive cells in each well were analysed for co-labelling with the cellular markers mouse anti-CD11b and mouse anti-GFAP. The same randomised selection method was used to study the expression of SR-BI in transfected cells.

Numbers of microglia were quantified based on CD11b expression in four randomly selected images (captured using a low magnification objective; 10x; one from each well quadrant) of each triplicate well. Using the same material for counting this total number of microglial cells, microglia were studied with regards to activation. This activation was measured by comparing the proportion of ramified cells, non-amoeboid activated cells and amoeboid activated cells within the microglial population at 24 h and 72 h after the start of exposure to

polycation/immunoporter/controls. Further information on this classification method is found in section 3.2.2.3.

4.2.5.3 Effects of immunogenes on cell viability

Another separate experiment assessed cell viability in cultures exposed to the final SR-BI^{Ab} - PEI immunogene, PEI - DNA and controls at 6 h and 24 h after the start of exposure. Cultures were incubated in DMEM for 5 min containing 10 µg/ml Hoechst 33258, 1 µg/ml calcein-acetoxymethyl (calcein-AM; Invitrogen Co.) and 25 µM propidium iodide (PI; Sigma-Aldrich Co.). This incubation mixture was replaced with DMEM, and cells were analysed immediately in fluorescence microscopy. Cell nuclei (as determined using Hoechst 33258) with incorporation of PI indicated that these cells had ruptured plasma membranes and nuclear envelopes. Live cells were identified based on their capacity to retain cytoplasmic calcein-AM. The proportion of PI-positive cells out of all Hoechst 33258-positive nuclei was calculated in four randomly selected images (captured using a low magnification objective; 10x; one from each well quadrant) in each of four identically treated wells. Control cultures were only exposed to calcein-AM / DMEM and PI / DMEM, separately, to confirm that no leakage occurred between fluorescence channels. The addition of 0.5 % v/v Triton-X100 to incubation mixtures of these two controls and also to the calcein-AM / PI / DMEM mixture, were used as positive controls for ruptured plasma membrane and nuclear envelope.

4.2.5.4 LPS treatment for microglial activation prior to immunogene transfection

LPS (Sigma-Aldrich Co.) was added to mixed glial cultures (confluent, 14 - 17 days old) at a concentration of 10 ng/ml for 24 h in DMEM/PEST (without FBS). Subsequently, the effect of microglial activation on expression of SR-BI and GFP was studied (as described previously).

4.2.6 Transfection by immunogenes in vivo

The transfection capacity of different batches of immunoporter was also tested *in vivo*. A stereotaxic single injection of SR-BI^{Ab} - PLL immunogene (containing up to 2 µg of SR-BI^{Ab} and 6 µg DNA) was performed into the lateral ventricle *(10 µl; AP -0.8, L -1.4, DV -3.5)* of adult rat. Rats were anaesthetised, placed in a stereotaxic frame and a burr hole drilled in the skull as described for stereotaxic injection in section 3.2.3.1.

Osmotic pump infusions of the final SR-BI^{Ab} - PEI immunogene (up to 20 µg SR-BI^{Ab} and 60 µg DNA) were subsequently performed into the hippocampus (*3 µl; AP -2.12, L -1.5, DV -4.0*). These osmotic pump infusions were carried out using the Alzet 1004 osmotic pump (Durect Co.) and the Alzet Brain Infusion kit 2 (Durect Co.) at a rate of 0.11 µl/h. Pumps were positioned under the skin between the shoulder blades of the rat using one small incision through the skin. Subsequent to small subcutaneous incisions, a catheter extending from the

pump was guided under the skin from the neck towards the top of the skull. The needle attached to the other end of the catheter was held in the position of infusion using dental cement, freshly made from mixing Jet acrylic powder (cross-linked, self curing; Lang dental Manufacturing Company, Inc.) and Self-cure acrylic repair material (Dentsply International Ltd.).

Rats were monitored daily until euthanized through intracardial perfusion 72 h after single stereotaxic injections and 14 days following initiation of osmotic pump infusions. Brains were post-fixed, incubated in sucrose and cut in 50 µm brain sections (see section 3.2.3.2). BSA/Triton IHC (see section 3.2.3.3) was used for brains injected with PLL immunogenes. An NHS/Triton IHC was used for brains injected/infused with PEI immunogenes. This NHS/Triton IHC was performed as described in section 3.2.3.3 except that blocking and permeabilisation was performed separately by initially blocking in 10 % v/v NHS / PBS for 60 min followed by permeabilising the tissue in 0.5 % v/v Triton-X100 / PBS (pH 7.4) for 30 min. All antibodies were incubated in 2 % v/v NHS / 0.2 % v/v Triton X-100 / PBS (pH 7.4), and primary antibodies were incubated for 72 h rather than O/N. All brains were analysed for GFP immunoreactivity and co-labelling with cellular markers (see section 2.3).

4.2.7 Microscopy

Images of brain tissue sections were captured using a BX50 fluorescence microscope (Olympus Co.) or a confocal microscope (Leica Microsystems GmbH). Cells grown in wells without coverslips were analysed directly in wells filled with PBS or DMEM using an IX71 inverted fluorescence microscope (Olympus Co.).

4.2.8 Statistical analysis

Quantitative results from microscopy analysis are presented as mean +/- standard deviation. Where multiple groups are compared, one-way and two-way ANOVAs were used to analyse for significance with p values < 0.05, unless otherwise stated. A Student Newman-Keuls post-hoc test was used to identify differences between specific groups. A two-tailed t-test was used to compare transfection efficiencies in LPS-treated cultures compared to control.

4.3 Results

4.3.1 Nucleofection of mixed glial cultures

The gWizGFP plasmid used in later immunogene incubations was initially tested using nucleofection to transfect cells grown in mixed glial cultures. A representative image of cells nucleofected with gWizGFP plasmid DNA is shown in Figure 4.5. The gWizGFP plasmid resulted in strong native GFP expression in

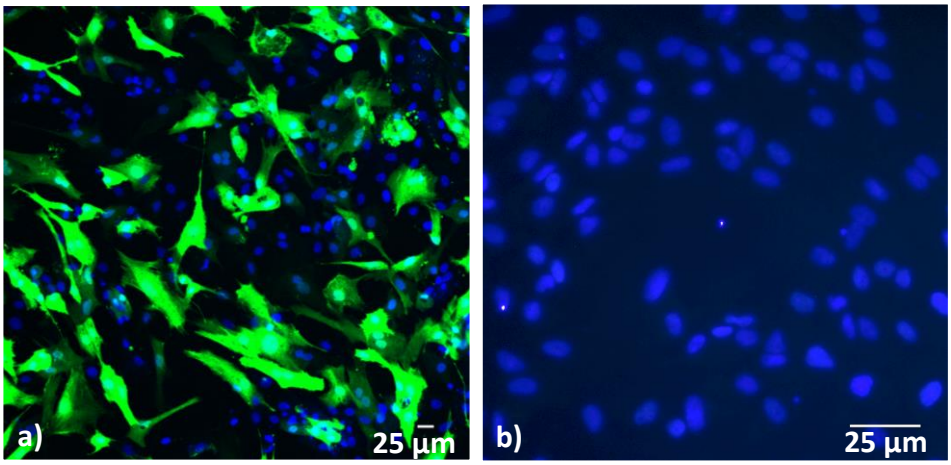

Figure 4.5 Nucleofection of mixed glial culture using gWizGFP plasmid DNA *as shown in representative images from fluorescence microscopy in one of thirteen independent experiments. a) Cells in mixed glial culture expressed GFP (green) after nucleofection, clearly showing that glial cells could be transfected using the gWizGFP plasmid. The majority of cells were co-stained with astrocytic markers, however microglial cells were also transfected (data not shown). b) Where DNA was replaced with an equal volume of water, no GFP immunoreactivity was detected. Nuclei were labelled with Hoechst 33258 (blue).*

glial cells and could therefore be used to transfect cells in these cultures. A majority of this expression was found in the astrocytic population (as determined using GFAP staining). Some GFP-positive / GFAP-negative cells with microglial morphology were also detected. At the time, the main point investigated was the capacity of glial cells to be transfected by the plasmid, and thus, transfection efficiencies and nature of cells transfected was not further investigated.

4.3.2 Construction of SR-BI^{Ab} - PLL immunoporters

Initial SR-BI^{Ab} - PLL immunoporter construction trials resulted in extensive antibody loss upon reaction with the SMPT cross-linker, and during the subsequent conjugation of SR-BI^{Ab} - SMPT with PLL - Traut's reagent. Thus, the yield of immunoporter was too low for testing transfection either in culture or in the intact brain (*n = 2*). This was not seen when constructing an immunoporter based on an antibody targeted against p75^{NTR} *(n = 3)*, suggesting that this reaction may be dependent on the properties of the antibody.

A number of modifications were made aimed at reducing precipitation and increasing recovery of the SR-BI^{Ab} - PLL immunoporter. Subsequent modifications also provided more efficient removal of unwanted reactants and products from the immunoporter and improved DNA binding of this construct. Key modifications involved changes in reagent concentrations and in the

composition of reaction buffers, and the use of Vivaspin® concentrators instead of polyethylene glycol for concentrating reaction mixtures and final immunoporters. In addition, the use of cation exchange instead of gel filtration was used to ensure complete separation of the immunoporter from unreacted antibody and PLL moieties.

These modifications substantially decreased the visible precipitation that developed both during the reaction of SR-BI^{Ab} with SMPT and during the subsequent conjugation of SR-BI^{Ab} with PLL. Furthermore, SDS-PAGE analysis of the final SR-BI^{Ab} - PLL immunoporter showed that no SR-BI^{Ab} moiety in this solution had the capacity to enter the gel, in contrast to unreacted SR-BI^{Ab} (Figure 4.6). Also, the final SR-BI^{Ab} - PLL immunoporter had a higher positive charge than previous SR-BI^{Ab} - PLL immunoporters. The earlier immunoporter was detected in the gel, indicating incomplete conjugation between SR-BI^{Ab} and PLL. As the final immunoporter could not be detected in the gel, it was determined that all SR-BI^{Ab} in this immunoporter was bound to PLL, resulting in a net positive charge that did not allow movement of SR-BI^{Ab} towards the anode.

The final SR-BI^{Ab} - PLL immunoporter (see protocol in section 4.2.1) had the capacity to bind DNA at an SR-BI^{Ab} : DNA w/w ratio of 1 : 5 (based on SR-BI^{Ab} protein at A_{280}; *n = 6*; Figure 4.7b). This was in contrast to an early SR-BI^{Ab} - PLL immunoporter (produced with an initial modification of changing the

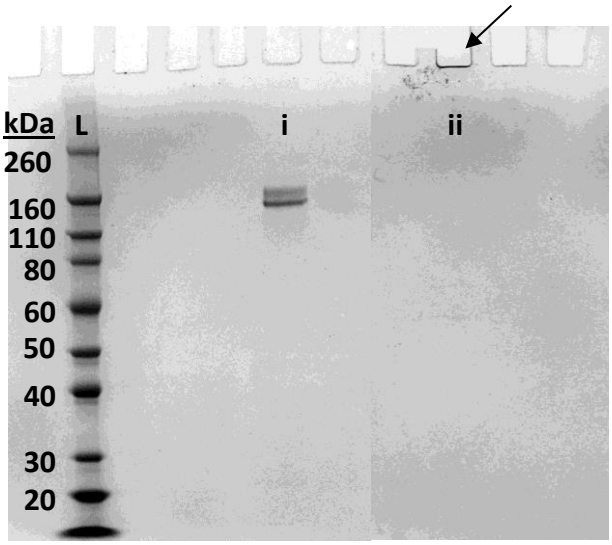

Figure 4.6 SDS-PAGE of SR-BI^{Ab} - PLL immunoporters*. In contrast to unreacted SR-BI^{Ab} (i), which has the capacity to enter an SDS-PAGE due to a slight negative charge, the final SR-BI^{Ab} - PLL immunoporter (see protocol in section 4.2.1) lacked the capacity to enter the gel (see arrow). This indicated that all SR-BI^{Ab} in the mixture was conjugated with PLL and that this conjugate had a strong positive charge. Samples were analysed using Brilliant Blue staining next to a Novex sharp pre-stained protein ladder (L) with marked sizes in kDa.*

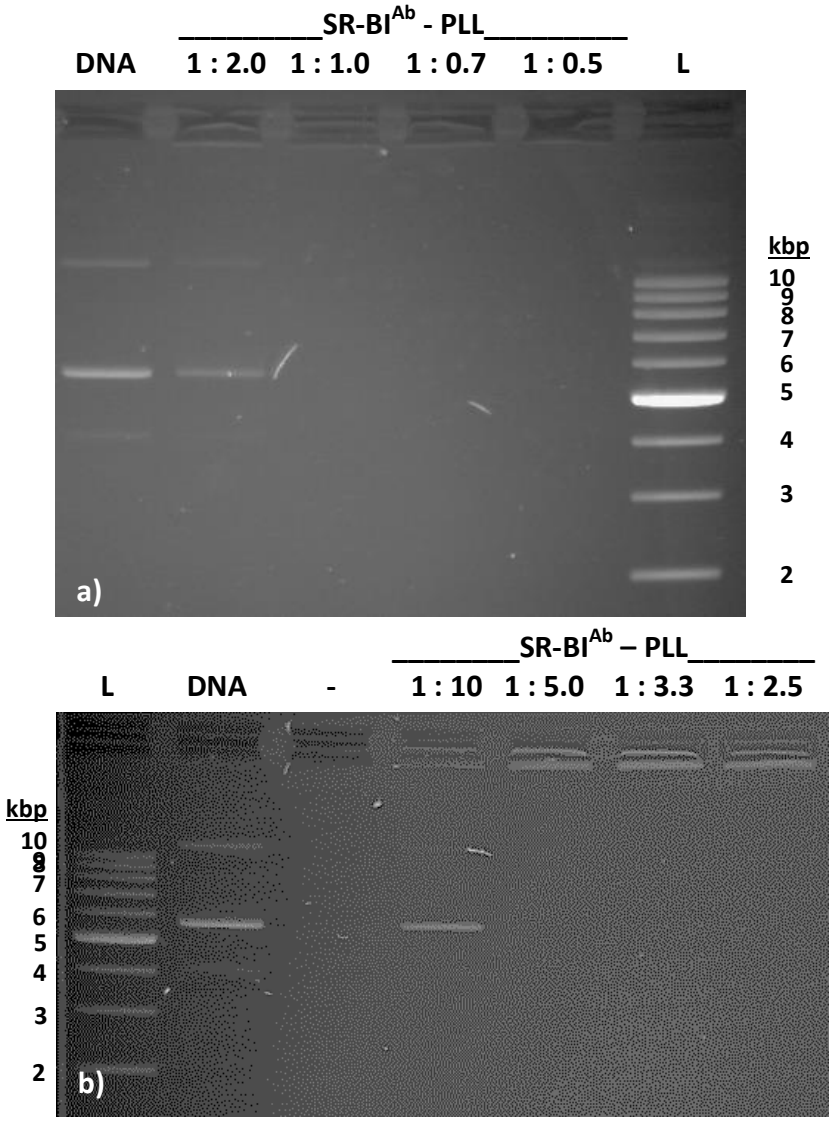

Figure 4.7 EMSA for SR-BIAb - PLL immunoporters *in 0.8 % agarose gels displaying plasmid DNA binding and retardation with increasing SR-BI^{Ab} : DNA w/w ratios from 1 : 10 to 1 : 0.5. a) An immunoporter constructed using the original protocol (see Appendix 1) with an initial modification of changing the SR-BI^{Ab} : SMPT w/w ratio from 1 : 20 to 1 : 5, displayed full DNA retardation (where no DNA enters the gel) at an SR-BI^{Ab} : DNA ratio of 1 : 1.0. b) Using the final protocol after modifications (see section 4.2.1), this was reached at an SR-BI^{Ab} : DNA ratio of 1 : 5.0. A supercoiled plasmid DNA ladder (L) with marked sizes in kbp was used for estimation of plasmid DNA size. Ethidium bromide was used for visualisation.*

SR-BI^{Ab} : SMPT w/w ratio from 1 : 20 to 1 : 5) where full DNA retardation was not achieved in an EMSA until an SR-BI^{Ab} : DNA w/w ratio of 1 : 1 (based on SR-BI^{Ab} protein at A_{280}; *n = 2*; Figure 4.7a). Tests using this early SR-BI^{Ab} - PLL immunogene (*n = 2*; 1.1 µg/ml), did not result in any GFP expression in mixed glial cells in culture.

In contrast, treatment of mixed glial cultures for 6 h with the final SR-BI^{Ab} - PLL immunogene resulted in GFP expression when assessed at 72 h after the start of exposure to the immunogene. Expression was limited to a few cells per well, and was seen at all concentrations tested (SR-BI^{Ab} concentration of 1, 2, or 8.5 µg/ml; in duplicates; n = 2; as shown using 2 µg/ml in Figure 4.8a). This transfection capacity was independent of changes in concentration, duration of treatment with the immunogene (up to 24 h) and post-incubation times (up to 172 h). Exposures to unbound DNA or to PLL - DNA alone did not result in any GFP-expressing cells. In cultures exposed to PLL and all SR-BI^{Ab} - PLL immunogenes, there was a clear decrease in cell number (using phase contrast microscopy; see Figure 4.8b). This finding suggested that the treatment caused cell death and/or inability of cells to remain attached to the cell culture wells. The transfection of a subpopulation of cells in culture indicated that the immunogene had the capacity to transfect glial cells. However, this was not investigated further due to low transfection rates and decreased cell numbers after exposure.

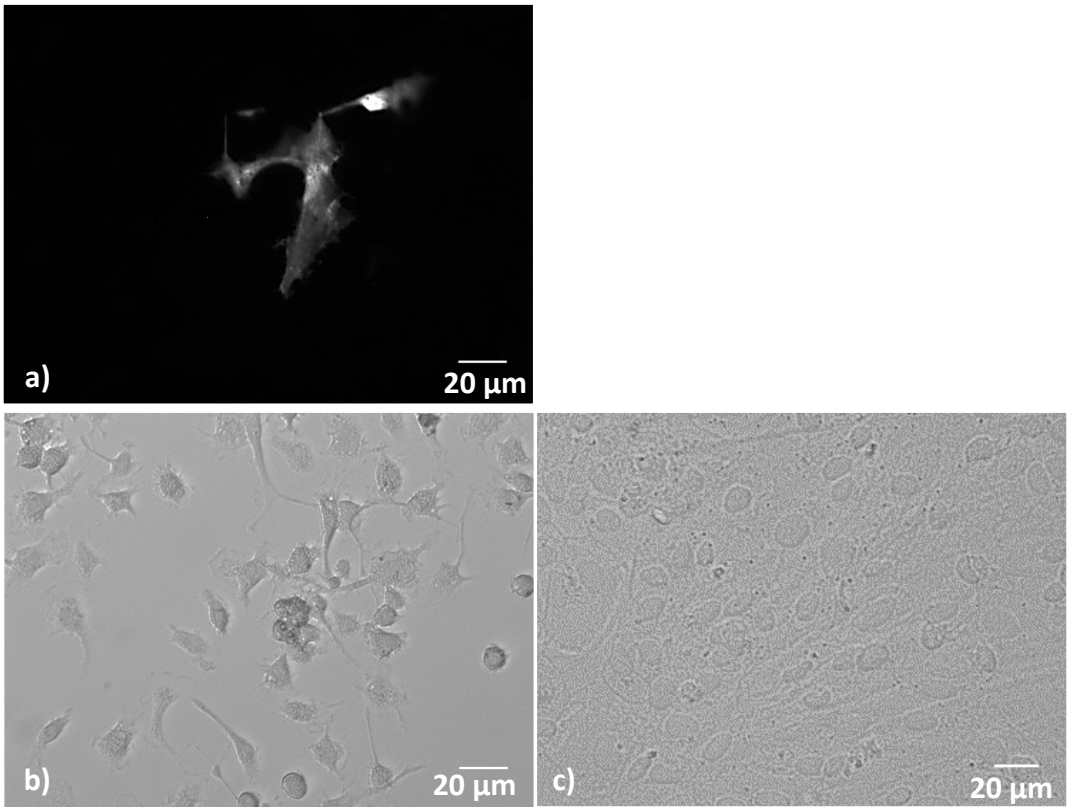

Figure 4.8 Exposure to the SR-BI^{Ab} - PLL immunogene in mixed glial cultures *resulted in GFP expression in sporadic astrocyte-looking cells (a; 2 µg/ml SR-BI^{Ab} - PLL). b) Consistently throughout all testing using this immunogene, phase contrast images showed a clear decrease in cell number (mostly astrocytes) in comparison to c) control cultures exposed to DNA alone. This decrease could be a result of cell death or lack of capacity to remain attached to the cell culture dish. Independent of the cause, the SR-BI^{Ab} - PLL immunogene was not analysed further due to the low degree of transfection and decreased cell numbers remaining after treatment.*

Test injections of the final SR-BI^{Ab} - PLL immunogene into the lateral ventricle of adult rat brain resulted in the expression of GFP in a subpopulation of periventricular glial-like cells in one of two injected animals (0.06 µg/µl; Figure 4.9). A low degree of glial activation was observed as determined using CD11b and GFAP staining.

In summary, the modifications of the protocol for the SR-BI^{Ab} - PLL immunoporter resulted in a preparation that was free from detectable unbound SR-BI^{Ab}, obtained in a higher yield than initial preparations and had good DNA-binding capacity. Most importantly, these initial studies demonstrated that an immunoporter based on the SR-BI^{Ab} had the capacity to transfect glial cells in culture, though with some toxicity, and glial-like cells of the adult rat brain.

4.3.3 Construction of SR-BI^{Ab} - PEI immunoporter

Due to the limited transgene expression achieved using SR-BI^{Ab} - PLL immunogenes, we investigated potential improvements in transfection capacity. One factor influencing transfection capacity is the choice of polycation. Changing from PLL to PEI could potentially increase transfection capacities in culture and *in vivo* due to the greater capacity of PEI to escape the endosomal/lysosomal pathway *(Boussif et al., 1995; Tinsley et al., 2004; Schaffert and Wagner, 2008)*.

The approach for constructing PEI-based immunoporters was adopted from unpublished work by the collaborating lab of Professor Robert Rush. After

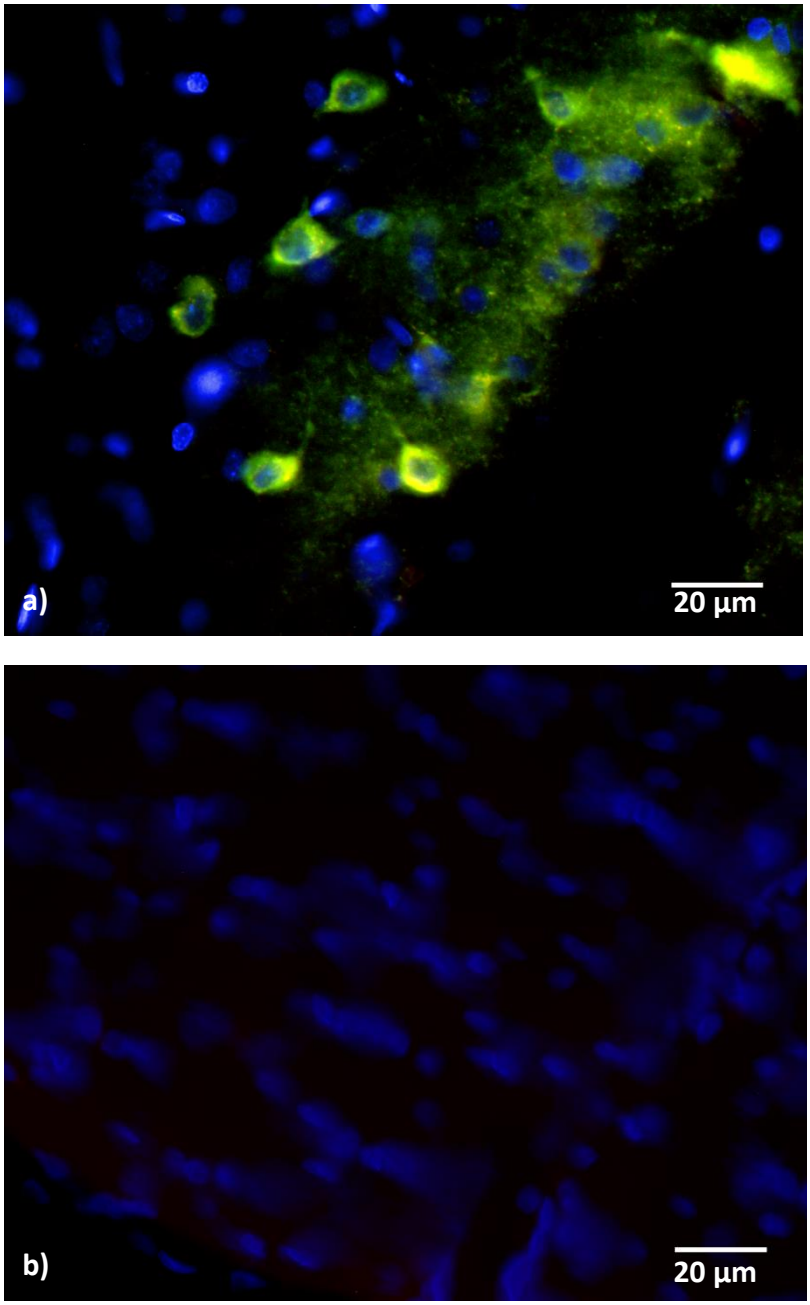

Figure 4.9 Initial intraventricular injection of SR-BI^{Ab} - PLL in adult rat brain *(n = 2) resulted in a) a sub-population of cells immunoreactive for GFP (green) in the periventricular area, as presented in an image from fluorescence microscopy. Pictures taken on the contralateral side away from the ventricle did not display any immunoreactivity (b). Nuclei were labelled with Hoechst 33258 (blue).*

initiating the development of an SR-BI^{Ab} - PEI immunoporter, the initial conjugate (see protocol in Appendix 2), only had modest capacity to bind DNA at SR-BI^{Ab} : DNA w/w ratios of up to 4 : 1. Full retardation of DNA was not reached in the tested conditions. However, a single preliminary study using 3 h treatments of mixed glial cultures with this immunogene (20 µg/ml) resulted in a few GFP-expressing cells. This showed that SR-BI^{Ab} - PEI had the capacity to transfect cells in culture, and to a larger extent than SR-BI^{Ab} - PLL. Thus, the construction protocol for the SR-BI^{Ab} - PEI immunoporter was modified to further increase transfection efficiencies.

Changes were initially focused on enhancing the capacity of SR-BI^{Ab} - PEI to bind DNA. This was done as a potential means to increase DNA delivery to cells and promote GFP expression. The DNA-carrying capacity of an immunoporter is dependent on its positive charge, which is dependent on the amount of PEI bound to the antibody. As a high amount of PEI per antibody would bind strongly to a cation exchange column, the elution of our immunoporter was expected at elutions using higher NaCl concentrations than 2 M, as in previous studies *(Blessing et al., 2001; Kircheis et al., 2001; Ogris et al., 2001; Kursa et al., 2003; Strehblow et al., 2005)*. In our studies, the initially used 1 : 4.5 SR-BI^{Ab} : SPDP molar ratio resulted in a 48 ± 15 % recovery (*n = 3*) in the 2 M NaCl fractions and none in the 3 M NaCl fractions. Thus, elution of our immunoporter was achieved at a lower ionic strength than observed in previous studies, which suggested that the cross-linking to the polycation was suboptimal.

Therefore, different SR-BI^{Ab} : SPDP molar ratios were tested in this reaction to increase the positive charge of the immunoporter. For the final immunoporter, the SR-BI^{Ab} : SPDP molar ratio was changed to 1.75 : 1, which resulted in 15 ± 2 % of the material eluted in the 3 M NaCl fraction (*n = 14*). This demonstrated that the conjugate had a higher positive charge and contained more PEI per antibody than previous batches of SR-BI^{Ab} - PEI immunoporter. Thus, this construct could potentially carry more DNA per immunoporter. It was therefore concluded that the decreased amount of SPDP added to the SR-BI^{Ab} lowered the degree of modification of the SR-BI^{Ab} and allowed for this to be eluted at 3 M NaCl rather than being subject to precipitation. The previous higher degree of visible precipitation after reaction with SPDP using SR-BI^{Ab} in comparison to other antibodies used for the same purpose (p75^{NTRAb}), suggests that this was due to characteristics of the antibody.

Construction of the SR-BI^{Ab} - PEI immunoporter using the final protocol described in section 4.2.2 resulted in a final yield of 4.2 ± 1.2 % (*n = 14*). Figure 4.10 summarises the amount of SR-BI^{Ab} recovered (based on A_{280} measurements) after five key steps. In EMSAs, full DNA retardation for the final immunoporter was observed at SR-BI^{Ab} : DNA w/w ratio of 1 : 1.3 (based on SR-BI^{Ab} protein at A_{280}; *n = 14*; Figure 4.11).

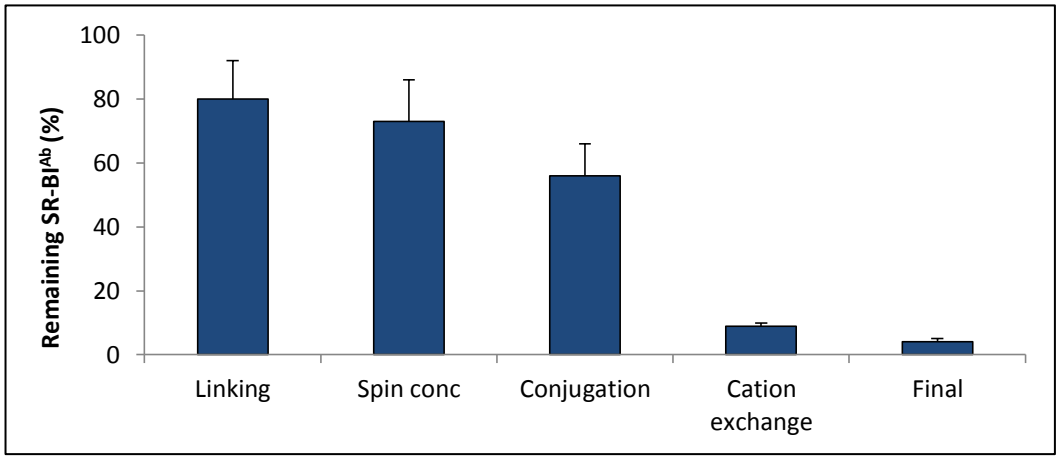

Figure 4.10 Antibody recovery of SR-BI^{Ab} - PEI immunoporter. *Diagram visualising the remaining proportion of SR-BI^{Ab} as determined at A_{280} after five key steps of the final SR-BI^{Ab} - PEI immunoporter protocol (see section 4.2.2; n = 14). Data are presented as mean + SD. The five key steps included: Linking (after antibody reaction with SPDP), Spin conc (following Vivaspin® concentrating steps of SR-BI^{Ab} after reaction with SPDP), Conjugation (after O/N incubation of SR-BI^{Ab} - SPDP with PEI-SPDP-SH), Cation exchange (following cation exchange separation of the immunogene from SR-BI^{Ab} alone) and Final (after the last step of Vivaspin® concentrating). Note that the majority of SR-BI^{Ab} is lost during the cation exchange step.*

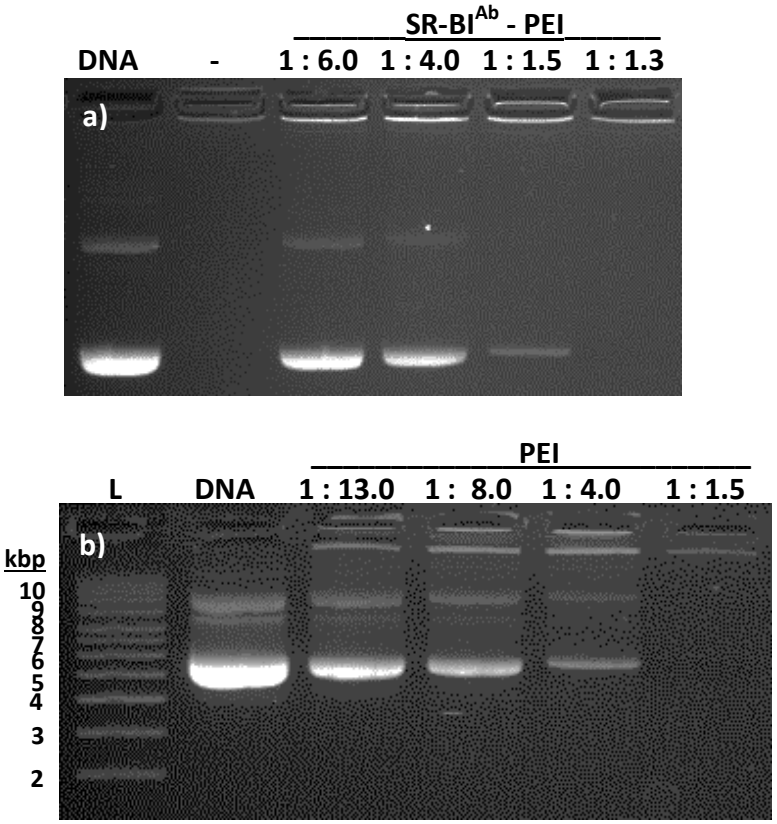

Figure 4.11 EMSAs for final SR-BI^{Ab} - PEI immunoporter and PEI alone. *a) EMSA displaying plasmid DNA binding and retardation by SR-BI^{Ab} - PEI immunoporter with SR-BI^{Ab} : DNA w/w ratios ranging from 1 : 6.0 to 1 : 1.3 (representative image of 15 EMSAs). Full DNA retardation was reached at a ratio of 1 : 1.3 for the final SR-BI^{Ab} - PEI immunoporter. b) DNA retardation was also seen upon the addition of PEI at PEI:DNA w/w ratios ranging from 1 : 13.0 to 1 : 1.5 (representative image of 3 EMSAs). Partial retardation of DNA occurred at the addition of lower amounts of SR-BI^{Ab} - PEI and PEI, as shown by a lower DNA amount detected in the gel compared to DNA alone. A supercoiled plasmid DNA ladder (L) with marked sizes in kbp was used for estimation of plasmid DNA size. Ethidium bromide was used for visualisation.*

4.3.4 Assessing the use of the SR-BI^{Ab} - PEI immunogene in culture

4.3.4.1 Transfection of glial cells in culture

Transfection was assessed after incubating mixed glial cultures with either 1 or 5 µg per well SR-BI^{Ab} - PEI immunogene, PEI-DNA alone (containing 1, 2.5 or 5 µg PEI per well) and DNA alone. Treatment with 1 µg SR-BI^{Ab} - PEI immunogene produced GFP expression that was detectable at 6 h (Figure 4.12a). Expression was subsequently analysed in cells fixed at 24 h and 72 h after the start of exposure (Figure 4.12b-c). GFP expression was seen in many cells in all cultures treated with the immunogene. Transfection efficiencies calculated for all cells independent of cell type after treating cultures with 1 µg SR-BI^{Ab} - PEI immunogene were 1.3 ± 0.2 % and 1.7 ± 0.6 % at 24 h and 72 h after the start of exposure, respectively (Figure 4.13). The maximum transfection efficiency in a single well was 2.4 %.

Increasing the amount to 5 µg of SR-BI^{Ab} - PEI immunogene added per well again resulted in GFP expression in most wells. Transfection efficiencies were not increased compared to treatment with 1 µg immunogene and the results were more variable. Half of the wells treated with 5 µg SR-BI^{Ab} - PEI immunogene produced similar transfection efficiencies to those with 1 µg immunogene whereas the other treated wells showed markedly lower GFP expression.

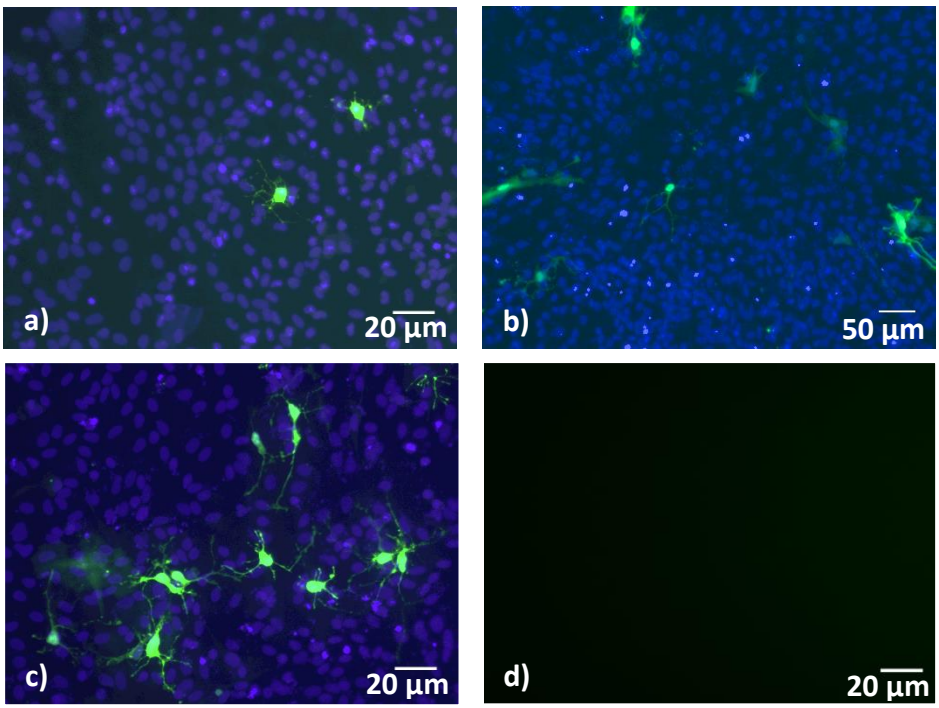

Figure 4.12 Transfection by SR-BI^{Ab} - PEI of cells in mixed glial cultures *as shown in representative images with GFP (green) after 6 h exposure to 1 µg SR-BI^{Ab} - PEI immunogene (based on SR-BI^{Ab} content) directly after 6 h exposure (a), 24 h (b) and 72 h (c) after the start of exposure. Pictures are taken from one of three independent experiments each. Note that many of these cells exhibit microglial morphologies. Nuclei were labelled with Hoechst 33258 (blue). Cultures exposed to only vehicle (modified HBSS buffer) did not display any immunoreactivity (d).*

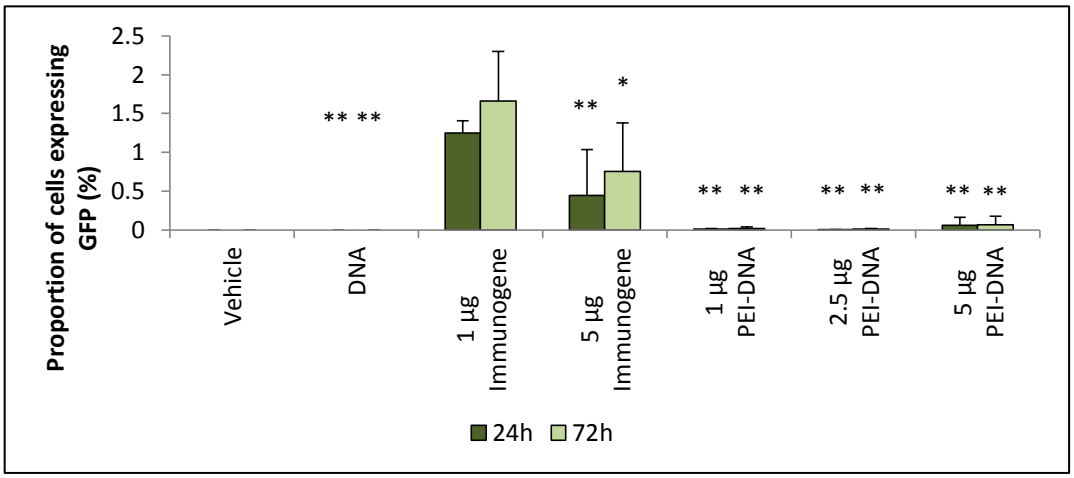

Figure 4.13 Transfection efficiencies in mixed glial cultures. *Proportion of Hoechst 33258-positive cells immunoreactive for GFP after 6 h exposure to vehicle (modified HBSS buffer), DNA alone, 1 µg / 5 µg SR-BI^{Ab} - PEI immunogene or 1 µg / 2.5 µg / 5 µg PEI - DNA per well at 24 h and 72 h after the start of exposure. Data are presented as mean + SD. Two-way ANOVA was used to compare all treatment conditions that included DNA plasmids (which excludes the vehicle treatment where no expression was expected). There was a highly significant overall effect of the different incubation conditions ($p < 0.01$) but no effect of the incubation time (24 h compared with 72 h) and no significant interaction. Subsequent comparison of the transfection efficiencies achieved with different treatment conditions (ANOVA with Student-Newman-Keuls post-hoc, n = 3 per group) demonstrated significant differences between cultures incubated with 1 µg SR-BI^{Ab} - PEI immunogene when compared with all other conditions at both time points * $p < 0.05$, ** $p < 0.01$ compared with the 1 µg SR-BI^{Ab} - PEI immunogene assessed at the same time point. No other differences between treatments were statistically significant.*

Transfection with 1 µg SR-BI^{Ab} - PEI immunogene was 120-fold higher than with PEI-DNA alone. Incubations with 1 µg PEI, which carried an amount of DNA equivalent to the immunoporter, resulted in detectable GFP expression in only half of the cultures and a maximum transfection efficiency of 0.04% in one of the cultures assessed at 72 h. Increasing the amount to 5 µg of PEI-DNA added per well again resulted in detectable GFP expression in only half of the wells. The highest individual efficiency was 0.19 %. No GFP expression was detected in any of the cultures treated with DNA alone.

Two-way ANOVA (with Student-Newman-Keuls post-hoc)) showed a statistically significant overall difference between the treatments ($p < 0.01$; Figure 4.13) and no significant effect of incubation time on GFP expression (24 h or 72 h). The treatment with 1 µg SR-BI^{Ab} - PEI immunogene was more efficient than the treatments with PEI-DNA and DNA alone and was also significantly different to the treatment with 5 µg SR-BI^{Ab} - PEI immunogene.

4.3.4.2 SR-BI^{Ab} - PEI immunogene transfection of astrocytes and microglia

In contrast to the microglia-specific uptake of the SR-BI^{Ab} (see section 3.3.3), the SR-BI^{Ab}-based immunogene transfected both microglia (Figure 4.14a) and astrocytes (Figure 4.14b) in mixed cultures. For 1 µg SR-BI^{Ab} - PEI per well, the proportion of transfected microglia and astrocytes was similar to the distribution of these cells in the original culture. An average of 10 % of transfected cells expressed the microglial marker CD11b (*n = 3*), with up to 20 % co-labelling in

Figure 4.14 Transfection of microglia and astrocytes by SR-BI^{Ab} PEI *(see figure text on next page)*

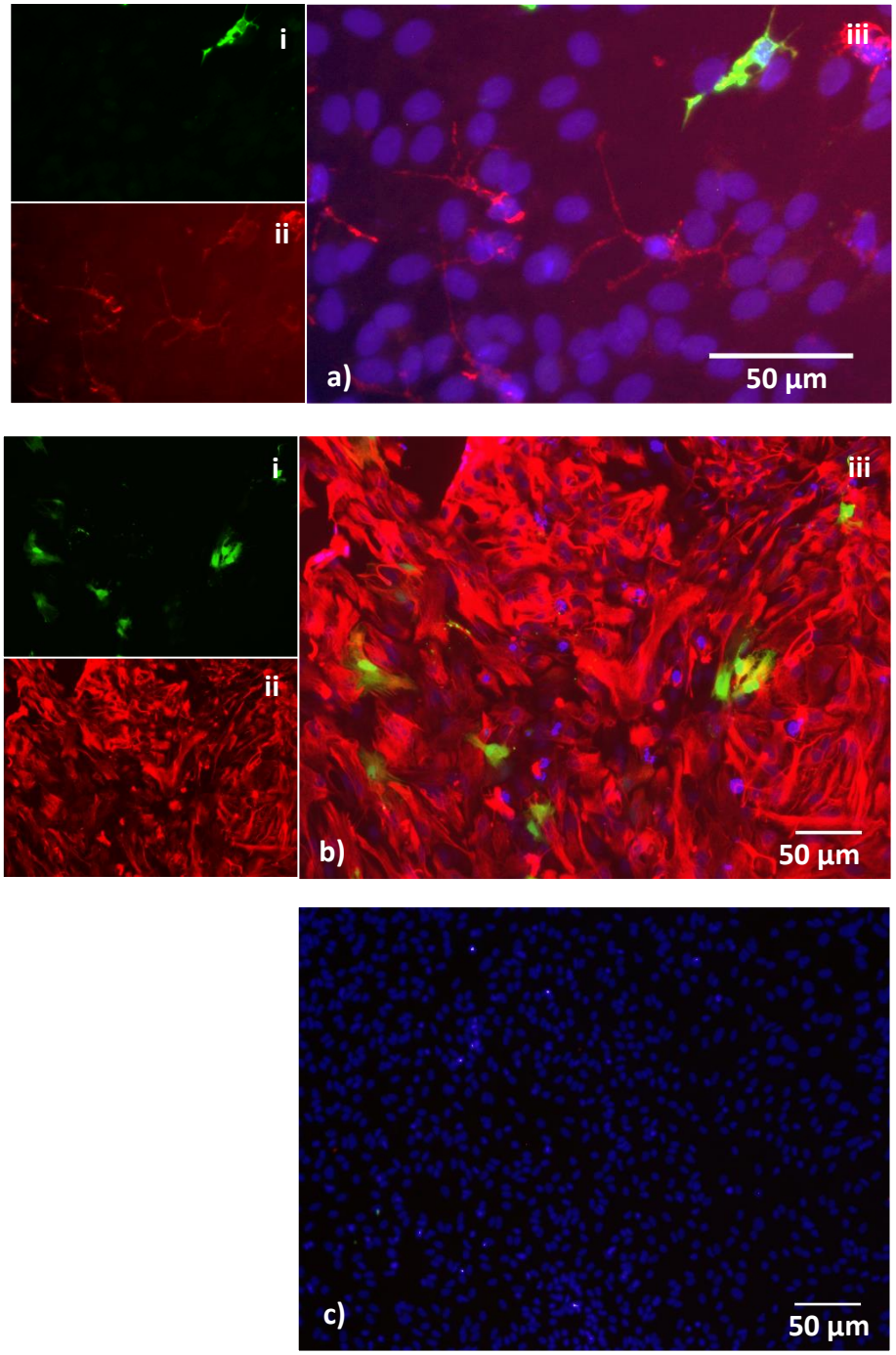

Figure 4.14 Transfection of microglia and astrocytes by SR-BI^{Ab} - PEI *(see previous page).* *Images from fluorescence microscopy showing cells immunoreactive for GFP (green in panels i of a and b) after 6 h exposure to 1 µg SR-BI^{Ab} - PEI per well (based on SR-BI^{Ab} protein content) in one of three independent experiments each. This GFP expression co-labelled with CD11b/c (red in panel a-ii) in cells with microglial morphology. GFP immunoreactivity also co-labelled with GFAP (red in panel b-ii) in cells with astrocytic morphology. Images were taken 24 h and 72 h after start of exposure in a) and b), respectively. Merged images are shown in (a-iii and b-iii). Note that microglial cells with ramified morphology exhibited GFP immunoreactivity in (a) and some might also be identified through morphology in (b). Cultures treated with secondary antibodies alone did not display any immunoreactivity (c). Nuclei were labelled with Hoechst 33258 (blue).*

individual wells. The majority of GFP-positive cells (45 - 80 %) were astrocytes that expressed GFAP. We also identified cells expressing GFP in which neither CD11b nor GFAP immunolabelling was detected. All of these cells had morphologies which were similar to either GFAP-positive astrocytes or CD11b-positive microglia. GFP-positive/GFAP-negative/CD11b-negative cells were not immunoreactive for markers of other potential cell populations, including NG2-positive glia and NeuN-positive neurons. Furthermore, no co-labelling was found with A2B5, a marker for stem cells that have been detected previously in mixed glial cultures *(Marek et al., 2008)*.

With regards to 1 µg / 2.5 µg / 5 µg PEI - DNA, averages of 13 - 63 % of cells transfected by these agents were identified as GFAP-positive astrocytes. In contrast to 1 µg of SR-BI^{Ab} - PEI immunogene, no GFP-positive cells were found to co-label with the microglial marker CD11b after exposure to PEI - DNA.

SR-BI expression was detected in all GFP-positive cells studied after exposure to the SR-BI^{Ab} - PEI immunogene (Figure 4.15a-b). In contrast, following PEI-DNA treatment, a few cells of the small GFP-expressing population were not immunreactive for SR-BI (*n = 3*; Figure 4.15c).

Figure 4.15 Specificity of transfection using SR-BI^{Ab} - PEI in contrast to PEI - DNA

(see figure text on the following page)

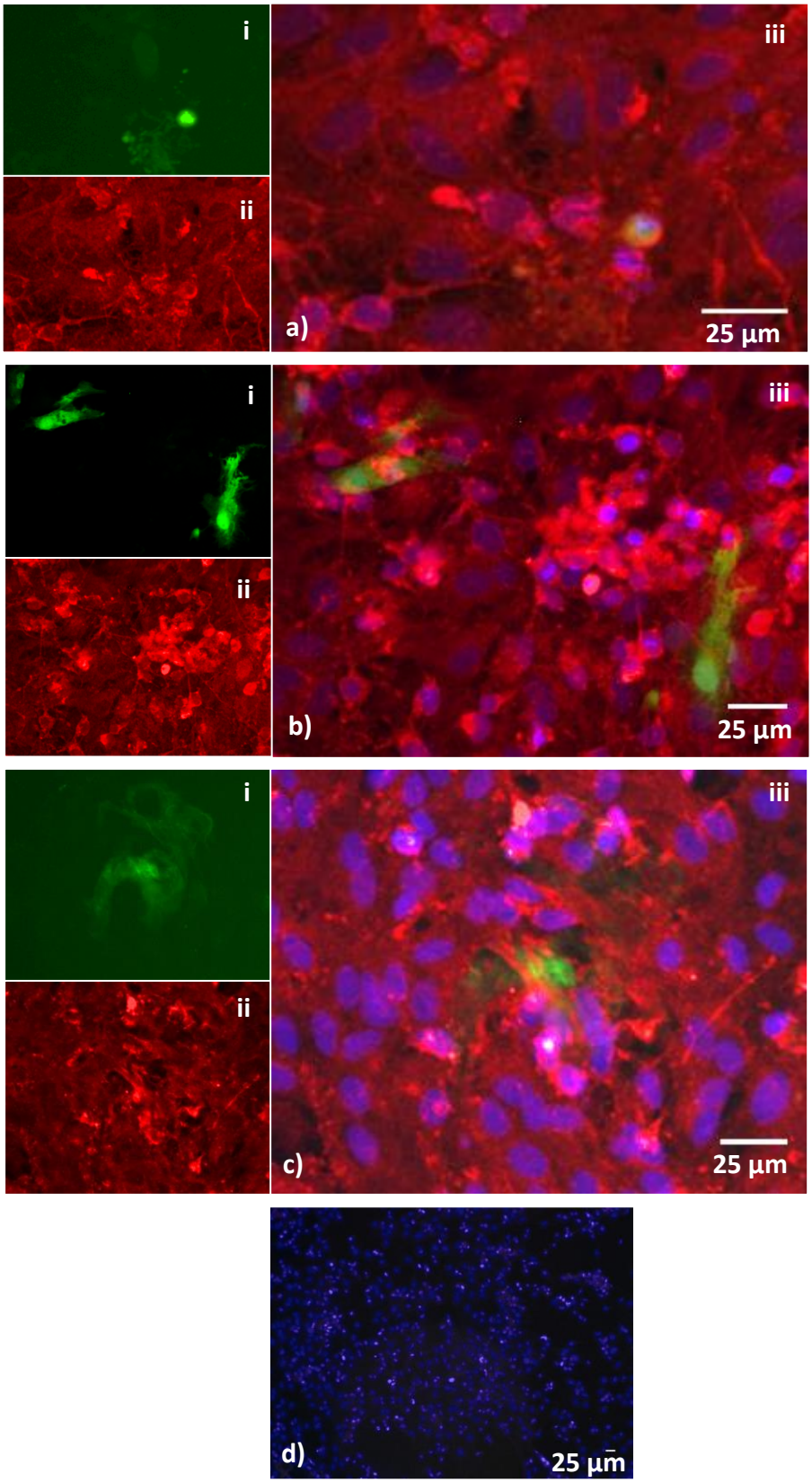

Figure 4.15 Specificity of transfection using SR-BI^{Ab} - PEI in contrast to PEI - DNA *(see previous page). Images from fluorescence microscopy displaying cells immunoreactive for GFP (green in panels i of a-c) and SR-BI (red in panels ii of a-c) in mixed glial cultures after 6 h exposure and 24 h post-incubation. Merged images are shown in panels iii of a-c. Exposure to 1 µg SR-BI^{Ab} - PEI immunogene per well (based on SR-BI^{Ab} content) resulted in the co-labelling of GFP with SR-BI in cells displaying both microglial (a) and astrocytic (b) morphologies. In contrast, as exemplified in (c), GFP-positive cells were identified after exposure to 5 µg PEI - DNA per well which did not express SR-BI. Cultures exposed to secondary antibodies alone did not display any immunoreactivity (d). Nuclei were labelled with Hoechst 33258 (blue).*

4.3.4.3 Assessment of toxicity in cultures after immunogene treatment

To initially assess for potential toxicity, total cell numbers were compared for the different treatments in the same cultures that had been analysed for transfection efficiency. No significant difference in cell numbers based on Hoechst 33258 counts was detected ($p > 0.05$; ANOVA, *n = 3* per group; Figure 4.16). Also, the proportion of microglia in the mixed glial cultures at 24 h and 72 h after the start of exposure did not change significantly in any tested condition ($p > 0.05$; ANOVA, *n = 3* per group*;* Figure 4.17).

In additional cultures, the effects of treatment were tested using calcein-AM / PI labelling (as previously described in section 4.2.5.3). Most cells showed calcein-AM fluorescence, indicating that they remained viable (as exemplified for vehicle-treated cultures and for cultures exposed to 1 µg SR-BI^{Ab} - PEI in Figure 4.18).

This conclusion was supported by the low numbers of PI-positive cells in most cultures. According to these studies, cultures exposed to 1 µg SR-BI^{Ab} - PEI per well did not result in any significant increase in PI-positive cells at either 6 h or 24 h ($p > 0.05$; ANOVA, *n = 3* per group*,* Figure 4.19). Analysis was limited to the samples where DNA was included. The amount of PI-positive cells was not significantly increased for any condition studied, however there was a higher variability between wells and experiments following exposure to the higher

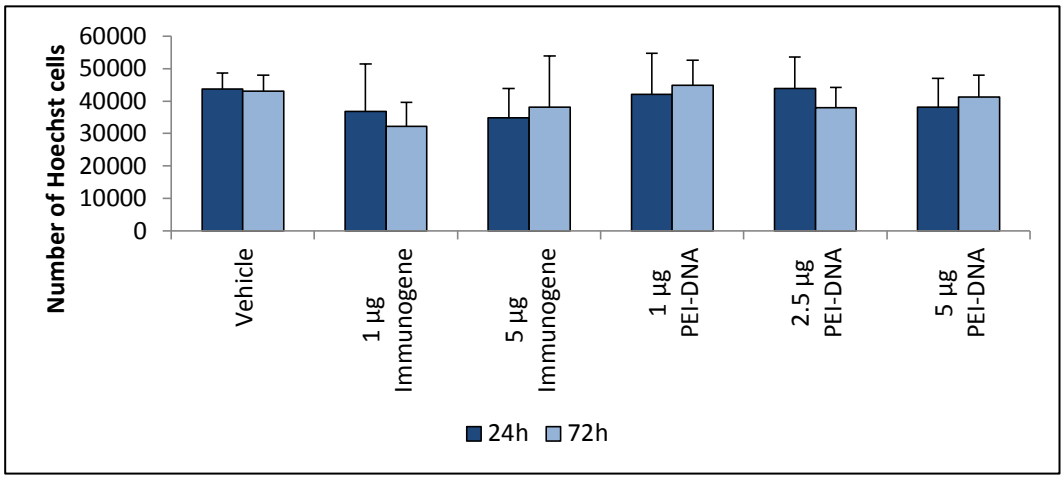

Figure 4.16 Cell numbers in glial cultures 24 h and 72 h after start of exposure *was not altered, as determined by the number of Hoechst-positive nuclei in wells exposed for 6 h to vehicle (modified HBSS buffer), 1 µg / 5 µg SR-BI^{Ab} - PEI immunogene or 1 µg / 2.5 µg / 5 µg PEI - DNA. Data are presented as mean + SD (p > 0.05; ANOVA, n = 3).*

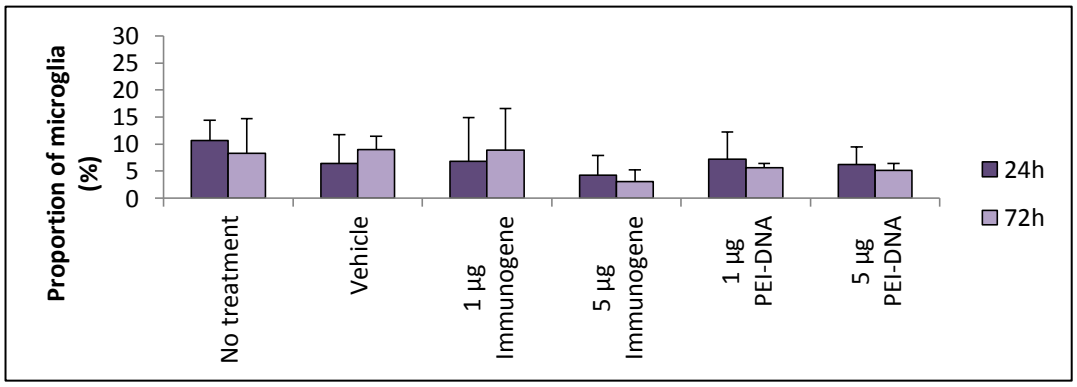

Figure 4.17 Proportion of microglia in glial cultures 24 h and 72 h after start of exposure*, as determined using CD11b/c staining. These cultures had been exposed to 6 h of no treatment (growth medium alone), vehicle (modified HBSS buffer), 1 µg / 5 µg SR-BI^{Ab} - PEI immunogene (based on SR-BI^{Ab} content) or 15 µg / 5 µg PEI - DNA per well. Data are presented as mean + SD. No significant change was detected (p > 0.05; ANOVA, n = 3).*

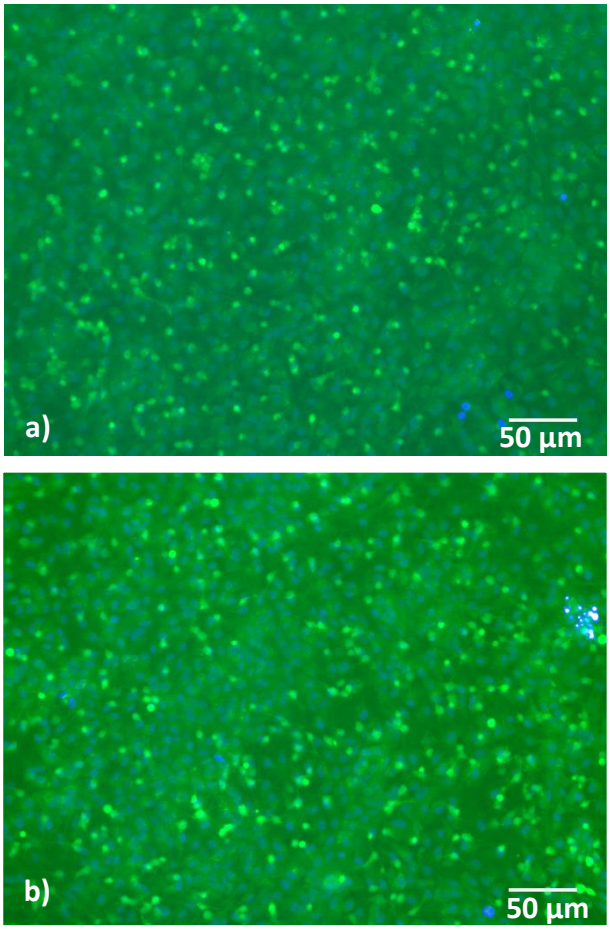

Figure 4.18 Calcein-AM incorporation in cells of mixed glial cultures. *These cultures were treated for 6 h with either vehicle (a; modified HBSS) or 1 µg SR-BI^{Ab} - PEI (b) in one of three independent experiments each. At 24 h after start of exposure, calcein-AM (green) was added to the cultures. There was no difference in calcein-AM incorporation between treated and non-treated cultures. Nuclei were labelled with Hoechst 33258 (blue).*

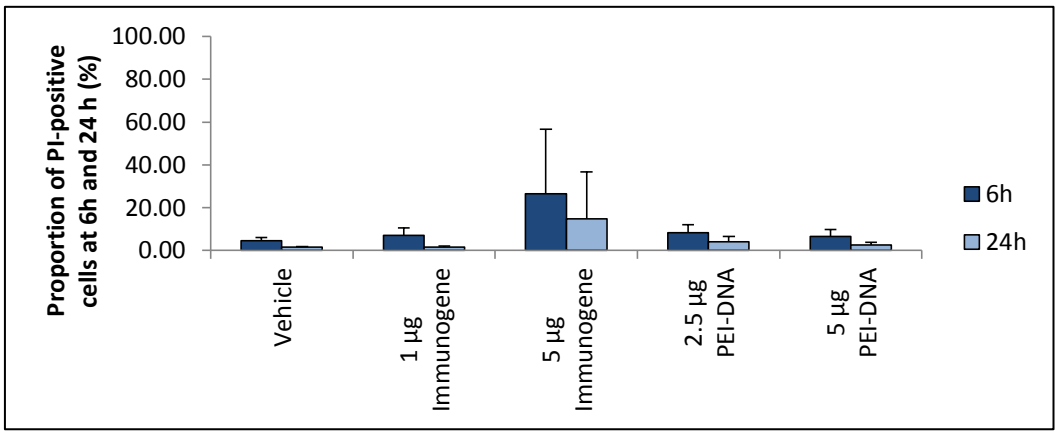

Figure 4.19 No significant cell death in glial cultures 6 h and 24 h after start of exposure. *The proportion of PI-positive nuclei out of total Hoechst 33258-positive nuclei was not significantly changed at any of the analysed time points after 6 h exposure to vehicle (modified HBSS buffer), 1 µg / 5 µg SR-BI^{Ab} - PEI immunogene or 2.5 µg / 5 µg PEI - DNA ($p > 0.05$; ANOVA, $n = 3$). Data are presented as mean + SD.*

amounts of immunogene. There was no evidence under any conditions for increases in the numbers of PI-positive cells at 24 h compared with 6 h. Indeed, mean values were generally lower, suggesting that some dead cells had detached from the culture during this period. Representative images are displayed for the selected conditions after 6 h exposure (Figure 4.20a-f) and at 24 h after the start of treatment (Figure 4.20g-l).

4.3.4.4 Effects on microglial activation by immunogene treatment

Exposure to various treatments could potentially alter activation of cells in culture. The possibility that immunogene treatment produced activation of microglia was tested based on the distribution of morphological profiles in this population (as described in section 3.2.2.3).

At 24 h and 72 h, untreated cultures contained approximately 20 % ramified microglia (Figure 4.21). This coincides with data in similarly prepared cultures of embryonic origin with this age in culture *(Szabo and Gulya, 2013)*. Remaining cells consisted of similar proportions of those with an amoeboid morphology and cells with short processes that resembled activated, but non-proliferative and non-phagocytic microglia described by others *(Giulian and Baker, 1986; Saura et al., 2003)*.

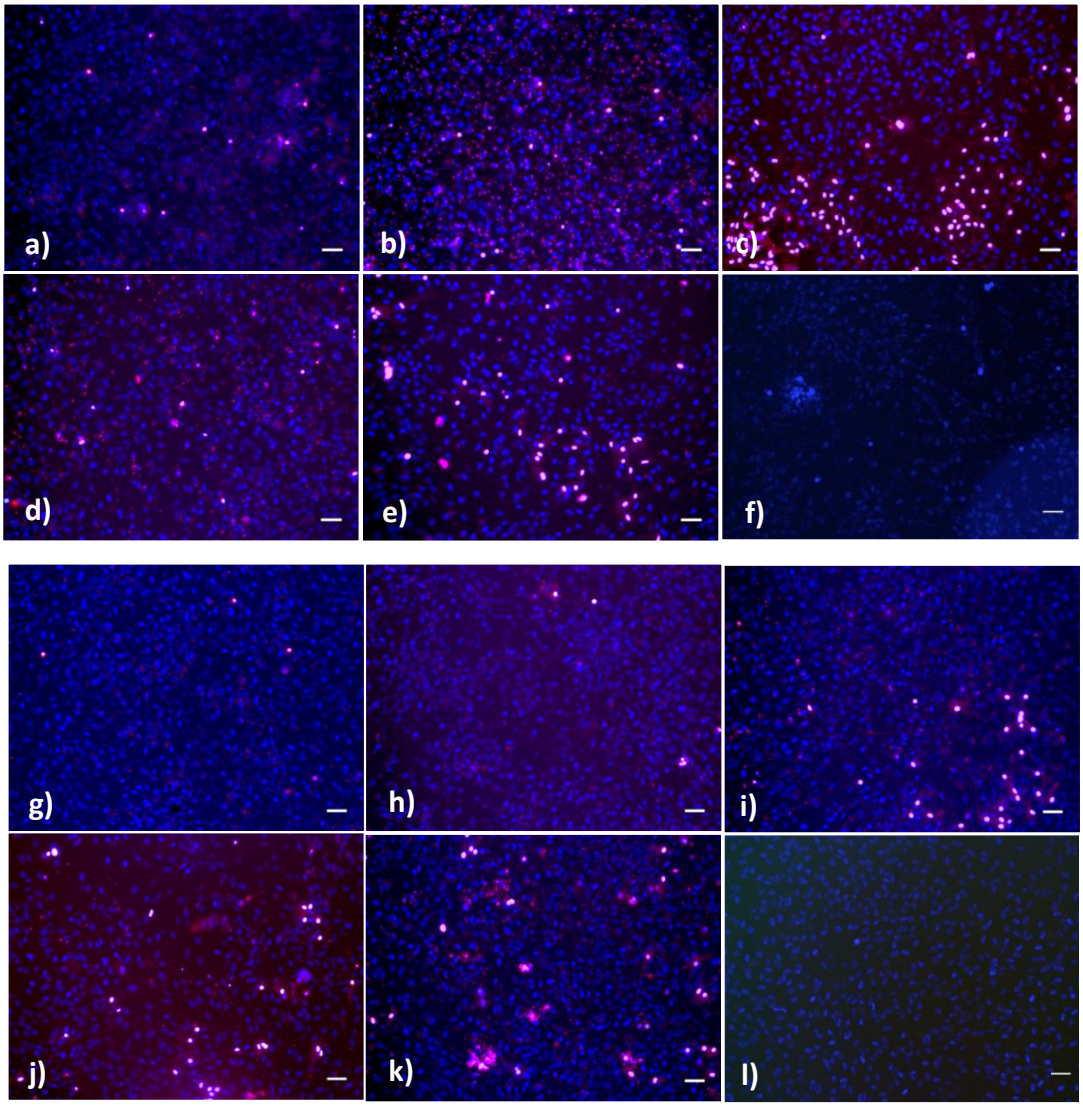

Figure 4.20 Images of cell death in glial cultures at 6 h and 24 h after start of exposure *showing PI (red) and Hoechst 33258 nuclear stain (blue) in merged images from one of three independent experiments each. Images were taken directly after 6 h exposure (a-f), and 24 h after the start of treatment (g-l). Cultures were treated with growth medium alone (a and g), 1 µg (b and h) or 5 µg (c and i) SR-BI^{Ab} - PEI immunogene per well, or to 2.5 µg (d and j) or 5 µg (e and k) PEI - DNA per well. Cultures treated without the addition of PI did not display any immunoreactivity (f and l). Scale bars = 50 µm.*

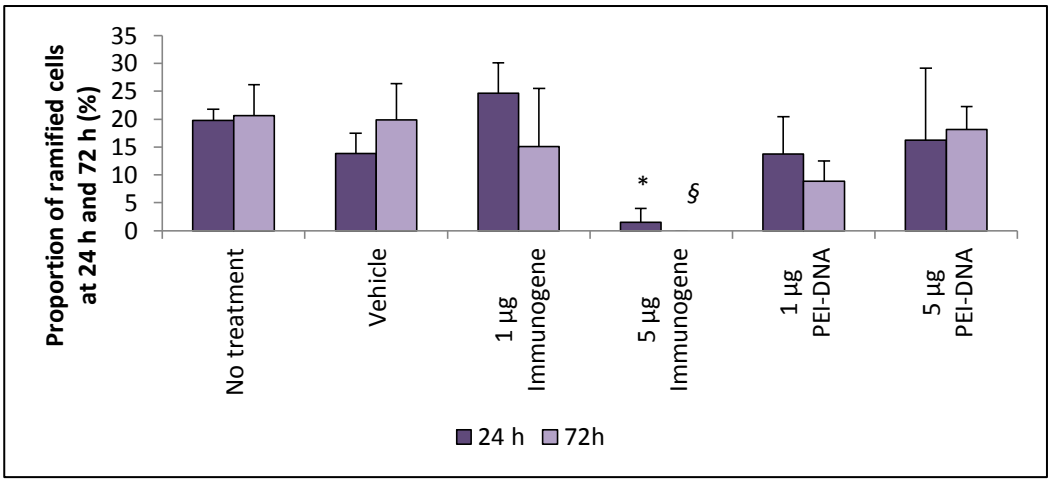

Figure 4.21 Proportion of ramified CD11b/c-positive microglia in mixed glial cultures 24 h and 72 h after start of treatment. *Cultures received 6 h of no treatment (growth medium alone), vehicle (modified HBSS buffer), 1 µg / 5 µg SR-BI^{Ab} - PEI immunogene (based on SR-BI^{Ab} content) or 1µg / 5 µg PEI - DNA per well. Data are presented as mean + SD. Two-way ANOVA revealed a highly significant treatment effect ($p < 0.001$), with no significant effect of incubation time and no significant interaction. Comparisons of individual treatment conditions (ANOVA with Student-Newman-Keuls post-hoc, n = 3 per group) are shown in the figure: * $p < 0.05$ compared with 1 µg immunogene and no treatment at 24 h; § $p < 0.05$ compared with all other treatments at 72 h except 1 µg PEI-DNA.*

Treatments using 1 µg SR-BI^{Ab} - PEI immunogene per well did not alter activation stages of these cells at either of the two time points. However, cell cultures treated with 5 µg SR-BI^{Ab} - PEI immunogene per well contained a significantly decreased proportion of ramified microglia. At 24 h, this was significantly decreased in comparison to untreated wells and to cells exposed to 1 µg SR-BI^{Ab} - PEI immunogene per well. For the 72 h time point, the population of ramified microglia after exposure to 5 µg SR-BI^{Ab} - PEI was completely abolished and was significantly decreased in comparison to all other conditions tested except 1 µg PEI ($p < 0.05$; ANOVA with Student-Newman-Keuls post-hoc, *n = 3* per group). This indicated that the immunogene treatment may affect microglial activation in a concentration-dependent manner.

There was also a significant overall effect of treatment on the proportion of amoeboid activated microglia ($p < 0.05$, two-way ANOVA, *n = 3* per group; Figure 4.22), consistent with an activation of the microglia by some treatments. Further analysis demonstrated that the proportion of amoeboid microglia at 24 h after treatment with 5 µg immunogene was significantly higher than seen following treatment with vehicle or 5 µg PEI-DNA ($p < 0.05$, two-way ANOVA with Student-Newman-Keuls post-hoc, *n = 3* per group). Due to the findings of less ramified and more amoeboid microglia after exposure to 5 µg SR-BI^{Ab} - PEI, 1 µg SR-BI^{Ab} - PEI was used in subsequent studies.

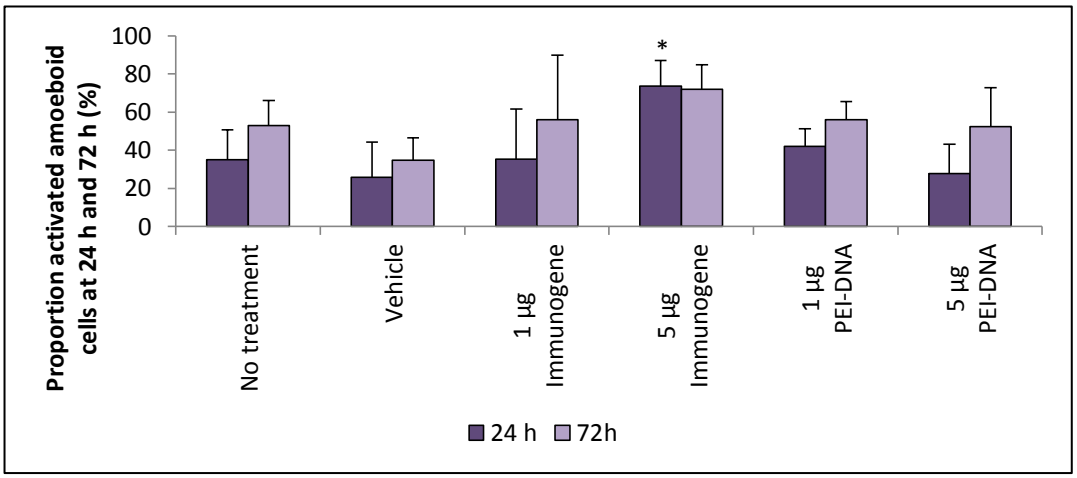

Figure 4.22 Proportion of activated amoeboid CD11b/c-positive microglia in mixed glial cultures 24 h and 72 h after start of exposure*. Cultures received 6 h of no treatment (growth medium alone), vehicle (modified HBSS buffer), 1 µg / 5 µg SR-BI^{Ab} - PEI immunogene (based on SR-BI^{Ab} content) or 1 µg / 5 µg PEI - DNA per well. Data are presented as mean + SD. Two-way ANOVA revealed a significant treatment effect ($p < 0.05$) with no significant effect of incubation time and no significant interaction. At 24 h, post-hoc analysis showed a significantly higher proportion of amoeboid microglia after exposure to 5 µg SR-BI^{Ab} - PEI in comparison to vehicle and to 5 µg PEI-DNA. No significant differences were detected at 72 h after start of treatment.*

4.3.4.5 Effects on immunogene transfection by prior activation of cultures

To test if the activation stage of the microglia affected transfection of these cells, cultures were treated with LPS, a previously used activator of microglia *(Saura, 2007)*, prior to exposure to the SR-BI^{Ab} - PEI immunogene. In these LPS - treated cultures, the majority of microglia had an activated morphology in comparison to control cultures (Figure 4.23).

For these set of experiments, transfection efficiencies in control cultures not exposed to LPS prior to immunogene transfection and post-incubation for 72 h was 1.7 ± 0.8 %, similar to what had been obtained previously. In LPS - treated cultures, the efficiency was 1.9 ± 0.4 %, demonstrating that microglial activation did not significantly change the extent of transfection in mixed glial culture by the SR-BI^{Ab} - PEI immunogene (two-tailed t-test, $p > 0.05$; *n = 3* per group). Also, expression of SR-BI remained in the majority of cells after exposure to this microglial activation agent as shown using IHC for SR-BI (*n = 3*), suggesting that the expression of this receptor is not greatly modified by activation.

4.3.5 Transfection by the SR-BI^{Ab} - PEI immunogene in vivo

Subsequent studies provided an initial test of the possibility that the SR-BI^{Ab} - PEI immunogene might also be suitable for transfecting glial cells in the adult rat brain. To increase the chances of achieving transfection in this initial study, the immunogene was infused into the hippocampus of two rats over 14 days using

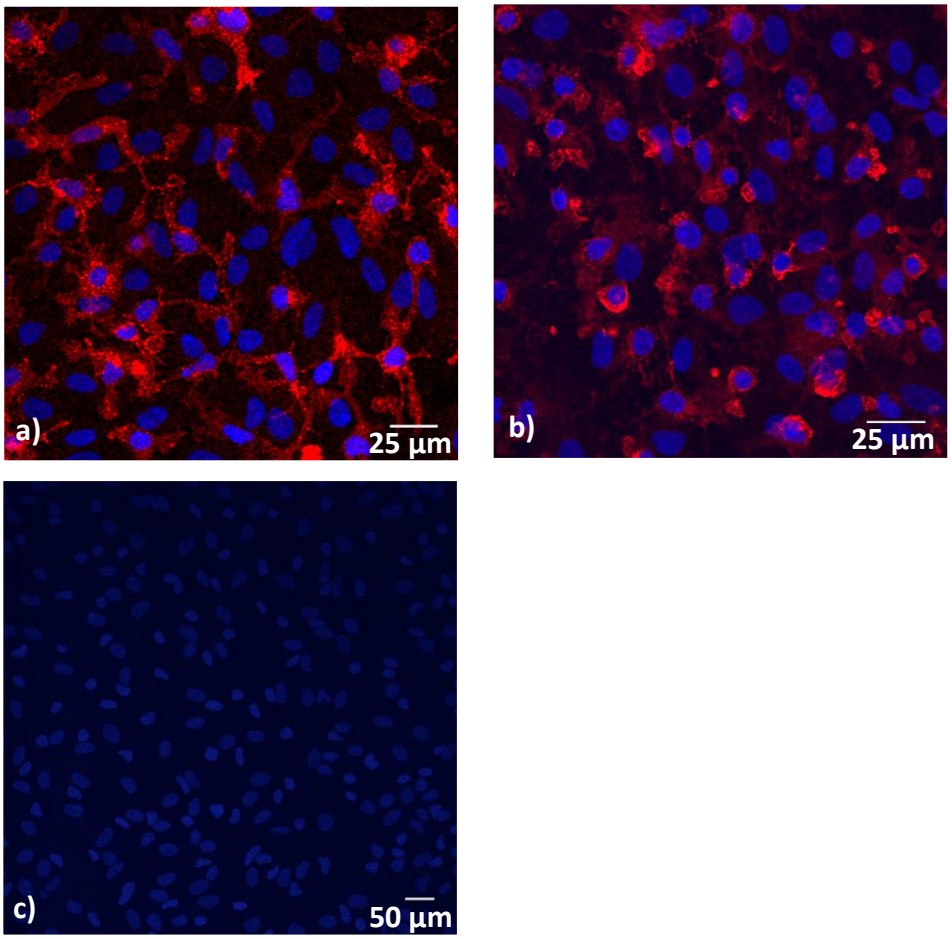

***Figure 4.23 Activation after LPS exposure in mixed glial culture**, as shown in representative images in one of three independent experiments. In b), the majority of CD11b/c-positive (red) microglia display an amoeboid morphology in comparison to non-treated culture controls which displayed a distribution of activation stages in culture (a) similar to that seen in previous studies, as shown in Figure 3.3. Cultures treated with secondary antibody alone did not display any immunoreactivity (c). Nuclei were labelled with Hoechst 33258 (blue).*

osmotic pumps. In the brains of these rats, GFP expression was found in many cells surrounding the site of infusion (Figure 4.24a-b). Almost all cells expressing GFP were also immunoreactive for CD11b (Figure 4.24c; see further characterisation of subsequent infusions in Chapter 5). Transfected cells were concentrated in the area of damage that developed as a result of the insertion of the infusion needle and subsequent infusion. However, transfected cells were also seen outside of the area of damage at distances up to 4.2 mm from the infusion site, and sporadic cells were detected close to the midline on the contralateral side of the brain.

4.4 Discussion

The results presented in this chapter demonstrate the capacity of immunogenes incorporating an antibody against SR-BI to produce transfection of glial cells in mixed glial culture and in the adult rat brain. In contrast to the predictions from investigations of SR-BI^{Ab} internalisation in glial cell cultures, both microglia and astrocytes in culture were transfected after the exposure to the SR-BI^{Ab} - PEI immunogene. Transfection was much more efficient using the SR-BI^{Ab} - PEI immunogene than PEI alone bound to DNA when compared on the basis of DNA content. Maximum transfection efficiency with the SR-BI^{Ab} - PEI immunogene was achieved under conditions that did not affect viability of the cells. Furthermore, transfection by this SR-BI^{Ab} - PEI immunogene did not alter the activation of microglia, as assessed from changes in morphology, and was not influenced by increases in activation stage of these cells.

Figure 4.24 Transfection after SR-BI^{Ab} - PEI infusions into adult rat hippocampus

(see figure text on the next page)

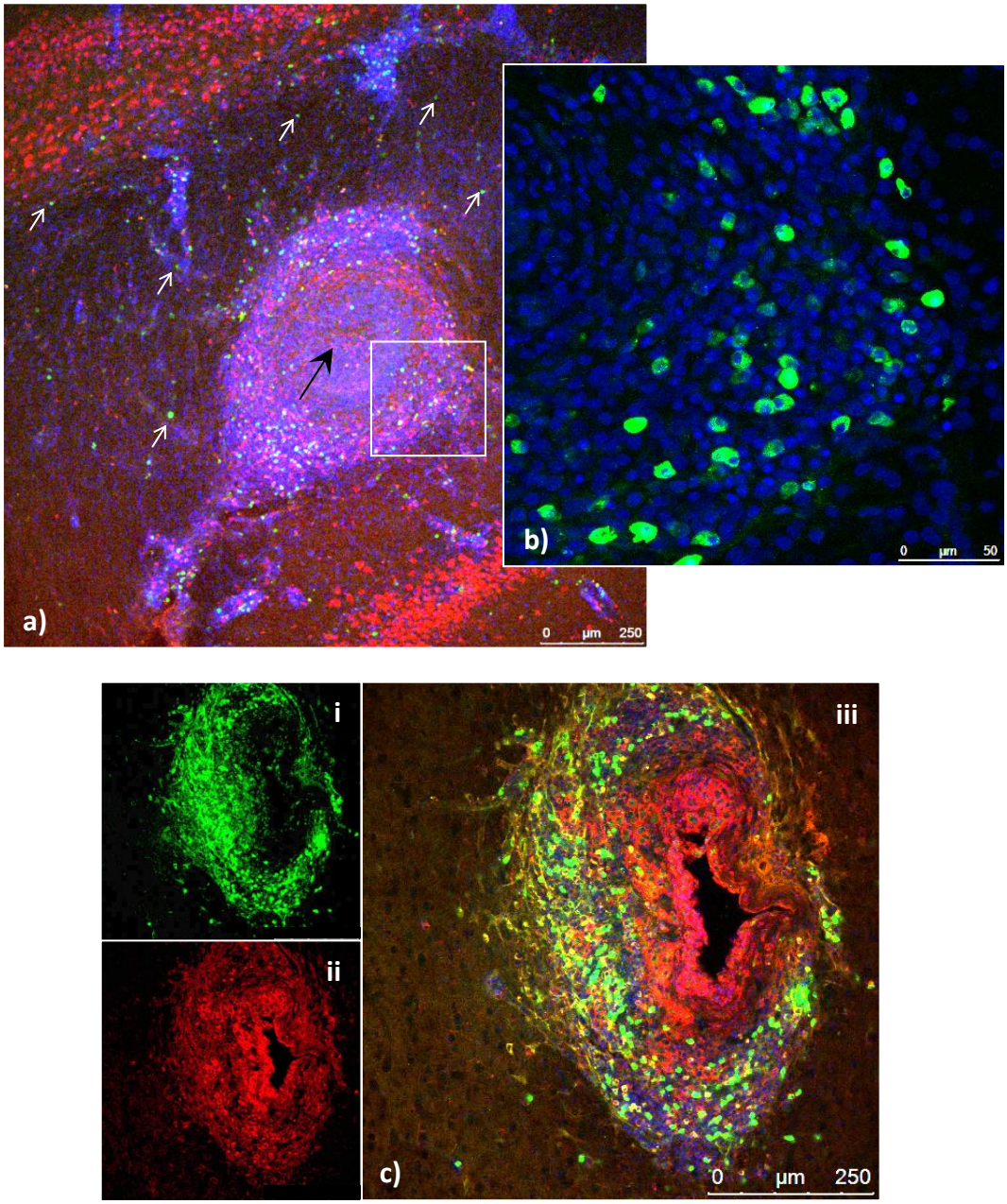

***Figure 4.24 Transfection after SR-BI^{Ab} - PEI infusions into adult rat hippocampus**, as shown in representative images (see previous page) from 50 µm horizontal sections in confocal microscopy from one of two brains. GFP immunoreactive cells (green) were found in a large area around the infusion site (a; large black arrow). In a picture from a different brain section with higher magnification (b), a widespread transfection of cells is visible around the site of infusion, in particular in the area of damage around the needle tract, which is demonstrated in more intense Hoechst 33258 nuclear staining (blue). Transfected cells were scattered (a; small white arrows) in an area up to 4.2 mm away from the infusion site. NeuN (red in panel a) visualised cell layers of the hippocampus. Also, the majority of cells immunoreactive for GFP (green in panel c-i) co-labelled with the microglial marker CD11b (red in panel c-ii), as shown in a merged image (panel c-iii). Brain sections exposed to secondary antibodies alone displayed no immunoreactivity with the exception of a few cells as shown in Figure 5.13f.*

Most interestingly, the findings from infusions of the SR-BI^{Ab} - PEI immunogene *in vivo* provided a proof of concept that such a conjugate could be used to selectively target microglia in the brain. Further development of this technique has the potential to provide novel approaches for manipulating the expression of key proteins in these cells. These initial findings led to a more detailed characterisation of transfection *in vivo*, which is further described in Chapter 5. The subsequent studies include evaluations of the distribution of GFP expression and the nature of the cells expressing this reporter gene. The chapter also investigates the effects of modifying the immunogene to promote the escape from the endosomal/lysosomal pathway, and to enhance nuclear translocation. The studies also examine the transfection produced using single intracerebral injections rather than long-term infusions.

4.4.1 The SR-BI^{Ab} - PEI immunogene transfects microglia of the adult rat brain

Although the initial *in vivo* studies were limited to investigations in two rats, they provide clear evidence that the SR-BI^{Ab} - PEI immunogene has the capacity to generate transfection of cells in brain tissue and that this transfection is highly selective for CD11b-positive cells. This finding is consistent with the selective internalisation of SR-BI^{Ab} into microglia but not in other cells in brain as reported in section 3.3.4.

As discussed for the antibody findings, this selective uptake could be due to the presence of SR-BI on microglia that was not detected by IHC either because the number of receptors were low or the epitopes detected by IHC were masked. Alternatively, the internalisation could involve cross reactivity of the antibody with other proteins or binding of other regions of the immunogene to the components in the cell membrane. The cellular specificity of the transfection was characterised in more detail in studies described in Chapter 5. These studies also investigated the efficiency of transfection compared with PEI - DNA or DNA alone and with an immunogene incorporating a different antibody. Infusions of a p75^{NTRAb}-based immunogene have not reported expression in microglia *(Berhanu and Rush, 2008)*.

Transfection with the SR-BI^{Ab} - PEI immunogene is similar to that produced in a single study using a viral vector *(Cucchiarini et al., 2003)*, although the viral transduction involved a single injection rather than an infusion (as used in our studies). The transfection capacity of our immunogene greatly exceeds that of other non-viral approaches, especially in the adult animal (see sections 1.4.2.1 on mechanic genetic modification and section 1.6 on genetic modification of microglia). Of the few published non-viral methods used in the intact CNS, most of these involve electroporation and generally do not discuss transfection of microglia or any cell-specific transgene expression *(Polazzi and Monti, 2010; Kofler and Wiley, 2011)*. Out of the methods that did produce transgene expression in microglia, this was not restricted to the microglial population

(Tanaka et al., 2000; Wang et al., 2007a). Our study demonstrates the only known avenue to selectively target microglial cells in the intact brain.

4.4.2 Transfection efficiencies by SR-BI^{Ab} - PEI immunogene in culture

The immunogene was initially characterised using mixed glial cultures to assess cell selectivity and transfection efficiencies compared with PEI - DNA alone. Further characterisation assessed whether treatment with immunogenes affected cell viability or the extent of activation of the microglia, and conversely whether promoting microglial activation affected transfection efficiency.

Treatments using 1 µg SR-BI^{Ab} - PEI immunogene in wells of mixed glial cultures resulted in consistent GFP expression. Transfection efficiencies using our immunogene resemble those reported using similar immunogenes and other non-viral methods to transfect cell lines. An immunoporter based on an antibody against epidermal growth factor receptor resulted in reporter gene expression in less than 2 % of cells in a human squamous carcinoma cell line *(Chen et al., 1994)*. Also, cell lines of neuronal origin have been transfected using similar conjugates with efficiencies between 5 and 8 % *(Martinez-Fong et al., 1999)*. Transfection efficiencies of other non-viral methods have rarely exceeded 20 % in microglial cell lines or primary glial cultures *(Wiesenhofer and Humpel, 2000; Jana et al., 2001; Mitrasinovic et al., 2001; Strehblow et al., 2005)*. Notably, these methods, which consist of mainly lipofection techniques, are not targeted

methods and thereby lack the capacity to discriminate between different cell populations.

The transfection efficiency of our SR-BI^{Ab} - PEI immunogene was significantly higher than that of PEI - DNA of equivalent amounts added per well. Comparing 1 µg PEI -DNA with 1 µg SR-BI^{Ab} - PEI immunoporter, these would according to EMSAs carry similar amounts of DNA (1.5 µg and 1.3 µg, respectively). Thus, the 120-fold higher transfection efficiency of 1 µg SR-BI^{Ab} - PEI immunogene compared to 1 µg PEI - DNA per well demonstrates a stronger capacity of the immunoporter than PEI itself to deliver DNA to cells in mixed glial cultures. There was limited GFP expression after PEI - DNA treatment. This is consistent with previous studies in which the use of immunoporters in culture has been shown superior to that of PEI - DNA *(Merdan et al., 2003; Zeng et al., 2007)* and PLL - DNA *(Chen et al., 1998a; Suh et al., 2001)*. Higher levels of transfection have been achieved using PEI - DNA in the C6 glioma cell line, with transfection efficiencies of up to 14 % *(Tinsley et al., 2004)*. Also, although primary cultures are generally harder to transfect *(Zou et al., 2010)*, transgene expression has been achieved in 0.95 ± 0.29 % of primary granule neurons using PEI - DNA *(Lambert et al., 1996)*. In the same study, 16 ± 1.3 % of superior cervical ganglia neurons have expressed the gene of interest after PEI - DNA exposure *(Lambert et al., 1996)*. The small number of reports on transfection of primary glia (and glial-derived cell lines) could partly reflect difficulties in achieving successful transgene expression in these cells *(Wu et al., 2000)*.

The transfection of 1.1 - 2.4 % of microglia is lower than the approximately 40 % of microglia shown to internalise the SR-BI^{Ab} in mixed glial culture (see section 3.3.3). This is consistent with other studies, where transfection efficiency is much lower than the degree of vector entry into cells. Lower transfection efficiencies are especially prominent after the use of non-viral vectors and may be due to factors including limited release from the endosomal/lysosomal pathway *(Young et al., 2003; Wagner, 2004; Blanchard et al., 2006; Lee et al., 2008; Howard, 2009; Ziello et al., 2010)*, slow intracellular movement *(Pollard et al., 2001; Askjaer et al., 2002; Bergen and Pun, 2007; Kwon et al., 2008a)*, limited nuclear translocation *(Navarro-Quiroga et al., 2002; Eguchi et al., 2005; Collins et al., 2007; Groppo et al., 2011)* and subsequent degradation of the DNA, as discussed in section 1.4.6. Furthermore, internalisation and subsequent intracellular transport is most likely size-dependent (see section 1.4.4.2) and could theoretically be less extensive for SR-BI^{Ab} - PEI than SR-BI^{Ab} alone *(Rejman et al., 2004)*

4.4.3 Transfection of microglia and astrocytes in culture by SR-BI^{Ab} - PEI

After exposure to the SR-BI^{Ab} - PEI immunogene, there was no evidence of selectivity of transfection between microglia and astrocytes in culture. This is consistent with the findings presented in section 3.3.2, where we demonstrated the presence of SR-BI on both cell types. However, the findings in Chapter 3 showed no evidence for SR-BI^{Ab} internalisation by astrocytes. Thus, transfection in culture could have been achieved due to mechanisms unrelated to SR-BI. The

transfection of astrocytes by the SR-BI^{Ab} - PEI immunogene could instead be due to a large number of PEI moieties on the SR-BI^{Ab} - PEI conjugate, which could accommodate for non-specific endocytosis.

SR-BI^{Ab} - PEI immunogenes did produce transfection in culture and although transfection was not restricted to microglia, the efficiency compared with PEI - DNA was more marked for this group. This may also be linked to the increased amount of PEI per construct, which may have enhanced the capacity of each immunoporter molecule to carry DNA and to escape the endosomal/lysosomal pathway through its postulated proton sponge effect. The increased release and DNA-carrying capacity could thus explain the resulting higher transfection efficiency than that exerted by PEI - DNA alone carrying the same amount of DNA.

Also, the immunogene had the capacity to transfect microglia, a cell type which has not been extensively transduced or transfected in the past. For 1 µg SR-BI^{Ab} - PEI immunogene, transfection in the microglial population was comparable to that available in mixed glial cultures. In contrast, PEI - DNA exposures rarely resulted in any GFP-expressing microglia, as determined using CD11b immunolabelling. Thus, treatments using the SR-BI^{Ab} - PEI immunogene resulted in significantly more transfected cells in comparison to PEI, and also in a larger proportion of microglia of lower activation stages. This demonstrates that the SR-BI^{Ab} - PEI immunogene was the only agent of those tested with the capacity to transfect microglia in culture.

There is a possibility that SR-BI mediated a less extensive internalisation into astrocytes in comparison to microglia (discussed in section 3.4.1). In comparison to the detection of antibody in internalisation experiments, transfection may require lower amounts of immunogene internalisation as one plasmid molecule gives rise to many replicates of the GFP reporter. Thus, the expression of GFP in astrocytes after treatment with the SR-BI^{Ab} - PEI immunogene could still be partly due to targeted internalisation of a low amount of internalised immunogene, potentially via SR-BI.

Another finding consistent with this possibility is that GFP-positive/SR-BI-negative cells were never found in cultures exposed to SR-BI^{Ab} - PEI, whereas PEI - DNA *per se* had the capacity to transfect cells that did not express this receptor. Another approach to determine receptor-specific transfection has been achieved in previous studies by demonstrating that the expression of a target receptor in cells in culture is necessary to achieve genetic modification *(Shimizu et al., 1996; Merdan et al., 2003; Zeng et al., 2007)*.

4.4.4 SR-BI^{Ab} - PEI transfects more cells in culture and in vivo than SR-BI^{Ab} - PLL

Previous studies have given evidence that PLL-based immunogenes and related vectors have the capacity to transfect cells of the CNS *(Navarro-Quiroga et al., 2002; Barati et al., 2006; Berhanu and Rush, 2008)*. The final SR-BI^{Ab} - PLL immunoporter produced in our work had the capacity to transfect glial cells in culture and in the adult rat brain. GFP-expressing cells arising from the

treatments using the SR-BI^{Ab} - PLL immunogene in culture and in the adult brain demonstrated that we were able to achieve transgene expression using this conjugate.

However, transfection efficiencies exerted by the SR-BI^{Ab} - PLL immunogene were lower, and not as consistent as that of the SR-BI^{Ab} - PEI immunogene. Multiple factors could contribute to these transfection efficiency differences: by affecting the capacity of the immunogenes to enter cells, or the subsequent processing of the polycation-DNA complex following cellular entry.

One potential factor is the escape from intracellular vesicles, for which PLL is known to be less efficient than PEI *(Wagner and Kloeckner, 2006)*. This may cause lower release of the DNA cargo from PLL, resulting in lower transfection efficiencies after exposures to our SR-BI^{Ab} - PLL immunogene. In contrast, PEI has been shown to have a higher transfection capacity, which may be attributed to its lower pK_a, by allowing for a more powerful capacity to escape the endosomal/lysosomal pathway *(Sonawane et al., 2003; Harada et al., 2006)*. PEI is often used in polycation-based genetic modification due to this characteristic *(Boussif et al., 1995; Wagner and Kloeckner, 2006; Xiong et al., 2007; Deng et al., 2011)*.

In addition, the SPDP cross-linker used in the construction of the SR-BI^{Ab} - PEI immunoporter introduces protected sulfhydryl groups with a decreased risk of oxidation *(Mattson et al., 1993)*. Thus, SPDP possesses higher stability when used for transfection in biological systems than many other cross-linkers *(Thorpe et al., 1987)*. This potentially gives the SR-BI^{Ab} - PEI immunoporter an advantage compared to SR-BI^{Ab} - PLL immunoporter with respect to degradability in the extracellular space that could otherwise separate the targeting moiety (the antibody) and the DNA-carrier before internalisation into target cells. Another possibility is that the size of the PLL construct is larger than that of PEI, which would impede internalisation and thereby lower transfection efficiencies.

The DNA-carrying capacity of the final SR-BI^{Ab} - PLL was higher in comparison to the final SR-BI^{Ab} - PEI. Molar ratios of SR-BI^{Ab} : SMPT in comparison to SR-BI^{Ab} : SPDP indicates that more SMPT were added per SR-BI^{Ab} on the PLL immunoporter than SPDP per SR-BI^{Ab} in the PEI immunoporter. This enables more PLL to bind to the SR-BI^{Ab} compared to PEI, thereby increasing its DNA-carrying capacity. Also, more extensive DNA-binding by PLL is expected at physiological pH due to its higher pK_a value than PEI.

4.4.5 Exposure to SR-BI^{Ab} - PEI in culture results in negligible cell toxicity

After having demonstrated that our SR-BI^{Ab} - PEI construct had the capacity to transfect cells in culture, we addressed the aspect of cell viability. Effects on cell viability has previously been shown to be an issue using polycation-based vectors

(Wolfert et al., 1999; Cho et al., 2003; Boeckle et al., 2004; Lv et al., 2006; Farrell et al., 2007; Xiong et al., 2007; Zeng et al., 2007; Feng et al., 2008; Deng et al., 2011). In our studies, only low levels of cell toxicity were observed after treatments with 1 µg SR-BI^{Ab} - PEI immunogene per well. There was a trend for higher mean values and more variability in the response after the addition of higher amounts of immunogene or PEI - DNA, which could suggest deleterious effects in some applications. Additional experiments would be needed to address this issue, but was not considered worthwhile as the increased concentrations of the immunogene were not associated with higher transfection efficiencies.

4.4.6 Small effect on microglial activation by the SR-BI^{Ab} - PEI immunoporter in culture

Ideally, changes in protein expression resulting from the expression of the delivered transgene should be induced by transfection without modifying other properties of the target cells. This is particularly an issue for microglia because of their propensity to be activated by many extracellular stimuli as part of their normal function *(Wu et al., 2000)*.

In our studies, two findings suggest that activation was not an issue for transfected microglia in culture. a) We detected GFP expression in cells with morphologies ranging from fully ramified to fully amoeboid. This suggests the immunogene had the capacity to transfect the full spectrum of microglial

activation stages. To further study the activation level of transfected cells, future studies may be supplemented with analysis of the expression of microglial activation markers, including cyclooxygenase 2, NO and TNF-α (see more info in section 1.2.3). b) Further supporting the notion that activation was not necessary for transfection, was the lack of change in proportion of microglia in the cultures and the distribution of different activation stages within this population after exposure to 1 µg SR-BI^{Ab} - PEI immunogene, as assessed using morphology studies, which provides a sensitive indicator of changes. The small effect on the degree of microglial activation after treatments using our immunogene indicates an advantage for our technique to that of viral transductions. A technique with low immunogenicity is essential in the study of ramified microglia in the healthy CNS environment. Also, transfection methods that do not exacerbate microglial activation will be beneficial for the use in treatment of neuropathology.

With regards to viral vectors, lentivirus is generally considered to produce little immunogenicity. However, studies on this matter have generally been conducted in cell lines *(Balcaitis et al., 2005)*. Such highly modified cells already produce higher degrees of cytokines and have more activated profiles than *in vivo* microglia and primary cultures *(Franco et al., 2006; De Vries and Boullerne, 2010; Graeber and Streit, 2010)*. Thus, immunogenicity of lentiviral and other viral vectors has not been fully elucidated in the healthy CNS environment, and may still affect microglial activation *in vivo*.

4.4.7 Microglial activation does not affect SR-BI expression or transfection by SR-BI^{Ab} - PEI in culture

In our studies, cells of higher activated stages were strongly represented in the microglial population transfected. This commonly found drawback using mixed glial cultures *(Szabo and Gulya, 2013)* is due to the fact that they contain cells that have been taken out of their natural environment in comparison to cells *in vivo* (see section 1.2.7). Possible effects of further microglial activation were directly investigated in our studies through incubation of cultures in LPS. Consistent with previous studies, microglial activation was observed in the form of morphological changes after exposure to LPS *(Liu et al., 2001; Wollmer et al., 2001; Saura, 2007; Kauppinen et al., 2008)*.

Activation of microglia using LPS prior to incubation with our immunogene did not affect transfection efficiencies in mixed glial cultures. This indicates that the capacity of the immunogene to transfect cells was not increased in cells of activated stages. Often accompanying an increased activation stage in microglia (and other cells), proliferation could also affect the capacity to transfect these cells. This is due to disintegration of the nuclear membrane during mitosis. However, no such effect was seen in the proliferating population of microglia in our studies in culture. Thus, the findings on the distribution of GFP expression in microglia and direct studies using LPS, suggest that transfection might not be limited by nuclear translocation. This is a surprising finding given other reports that this is commonly a limiting step (see section 1.4.6.3).

Also, we did not detect any obvious changes in SR-BI expression after LPS treatment. This finding was consistent with that in untreated cultures, where microglia of all activation stages had similar expression levels of this receptor (see section 3.3.2). However, this finding was in contrast to previous studies where it has been demonstrated that changes in activation stage often result in changes in receptor expression, including a reported decrease in SR-BI expression in a macrophage-like RAW 264.7 cell line upon similar LPS treatment to what was used in our studies *(Baranova et al., 2002)*. Our results indicate that activation of microglia does not cause any obvious changes in SR-BI expression. Thus, if SR-BI is contributing to the uptake of the immunogene, this is available in both ramified cells and in cells of higher activation stages. A shortcoming of this approach was that LPS was used to alter the activation stage of a cell population in culture of which the majority was already in activated stages. Thus, only a small proportion of cells would be affected. Another potential experiment to analyse the effect of activation stages on microglial transfection by our immunogenes would be to use a preceding treatment to promote ramification using agents as discussed in section 1.2.3.1.

4.4.8 Concluding remarks

In conclusion, the data presented in this chapter describe the first ever attempt to perform transient, targeted gene delivery specifically into microglial cells of the CNS. We have developed a system based on immunogenes, with the capacity to specifically target and transfect microglia in culture and in the adult rat brain.

Our final SR-BI^{Ab} - PEI immunogene was produced based on previous immunogenes used to target other cell types. There are many factors which affect the transfection capacity of transient vector-based genetic modification agents. The vector is required to be internalised into its target cells, the DNA should be released from the targeting moiety of the vector, enter the cytosol and be translocated into the nucleus. Modifications can be made that have the potential to circumvent potential obstacles in this intracellular pathway. Such modifications were investigated in the next chapter to improve transfection efficiencies *in vivo*.

CHAPTER 5: TRANSFECTION OF MICROGLIA *IN VIVO*: CHARACTERISATION AND MODIFICATIONS TO IMPROVE EFFICIENCY OF SR-BI^{AB} - PEI

5.1 Introduction

Results in the previous chapter demonstrated that a construct based on SR-BI^{Ab} can specifically target and produce transfection in microglia in the adult rat brain. This proof of concept was obtained using pump infusions into the rat hippocampus over 14 days, after which we found a large number of cells immunoreactive for GFP spread around the infusion site. Further characterisation of infusions with regards to transfection efficiencies and cell specificity using the SR-BI^{Ab} - PEI immunogene is presented in this chapter.

To broaden the use of the immunogene for microglial studies in the healthy adult brain, further modifications to enhance transfection efficiencies of this construct were also tested. This included two approaches; the addition of peptides which could enhance the release of the immunogene and its DNA cargo into the cytosol (section 5.1.1), and the addition of peptides which were aimed at enhancing nuclear translocation of the DNA (section 5.1.2)

Also, if results using infusions could be obtained using a single injection, the immunogene method would be comparable to that reported in a viral transduction study using cell-specific promoters to limit expression to microglia *(Cucchiarini et al., 2003)*. The additional peptide changes were also tested in their capacity to enhance transfection of the immunogene after single injections.

5.1.1 Increasing release of non-viral vectors into the cytosol

It is not known whether our SR-BI^{Ab} - based immunogene is internalised via classical receptor-mediated endocytosis pathways. However, the higher transfection efficiencies using immunogenes based on PEI in contrast to those based on PLL (as discussed in section 4.4.4), indicate that one restricting step in our non-viral constructs may be limited release from acidic intracellular vesicles.

After internalisation via receptor-mediated endocytosis before entering the nuclear compartment, internalised DNA is found in vesicles with gradually decreasing pH and increasing amount of degrading enzymes *(Ziello et al., 2010)*. Upon acidification by the surplus H^+ influx in these acidic intracellular vesicles, synthetic polycations such as PEI have been suggested to promote release from the endosomal/lysosomal pathway, as discussed in section 1.4.6.1 *(Sonawane, Szoka et al. 2003; Fabre and Collins 2006)*. This finally ruptures the acidic compartment and causes release of its contents into the cytosol. However, this release is not a consistent feature for all adaptations of PEI and related polycations. Other agents have therefore been used to enhance this process, including the lysosomotropic agent chloroquine *(Zauner et al., 1998; Barati et al., 2002; Blanchard et al., 2006)* and thermal sensitive polymers *(Lee et al., 2008)*.

Another approach to enhance release from acidic intracellular compartments takes advantage of the capacity of viruses to escape these vesicles. The HA2 subunit, a component in the envelope of influenza virus, is one component that promotes viral escape *(Liou et al., 2012)*. At physiological pH, the hydrophobic N-terminal sequence of HA2 is encapsulated by the rest of the peptide sequence. Upon acidification, structural changes of the HA2 allows for the insertion of its N-terminal peptide into endosomal membranes *(Cho et al., 2003; Endoh and Ohtsuki, 2009; Liou et al., 2012)*. This causes the formation of pores and subsequently solubilises the endosomal/lysosomal membrane, causing leakage of up to 90 % of vesicle contents into the cytosol *(Wharton et al., 1988; Endoh and Ohtsuki, 2009; Liou et al., 2012)*.

Peptide sequences from the N-terminal region of HA2 and other proteins have been widely used to promote release of vesicle contents into the cytosol *(Skehel and Waterfield, 1975; Wharton et al., 1988; Déas et al., 2002; Navarro-Quiroga et al., 2002; Berhanu and Rush, 2008; Liou et al., 2012)*. These sequences have the capacity to increase transfection efficiencies of non-viral vectors, especially PLL-based constructs *(Plank et al., 1992; Midoux et al., 1993; Navarro-Quiroga et al., 2002; Berhanu and Rush, 2008)*. For example, a HA2 peptide has been used to enhance transfection via p75^{NTR}, as discussed in the previous chapter *(Berhanu and Rush, 2008)*. The same HA2 peptide has been used in a neurotensin-PLL construct with the purpose of enhancing transfection of dopaminergic neurons in the substantia nigra. The addition of HA2 to this

immunoporter-like construct resulted in transgene expression from 48 h up to 60 days after transfection *(Navarro-Quiroga et al., 2002)*. Another HA2 analogue has been used in an antibody-histone-neutravidin construct to increase transfection efficiencies in cells of a renal carcinoma cell line (15 % with the peptide in comparison to 5 % without this addition). More importantly for our studies, *in vivo* application of this HA2 peptide in a similar construct enhanced its capacity to produce β-gal expression in tumours expressing the antigen to which the antibody was targeted *(Déas et al., 2002)*.

Peptides with the capacity to produce pores in intracellular vesicles could be useful additions to the SR-BI^{Ab} - PEI immunogene if the extent of release from intracellular vesicles limits the process of transfection. These peptides have been used in non-viral vectors linked either via disulphide bonds (for example using cross-linkers, see section 4.1.2) or via peptide bonds in a fusion peptide with other vector components. The former linkage is favoured in part because it is more readily achieved. Furthermore, disulphide bonds are stable in the extracellular space where this is needed for appropriate delivery of the entire non-viral vector into target cells. After delivery, these disulphide bonds are presumably broken in the reducing environment of the cell *(Gosselin et al., 2002; Saito et al., 2003; Schaffert and Wagner, 2008)*, thereby releasing PEI - DNA from the targeting antibody moiety and from the pore-forming HA2 peptide. This is thought to occur already in the endosome where several reducing processes have been identified *(Saito et al., 2003)*. This is in contrast to HA2/vector moiety

fusion proteins, which due to the peptide bond have shown difficulties in escaping intracellular vesicles, although most other particles in the same vesicles are delivered to the cytosol *(Lee et al., 2011)*.

5.1.2 Increasing nuclear translocation of DNA delivered by non-viral vectors

After DNA has been internalised via receptor-mediated delivery and subsequently released into the cytosol, this nucleic acid is required to enter the transcriptional machinery in the nucleus of the cell to result in transgene expression. Translocation into the nucleus through nuclear pores occurs via passive diffusion for smaller molecules. For macromolecules of over 9 nm in diameter, this translocation occurs via an active mechanism involving importins which detect NLSs *(Zanta et al., 1999; Talsma et al., 2006; Collins et al., 2007; Vandenbroucke et al., 2007)*. The NLS transport mechanism is used by many viruses to enter the nucleus *(Ishii et al., 1996; Groppo et al., 2011)*.

This enhancement of nuclear translocation has been shown to increase the amount and rate of reporter gene expression for similar constructs to our immunogene, including PLL and PEI - based constructs, as discussed in section 1.4.6.3 *(Sebestyen et al., 1998; Zanta et al., 1999; Chan and Jans, 2001; Navarro-Quiroga et al., 2002; van der Aa et al., 2005; Talsma et al., 2006; Collins et al., 2007; Berhanu and Rush, 2008)*. Two frequently used synthetic NLS peptides have been obtained from SV40 major capsid protein Vp1 *(Navarro-Quiroga et*

al., 2002; Berhanu and Rush, 2008) and SV40 large T antigen *(Sebestyen et al., 1998; Collins et al., 2007)*. These peptides have been incorporated into non-viral vectors either via covalent bonds *(Sebestyen et al., 1998)* or, more simply, by mixing the peptide with the vector *(Collins et al., 2007; Berhanu and Rush, 2008)*.

5.1.3 Aims

Studies described in this chapter were aimed in part at characterising the transfection produced by infusion of the SR-BI^{Ab} - PEI immunogene into the hippocampus by assessing the number of transfected cells, their spatial distribution around the site of infusion and cell specificity.

Also, based on previous enhancements of release into the cytosol and of nuclear translocation for non-viral transfection agents, we describe the development and use of three other versions of SR-BI^{Ab} - PEI immunoporters for *in vivo* testing.

The capacity of HA2 peptides to enhance transfection efficiencies was tested through attachment to the PEI moiety carrying the nucleic acid. HA2 peptides were specifically added onto PEI to promote release of the DNA (bound to PEI through charge) from intracellular vesicles after the breaking of the disulphide bond between SR-BI^{Ab} and PEI (Figure 5.1).

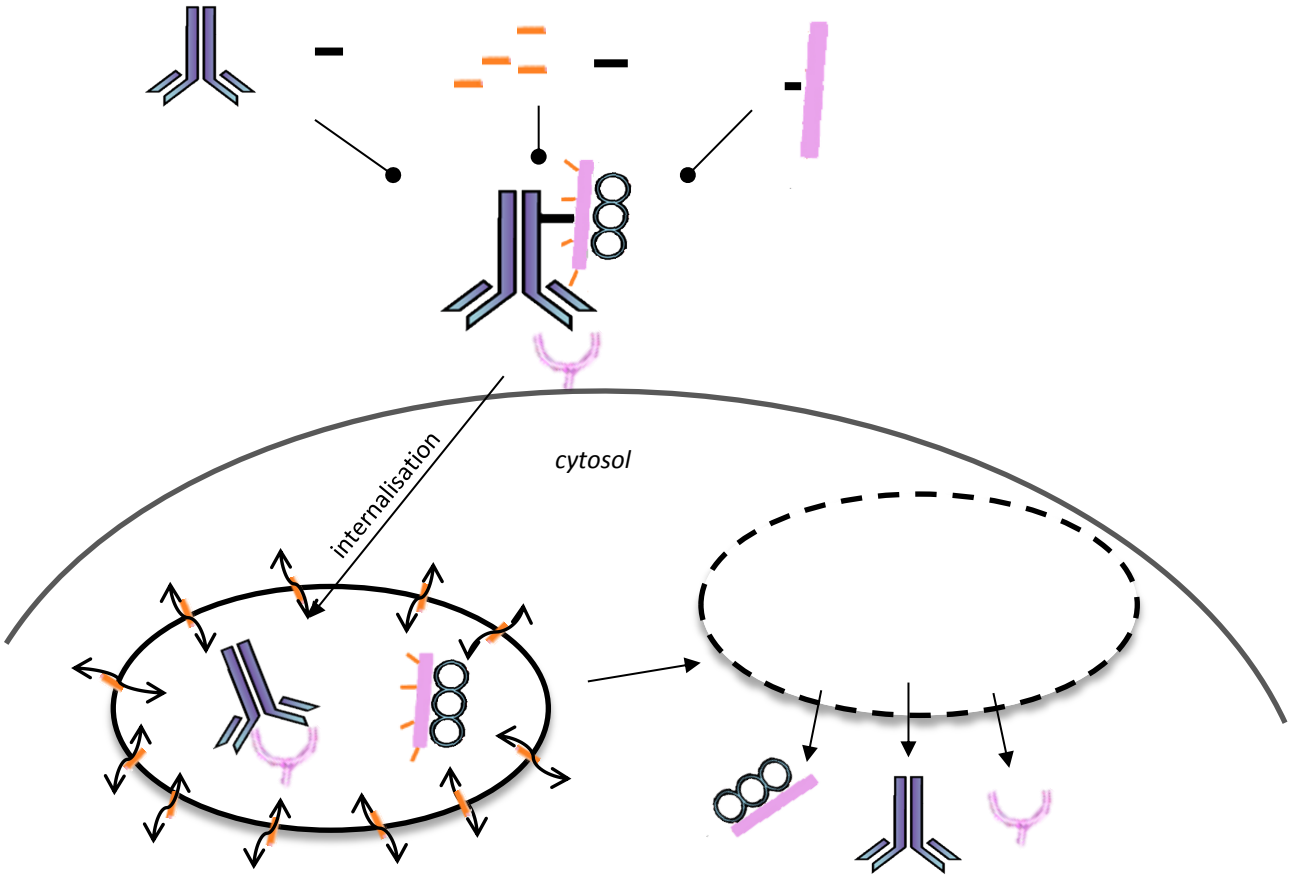

Figure 5.1 Schematic diagram of a HA2 peptide addition to SR-BI^{Ab} - PEI and its potential to enhance release from intracellular vesicles. *HA2 peptide (orange) was linked to SR-BI^{Ab} - PEI immunoporter by first reacting HA2 with SPDP (small, black rectangle) and thereafter combining this with the previously reacted SR-BI^{Ab} - SPDP (Y-shaped) and PEI-SPDP-SH (pink large rectangle). After entering the cell through receptor-mediated (pink, y-shaped object) endocytosis or other internalisation pathways, HA2 peptide has the capacity to form pores in the membrane of intracellular vesicles, causing leakage (see curved arrows) of its contents, including DNA (blue circles) into the cytosol.*

Secondly, the addition of the Vp1 NLS peptide was added to investigate whether its capacity to enhance nuclear translocation could increase transfection efficiencies of the SR-BI^{Ab} - PEI immunogene (Figure 5.2). As the DNA is the only moiety of the immunogene complex required to enter the nucleus for proper transfection, the NLS peptide was to be mixed with the DNA before this complex was combined with the SR-BI^{Ab} - PEI immunoporter. Although the mechanism through which NLSs enhance transfection efficiencies is yet to be determined, the use of an NLS peptide offered a potential approach to increase transgene expression by our SR-BI^{Ab} - PEI immunogene. Immunogenes incorporating both modifications were also constructed and tested.

Thus, the aims of this chapter were to:

a) provide a detailed characterisation of the pattern and cell specificity of transfection produced by infusions of the SR-BI^{Ab} - PEI immunogene into the hippocampus
b) test whether the addition of a HA2 peptide and/or an NLS peptide has the capacity to increase transfection efficiencies after infusions of SR-BI^{Ab} - PEI
c) test the efficiency of transfection following single intracerebral injections of SR-BI^{Ab} - based immunogenes

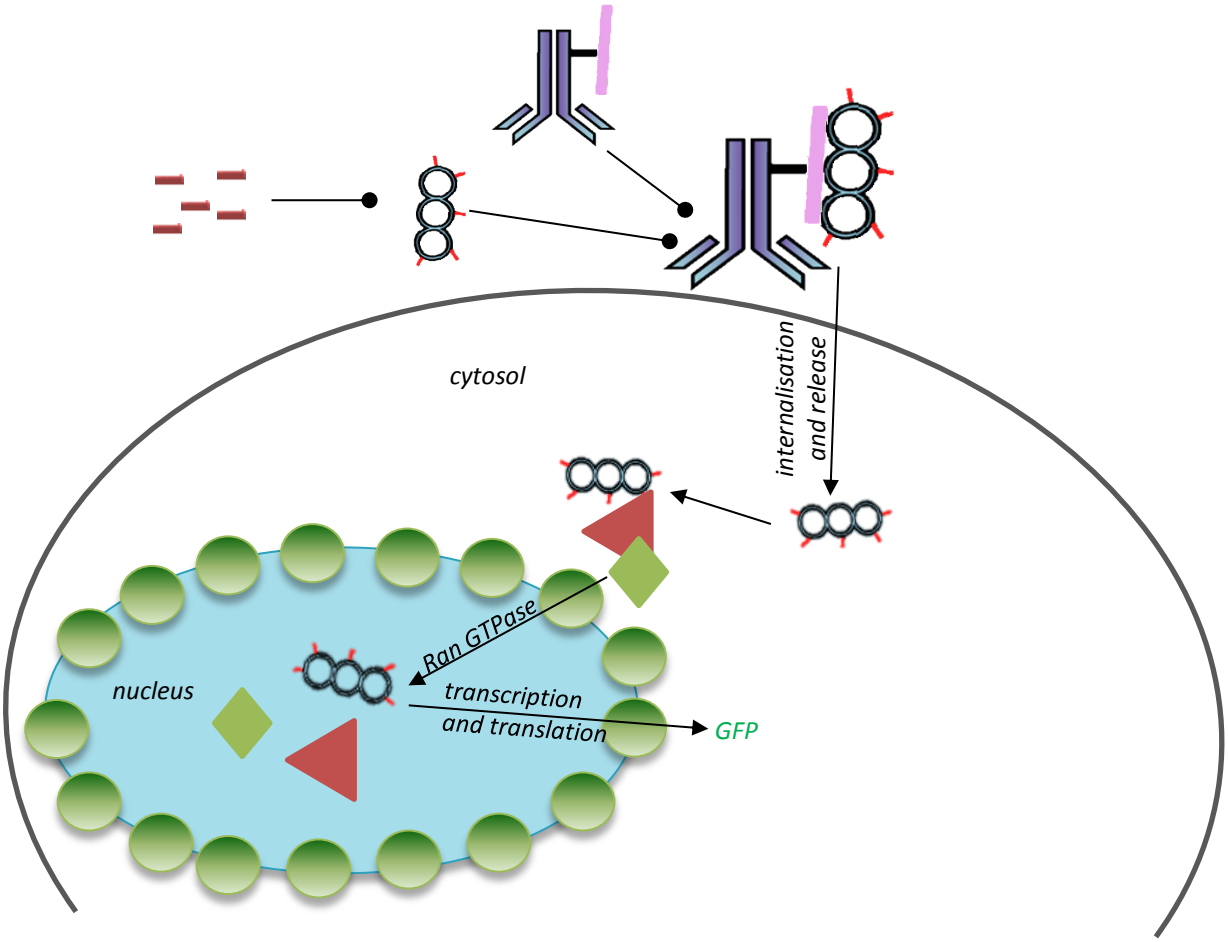

Figure 5.2 Schematic diagram of the addition of NLS peptide to the immunogene and its potential to enhance nuclear import. *NLS peptide (red small rectangles) derived from SV40 major capsid protein Vp1 was mixed with plasmid DNA (blue circles) prior to the combination of NLS-DNA with SR-BI^{Ab} - PEI (or SR-BI^{Ab} - PEI - HA2) immunoporter. NLS peptide is believed to bind endogenous importin α (red triangle), forming a ternary complex with importin β (green diamond). This complex enter the nucleus through nuclear pores (green spheres) of the nuclear membrane, where Ras-related nuclear protein guanosine tri phosphatase (Ran GTPase) finalises delivery of the ternary complex. After transcription of the delivered DNA, translation in the cytoplasm can give rise to the encoded protein (which in our study was GFP).*

5.2 Materials and methods

5.2.1 Addition of HA2 peptide to the immunoporter

The method for adding the HA2 peptide to the immunoporter was adapted from Berhanu and Rush (2008). HA2 peptide (single letter amino acid sequence G L F E A I A E F I E G G W E G L I E G C A K K K; Auspep; custom-ordered, freeze-dried) was weighed up using a microbalance (C-31; Cahn Instruments, Inc.) and dissolved in GIBCO H_2O at a concentration of approximately 2.5 mg/ml. A_{280} was measured on a NanoDrop™ 8000 micro-volume UV-vis spectrophotometer and peptide concentration was calculated using a formula for small peptide concentration (see Table 5.1). From this, HA2 peptide (100 µg; 13.3 µM final concentration) and SPDP (26.7 µM) were mixed in a total volume of 2.8 ml IRB2 and incubated at RT for 30 min with shaking (60 rpm). A Microsep™ centrifugal device (1 kDa MWCO; Pall Life Sciences Co.) was washed in 70 % v/v ethanol through centrifugation. To concentrate the construct and remove most of the unreacted SPDP, the reaction mix was centrifuged (3680*g*) in the Microsep™ device until the volume reached 200 µl. A_{280} was measured on a NanoDrop™ 8000 micro-volume UV-vis spectrophotometer to calculate the peptide concentration in the solution remaining in the Microsep™ centrifugal device. Using the same concept as for previous PLL-based constructs *(Navarro-Quiroga et al., 2002; Berhanu and Rush, 2008)*, HA2-SPDP and PEI-SPDP-SH were simultaneously added to SR-BI^{Ab}-SPDP at a molar ratio of 0.5 : 1.38 : 1,

incubated 24 h at RT and continued along the previously described protocol for immunoporter construction (see section 4.2.2).

Table 5.1 Formula for calculating the concentration of HA2 peptide in solution.

$\rho = \frac{A_{280} \cdot MW_{pept}}{(n_W \cdot e_W)+(n_Y \cdot e_Y)} = \frac{A_{280} \cdot 2696.13}{(1 \cdot 556)+(0 \cdot 120)} = \frac{A_{280} \cdot 2696.13}{556}$
A_{280}= *absorbance measurement at 280 nm*
MW_{pept}=molecular weight (Da) of whole peptide
n_W/n_Y= number of tryptophan / tyrosine in whole peptide. For the HA2 peptide used in this work, this is 1 and 0, respectively.
e_W/e_Y = extinction coefficient of chromophoric residues at 280 nm at neutral pH, using a 0.1 cm cell.
e_W = 556 absorbance units/mmole per 0.1 cm cell (as in NanoDrop™ 8000) for tryptophan
e_Y = 120 absorbance units /mmole per 0.1 cm cell (as in NanoDrop™ 8000) for tyrosine

5.2.2 Preparation and characterisation of NLS peptide

Similarly to the procedure described by Berhanu and Rush (2008), NLS peptide was directly mixed with the DNA prior to immunogene formation. NLS peptide (single letter amino acid sequence M A P T K R K G S C P G A A P N K P K; Auspep; custom-ordered, freeze-dried) was weighed using a microbalance C-31 and dissolved in GIBCO H_2O to a final concentration of approximately 4 µg/µl. As this peptide does not contain any tryptophan or tyrosine residues that can be detected at $A_{280,}$ concentration of this peptide in solution was estimated using

A_{220} measurement of a diluted stock and comparing this to a linear standard curve obtained from A_{220} measurements of 0.2, 0.3, 0.4 and 0.5 µg/µl BSA.

NLS was mixed with plasmid DNA (also dissolved in GIBCO H_2O) and analysed in EMSAs. The same assay was used to study the interaction of NLS - DNA with immunoporters.

5.2.3 The effect on transfection efficiencies in vivo after infusing SR-BI^{Ab} - PEI immunogenes with peptide additions

Rats were infused with one of the following immunogenes: without any peptide addition (SR-BI^{Ab} - PEI; *n = 3*), with the addition of HA2 peptide (SR-BI^{Ab} - PEI - HA2; *n = 3*), the addition of NLS peptide (SR-BI^{Ab} - PEI - NLS; *n = 3*) or the addition of both HA2 and NLS peptides (SR-BI^{Ab} - PEI - HA2 - NLS; *n = 3*). Immunogenes were prepared as described in section 4.2.4 with modifications for some studies as described in 5.2.1 and/or 5.2.2. Infusions into rat hippocampus (see section 4.2.6), brain preparation and sectioning (see section 3.2.3.2) were performed as described previously. As mentioned in section 4.2.2, a second immunogene that was targeted at a protein which was not normally expressed by microglia (p75^{NTR}) was used for control purposes. This p75^{NTRAb} - PEI immunoporter and also PEI carrying corresponding DNA amounts were infused in the same location (*n = 3* per group).

5.2.4 Intracerebral injections of the SR-BI^{Ab} - PEI immunogene with peptide additions

Intracerebral injections (up to 2 µg of immunoporter and 6 µg DNA) of three immunogene versions; without any peptide addition (SR-BI^{Ab} - PEI; *n = 3*), with the addition of HA2 peptide (SR-BI^{Ab} - PEI - HA2; *n = 3*) or with the addition of NLS peptide (SR-BI^{Ab} - PEI - NLS; *n = 3*), were performed as described in section 3.2.3.1. PEI - DNA and a p75^{NTRAb} - PEI immunoporter carrying corresponding DNA amounts were also injected into the same location (*n = 3*). Animals subject to these intracerebral injections were sacrificed 72 h after injection and brains prepared for IHC (see section 3.2.3.2).

5.2.5 IHC and microscopy

NHS/Triton IHC (see section 3.2.3.3 with modifications in the end of section 4.2.6) and subsequent confocal microscopy (Leica Microsystems GmbH) was used to study transfection in 50 µm horizontal brain sections. For infused brains, the number of cells immunoreactive for GFP was counted in two entire brain sections at each of five levels (separated by 0.5 mm) between the site of injection and 2 mm dorsal to this site. These values were used to calculate an estimated number of cells immunoreactive for GFP in a 2 mm slice of each brain and offered an initial comparison of transfection efficiencies obtained after the addition of HA2 and/or NLS peptides. The same approach was taken with regards to brains with single injections where GFP numbers were counted at four levels in a 1.5 mm slice.

GFP-positive cells were also analysed for immunolabelling for the microglial marker mouse anti-CD11b/c, the marker for activated microglia anti-CD68, the astrocytic marker mouse anti-GFAP, the glial progenitor marker NG2 and the neuronal marker NeuN.

5.2.6 Statistical analysis

Quantitative results from microscopy analysis are presented as mean +/- standard deviation. Where multiple groups are compared, one-way and two-way ANOVA was used to analyse for significance with p values < 0.05.

5.3 Results

5.3.1 Addition of HA2 peptide and NLS peptide to SR-BI^{Ab} - PEI immuongene

Including the HA2 peptide in the immunoporter construction protocol did not cause any changes in final yield or in the proportion of SR-BI^{Ab} protein left at selected steps throughout the protocol (Figure 5.3). Also, the HA2 peptide did not majorly affect the DNA-binding capacity of PEI in the SR-BI^{Ab}-based immunoporter as demonstrated in EMSAs (Figure 5.4).

The addition of NLS reduced the mobility of the DNA in the EMSA (Figure 5.5). This DNA retardation increased with higher NLS concentration. Based on this assay and in line with previous work of other research groups

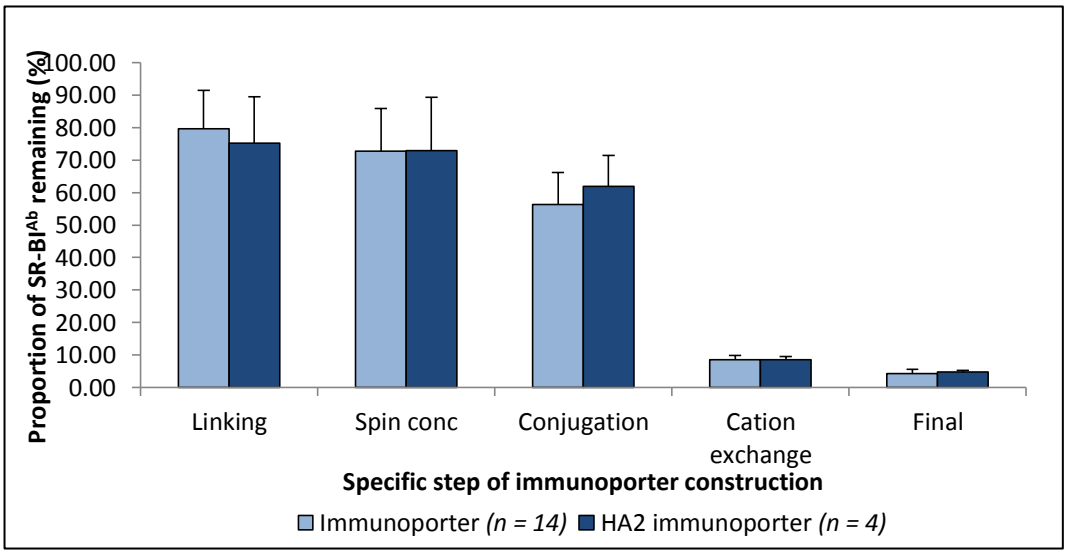

Figure 5.3 Antibody recovery of the SR-BI^{Ab} - PEI - HA2 immunoporter *(n = 4; dark blue) was not different from that recovered during the construction of SR-BI^{Ab} - PEI (n = 14; light blue) at five key steps of the immunoporter construction protocols. Recovery was assessed from protein content based on A_{280} measurements. The key steps measured included; Linking (after antibody reaction with SPDP), Spin conc (following Vivaspin concentrating steps of SR-BI^{Ab} after reaction with SPDP), Conjugation (after O/N incubation of SR-BI^{Ab} - SPDP with PEI-PSDP, and HA2-SPDP if applicable), Cation exchange (following cation exchange separation separated from SR-BI^{Ab} alone) and Final (after the last step of Vivaspin concentrating). Data are presented as mean + SD. The majority of SR-BI^{Ab} was lost during the cation exchange step in both protocols.*

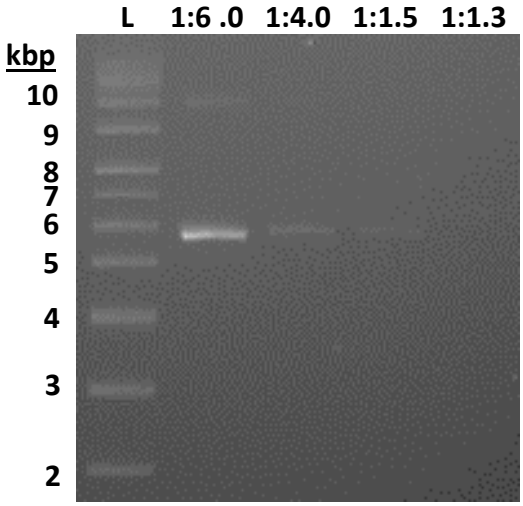

Figure 5.4 EMSA for SR-BI^{Ab} - PEI - HA2 immunoporter *displaying plasmid DNA binding and retardation with increasing SR-BI^{Ab} : DNA w/w ratio of 1 : 6.0 to 1 : 1.3. Note that full DNA retardation was reached at a ratio of 1 : 1.3, similarly to previous SR-BI^{Ab} - PEI immunoporters without the HA2 peptide addition. DNA ladder (L) with marked sizes in kbp. Ethidium bromide was used for visualisation.*

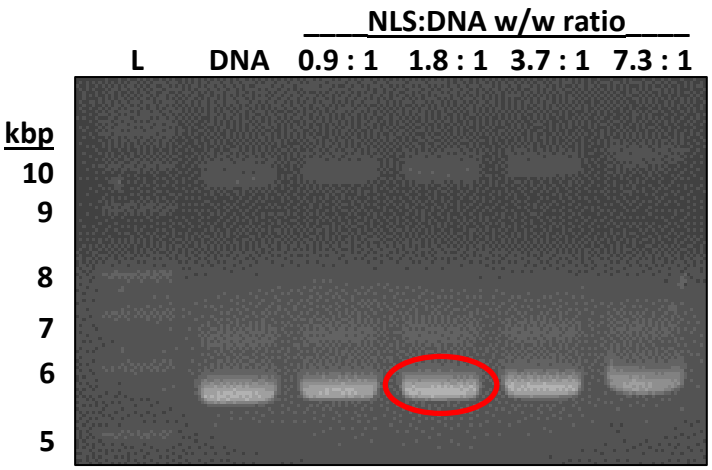

Figure 5.5 EMSA of NLS peptide showing plasmid DNA binding and retardation *at a range of NLS : DNA w/w ratios from 0.9 : 1 to 7.3 : 1 (representative image of 5 EMSAs). A w/w ratio of 1.8 µg NLS per 1 µg of DNA was chosen (circled in red) as this resulted in a small degree of DNA retardation, as seen by the shorter movement of the DNA through the gel. This was thought to potentially increase nuclear affinity without any large effects on the binding of the DNA to the immunoporter in immunogene formation. Note that the DNA is progressively retarded when analysing the gel from left to right. DNA ladder (L) with marked sizes in kbp. Ethidium bromide was used for visualisation.*

(Navarro-Quiroga et al., 2002), an NLS : DNA w/w ratio of 1.8 : 1 was chosen for *in vivo* experiments (circled in Figure 5.5). This ratio involved slight DNA retardation compared to DNA alone.

When mixing DNA with this ratio of NLS prior to immunogene formation, DNA retardation was similar to those for the SR-BI^{Ab} - PEI - HA2 immunoporter alone (Figure 5.6). This showed only a slight change in the DNA retardation by the immunogene in the presence of NLS, which was not considered to interfere with subsequent experiments.

5.3.2 GFP expression following immunogene infusions

GFP expression arising from the SR-BI^{Ab} - PEI immunogene was most prominent in an area of damage produced as a response to the brain infusion. Cells immunoreactive for GFP were also found outside this region in all but one of the brains, and accounted for up to 33 % of the total cells counted in individual brains. Cells expressing GFP were detected well over 2 mm from the infusion site dorsally, and over 4 mm laterally.

The extent of co-labelling between GFP and markers of specific cell populations was quantified in three brains infused with SR-BI^{Ab} - PEI. This was analysed in randomly selected horizontal slices from the infusion site and up to 1 mm dorsal to this site. In this analysis, out of the 582 cells expressing GFP, most were

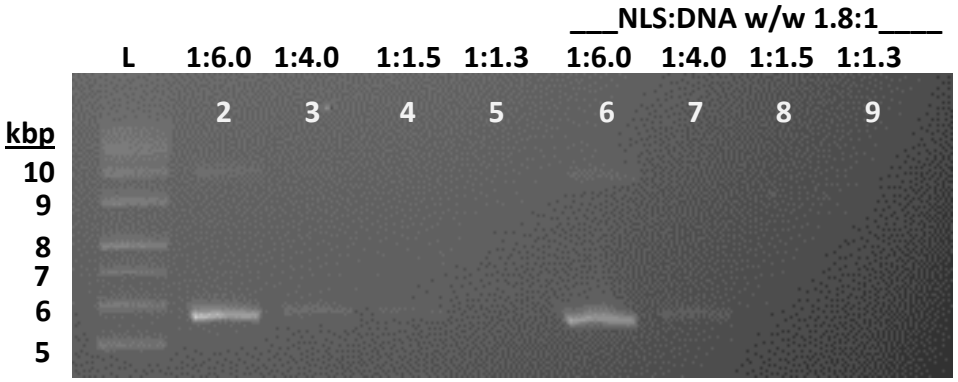

Figure 5.6 EMSA of SR-BI^{Ab} - PEI - HA2 in the presence of an NLS peptide *showing plasmid DNA binding and retardation by SR-BI^{Ab} - PEI - HA2 immunoporter alone (well 2 through 5) and in the presence of an NLS peptide (well 6 through 9; 1.8 : 1 w/w ratio of NLS : DNA). Full DNA retardation was obtained at SR-BI^{Ab} : DNA w/w ratio of 1 : 1.3 and 1 : 1.5 for SR-BI^{Ab} - PEI - HA2 and SR-BI^{Ab} - PEI - HA2 - NLS, respectively (representative image of 4 EMSAs). DNA ladder (L) with marked sizes in kbp. Ethidium bromide was used for visualisation.*

immunoreactive for the microglial marker CD11b/c (83 ± 5%; Figure 5.7). Only three GFP-positive cells were immunoreactive for the astrocytic marker GFAP, and these were all found in a single section from one brain (Figure 5.8a). No co-labelling of GFP was detected with the neuronal marker NeuN (Figure 5.8b) or for NG2 (Figure 5.8c), a marker for a subpopulation of NG2-positive glia and for potentially infiltrating monocytes *(Matsumoto et al., 2007)*.

Most cells expressing GFP had a rounded amoeboid-like morphology but occasional transfected ramified cells were also seen (Figure 5.7c). Within the population of transfected cells, 67 ± 18% were immunoreactive for the marker for activated microglia CD68 (Figure 5.8d). This protein is a marker for phagocytic microglia and macrophages, further supporting the high activation of many of the transfected cells.

In contrast to the extensive GFP expression produced with SR-BI^{Ab} - based immunogenes, no detectable GFP expression was found in any cell type after infusions of a p75^{NTRAb} - based immunogene *(n = 3*; Figure 5.9a*)*. Also, infusions of PEI - DNA alone did not result in transfection *(n = 3*; Figure 5.9b*)*.

5.3.3 Analysis of transfection capacities after infusions of immunogenes with peptide additions

Infusions of each of the immunogene versions with HA2 and/or NLS produced

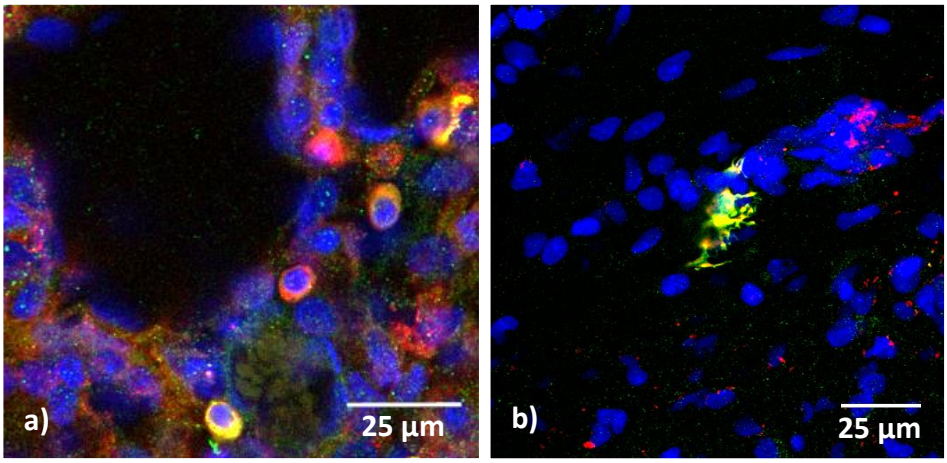

Figure 5.7 Transfection of microglia after SR-BI^{Ab} - PEI infusions into the adult rat hippocampus *as shown in images from 50 µm horizontal sections analysed in confocal microscopy in one of three independent experiments. Most of the cells immunoreactive for GFP (green) co-labelled with the microglial marker CD11b (red). The majority of thse cells had a rounded, amoeboid-like morphology (a). However, microglia with ramified morphology were also found to express GFP (b). Brain sections exposed to Alexa Fluor^{647} secondary antibody alone displayed no immunoreactivity (see Figure 5.9c). Nuclei were labelled with Hoechst 33258 (blue).*

Figure 5.8 Transfection of cells after SR-BI^{Ab} - PEI infusions into the adult rat hippocampus *(see figure text on next page)*

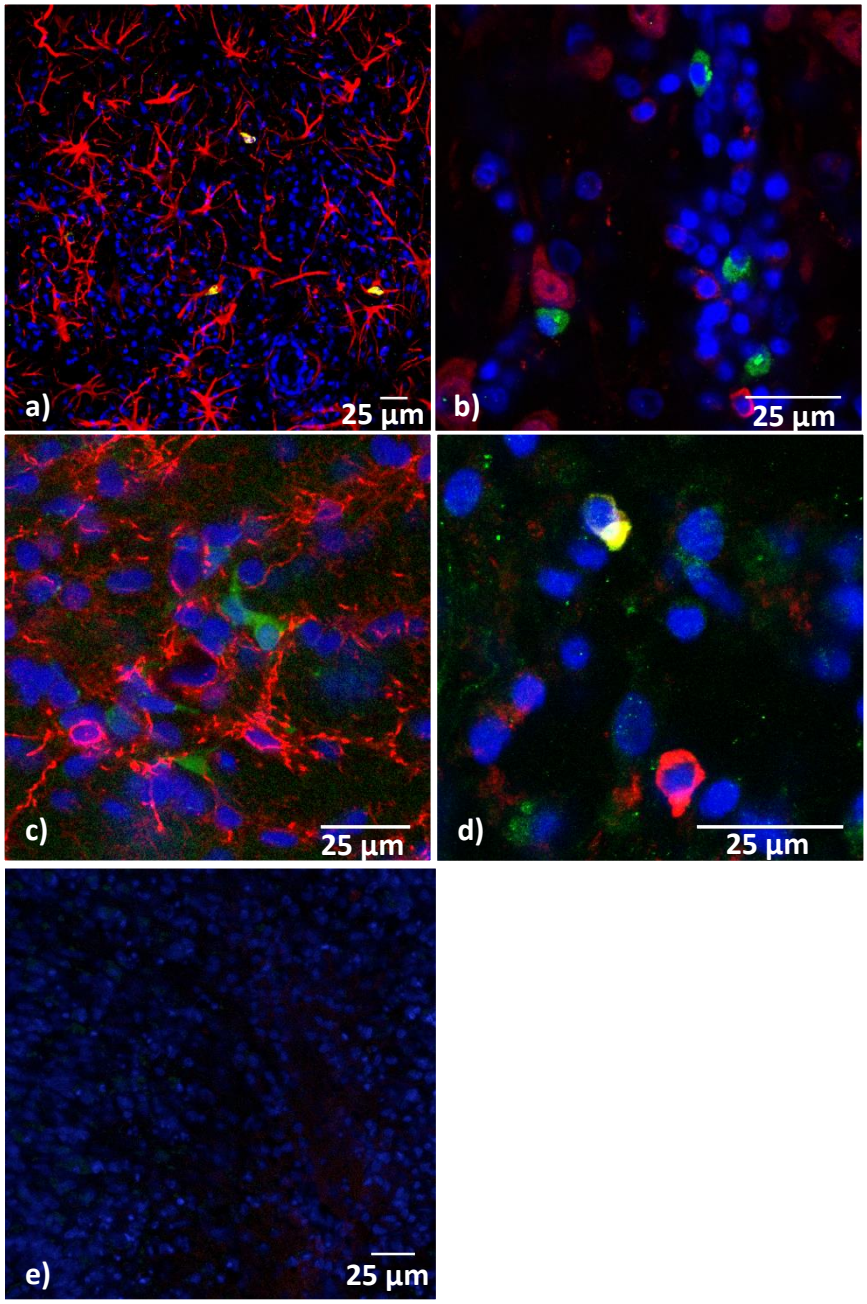

Figure 5.8 Transfection of cells after SR-BI^{Ab} - PEI infusions into the adult rat hippocampus *(see previous page) as shown in 50 µm horizontal rat brain sections analysed in confocal microscopy. Only a total of three GFAP-positive astrocytes (a; red) in all brains investigated were found immunoreactive for GFP (green; a-d). No co-labelling with GFP was found with NeuN (b; red) or the glial progenitor marker NG2 (c; red). GFP expression was found in cells positive for CD68, a marker for activated microglia (d; red). Brain sections exposed to Alexa Fluor^{647} secondary antibody alone displayed no immunoreactivity (e). Nuclei were labelled with Hoechst 33258 (blue).*

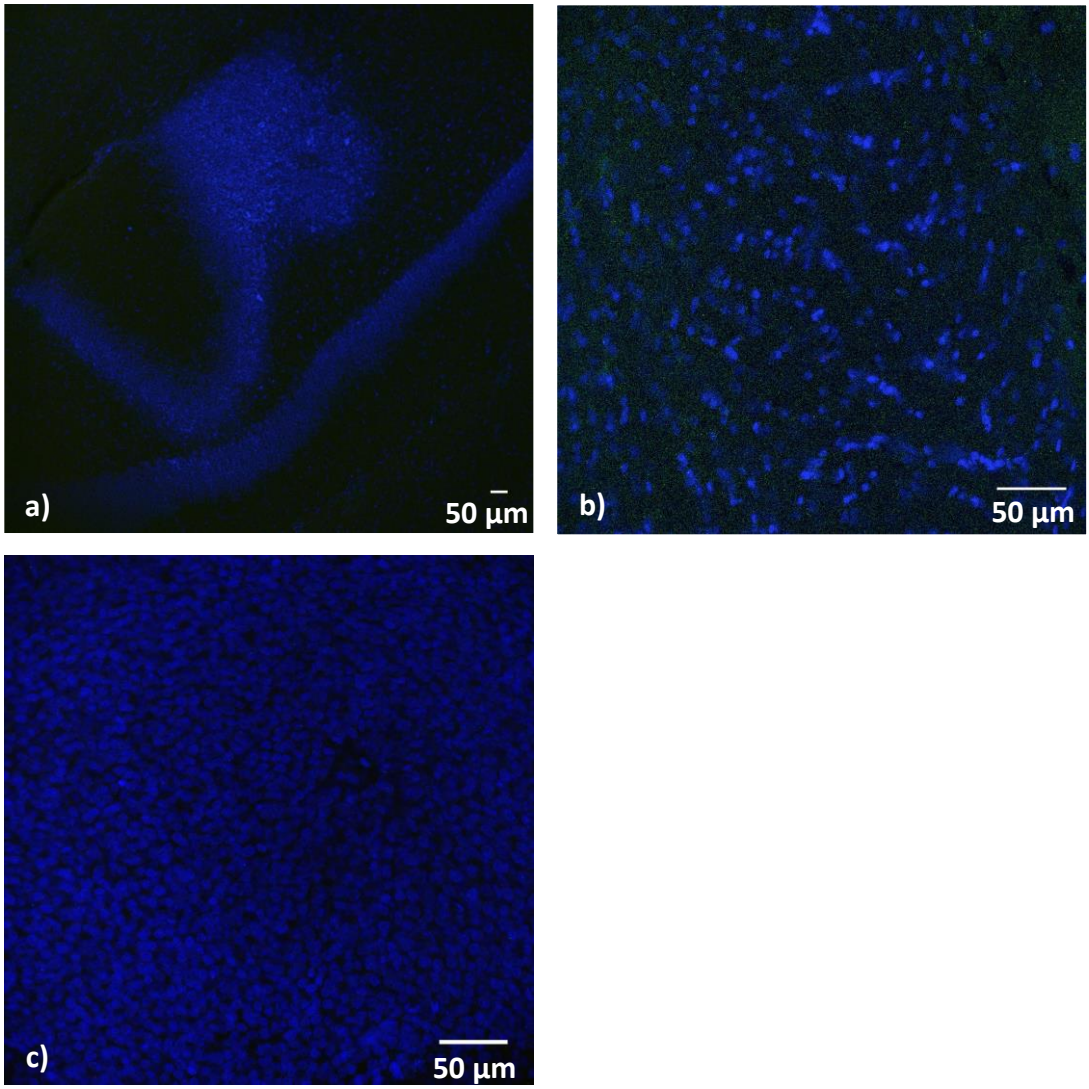

***Figure 5.9 Lack of GFP-positive cells after control infusions into adult rat hippocampus**, as shown in representative images from 50 µm horizontal sections in confocal microscopy from one of three independent experiments each. No GFP immunoreactivity was found in sections from brains infused with PEI-DNA (a) or the p75^{NTRAb} - PEI immunogene (b). There was also no immunoreactivity in brain sections exposed to secondary antibodies alone (c). Nuclei were labelled with Hoechst 33258 (blue).*

similar numbers of cells immunoreactive for GFP. Representative images for all conditions are presented in Figure 5.10. Infusions with SR-BI^{Ab} - PEI resulted in expression of GFP in 932 ± 275 cells in the 2 mm block of tissue which was used for analysis. Treatment with the other immunogene versions did not result in any difference in the number of cells expressing GFP (Figure 5.11; $p > 0.05$, ANOVA, *n = 3* per group).

Also, there was no significant difference in the location of the GFP-positive cells. The proportion of cells immunoreactive for GFP outside the area of damage compared to those found in this area did not differ between the four versions of the immunogene ($p > 0.05$, ANOVA, *n = 3* per group). There was also no significant difference in the pooled mean values for all 12 brains with respect to the number of GFP-positive cells found at the five levels studied; from the infusion site and at the four successive 0.5 mm intervals dorsal to the injection site (Figure 5.12; $p > 0.05$; two-way ANOVA, *n = 3* per group). This demonstrates the extensive spread of the immunogene in the brain under the infusion conditions.

The number of GFP-positive cells in a 2 mm block of tissue varied considerably between individual animals across the four groups. This ranged from a minimum of 124 cells for one of the rats infused with SR-BI^{Ab} - PEI - NLS up to almost 2200 cells in a rat infused with the SR-BI^{Ab} - PEI - HA2 immunogene. Because of the

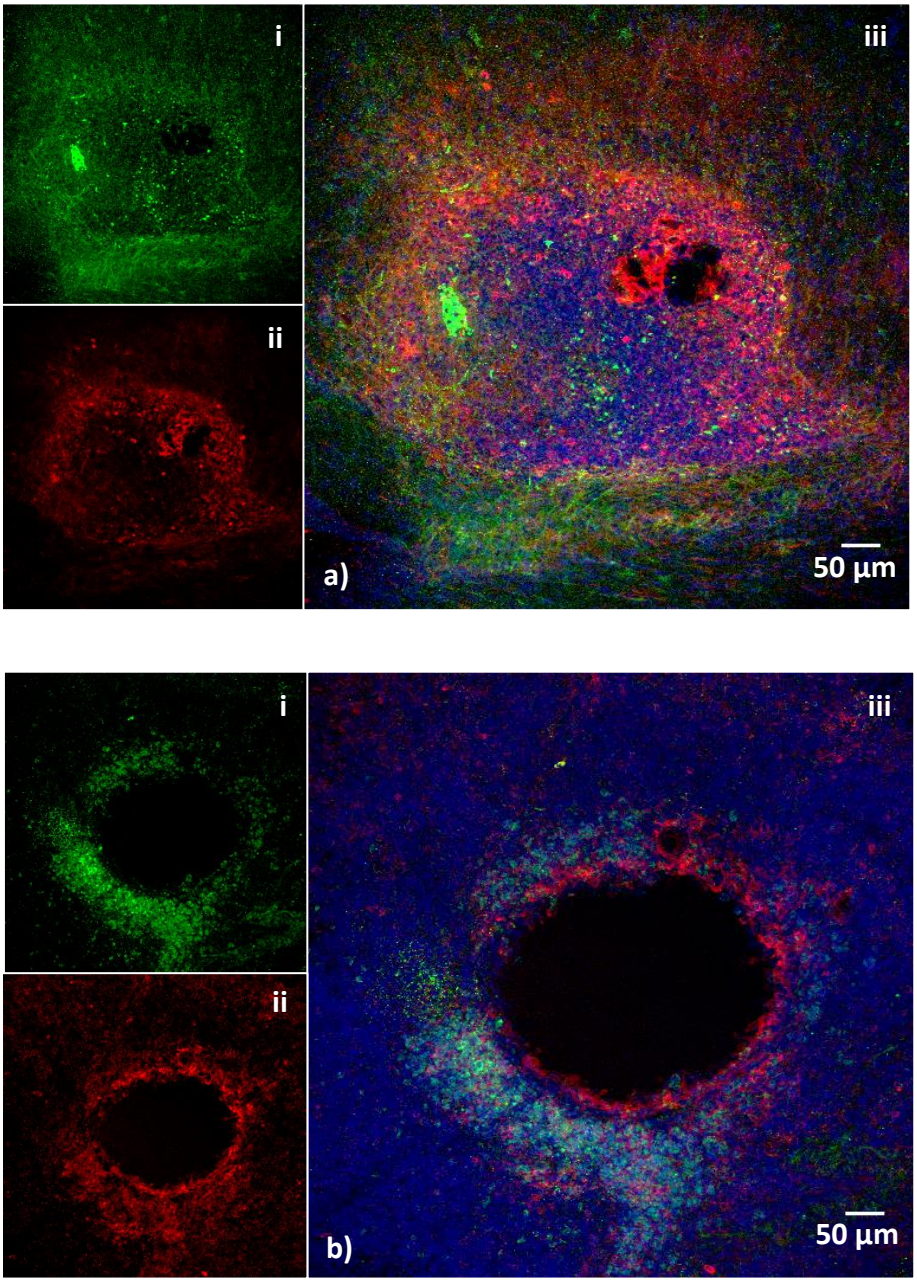

Figure 5.10 Infusions of four versions of the SR-BIAb - PEI immunogene into rat hippocampus *(see figure text two pages forward)*

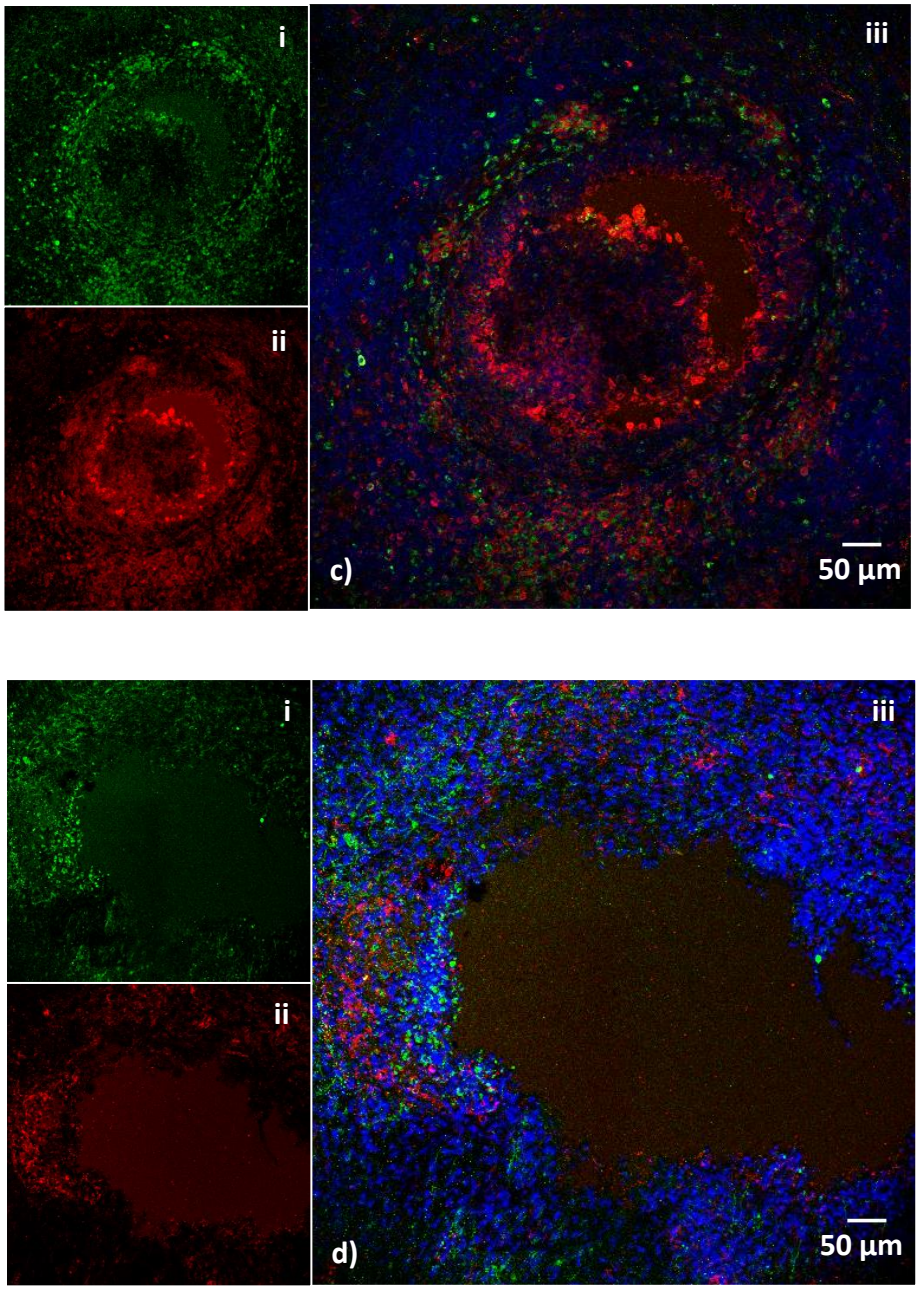

Figure 5.10 Infusions of four versions of the SR-BI^{Ab} - PEI immunogene into rat hippocampus, continued *(see figure text on the next page)*

Figure 5.10 Infusions of four versions of the SR-BI^{Ab} - PEI immunogene into rat hippocampus *(see two previous pages) Representative images from one of three independent experiments, showing cells immunoreactive for GFP (green in panel i of each image) and CD11b/c (red in panel ii of each image) around the area of damage after infusions with SR-BI^{Ab} - PEI (a), SR-BI^{Ab} - PEI - NLS (b), SR-BI^{Ab} - PEI - HA2 (c) and SR-BI^{Ab} - PEI - HA2 – NLS (d). Merged images are shown in panel iii of each image. Note the high number of cells immunoreactive for GFP in each image. Brain sections exposed to secondary antibodies alone displayed no immunoreactivity with the exception of a few cells positive for the Alexa Fluor^{647}, most likely due to the detection of SR-BI^{Ab} of mouse origin (see figure 5.13f). Nuclei were labelled with Hoechst 33258 (blue).*

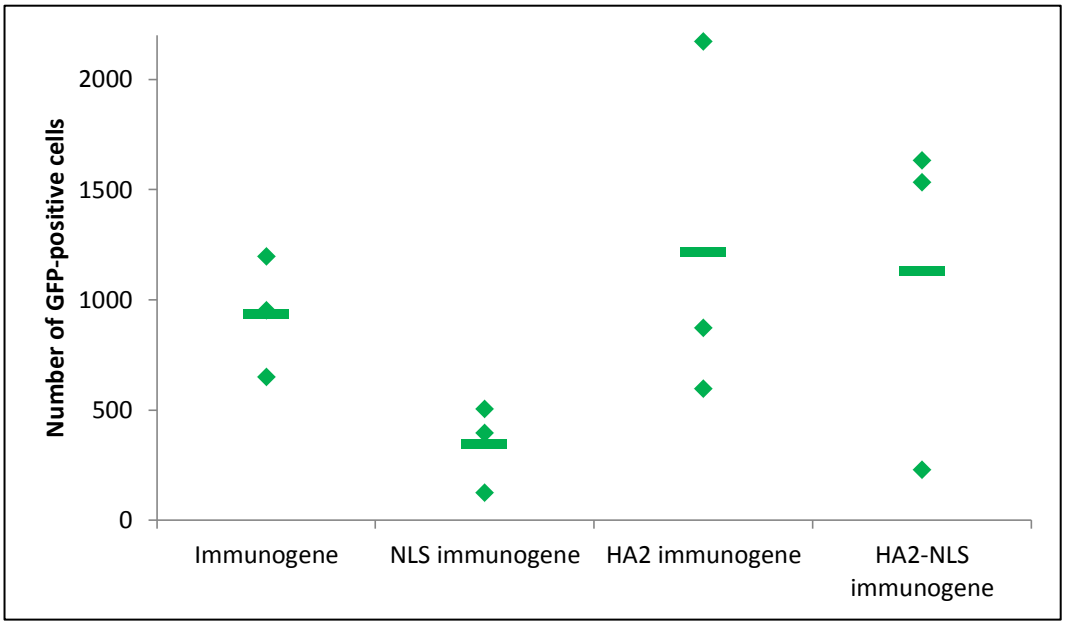

Figure 5.11 Numbers of transfected cells in 2 mm thick horizontal blocks of the brain following infusions of four versions of SR-BI^{Ab} - PEI immunogenes *into the hippocampus (n = 3 of each; diamonds). The mean values for each immunogene version are illustrated as horizontal bars. Transfected cells were calculated based on counting two entire horizontal sections at five levels, starting at the injection site and in four successive 0.5 mm intervals dorsal to this site. No significant change was detected between the four versions of the SR-BI^{Ab} - PEI immunogene: SR-BI^{Ab} - PEI, SR-BI^{Ab} - PEI - NLS, SR-BI^{Ab} - PEI - HA2 or SR-BI^{Ab} - PEI - HA2 - NLS. ($p > 0.05$; ANOVA, n = 3 of each).*

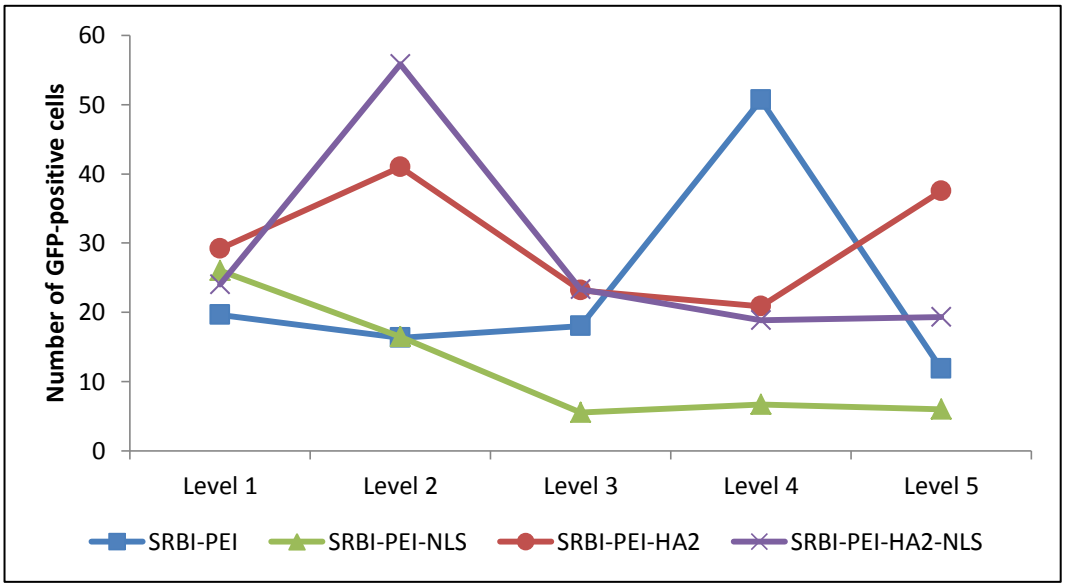

Figure 5.12 GFP immunoreactivity is not significantly changed between levels within the 2 mm slice for either immunogene version *($p > 0.05$; two-way ANOVA, $n = 3$).* ***Each*** *data set represents pooled mean values of GFP-expressing cell counts per 50 µm horizontal section for three brains injected with SR-BI^{Ab} - PEI, SR-BI^{Ab} - PEI - NLS, SR-BI^{Ab} - PEI - HA2 or SR-BI^{Ab} - PEI - HA2 - NLS, respectively. These numbers were calculated based on the number cells immunoreactive for GFP in two entire horizontal sections on each level, starting at the injection site (Level 5) and in four successive 0.5 mm intervals dorsal to this site (Level 4 to Level 1).*

considerable inter-animal variability, small effects on transfection efficiency arising from the modifications to the immunogene constructs might not have been detected. Nonetheless, the findings strongly suggest that none of the modifications caused substantial differences in GFP expression that would most likely be needed to justify recurrent use of the immunogene. Thus, investigations in additional animals were felt not to be warranted.

5.3.4 GFP expression following intrahippocampal injections of immunogenes

To explore the possibility of achieving transfection with a single injection rather than prolonged infusion, three immunogene versions (SR-BI^{Ab} - PEI, SR-BI^{Ab} - PEI - NLS and SR-BI^{Ab} - PEI - HA2; *n = 3* per group) were injected separately into the hippocampus of adult rat brain. These single injections again resulted in transfection of cells, albeit at much lower efficiencies than produced by infusions. Based on preliminary analysis of the brains following single injections, transfected cells were less widespread than with infusions and all were found within a distance of 1.5 mm dorsally from the injection site. Thus, tissue sections extending 1.5 mm dorsal to the injection site were subsequently analysed.

GFP-positive cells were detected in 8 of 9 brains. Only for one of the rats injected with SR-BI^{Ab} - PEI - NLS, no transfected cells were detected. The mean total number of GFP-positive cells in all rats calculated for the 1.5 mm block of tissue analysed was 28. A maximum of 75 cells was found in one of the rats infused

with the SR-BI^{Ab} - PEI - HA2 immunogene. No significant differences between the three immunogene versions were found for the mean number of GFP-positive cells detected ($p > 0.05$, ANOVA, $n = 3$ per group). Also, no differences in morphology of these cells were found. No GFP expression was detected after injections of either PEI - DNA ($n = 3$) or the p75^{NTRAb} - PEI immunogene ($n = 3$).

As for the infusions, almost all cells transfected following injections (in proximity to or far away from the area of damage) were immunoreactive for CD11b/c (Figure 5.13a-b). In these brains, a smaller area of damage was observed than that caused by infusions (compare accumulation of CD11b/c staining in Figure 5.13 c and d). The majority of GFP-positive cells after intracerebral injections had rounded amoeboid morphologies. They were all found outside, however in close proximity to, this area of damage.

5.4 Discussion

5.4.1 Transfection of microglia in the adult rat brain

In this chapter, we demonstrate that the SR-BI^{Ab} - PEI immunogene produces transfection of many cells within several mm of the site of infusion. Also, this immunogene approach was highly selective for microglia and/or related cells, as shown using CD11b/c co-labelling. This was consistent with the selective

Figure 5.13 Transfection of a small population of cells after single intrahippocampal injections of SR-BI^{Ab} - PEI

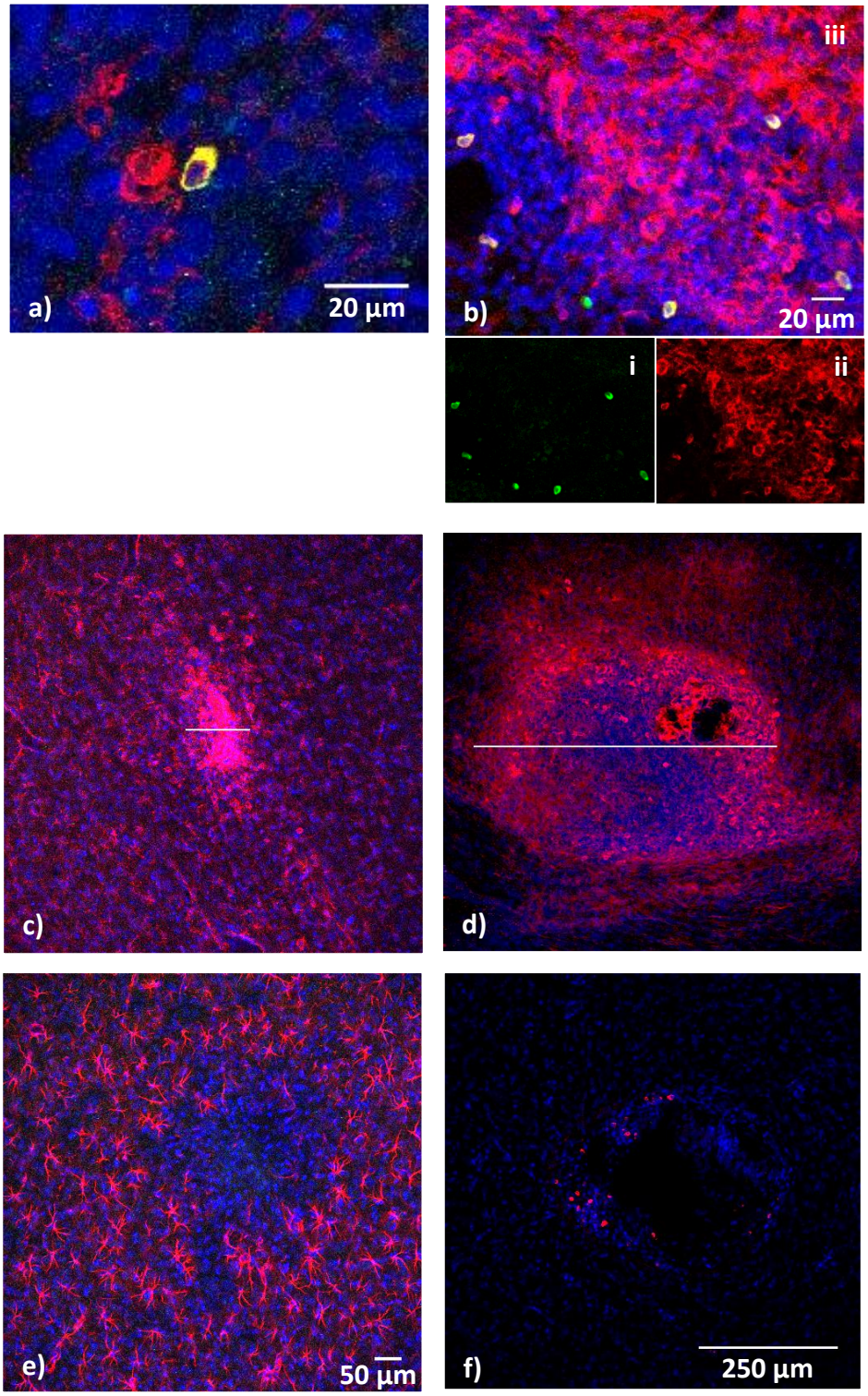

Figure 5.13 Transfection of a small population of cells after single intrahippocampal injections of SR-BI^{Ab} - PEI *(see previous page), as shown in images from 50 µm horizontal rat brain sections analysed in confocal microscopy from one of three independent experiments. GFP immunoreactivity (green in a and b-i) was found in a small population of cells around the injection site. Essentially all GFP-positive cells co-labelled with the microglial marker CD11b/c (red in a and b-ii). This was true for cells localised in the area of damage (b) and for cells found outside this area (a) as shown in merged images (a and b-iii). No transfected cells co-labelled with GFAP or NeuN. There was an accumulation of CD11b-positive cells (c; red) including activated resident microglia in the area of damage after a single injection (c; 120 µm wide as shown in white line). This area was smaller in comparison to the damaged area seen after an infusion with the same immunogene (d; 560 µm as shown in white line). GFAP-positive astrocytes were also seen in close proximity to the area of damage after single injections (e). Brain sections exposed to secondary antibodies alone displayed no immunoreactivity with the exception of a few cells in the far-red channel (f). This was most likely detection of the SR-BI^{Ab} that was of mouse origin. Nuclei were labelled with Hoechst 33258 (blue).*

internalisation of SR-BI^{Ab} into CD11b/c-positive cells of the brain (see section 3.3.4). However, the finding of CD11b/c-specific transfection was in contrast to the lack of SR-BI immunoreactivity in these cells (see section 3.3.4).

Interestingly, transfection was produced using all immunogene constructs incorporating SR-BI^{Ab}, but not the construct built on an antibody targeting p75^{NTRAb} which is not normally expressed by microglia. This observation indicates that specific features of SR-BI^{Ab} were apparently important for the transfection process. The finding is consistent with what had been seen after injection of the SR-BI^{Ab} alone which also showed selectivity for microglial cells, in contrast to the injection of Nrf2^{Ab} and X63^{Ab} which did not result in any internalisation in the adult rat brain (see section 3.3.4). Other antibodies against cell surface receptors have been injected into the adult rodent brain *(Book et al., 1992; Gu et al., 2000; Browne et al., 2001; Berhanu and Rush, 2008)*, where internalisation has been found in specific cell populations. In these studies, microglia were not represented.

The widespread transfection of microglia using the immunogene contrasted with the lack of any transfection when PEI carrying the same amount of DNA was infused into the brain. As with the lack of transfection following infusion of the immunogene based on the p75^{NTRAb}, this finding with PEI - DNA indicates that the transfection with the SR-BI^{Ab} - based immunogene was unlikely to result from

non-selective uptake of material in the extracellular space by microglia and adds support for a specific role for the SR-BI^{Ab} component of the immunogene in this process.

Similar low transfection capacities by PEI - DNA in the intact brain have been documented previously, for example after injections into the ventricle of the adult rodent brain *(Goula et al., 1998)*. Improvements of PEI transfection have been made using chemical modifications and also after controlling variables affecting the formation of the PEI - DNA complex using for example dextran *(Corso et al., 2005)*. Together with others, this study achieved high transfection efficiencies in cells of the postnatal brain at comparable levels to viral transduction *(Boussif et al., 1995; Goula et al., 1998; Corso et al., 2005; Posadas et al., 2010)*. However, these studies did not result in targeted delivery of the transgene and also did not produce any transgene expression in microglia. In contrast, the SR-BI^{Ab} - PEI immunogene provides a potentially powerful tool specifically transfecting the microglial population.

The selectivity of the immunogene *in vivo* also contrasted with transfection seen in culture using the same immunogene, where both astrocytes and microglia were transfected (see section 4.3.4.2). The different transfection profile in culture in comparison to the *in vivo* setting, may be due to several reasons, including: a) the different developmental stage of the cells, b) the extraction of

cells from their natural environment (previously mentioned in section 1.4.1) c) the different conditions encountered in a narrow layer of cells on a dish or d) the different cellular interactions.

As previously described in sections 1.2.5 - 1.2.6, immunolabelling of highly activated resident microglia may be hard to distinguish from that of monocytes which can infiltrate the tissue in response to injury. Resident microglia acquire a more activated morphology in response to injury and new tissue macrophages in the CNS acquire a phenotype that is similar to resident microglia with regards to protein expression and morphology *(Lucin and Wyss-Coray, 2009; Kettenmann et al., 2011)*. Blood-derived macrophages and neutrophils found in the CNS after injury express CD11b/c and CD68 *(Tanaka et al., 2003; Matsumoto et al., 2007)*. Thus, it is not possible to unequivocally determine whether the GFP-expressing cells found in our study are resident microglia or cells entering from the blood in response to injury.

However, monocytes have been shown to express NG2 after infiltrating the brain in contrast to resident microglia *(Matsumoto et al., 2007)*. NG2 was not detected in any GFP-positive cells after infusions of the SR-BI^{Ab} - PEI immunogenes. Also, potentially infiltrating neutrophils have characteristic polymorph nuclei which were not detected in the transfected CD11b-positive population in our studies. In addition, the seminal study by Ajami et al. (2007) suggests that infiltration by

potential microglial progenitors such as monocytes is non-existent in a facial nerve axotomy model and that the proliferation of resident microglia sustains this population throughout life.

In addition to this, several other factors indicate that many of the transfected cells in our studies were microglia rather than infiltrated monocytes. Firstly, this is suggested by the detection of a large number of cells outside the area of damage. The spread of GFP-positive cells in our study is wider than what has been seen for the spread of potential microglial progenitors after injury in the CNS. For example, in a spinal cord nerve injury model, GFP-positive infiltrating cells were found in an area of approximately 1 mm in diameter at 14 days after injury *(Zhang et al., 2007a)*. In a similar study of the brain in which animals were exposed to a peripheral organ-specific inflammatory injury, monocyte infiltration after 10 days was restricted to the choroid plexus and to perivascular and periventricular regions *(D'Mello et al., 2009)*. Also, the injection of specific amyloid-β isoforms into the mouse hippocampus has resulted in infiltration of potential microglial progenitors into this area and up to approximately 600 µm away from the injection site *(Simard et al., 2006)*. It would also be expected that chemokine stimuli by activated cells in the vicinity of the infusion would attract infiltrated progenitors *(Zhang et al., 2007a)* rather than resulting in movement of these cells up to 4 mm away from the infusion site.

The finding of GFP immunoreactivity in cells with ramified morphology is also consistent with a prominent expression of the transgene in the resident microglial population. This morphology is only seen in non-proliferative microglia, which are acting as surveyors in the CNS parenchyma, rather than phagocytes of dying cells or cell debris. Infiltrated monocytes would not be expected to have acquired ramified morphologies after 14 days as they are in the vicinity of an area of damage, which would more likely result in the preservation of an activated phenotype.

5.4.1.1 The majority of transfected microglia are activated

The majority of GFP-positive cells found after immunogene infusions had an amoeboid activated morphology, and a large proportion of these cells expressed the marker for activated microglia CD68. This finding raised the question what caused the activation of these GFP-positive cells. Several factors could contribute, as discussed below.

Microglia around the infusion site are expected to be activated in response to the tissue injury induced by the needle and the prolonged period of infusion. Regardless of their activation stage, these microglia are more likely to be transfected due to their location in the area where the immunogene is infused. Furthermore, cells of the activated, amoeboid microglial population are much more likely to proliferate. Immunogenes infused into the adult rat hippocampus may more easily result in GFP expression in such a dividing cell. This is due to the

fact that DNA can more easily enter the nucleus during mitosis, as previously shown in cultured cell lines *(van der Aa et al., 2005)*. However, amoeboid cells expressing GFP were found far away from the infusion site. It is possible that resident microglia of lower activation stages at great distances from the infusion site had been transfected, and that these cells might have been activated after the transfection process. In order to determine whether the immunogene has the capacity to transfect resident ramified microglia, the characteristics of the immunogene must be changed. These changes are required to result in an immunogene with similar levels of transfection even after a single intracerebral injection without substantial activation of microglia.

Studies in culture using our SR-BI^{Ab} - PEI immunogene had also shown that the prior activation of microglia using LPS did not increase transfection levels (see section 4.3.4.5). Thus, the proximity to the infusion site and/or the mitotic state of these cells is unlikely to fully account for the transfection of an amoeboid microglial population in the adult rat brain.

A further possibility is that the transfection process results in microglial activation. The binding and/or internalisation of the SR-BI^{Ab}, the presence of PEI, the detection by the microglia of DNA derived from bacteria, or the expression of GFP could possibly lead to activation of the microglia exposed to the SR-BI^{Ab} - PEI immunogenes. PEI has been shown to cause microglial activation in previous studies. For example, increased CD11b expression has been detected after injection of 25 kDa PEI in rat spinal cord *(Zeng et al., 2007)*. However, the

potential immunogenicity effect of PEI from our injections/infusions was considered negligible as injections of PEI - DNA alone also did not result in any extensive glial activation in comparison to that of SR-BI^{Ab}. We also do not report any obvious activation of microglia through the binding and/or internalisation of SR-BI^{Ab} on microglial cells in culture (see section 3.3.3) or after intracerebral injections of SR-BI^{Ab} alone (see section 3.3.4), SR-BI^{Ab} - PLL immunogene (see section 4.3.2) or SR-BI^{Ab} - PEI immunogene (see section 5.3.4) into the adult brain.

With regards to potential activation of cells due to the presence of DNA derived from bacteria, this has been observed in cell lines derived from cells belonging to the innate immune system. This is most likely due to the lack of methylation at key sites of the bacterial DNA *(Hacker et al., 2002; Nonnenmacher et al., 2003)*. Though the possibility of activation by bacterial DNA is less likely by the absence of a similar effect on macrophages in primary culture *(Yasuda et al., 2004)*, there might still be a possibility that the bacteria-derived plasmid used in our studies could have contributed to microglial activation.

Protein expression from the transgene could also potentially trigger activation of microglia. However, to our knowledge, there is no published material showing increased activation of any cell type upon GFP expression. This reporter gene produces a protein with little, if any, effect on the cell with respect to toxicity, cell growth and function *(Rosochacki and Matejczyk, 2002)*.

In conclusion, we have not identified a specific cause for the majority of transfected cells being activated in our studies. However, a combination of several of the factors identified above may have contributed to this finding. The lower number of ramified microglia expressing GFP illustrates the difficulties in achieving transfection in these cells. However, the findings in this work offer a first step towards selective transfection of the microglial population. Further studies involving longer infusion times, or the removal of the cannula and longer subsequent waiting times, may give a higher proportion of ramified GFP-positive microglia. However, the changes with the highest potential to reach the ramified microglial population, involved the change of the immunogene construct itself (see section 5.4.2 below).

5.4.2 Transfection capacities after infusions of immunogenes with peptide additions

In this chapter, we achieved extensive GFP expression specifically within the microglial population of the adult rat hippocampus using all four versions of the SR-BI^{Ab} - PEI immunogene. The attempts to increase the release of the SR-BI^{Ab} - PEI construct into the cytosol and entry into the nucleus of the DNA cargo through the addition of HA2 peptide and NLS peptide, respectively, did not increase transfection efficiencies. Possible explanations for this are discussed in the following sections.

It is important to note that the analysis of transfection capacities was limited due to the low numbers of animals included in the study. The limitation in numbers of injected animals was partially due to the low yield after the three-day immunoporter production protocol. Each batch could be used to infuse a maximum of two rat brains. In spite of the low power of the study, none of the animals showed any dramatic differences in the number of GFP-positive cells that would probably be required for recurrent use of the immunogene. Thus, we did not analyse the effects of HA2 and NLS additions any further.

5.4.2.1 Addition of HA2 peptide - studying effects on transfection in vivo

The addition of the HA2 peptide was not only interesting as a means of improving transfection efficiency of our immunogene, but also provided an approach to investigate the mechanism of internalisation and subsequent intracellular pathways of this construct. One possible explanation for the lack of increase in transfection capacity of the SR-BI^{Ab} - PEI - HA2 immunoporter compared to SR-BI^{Ab} - PEI is that HA2 may have a limited effect on improving the intrinsic capacity of PEI to escape acidic intracellular vesicles *(Wagner and Kloeckner, 2006)*. It is possible that the capacity of PEI to escape acidic vesicles may already induce sufficient release into the cytosol, making other parts of the intracellular pathway more limiting in the transfection by our SR-BI^{Ab} - PEI immunogene.

An alternative explanation is suggested by the finding that the addition of an analogue to the HA2 peptide used in this project, could induce release of PLL - DNA into the cytosol, but subsequently inhibited nuclear translocation of the plasmid DNA cargo *(Parker et al., 2005)*. This is most likely due to the displacement of DNA from the polycation moiety to the slightly charged HA2 peptide *(Parker et al., 2005; Fabre and Collins, 2006)*.

Interference with internalisation of the immunogene may also be caused by the addition of the HA2 peptide. Endocytosis is favourable for particle sizes < 200 nm via clathrin-mediated pathways and possible for particles up to 500 nm via caveolae *(Rejman et al., 2004; Germershaus et al., 2006)*. Determination of particle sizes using dynamic light scattering *(Fabre and Collins, 2006; Germershaus et al., 2006; Yu et al., 2007)* has shown that condensation of plasmids of similar size as gWizGFP using cationic lipids or polymers results in spheres with sizes ranging from 25 nm *(Blessing et al., 1998)* to 190 nm *(Zeng et al., 2007)*. For entire immunogene constructs, it has been shown that a construct based on a pegylated monoclonal antibody coupled with PEI, form complexes with DNA of sizes between 125 nm and 180 nm *(Germershaus et al., 2006)*. Other investigations have indicated that PEI immunogenes similar to those used in our study are less than 100 nm (Rogers, M-L and Rush R.R., unpublished results). Thus, it is likely that entry of our unmodified SR-BI^{Ab} - PEI immunogene was not greatly influenced by size.

However, the presence of HA2 peptides in the immunoporter construct may increase its size, resulting in reduced internalisation of the immunogene into cells. Such reduced uptake might have counteracted any potential improvements in transfection due to increased endosomal/lysosomal release of DNA produced by HA2. Information on immunogene sizes obtained from dynamic light scattering might be used as guidance for preparation of immunogene constructs. If future analysis indicates a large size of our construct, the presence of agents such as 5 % dextran is a potential method to decrease the particle size of some polycations when complexed to DNA *(Fabre and Collins, 2006)*.

5.4.2.2 Addition of NLS peptide - studying effects on transfection in vivo

The NLS : DNA w/w ratio of 1.8 : 1 was similar to the use of this peptide in other non-viral constructs *(Navarro-Quiroga et al., 2002; Berhanu and Rush, 2008)*. Although no significant difference was detected for the number of GFP-expressing cells after the infusion of SR-BI^{Ab} - PEI - NLS compared to SR-BI^{Ab} - PEI, this may have been inhibited due to other complications caused by the addition of this peptide. For example, similar effects on particle size as postulated for the addition of the HA2 peptide (discussed in the previous section) could have inhibited any impact by enhanced nuclear translocation.

There has also been a debate whether plasmid DNA molecules are too large to cross the nuclear envelope. As mentioned previously, polymer-plasmid

complexes have sizes of approximately 25 nm *(Blessing et al., 1998)*. This size is near the limit for successful importin-dependent nuclear transport *(Gorlich and Mattaj, 1996; Ohno et al., 1998; Zanta et al., 1999)*. However, one study reports the nuclear translocation of complexes of up to 50 nm after the addition of an NLS peptide *(Eguchi et al., 2005)*. Nuclear translocation of DNA has also been detected in cells transfected by PEI after cell cycle arrest in a phase where mitosis is inhibited *(Escriou et al., 2001)*. This study indicates that plasmid DNA has the capacity to enter the nucleus of non-dividing cells via importin-dependent nuclear transport.

It has also been suggested that the addition of SV40 large T antigen NLS has the capacity to enhance transfection efficiencies in only non-dividing cells, but not in dividing cells *(Collins et al., 2007)*. Thus, there is a possibility that the addition of NLS peptides may not affect transfection in strongly dividing cells such as that of the microglial population in the area of damage caused by our injections/infusions. The same study also showed that transfection was increased when using a mutated version of the peptide. This mutated peptide did not harbour nuclear targeting characteristics, which suggests that it was the mere compaction of DNA by the slight positive charge of the two peptides that enhanced the delivery of the DNA to the cells, rather than inducing nuclear translocation. It was therefore hypothesised that, after endocytosis, DNA delivery to the nucleus was instead inhibited by the binding to either of these peptides *(Collins et al., 2007)*.

An alternative approach to using NLS peptides to promote DNA entry into the nucleus is the use of so-called DNA-targeting sequences (DTS; *Lam and Dean, 2010)*. These sequences are incorporated directly into the plasmid DNA, and attract the binding of ubiquitously expressed transcription factors with NLS peptide sequences in the cytoplasm. Via these endogenous NLS peptides, nucleic acids of interest can be imported through the NPCs. The use of DTS has increased over recent years. Many, but not all, eukaryotic promoters, include DTS sequences that enhance nuclear translocation *(Lam and Dean, 2010)*. Cell-specific promoters with this characteristic have therefore been used to transfect a variety of cell types *(Brenner et al., 1994; Tsien et al., 1996; Klein et al., 1998; Cucchiarini et al., 2003; Miller and Dean, 2008; Bradford et al., 2009)*. A future alternative to the NLS peptides used in this work would be to exchange the currently used CMV promoter for a cell-specific promoter with the capacity to bind endogenous NLS peptides.

5.4.3 Concluding remarks

These studies demonstrate that SR-BI^{Ab} - PEI immunogenes can produce extensive transfection of microglia in the brain. Transfection was highly selective as it was almost completely undetectable in other neural cell populations, although blood-derived CD11b/c-positive cells may also be affected. To our knowledge, this is the only report of a non-viral transfection specifically targeting microglia in the CNS.

Transfection was extensive following infusion of the immunogene and was also produced in many cells surrounding the sites of individual intracerebral injections. Improvements in the efficiency of transfection are likely to be needed for routine use of these immunogenes. Modifications directed at promoting escape from endosomes/lysosomes and entry of DNA into the nucleus did not improve transfection. However, as discussed in Chapter 6, there are other approaches that could be tested to achieve this outcome. Furthermore, the evidence for the highly targeted actions of the SR-BI^{Ab} points to alternative uses of this protein to manipulate microglial function in the brain.

CHAPTER 6: SUMMARY AND FUTURE STUDIES

Two major conclusions arising from this work are as follows:

a) An antibody targeted at an extracellular epitope of SR-BI provides an effective mechanism for the highly selective delivery of substances to microglia in the adult brain.

b) An immunogene containing the SR-BI^{Ab} and the polycation PEI can selectively transfect microglia in the brain. Thus, such constructs have the capacity to be internalised by microglia and can overcome intracellular barriers associated with escape from vesicles and entry of DNA into the nucleus.

To our knowledge, this is the only report of the use of a non-viral vector to produce selective microglial transfection in the CNS. The only other approach producing a similar outcome involved an AAV vector, for which selectivity was achieved using a microglial-specific promoter rather than targeted delivery of the DNA as in the present investigations. An immunogene approach avoids the potential impact of vector entry into other cells, as well as possible deleterious responses that are detected in the presence of viral vectors in the CNS *(Askjaer et al., 2002; Bhat and Fan, 2002; Raper et al., 2003; Gaspar et al., 2004; Fabre and Collins, 2006; Manfredsson and Mandel, 2010; Thaci et al., 2011)*.

Using the SR-BI^{Ab} - based immunogene, widespread transfection of CD11b/c-positive cells was achieved after infusions over an extended period into the brain

tissue. The lack of detected immunoreactivity for the target SR-BI in IHC suggested that this protein might not be present in the mature rat brain. However, the cell-specific internalisation of another SR-BI^{Ab} with a different target to that used for IHC, together with the lack of internalisation of other antibodies and the selectivity of transfection achieved with the SR-BI^{Ab} - PEI immunogene, point strongly to SR-BI being expressed by microglia.

The SR-BI antibody used for IHC had the capacity to label astrocytes and microglia in culture, consistent with previous reports *(Alarcon et al., 2005; Zhang et al., 2006)*. Thus, this antibody had the capacity to recognise the relevant protein, at least in cells derived from the immature brain. The lack of detectable immunolabelling in brain tissue could reflect a real absence of the protein in the adult rat, or levels of expression below the sensitivity of detection of IHC protocols. Alternatively, this finding could result from a masking of the SR-BI protein or structural modifications associated with maturation of the animal. The absence of detectable immunolabelling despite the use of several antigen retrieval techniques makes a reversible masking of the antigenic sites less likely. Modifications to SR-BI which could potentially limit interactions with the antibody used for IHC but not with that used for internalisation remains a strong possibility.

Regardless of the detailed interpretation, all our findings in rat brain suggest substantial differences in SR-BI expression compared with that in adult mouse and human *(Husemann and Silverstein, 2001; Husemann et al., 2002)*. In these species, expression was found to be restricted to astrocytes in the mature brain. Further studies are needed to investigate the basis for this apparent species difference and the implications for microglial and astrocytic function. The internalisation of antibodies directed at extracellular sites of SR-BI has not been investigated in mice and such studies are not plausible in humans. Thus, the possibility remains that molecular complexes incorporating SR-BI^{Ab} might also selectively target microglia in these species.

Infusions of immunogenes were used in our studies to maximise the chances of detecting transfection. However, such a procedure is not likely to be useful for routine applications due to the associated tissue damage. In our studies, single injections of the immunogene successfully induced transfection of microglia, while resulting in little tissue damage. However, modifications that can increase transfection efficiency will be needed if the technique is to be widely adopted.

As part of our studies, two approaches were tested that aimed to improve the transfection efficiency of the immunogene: a) the incorporation of HA2 in the construct to promote disruption of endosomes/lysosomes or other vesicles resulting from the internalisation of the immunogenes and b) the addition of NLS

to facilitate DNA entry into the nucleus. We acknowledge the use of low animal numbers in this work and that there is a possibility of finding increased GFP expression in an experiment of higher power. However, no substantial increase was found in the use of any immunogene version and was thus not further analysed. The finding that immunogene modifications did not substantially improve the transfection efficiency may indicate that they did not have the capacity to overcome intracellular barriers to transfect microglia, even though they have been effective in other cells *(Navarro-Quiroga et al., 2002; Berhanu and Rush, 2008)*. Other approaches such as the use of DTS to promote DNA entry into the nucleus might prove to be more effective (see section 5.4.2.2).

Alternatively, the lack of improvement with the modified immunogenes could indicate that steps required for immunogene trafficking other than disruption of endosomes and nuclear entry of DNA might have bigger roles in limiting transfection. One step that could potentially contribute is uptake of immunogenes into microglia. The internalisation might be limited due to the size of these molecular complexes. Thus, modifications to reduce immunogene size could increase transfection efficiencies. As previously mentioned, antibody fragments rather than entire antibodies may be used to deliver nucleic acids to cells *(Chen et al., 1998b; Merdan et al., 2003; Germershaus et al., 2006)*. In one study, the antigen-binding fragments (Fab fragments) of a murine IgG antibody against epidermal growth factor receptor were used to produce transfection. Expression of β-galactosidase reporter was achieved in 2 % of cells in a human

squamous carcinoma cell line, which was a 20 - 100 fold increase compared to when the whole antibody was included in the immunoporter construct *(Chen et al., 1998b)*. This finding indicated that a construct of smaller size may more easily produce transfection *(Rejman et al., 2004; Germershaus et al., 2006)*. Similar methods have been used to transfect other carcinoma cell lines using pegylated PEI bound to an entity that recognised receptors up-regulated in tumourogenic cells *(Merdan et al., 2003)*. This entity was produced through treatment of pepsin and resulted in two connected Fab fragments ($F(Ab')_2$). Potentially, the use of a smaller derivative of the SR-BI^{Ab} in form of its Fab fragments could lower steric hindrance, resulting in more binding of DNA to the PEI. This may further increase transfection efficiencies by our SR-BI^{Ab} - PEI immunogene.

The selectivity of SR-BI^{Ab} uptake also provides an excellent basis for developing additional approaches to modify microglial function *in vivo*. One alternative would be to deliver nucleic acids other than DNA, including siRNAs. The use of siRNAs can inhibit translation of endogenous mRNA targets and only requires delivery to the cytosol, rather than the nucleus. Knock-down of endogenous genes in culture and *in vivo* has been valuable for the determination of function and importance in various diseases and injuries *(Kim et al., 2011)*, including that of the CNS *(Kumar et al., 2007; Posadas et al., 2010)*. Therefore, an extended use of our immunoporter may involve the transfection of siRNAs rather than plasmid DNA.

The same SR-BI^{Ab} may also be used for delivery of molecules other than nucleic acids to modify microglial function. Similar approaches to the work presented in this thesis have been used to deliver toxins to other cells in organs outside the CNS, with a focus on treating various cancers *(Thorpe et al., 1987; Shimizu et al., 1996; Uherek et al., 1998; Omelyanenko et al., 2003; Saito et al., 2003; Germershaus et al., 2006; Yip et al., 2007)*.

Modifications to improve transfection efficiencies with the immunogene or to develop other complexes incorporating the SR-BI^{Ab} would also provide useful tools for studying glial cells in culture. In our studies, the exposure of the SR-BI^{Ab} - PEI immunoporter led to GFP reporter expression in up to 2.4 % of cells in mixed glial culture. This transfection efficiency was 120-fold higher than that of PEI carrying similar amounts of DNA, demonstrating a higher capacity of the immunoporter than PEI itself to transfect cells in mixed glial culture. Thus, the inclusion of the SR-BI^{Ab} in the construct increased gene delivery and transfection efficiency in mixed glial cultures. Transfection efficiencies using our immunoporter match those of other immunoporter techniques *(Chen et al., 1994)* and are similar to those of other non-viral methods in microglial cell lines or primary glial cultures *(Wiesenhofer and Humpel, 2000; Jana et al., 2001; Mitrasinovic et al., 2001)*.

In contrast to the findings in brain, the immunogene in mixed glial cultures was equally effective in producing transfection in microglia and astrocytes. This use of immunogenes would thus have advantages for transiently modifying proteins in both types of glial cells concurrently. Alternatively, selectivity might be achieved by incorporating cell-specific promoters, including the GFAP promoter *(Brenner et al., 1994; Bradford et al., 2009; Xu et al., 2010)* or the F4/80 promoter *(Cucchiarini et al., 2003)* for astrocytes and microglia, respectively. Another option would be to deliver siRNA directed at proteins expressed by only one of these cell types.

In conclusion, we have developed a non-viral construct targeting SR-BI. This immunoporter can deliver DNA and potentially other nucleic acids, drugs and toxins to microglia in the adult rat brain. This is the first non-viral method ever targeted at the microglial population. Manipulation of microglial functions using the $SR\text{-}BI^{Ab}$ - PEI immunogene or other constructs incorporating the $SR\text{-}BI^{Ab}$ has good potential to provide valuable insights into the resident immunocompetent cell population of the CNS.

CHAPTER 7: APPENDICES

Appendix 1 – Initial poly-L-lysine immunoporter construction protocol

Constructing conjugate

1) Prepare **buffers** (Sterile-filter all. De-gas all but Traut's buffer for 30 min);

Traut's buffer
(for dissolving of Traut's reagent)

Amount	Descripton
663 µl (=0.745 g)	Triethanolamine
2.37 g	NaCl
0.29 g	EDTA
up to 100 ml	dH_2O
Equlibriate to pH 7.5	

Activation buffer
(improves efficiency of linking reaction)

Amount	Descripton
11.5 g	Na_2HPO_4
2.9 g	NaH_2PO_4
8.7 g	EDTA
7.5 g	NaCl
up to 1 l	dH_2O
Equilibriate to pH 7.5 using NaOH	

PBS-sodium azide
(for packing Sephacryl-200 column)

Amount	Descripton
0.98 g	Sodium azide
50 ml	20 X PBS
up to 1 l	dH_2O

20 % Ethanol
(for washing FPLC)

Amount	Descripton
200 ml	Absolute ethanol
up to 1 l	dH_2O

2) Prepare **Antibody (Ab)**

MW of IgGs is 150 kDA ≥3 mg is needed for each immunogene.

$\rho =$ mg/ml $V = \frac{m}{\rho} = \frac{3mg}{} =$ ml

Make final c between 1.5 and 2.5 mg/ml by diluting with sterile 1X PBS.

$$n_{Ab} = \frac{m}{MW_{Ab}} = \frac{0.003g}{150000Da} = 0.02\mu moles$$

If Ab lyophilized, dissolve in dH_2O ('cause it already contains PBS), if not; dilute in 1x PBS. OBS! The Ab used should have been tested by injecting it directly into the rat brain (~50 µg). It should also be tested by staining brain tissue sections.

3) Prepare **Sulfo-LC-SMPT** (*4-Sulfosuccinimidyl-6-methyl-a-(2-pyridyldithio)toluamido]hexanoate, Pierce Biotechnologies #21568, 50 mg)*

$MW_{Sulfo\text{-}LC\text{-}SMPT}$ = 636. Calculate;

$$n_{Sulfo-LC-SMPT} = 20 \cdot n_{Ab} = 20 \cdot 0.02\mu moles = 0.4\mu moles$$

$$m_{Sulfo-LC-SMPT} = n_{Sulfo-LC-SMPT} \cdot MW_{Sulfo-LC-SMPT} = 0.4\mu moles \cdot 636 = 0.25mg$$

Weigh up as little as possible (maximum 3.75 mg) in an eppendorf, spin down a few seconds and add DMF. Calculate;

$$V_{DMF\,added} = \frac{m_{\text{Sulfo-LC-SMPT added}}}{c_{\text{Sulfo-LC-SMPT stock}}} = \frac{mg}{2.5mg/ml} = \qquad ml$$

Discard this stock after use.

The added volume of Sulfo-LC-SMPT will be a tenth of the volume of the Ab for each linking. Calculate; $V_{SulfoLCSMPT} = \frac{2ml}{10} = 200\mu l$

Ingredient	**v**	**[orig]**	**Wanted**
Sulfo-LC-SMPT	*100 µl*	*2.5mg/ml*	*0.25 mg*
DMF	*100 µl*	-	up to total
TOTAL	*200 µl*		

4) Prepare **PLL** *(Poly-L-lysine Sigma-Aldrich #P2636-100MG)*

MW_{PLL} = 45.8 kDa (varies in each lot)

Calculate; $n_{PLL} = 2 \cdot n_{Ab} = 2 \cdot 0.02\mu moles = 0.04\mu moles$

$m_{PLL} = n_{PLL} \cdot MW_{PLL} = 0.04\mu moles \cdot 45.8kDa = 1.8mg$

Weigh up as little as possible (this amount is hard to get exact) in an eppendorf, spin down a few seconds and add activation buffer to make up (Calculate) 50 mg/ml stock (or use old one if kept in fridge for no longer than 2 years) $V_{Activationbuffer\,added} = \frac{m_{PLL\,added}}{\rho_{\text{PLL stock}}} \frac{mg}{50mg/ml} = \qquad \mu l$

Sterile-filter solution and keep in fridge (stable for 2 years).

The wanted concentration of PLL is between 1.5-2.5 mg/ml. Since I want 1.8 mg total, I could simply take out the amount I want from the stock and dilute it into 1000 µl total.

Ingredient	**v**	**[orig]**	**[wanted]**
PLL	*36 µl*	*50 mg/ml*	*1.8 mg*
Activation buffer	*964 µl*	-	up to total
TOTAL (v_{PLL})	*1000 µl*		

5) Prepare **Traut's reagent** *(2-Iminothiolane•HCl, Pierce Biotechnologies #26101, 500 mg)*

$MW_{Trautreag}$ = 137 Traut's reagent is a PLL activator.

Calculate; $n_{Trautreag} = 20 \cdot n_{PLL} = 20 \cdot 0.04\mu moles = 0.8\mu moles$

$m_{Trautreag} = n_{Trautreag} \cdot MW_{Trautreag} = 0.8\mu moles \cdot 137 = 109.6\mu g = 0.11mg$

Weigh up as little as possible (maximum 3.75 mg) in an eppendorf, spin down a few seconds and add a volume of Traut's buffer to make up a 2 mg/ml solution. Calculate;

$$V_{Trautsbuffr\,added} = \frac{m_{Trautreagadded}}{\rho_{\text{Trautreag stock}}} \frac{mg}{2.5mg/ml} = \qquad \mu l$$

Discard this stock after use.

Ingredient	Volume	[orig]	[wanted]
Traut's reagent	*44 µl*	*2.5 mg/ml*	*0.11 mg*
Traut's buffer	*56 µl*	-	up to total
TOTAL	*100 µl*		v_{PLL} / 10

6) **Ab linking and PLL linking** (in parallel)
   a. Directly mix the following in a 15 ml Falcon tubes and shake;

Ingredient	Volume	[orig]	Wanted
Ab	*2 ml*	*1.5 mg/ml*	*3 mg*
Sulfo-LC-SMPT mix	*200 µl*		$V_{Ab}/10$
TOTAL	*2.2 ml*		

   b. Mix by inverting the tube.
   c. De-gas Ab mix for 10 minutes.
   d. Meanwhile, mix the following in another 15 ml Falcon tube and shake;

Ingredient	Volume	[orig]	Wanted
PLL mix	*1 ml*		*1.8 mg*
Traut's reagent mix	*100 µl*		V_{PLL}/ 10
TOTAL	*1.1 ml*		

   De-gas PLL mix for 10 minutes and flush Ab mix with N_2 gas for 10 minutes. Then flush the PLL mix with N_2 gas for 10 minutes.
   N_2-flushing is used to prevent O_2 from oxidising the Ab and also because it inhibits the linking reaction
   e. Check pH using pH indiciator strip.
   f. Incubate @ RT, slow shaking, 1h. (Start PLL linking – see below)
   g. De-salt Ab with Sephadex G25 and concentrate using dialysis tubing (see separate protocol)

7) **Constructing conjugate**
   a. Transfer the linked Ab and PLL mixes from dialysis tubing into a new, sterile vial.
   b. Check pH using pH indiciator strip.
   c. Incubate @ 4˚C O/N.

8) **L-cysteine** incubation.
   Use a stock of 200 mM (0.2 M) L-cysteine to add to the total volume (final conc 20 mM), 2h, RT. $\frac{V_{L-cysteine}}{V_{L-cysteine}+V_{conj}} = \frac{20mM}{200mM} \rightarrow V_{L-cysteine} = \frac{V_{conj}}{9}$

9) If precipitation exists, put in 15 ml Falcon tube and **centrifuge** for 5 min at maximum speed (20 000 *g;* at least 2 000 *g*) in a benchtop centrifuge. Keep pellet in fridge until after finished purification. This centrifugation step is made instead of filtering through 0.22 µm filter since this may cause the loss of conjugate.
10) **Purify conjugate** using Sephacryl-HR-200 (see separate protocol).

11) **Dialyze** in 0.9 % NaCl three times á 6 hours.

12) **Check pH** using pH indiciator strip.

13) **Constructing immunogene**; *Includes the addition of DNA to the conjugate to construct an immunogene.* Analyse this using a DNA retardation assay.

Sephadex G25 de-salting and concentrating Ab and PLL

Sephadex G25 (*Pharmacia Fine Chemicals, Uppsala, Sweden, 500 g, retrieve from* Amersham Biosciences- a part of GE health care - *http://www4.gelifesciences.com/aptrix/upp01077.nsf/Content/australia_homepage)*

1) Prepare Sephadex G25; Boil 50 ml dH_2O for 3 min in microwave. Add 3 g Sephadex G25 and let swell and cool down.
2) When ready to purify Ab, fill an empty column (buy?) with Sephadex G25. Put waste beaker under column. Add, in total, 20 ml activation buffer using plastic transfer pipette to equilibrate column.
3) Swap waste beaker for Falcon tube and add Ab mix to column using plastic transfer pipette. Let column absorb Ab mix and then start adding Activation buffer.
4) Withdraw the first 7 mls of flow-through in 1 ml aliquots, which should contain the majority of the Ab. Measure on spectrophotometer @ 280 nm and determine the amount of Ab recovered.
5) Swap Falcon tube for waste beaker and rinse column with 20 ml activation buffer to remove salt.
6) Add PLL mix to column using plastic transfer pipette. Let column absorb PLL mix and start adding Activation buffer. Let the first 2 ml pass through into waste beaker. Swap waste beaker for Falcon tube and withdraw the following 7 ml, which should contain the majority of the PLL.
7) Mix the Ab mix and the PLL mix and put in a 2 dm dialysis tube.
8) Put dialysis tube in polyethyleneglycol and concentrate it to 1.5-3 mg/ml.

Appendix 2 – Initial polyethylenimine immunoporter construction protocol

Day 1 Buffer preparation and PEI preparation

(Adapted from Blessing et al., 2001; and Germershaus et al., 2006 and Kircheis et al., 1997)

- ❑ 1 M HEPES *(Sigma-Aldrich, #H4034, FW = 238.3 g/mol)*; 59.6 g in 250 ml dH_2O.
- ❑ 5 M NaCl *(Sigma-Aldrich, #S9625, FW = 58.44 g/mol)*: 292.2 g (192 g + 100 g) in 1 L dH_2O.
- ❑ 0.2 M EDTA *(FW=372.24 g/mol)*; 7.4 g in 100 ml dH_2O *(stable for months @4˚C)*
- ❑ 5M NaOH *(FW 40g/mol)*; 40 g in 200 ml dH_2O.
- ❑ Prepare the following buffers; *OBS! Store all in 4˚C, in dark (using aluminium foil) OBS! Make up buffers fresh and sterile-filter fresh just before immunogene construction starts.*
  1) 20 mM HEPES, pH 7.4 (salt-free 20 mM HEPES pH 7.4)
  2) 20 mM HEPES, 0.15M NaCl, pH 7.4
  3) 20 mM HEPES, 0.25M NaCl pH 7.9
  4) 20 mM HEPES, 1M NaCl, pH 7.6
  5) 20 mM HEPES, 2M NaCl, pH 7.6
  6) 20 mM HEPES, 3M NaCl, pH 7.6
  7) 20 mM HEPES, 0.5 M NaCl, pH 7.6

V										Total V	
1	2	3	4	5	6	7			Ingredient	needed	
10	10	10	10	10	10	10	*ml*		1 M HEPES	60	*ml*
0	15	25	100	200	300	50	*ml*		5 M NaCl	640	*ml*
500	500	500	500	500	500	500	*ml*		dH2O up to TOTAL		
7.4	*7.4*	*7.9*	*7.6*	*7.6*	*7.6*	*7.6*			*wanted pH*		
									final pH		

- ❑ **PEI preparation (~3h with protein assay)**
  - ❑ Weigh out ____ mg (> 100 mg) of Polyethyleneimine (PEI, *Sigma-Aldrich # 408727 – this is a liquid*) using cut-off pipette tip into 15 ml Falcon tube.
  - ❑ Just before putting the original PEI bottle back, flush the top with N_2 gas.
  - ❑ Add ____ ml (~10) of sterile dH_2O. (This will give a pH of ~11).
  - ❑ Shake vigorously to dissolve PEI.
  - ❑ Put small magnetic stirrer into tube and add full strength HCl, drop by drop, (~250 µl) until pH is exactly 7; _____.
  - ❑ Sterile-filter through 0.22 µm syringe filter.
  - ❑ Equilibrate PD10 column with ~25 ml 20 mM HEPES, 0.25M NaCl pH 7.9.
  - ❑ Add 2.5 ml (3 x ~830µl) of PEI solution at a time to column and collect in 1 ml fractions.

- ❑ Assay for PEI using Biorad assay using PEI stock as standard curve *(see separate protocol)*.
- ❑ PEI concentration: _____ mg/ml
- ❑ Store this PEI in fridge until used *(preferably the next day, but in theory this is stable for months @ 4˚C)*.
- ❑ Throw this PD10 column away.

Day 2 PEI thiolation and Ab preparation

- ❑ **PEI Thiol-functionalisation** → *thiol-functionalised PEI (PEI-SH) in 20 mM HEPES 0.25M NaCl pH 7.9 (ideally 3 per molecule of PEI)*
  - ❑ Make up 10 mM SPDP stock by mix ~2.5 mg of SPDP *(Sigma Aldrich, #P3415, 312.37 g/mol)* in ~800 µl of 100 % EtOH

$$V_{EtOH} = \frac{m_{SPDP}}{c_{SPDP} \cdot MW_{SPDP}} = \frac{g}{10 \cdot 10^{-3} M \cdot 312.37 g/mol} = \frac{g}{3.1237} =$$

  - ❑ Shake SPDP slowly for 15 min to ensure dissolving.
  - ❑ Based on quantification in Bio-rad assay, withdraw 25 mg of PEI (→ 1 µmoles of PEI).
  - ❑ Add 197 µl of 10 mM SPDP ethanolic solution in 5 ml yellow-cap tube to add 1.975 µmoles SPDP to 1 µmoles of PEI.
  - ❑ Mix @ RT, 1 hour, gentle shaking, in dark.
  - ❑ Equilibrate PD10 column with ~25 ml 20 mM HEPES, 0.25M NaCl pH 7.9.
  - ❑ Add PEI-SPDP mix to column and collect in 1 ml fractions. (Re-use this column for the next PEI PD10 separation further down)
  - ❑ Assay for PEI in pooled fractions using Biorad assay with PEI stock as standard curve *(see separate protocol)*
  - ❑ PEI concentration: _____ mg/ml.
  - ❑ Prepare 25 mg/ml (0.16 M) DTT *(Sigma-Aldrich, # D9779, 154.3 g/mol)* stock (daily, fresh stock).
  - ❑ Based on quantification in Bio-rad assay, withdraw 20 mg PEI-PDP (→0.8 µmoles).
  - ❑ Mix PEI-PDP with 157 µl of DTT (→ 25 µmoles, → ~30 molar excess of DTT over PEI-PDP) in 5ml tube.
  - ❑ Flush with N_2 gas for 2 min and air tight.
  - ❑ Incubate @ RT, 1 h, gentle shaking, in dark. (Start underlined part of Ab-SPDP linking below)
  - ❑ Equilibrate PD10 column with ~25ml (the same column as previous PEI column in this protocol) with 20 mM HEPES, 0.25M NaCl pH 7.9 (Kircheis et al., 1997).
  - ❑ Add PEI-PDP mix to column and collect in 1 ml fractions.
  - ❑ Assay for PEI using Biorad assay using PEI stock as standard curve *(see separate protocol)*.
  - ❑ PEI concentration: _____ mg/ml.
  - ❑ Throw away this PD10 column.

- ❑ **Ab-SPDP linking;** → *Ab-PDP ready for conjugation (Ab concentration known), ideally with one SPDP per Ab molecule.*

- ❑ Make up 5.5 mg freeze-dried Ab (0.033 u mol) in 1 ml dH_2O.
- ❑ Equilibrate PD10 column with ~25ml 20 mM HEPES, 0.25M NaCl pH 7.9.
- ❑ Add Ab solution to column and collect in 1 ml fractions.

- ❑ Measure A_{280} to find Ab

1	2	3	4	5	6	7	8

- ❑ Pool fractions containing Ab and make sure that 5 mg is present in 1 ml.

$$c = \frac{A_{280}}{1.35} = \frac{\qquad}{1.35} = \qquad mg/ml \; m = c \cdot V = \qquad \cdot \qquad = [\qquad mg]$$

$$V = \frac{m}{c} = \frac{5mg}{\qquad} = \qquad ml$$

- ❑ <u>Start this during the a half hour into the 1 h incubation period of PEI-PDP thiolation;</u> For each 1 mg of Ab, add 2.5 µl of 10 mM ethanolic solution of SPDP. *(slightly different amount compared to Kircheis et al., 1997 article)*.

$V = 2.5\mu l \cdot \qquad mg = \qquad \mu l$

- ❑ Incubate @ RT, 2 h (not more or less!).

- ❑ Equilibrate PD10 column with ~25ml 20 mM HEPES, 0.25M NaCl pH <u>7.9</u> (Kircheis et al., 1997).
- ❑ Add Ab-SPDP mix to column and collect in 1 ml fractions.
- ❑ Measure A_{280} to find Ab

1	2	3	4	5	6	7	8

1	2	3	4	5	6	7	8

- ❑ Pool fractions containing Ab and measure A_{280} *(important, use other means if interference exists)*.

$$c = \frac{A_{280}}{1.35} = \frac{\qquad}{1.35} = \qquad mg/ml \; m = c \cdot V = \qquad \cdot \qquad = [\qquad mg]$$

(M-L had 4.6 mg left out of 5.5 mg here)

- ❑ Concentrate using Agilent spin concentrator with 100 kDa cut-off to ensure concentration > 1.5 mg/ml (*2.0 mg/ml is good, M-L had 1.8 mg/ml last time*). $V \leq \frac{mg}{mg/ml} =$
- ❑ Final V_{Ab} =

- **Ab-PEI conjugation** *in 3 different ratios (all in 20 mM HEPES 0.25M NaCl, pH 7.9, 1 mM EDTA (protects conjugation; Kircheis et al., 1997)* → three conjugates, to see which ratios give most specific transfection and best recovery of conjugate.

  - Mix all the Ab-PDP that is left with PEI-SH in a 2:1 mole ratio in a 5 ml tube.

    $m_{PEI} = n_{PEI} \cdot MW_{PEI} = (2 \cdot n_{Ab}) \cdot 25000 g/mol = 50000 \cdot n_{Ab} =$

    $= 50000 \cdot \frac{m_{Ab}}{150000 g/mol} = \frac{m_{Ab}}{3} = \frac{\quad}{3} = \qquad g$

    $V_{PEI} = \frac{m_{PEI}}{\rho_{PEI}} = \frac{g}{g/l}$
  - Measure A_{343} to use as blank; ☐
  - Add 0.2 M EDTA to final concentration of 1 mM.

    $\frac{V_{EDTA}}{V_{EDTA} + V_{Ab-PEI}} = \frac{1mM}{200mM} \rightarrow V_{EDTA} = \frac{V_{Ab-PEI}}{199} = \frac{\quad}{199} =$
  - Degas 2 min and flush with N_2 gas 2 min.
  - Incubate @ RT, 24 h *(M-L did 22 h last time, this should not matter)*, gentle shaking. Start time: ☐.

Day 3 Purification of Ab-PEI conjugate

- Equilibrate PD10 column with ~25ml 20 mM HEPES, 0.25M NaCl pH 7.9 (Kircheis et al., 1997).
- Add Ab-PEI mix to column and collect in 1 ml fractions.
- Measure A_{280} *(~fractions 2-4)* and A_{343} *(~fractions 6-11)* simultaneously;

1	2	3	4	5	6	7	8

9	10	11	12

- Pool fractions containing Ab-PEI mix.
- **Cation exchange**
  - Fill syringe with start buffer, remove stopper and connect the column to the syringe (with the provided adaptor), "drop to drop" to avoid introducing air into column.
  - Remove the snap-off end at the column outlet.
  - Wash column with 4 ml of sterile dH_2O.
  - Wash column with 4 ml of 20 mM HEPES, 0.5M NaCl, pH 7.6.
  - Charge column with 4 ml 20 mM HEPES, 1M NaCl, pH 7.6.
  - Re-equilibrate column with 4 ml 20 mM HEPES, 0.5M NaCl, pH 7.6.
  - Load conjugate mixture (~7ml) onto column 3 times. Measure A_{280} of FT; _____
  - Wash column to remove unbound protein, and measure A_{280} on fractions until 0.
  - Elute with 20 mM HEPES, 1M NaCl, pH 7.6.
  - Elute with 20 mM HEPES, 2M NaCl, pH 7.6
  - Elute bound protein with 20 mM HEPES, 3M NaCl, pH 7.6

- ❑ Measure A_{280} on all fractions

	1	2	3	4	5	6
FT						
0.5 M (wash)						
1M						
2M						
3M						

M-L had 0.22 mg Ab in FT and no Ab in wash.

- ❑ Pool 2 M fractions containing Ab
- ❑ Pool 3 M fractions containing Ab.
- ❑ Wash column with 4 ml 20 mM HEPES, 0.5 M NaCl, pH 7.6.
- ❑ Wash column with 4 ml of filtered dH_20.
- ❑ Let at least 1 column volume of 20% EtOH, 0.2M sodium acetate go through column for storage.

❑ Quantify protein using $A_{280;}$

$$c = \frac{A_{280}}{1.35} = \frac{\quad}{1.35} = \qquad mg/ml\ m = c \cdot V = \qquad \cdot \qquad = [\qquad mg]$$

$$c = \frac{A_{280}}{1.35} = \frac{\quad}{1.35} = \qquad mg/ml\ m = c \cdot V = \qquad \cdot \qquad = [\qquad mg]$$

❑ Desalt Ab-PEI conjugate using an Agilent spin column with 100 kDa.

- ❑ Top up sample with salt-free HEPES, pH 7.4 (20 mM HEPES pH 7.4 w/o NaCl) up to 4 ml and centrifuge @ 2000g, 12 min → v ~ 2ml.
- ❑ Top up again to 4 ml with salt-free HEPES and centrifuge again @ 2000g, 12 min.
- ❑ Top up once more to 4 ml with salt-free HEPES and centrifuge @ 2000g, 12 min.
- ❑ Top up using 20 mM HEPES, 0.15 M NaCl, pH 7.4 and centrifuge @ 2000g, 12 min.
- ❑ Top up again using 20 mM HEPES, 0.15 M NaCl, pH 7.4 and centrifuge @ 2000g, 12 min.
- ❑ Top up again using 20 mM HEPES, 0.15 M NaCl, pH 7.4 and centrifuge @ 2000g, 25 min. (total 6 spins) → v ~ 200-500 ul (depending on quantity recovered of conjugate, don't let c > 3 mg/ml protein.

❑ Quantify protein using $A_{280;}$ for both 2M and 3M pools;

$$c = \frac{A_{280}}{1.35} \cdot DF = \frac{\quad}{1.35} \cdot \frac{\quad}{\quad} = \qquad mg/ml\ m = c \cdot V = \qquad \cdot \qquad = [\qquad mg]$$

$$c = \frac{A_{280}}{1.35} \cdot DF = \frac{\quad}{1.35} \cdot \frac{\quad}{\quad} = \qquad mg/ml\ m = c \cdot V = \qquad \cdot \qquad = [\qquad mg]$$

❑ Freeze-dry conjugate in 20 µg aliquots.

CHAPTER 8: BIBLIOGRAPHY

ACTON, S., RIGOTTI, A., LANDSCHULZ, K. T., XU, S., HOBBS, H. H. & KRIEGER, M. 1996. Identification of scavenger receptor SR-BI as a high density lipoprotein receptor. *Science,* 271*,* 518-20.

ACTON, S. L., SCHERER, P. E., LODISH, H. F. & KRIEGER, M. 1994. Expression cloning of SR-BI, a CD36-related class B scavenger receptor. *J Biol Chem,* 269*,* 21003-9.

ADAMS, R. A., BAUER, J., FLICK, M. J., SIKORSKI, S. L., NURIEL, T., LASSMANN, H., DEGEN, J. L. & AKASSOGLOU, K. 2007. The fibrin-derived gamma377-395 peptide inhibits microglia activation and suppresses relapsing paralysis in central nervous system autoimmune disease. *J Exp Med,* 204*,* 571-82.

AIHARA, N., TANNO, H., HALL, J. J., PITTS, L. H. & NOBLE, L. J. 1994. Immunocytochemical localization of immunoglobulins in the rat brain: relationship to the blood-brain barrier. *J Comp Neurol,* 342*,* 481-96.

AJAMI, B., BENNETT, J. L., KRIEGER, C., TETZLAFF, W. & ROSSI, F. M. 2007. Local self-renewal can sustain CNS microglia maintenance and function throughout adult life. *Nat Neurosci,* 10*,* 1538-43.

AKAMATSU, W., OKANO, H. J., OSUMI, N., INOUE, T., NAKAMURA, S., SAKAKIBARA, S., MIURA, M., MATSUO, N., DARNELL, R. B. & OKANO, H. 1999. Mammalian ELAV-like neuronal RNA-binding proteins HuB and HuC promote neuronal development in both the central and the peripheral nervous systems. *Proc Natl Acad Sci U S A,* 96*,* 9885-90.

ALARCON, R., FUENZALIDA, C., SANTIBANEZ, M. & VON BERNHARDI, R. 2005. Expression of scavenger receptors in glial cells - Comparing the adhesion of astrocytes and microglia from neonatal rats to surface-bound beta-amyloid. *Journal of Biological Chemistry,* 280*,* 30406-30415.

ALBANESI, M. & DAERON, M. 2012. The interactions of therapeutic antibodies with Fc receptors. *Immunol Lett,* 143*,* 20-7.

ALBERTS, B., JOHNSON, A., LEWIS, J., RAFF, M., ROBERTS, K. & WALTER, P. 2008. *Molecular biology of the cell,* New York, Garland Sicience, Taylor & Francis Group.

ALOISI, F. 2001. Immune function of microglia. *Glia,* 36*,* 165-79.

ALOISI, F., RIA, F., PENNA, G. & ADORINI, L. 1998. Microglia are more efficient than astrocytes in antigen processing and in Th1 but not Th2 cell activation. *J Immunol,* 160*,* 4671-80.

ANDERSON, A. C., ANDERSON, D. E., BREGOLI, L., HASTINGS, W. D., KASSAM, N., LEI, C., CHANDWASKAR, R., KARMAN, J., SU, E. W., HIRASHIMA, M., BRUCE, J. N., KANE, L. P., KUCHROO, V. K. & HAFLER, D. A. 2007. Promotion of tissue inflammation by the immune receptor Tim-3 expressed on innate immune cells. *Science,* 318*,* 1141-3.

ARAQUE, A. & NAVARRETE, M. 2010. Glial cells in neuronal network function. *Philos Trans R Soc Lond B Biol Sci,* 365*,* 2375-81.

ARAVALLI, R. N., HU, S. & LOKENSGARD, J. R. 2008. Inhibition of toll-like receptor signaling in primary murine microglia. *J Neuroimmune Pharmacol,* 3*,* 5-11.

ASCHNER, M. 2000. Neuron-astrocyte interactions: implications for cellular energetics and antioxidant levels. *Neurotoxicology,* 21*,* 1101-7.

ASKJAER, P., GALY, V., HANNAK, E. & MATTAJ, I. W. 2002. Ran GTPase cycle and importins alpha and beta are essential for spindle formation and nuclear envelope assembly in living Caenorhabditis elegans embryos. *Molecular Biology of the Cell,* 13*,* 4355-4370.

BABITT, J., TRIGATTI, B., RIGOTTI, A., SMART, E. J., ANDERSON, R. G., XU, S. & KRIEGER, M. 1997. Murine SR-BI, a high density lipoprotein receptor that mediates selective lipid uptake, is N-glycosylated and fatty acylated and colocalizes with plasma membrane caveolae. *Journal of Biological Chemistry,* 272*,* 13242-13249.

BACKOS, D. S., FRANKLIN, C. C. & REIGAN, P. 2012. The role of glutathione in brain tumor drug resistance. *Biochem Pharmacol,* 83*,* 1005-12.

BADOER, E. 2010. Microglia: activation in acute and chronic inflammatory states and in response to cardiovascular dysfunction. *Int J Biochem Cell Biol,* 42*,* 1580-5.

BALAZS, Z., PANZENBOECK, U., HAMMER, A., SOVIC, A., QUEHENBERGER, O., MALLE, E. & SATTLER, W. 2004. Uptake and transport of high-density lipoprotein (HDL) and HDL-associated alpha-tocopherol by an in vitro blood-brain barrier model. *J Neurochem,* 89*,* 939-50.

BALCAITIS, S., WEINSTEIN, J. R., LI, S., CHAMBERLAIN, J. S. & MOLLER, T. 2005. Lentiviral transduction of microglial cells. *Glia,* 50*,* 48-55.

BALICKI, D., REISFELD, R. A., PERTL, U., BEUTLER, E. & LODE, H. N. 2000. Histone H2A-mediated transient cytokine gene delivery induces efficient antitumor responses in murine neuroblastoma. *Proc Natl Acad Sci U S A,* 97*,* 11500-4.

BANATI, R. B., GEHRMANN, J., SCHUBERT, P. & KREUTZBERG, G. W. 1993. Cytotoxicity of microglia. *Glia,* 7*,* 111-8.

BARANOVA, I., VISHNYAKOVA, T., BOCHAROV, A., CHEN, Z., REMALEY, A. T., STONIK, J., EGGERMAN, T. L. & PATTERSON, A. P. 2002. Lipopolysaccharide down regulates both scavenger receptor B1 and ATP binding cassette transporter A1 in RAW cells. *Infect Immun,* 70*,* 2995-3003.

BARATI, S., CHEGINI, F., HURTADO, P. & RUSH, R. A. 2002. Hybrid tetanus toxin C fragment-diphtheria toxin translocation domain allows specific gene transfer into PC12 cells. *Exp Neurol,* 177*,* 75-87.

BARATI, S., HURTADO, P. R., ZHANG, S. H., TINSLEY, R., FERGUSON, I. A. & RUSH, R. A. 2006. GDNF gene delivery via the p75(NTR) receptor rescues injured motor neurons. *Experimental Neurology,* 202*,* 179-188.

BARGER, S. W., GOODWIN, M. E., PORTER, M. M. & BEGGS, M. L. 2007. Glutamate release from activated microglia requires the oxidative burst and lipid peroxidation. *J Neurochem,* 101*,* 1205-13.

BASS, N. H., HESS, H. H., POPE, A. & THALHEIMER, C. 1971. Quantitative cytoarchitectonic distribution of neurons, glia, and DNa in rat cerebral cortex. *J Comp Neurol,* 143*,* 481-90.

BATCHELOR, P. E., LIBERATORE, G. T., WONG, J. Y., PORRITT, M. J., FRERICHS, F., DONNAN, G. A. & HOWELLS, D. W. 1999. Activated macrophages and microglia induce dopaminergic sprouting in the injured striatum and

express brain-derived neurotrophic factor and glial cell line-derived neurotrophic factor. *J Neurosci,* 19*,* 1708-16.

BATCHELOR, P. E., PORRITT, M. J., MARTINELLO, P., PARISH, C. L., LIBERATORE, G. T., DONNAN, G. A. & HOWELLS, D. W. 2002. Macrophages and Microglia Produce Local Trophic Gradients That Stimulate Axonal Sprouting Toward but Not beyond the Wound Edge. *Mol Cell Neurosci,* 21*,* 436-53.

BATTISTA, D., FERRARI, C. C., GAGE, F. H. & PITOSSI, F. J. 2006. Neurogenic niche modulation by activated microglia: transforming growth factor beta increases neurogenesis in the adult dentate gyrus. *Eur J Neurosci,* 23*,* 83-93.

BAUER, M., KRISTENSEN, B. W., MEYER, M., GASSER, T., WIDMER, H. R., ZIMMER, J. & UEFFING, M. 2006. Toxic effects of lipid-mediated gene transfer in ventral mesencephalic explant cultures. *Basic Clin Pharmacol Toxicol,* 98*,* 395-400.

BECHMANN, I., KWIDZINSKI, E., KOVAC, A. D., SIMBURGER, E., HORVATH, T., GIMSA, U., DIRNAGL, U., PRILLER, J. & NITSCH, R. 2001. Turnover of rat brain perivascular cells. *Exp Neurol,* 168*,* 242-9.

BERGEN, J. M. & PUN, S. H. 2007. Evaluation of an LC8-binding peptide for the attachment of artificial cargo to dynein. *Mol Pharm,* 4*,* 119-28.

BERHANU, D. A. & RUSH, R. A. 2008. Targeted silencing of TrkA expression in rat forebrain neurons via the p75 receptor *Neuroscience,* 153 1115-1125.

BESSIS, A., BECHADE, C., BERNARD, D. & ROUMIER, A. 2007. Microglial control of neuronal death and synaptic properties. *Glia,* 55*,* 233-8.

BHAT, N. R. & FAN, F. 2002. Adenovirus infection induces microglial activation: involvement of mitogen-activated protein kinase pathways. *Brain Res,* 948*,* 93-101.

BIBER, K., NEUMANN, H., INOUE, K. & BODDEKE, H. W. 2007. Neuronal 'On' and 'Off' signals control microglia. *Trends Neurosci,* 30*,* 596-602.

BIEBER, T., MEISSNER, W., KOSTIN, S., NIEMANN, A. & ELSASSER, H. P. 2002. Intracellular route and transcriptional competence of polyethylenimine-DNA complexes. *J Control Release,* 82*,* 441-54.

BIFFI, A., DE PALMA, M., QUATTRINI, A., DEL CARRO, U., AMADIO, S., VISIGALLI, I., SESSA, M., FASANO, S., BRAMBILLA, R., MARCHESINI, S., BORDIGNON, C. & NALDINI, L. 2004. Correction of metachromatic leukodystrophy in the mouse model by transplantation of genetically modified hematopoietic stem cells. *J Clin Invest,* 113*,* 1118-29.

BLANCHARD, E., BELOUZARD, S., GOUESLAIN, L., WAKITA, T., DUBUISSON, J., WYCHOWSKI, C. & ROUILLE, Y. 2006. Hepatitis C virus entry depends on clathrin-mediated endocytosis. *J Virol,* 80*,* 6964-72.

BLASCHKE, A. J., STALEY, K. & CHUN, J. 1996. Widespread programmed cell death in proliferative and postmitotic regions of the fetal cerebral cortex. *Development,* 122*,* 1165-74.

BLESSING, T., KURSA, M., HOLZHAUSER, R., KIRCHEIS, R. & WAGNER, E. 2001. Different strategies for formation of PEGylated EGF-conjugated PEI/DNA Complexes for targeted gene delivery. *Bioconjugate Chemistry,* 12 529-537.

BLESSING, T., REMY, J. S. & BEHR, J. P. 1998. Monomolecular collapse of plasmid DNA into stable virus-like particles. *Proc Natl Acad Sci U S A,* 95*,* 1427-31.

BOCKSTAEL, O., CHTARTO, A., WAKKINEN, J., YANG, X., MELAS, C., LEVIVIER, M., BROTCHI, J. & TENENBAUM, L. 2008. Differential transgene expression profiles in rat brain, using rAAV2/1 vectors with tetracycline-inducible and cytomegalovirus promoters. *Human gene therapy,* 19*,* 1293-1305.

BOECKLE, S., VON GERSDORFF, K., VAN DER PIEPEN, S., CULMSEE, C., WAGNER, E. & OGRIS, M. 2004. Purification of polyethylenimine polyplexes highlights the role of free polycations in gene transfer. *Journal of Gene Medicine,* 6*,* 1102-1111.

BOOK, A. A., WILEY, R. G. & SCHWEITZER, J. B. 1992. Specificity of 192 IgG-saporin for NGF receptor-positive cholinergic basal forebrain neurons in the rat. *Brain Res,* 590*,* 350-5.

BOUSSIF, O., LEZOUALCH, F., ZANTA, M. A., MERGNY, M. D., SCHERMAN, D., DEMENEIX, B. & BEHR, J. P. 1995. A Versatile Vector for Gene and Oligonucleotide Transfer Into Cells in Culture and In-Vivo - Polyethylenimine. *Proceedings of the National Academy of Sciences of the United States of America,* 92*,* 7297-7301.

BOUTIN, C., DIESTEL, S., DESOEUVRE, A., TIVERON, M. C. & CREMER, H. 2008. Efficient in vivo electroporation of the postnatal rodent forebrain. *PLoS One,* 3*,* e1883.

BRADFORD, J., SHIN, J. Y., ROBERTS, M., WANG, C. E., LI, X. J. & LI, S. 2009. Expression of mutant huntingtin in mouse brain astrocytes causes age-dependent neurological symptoms. *Proc Natl Acad Sci U S A,* 106*,* 22480-5.

BRANDENBURG, L. O., KOCH, T., SIEVERS, J. & LUCIUS, R. 2007. Internalization of PrP106-126 by the formyl-peptide-receptor-like-1 in glial cells. *J Neurochem,* 101*,* 718-28.

BRENNER, M., KISSEBERTH, W. C., SU, Y., BESNARD, F. & MESSING, A. 1994. Gfap Promoter Directs Astrocyte-Specific Expression in Transgenic Mice. *Journal of Neuroscience,* 14*,* 1030-1037.

BREUNIG, M., HOZSA, C., LUNGWITZ, U., WATANABE, K., UMEDA, I., KATO, H. & GOEPFERICH, A. 2008. Mechanistic investigation of poly(ethylene imine)-based siRNA delivery: disulfide bonds boost intracellular release of the cargo. *J Control Release,* 130*,* 57-63.

BRIGHTMAN, M. W. & REESE, T. S. 1969. Junctions between intimately apposed cell membranes in the vertebrate brain. *J Cell Biol,* 40*,* 648-77.

BROWNE, S. E., LIN, L., MATTSSON, A., GEORGIEVSKA, B. & ISACSON, O. 2001. Selective antibody-induced cholinergic cell and synapse loss produce sustained hippocampal and cortical hypometabolism with correlated cognitive deficits. *Exp Neurol,* 170*,* 36-47.

BUECHLER, C., RITTER, M., QUOC, C. D., AGILDERE, A. & SCHMITZ, G. 1999. Lipopolysaccharide inhibits the expression of the scavenger receptor Cla-1 in human monocytes and macrophages. *Biochem Biophys Res Commun,* 262*,* 251-4.

BURUDI, E. M., RIESE, S., STAHL, P. D. & REGNIER-VIGOUROUX, A. 1999. Identification and functional characterization of the mannose receptor in astrocytes. *Glia,* 25*,* 44-55.

BUSHONG, E. A., MARTONE, M. E., JONES, Y. Z. & ELLISMAN, M. H. 2002. Protoplasmic astrocytes in CA1 stratum radiatum occupy separate anatomical domains. *J Neurosci,* 22*,* 183-92.

BUSS, R. R., SUN, W. & OPPENHEIM, R. W. 2006. Adaptive roles of programmed cell death during nervous system development. *Annu Rev Neurosci,* 29*,* 1-35.

BUTCHI, N. B., DU, M. & PETERSON, K. E. 2010. Interactions between TLR7 and TLR9 agonists and receptors regulate innate immune responses by astrocytes and microglia. *Glia,* 58*,* 650-64.

CAI, L., JI, A., DE BEER, F. C., TANNOCK, L. R. & VAN DER WESTHUYZEN, D. R. 2008. SR-BI protects against endotoxemia in mice through its roles in glucocorticoid production and hepatic clearance. *J Clin Invest,* 118*,* 364-75.

CALDERO, J., BRUNET, N., CIUTAT, D., HEREU, M. & ESQUERDA, J. E. 2009. Development of microglia in the chick embryo spinal cord: implications in the regulation of motoneuronal survival and death. *J Neurosci Res,* 87*,* 2447-66.

CALVO, D., GOMEZ-CORONADO, D., LASUNCION, M. A. & VEGA, M. A. 1997. CLA-1 is an 85-kD plasma membrane glycoprotein that acts as a high-affinity receptor for both native (HDL, LDL, and VLDL) and modified (OxLDL and AcLDL) lipoproteins. *Arterioscler Thromb Vasc Biol,* 17*,* 2341-9.

CALVO, D. & VEGA, M. A. 1993. Identification, primary structure, and distribution of CLA-1, a novel member of the CD36/LIMPII gene family. *J Biol Chem,* 268*,* 18929-35.

CARDONA, A. E., PIORO, E. P., SASSE, M. E., KOSTENKO, V., CARDONA, S. M., DIJKSTRA, I. M., HUANG, D., KIDD, G., DOMBROWSKI, S., DUTTA, R., LEE, J. C., COOK, D. N., JUNG, S., LIRA, S. A., LITTMAN, D. R. & RANSOHOFF, R. M. 2006. Control of microglial neurotoxicity by the fractalkine receptor. *Nat Neurosci,* 9*,* 917-24.

CARLSSON, J., DREVIN, H. & AX,N, R. 1978. Protein thiolation and reversible protein-protein conjugation. N-Succinimidyl 3-(2-pyridyldithio)propionate, a new heterobifunctional reagent. *The Biochemical Journal,* 173 723-737.

CEPKO, C. L., AUSTIN, C. P., YANG, X., ALEXIADES, M. & EZZEDDINE, D. 1996. Cell fate determination in the vertebrate retina. *Proc Natl Acad Sci U S A,* 93*,* 589-95.

CHAN, C. K. & JANS, D. A. 2001. Enhancement of MSH receptor- and GAL4-mediated gene transfer by switching the nuclear import pathway. *Gene Therapy,* 8*,* 166-171.

CHAN, W. Y., KOHSAKA, S. & REZAIE, P. 2007. The origin and cell lineage of microglia: new concepts. *Brain Res Rev,* 53*,* 344-54.

CHANG LING, T. & STONE, J. 1991. Factors determining the morphology and distribution of astrocytes in the cat retina: a 'contact-spacing' model of astrocyte interaction. *J Comp Neurol,* 303*,* 387-99.

CHAO, C. C., HU, S., MOLITOR, T. W., SHASKAN, E. G. & PETERSON, P. K. 1992. Activated microglia mediate neuronal cell injury via a nitric oxide mechanism. *J Immunol,* 149*,* 2736-41.

CHASTAIN, E. M., DUNCAN, D. S., RODGERS, J. M. & MILLER, S. D. 2011. The role of antigen presenting cells in multiple sclerosis. *Biochim Biophys Acta,* 1812*,* 265-74.

CHEN, H., MCCARTY, D. M., BRUCE, A. T. & SUZUKI, K. 1998a. Gene transfer and expression in oligodendrocytes under the control of myelin basic protein transcriptional control region mediated by adeno-associated virus. *Gene Ther,* 5*,* 50-8.

CHEN, J., GAMOU, S., TAKAYANAGI, A., OHTAKE, Y., OHTSUBO, M. & SHIMIZU, N. 1998b. Receptor-mediated gene delivery using FAb fragments of anti-epidermal growth factor receptor antibodies: Improved immunogene approach. *Cancer gene therapy,* 5*,* 357-364.

CHEN, J. B., GAMOU, S., TAKAYANAGI, A. & SHIMIZU, N. 1994. A Novel Gene Delivery System Using Egf Receptor-Mediated Endocytosis. *Febs Letters,* 338*,* 167-169.

CHEN, Z. Y., YANT, S. R., HE, C. Y., MEUSE, L., SHEN, S. & KAY, M. A. 2001. Linear DNAs concatemerize in vivo and result in sustained transgene expression in mouse liver. *Mol Ther,* 3*,* 403-10.

CHINETTI, G., GBAGUIDI, F. G., GRIGLIO, S., MALLAT, Z., ANTONUCCI, M., POULAIN, P., CHAPMAN, J., FRUCHART, J. C., TEDGUI, A., NAJIB-FRUCHART, J. & STAELS, B. 2000. CLA-1/SR-BI is expressed in atherosclerotic lesion macrophages and regulated by activators of peroxisome proliferator-activated receptors. *Circulation,* 101*,* 2411-7.

CHIOU, H., TANGCO, S., LEVINE, S., ROBERTSON, D., KORMIS, K., WU, C. H. & WU, G. Y. 1994. Enhanced resistance to nuclease degradation of nucleic acids complexed to asia-glycoprotein-polylysine carriers. *Nucleic Acids Research,* 22 5439-5446.

CHO, Y. W., KIM, J. D. & PARK, K. 2003. Polycation gene delivery systems: escape from endosomes to cytosol. *J Pharm Pharmacol,* 55*,* 721-34.

CHOI, Y. H., LIU, F., CHOI, J. S., KIM, S. W. & PARK, J. S. 1999. Characterization of a Targeted Gene Carrier, Lactose-Polyethylene Glycol-Grafted Poly-L-Lysine, and Its Complex with Plasmid DNA. *Human Gene Therapy,* 10 2657-2665.

CHOI, Y. R., CHAE, S. Y., AHN, C. H., LEE, M., OH, S., BYUN, Y., RHEE, B. D. & KO, K. S. 2007. Development of polymeric gene delivery carriers: PEGylated copolymers of L-lysine and L-phenylalanine. *Journal of Drug Targeting,* 15*,* 391-398.

CHURNEY, L. 1942. The osmotic properties of the nucleus. *The Biological Bulletin,* 82*,* 52-67.

COHEN, S. 1960. Purification of a Nerve-Growth Promoting Protein from the Mouse Salivary Gland and Its Neuro-Cytotoxic Antiserum. *Proc Natl Acad Sci U S A,* 46*,* 302-11.

COHEN, S. N., CHANG, A. C., BOYER, H. W. & HELLING, R. B. 1973. Construction of biologically functional bacterial plasmids in vitro. *Proc Natl Acad Sci U S A,* 70*,* 3240-4.

COLLINS, E., BIRCHALL, J. C., WILLIAMS, J. L. & GUMBLETON, M. 2007. Nuclear localisation and pDNA condensation in non-viral gene delivery. *J Gene Med,* 9*,* 265-74.

CONNELLY, M. A., KELLNER-WEIBEL, G., ROTHBLAT, G. H. & WILLIAMS, D. L. 2003. SR-BI-directed HDL-cholesteryl ester hydrolysis. *J Lipid Res,* 44*,* 331-41.

CORSO, T. D., TORRES, G., GOULAH, C., ROY, I., GAMBINO, A. S., NAYDA, J., BUCKLEY, T., STACHOWIAK, E. K., BERGEY, E. J., PUDAVAR, H., DUTTA, P., BLOOM, D. C., BOWERS, W. J. & STACHOWIAK, M. K. 2005. Assessment of viral and non-viral gene transfer into adult rat brains using HSV-1, calcium phosphate and PEI-based methods. *Folia Morphol (Warsz),* 64*,* 130-44.

COWAN, W. M., FAWCETT, J. W., O'LEARY, D. D. & STANFIELD, B. B. 1984. Regressive events in neurogenesis. *Science,* 225*,* 1258-65.

CUCCHIARINI, M., REN, X. L., PERIDES, G. & TERWILLIGER, E. F. 2003. Selective gene expression in brain microglia mediated via adeno-associated virus type 2 and type 5 vectors. *Gene Ther,* 10*,* 657-67.

CUNNINGHAM, C., WILCOCKSON, D. C., CAMPION, S., LUNNON, K. & PERRY, V. H. 2005. Central and systemic endotoxin challenges exacerbate the local inflammatory response and increase neuronal death during chronic neurodegeneration. *J Neurosci,* 25*,* 9275-84.

CURIEL, D. T., AGARWAL, S., WAGNER, E. & COTTEN, M. 1991. Adenovirus enhancement of transferrin-polylysine-mediated gene delivery. *Proc Natl Acad Sci U S A,* 88*,* 8850-4.

D'MELLO, C., LE, T. & SWAIN, M. G. 2009. Cerebral microglia recruit monocytes into the brain in response to tumor necrosis factoralpha signaling during peripheral organ inflammation. *J Neurosci,* 29*,* 2089-102.

DALMAU, I., VELA, J. M., GONZALEZ, B., FINSEN, B. & CASTELLANO, B. 2003. Dynamics of microglia in the developing rat brain. *J Comp Neurol,* 458*,* 144-57.

DANBOLT, N. C. 2001. Glutamate uptake. *Prog Neurobiol,* 65*,* 1-105.

DAO THI, V. L., DREUX, M. & COSSET, F. L. 2011. Scavenger receptor class B type I and the hypervariable region-1 of hepatitis C virus in cell entry and neutralisation. *Expert Rev Mol Med,* 13*,* e13.

DAS, P., HOWARD, V., LOOSBROCK, N., DICKSON, D., MURPHY, M. P. & GOLDE, T. E. 2003. Amyloid-beta immunization effectively reduces amyloid deposition in FcRgamma-/- knock-out mice. *J Neurosci,* 23*,* 8532-8.

DAVOUST, N., VUAILLAT, C., ANDRODIAS, G. & NATAF, S. 2008. From bone marrow to microglia: barriers and avenues. *Trends Immunol,* 29*,* 227-34.

DE SIMONE, R., AJMONE-CAT, M. A., CARNEVALE, D. & MINGHETTI, L. 2005. Activation of alpha7 nicotinic acetylcholine receptor by nicotine selectively up-regulates cyclooxygenase-2 and prostaglandin E2 in rat microglial cultures. *Journal of neuroinflammation,* 2*,* 4.

DE VRIES, G. H. & BOULLERNE, A. I. 2010. Glial cell lines: an overview. *Neurochem Res,* 35*,* 1978-2000.

DE VRY, J., MARTINEZ-MARTINEZ, P., LOSEN, M., TEMEL, Y., STECKLER, T., STEINBUSCH, H. W., DE BAETS, M. H. & PRICKAERTS, J. 2010. In vivo

electroporation of the central nervous system: a non-viral approach for targeted gene delivery. *Prog Neurobiol,* 92*,* 227-44.

DEAN, D. A., DEAN, B. S., MULLER, S. & SMITH, L. C. 1999. Sequence requirements for plasmid nuclear import. *Exp Cell Res,* 253*,* 713-22.

DÉAS, O., ANGEVIN, E., CHERBONNIER, C., SENIK, A., CHARPENTIER, B., LEVILLAIN, J. P., OOSTERWIJK, E., HIRSCH, F. & DURRBACH, A. 2002. In vivo-targeted gene delivery using antibody-based nonviral vector. *Human Gene Therapy,* 13*,* 1101-1114.

DEL-RIO HORTEGA, P. 1932, ' Microglia, 'in: PENFIELD, W. (ed.) *Cytology and cellular pathology of the nervous system,* Paul B. Hoeber, New York, pp. 481-534

DEL BIGIO, M. R. 2010. Ependymal cells: biology and pathology. *Acta Neuropathol,* 119*,* 55-73.

DENES, A., THORNTON, P., ROTHWELL, N. J. & ALLAN, S. M. 2010. Inflammation and brain injury: acute cerebral ischaemia, peripheral and central inflammation. *Brain Behav Immun,* 24*,* 708-23.

DENG, J. Z., SUN, Y. X., WANG, H. Y., LI, C., HUANG, F. W., CHENG, S. X., ZHUO, R. X. & ZHANG, X. Z. 2011. Poly(beta-amino amine) cross-linked PEIs as highly efficient gene vectors. *Acta Biomater,* 7*,* 2200-8.

DERMIETZEL, R., HERTBERG, E. L., KESSLER, J. A. & SPRAY, D. C. 1991. Gap junctions between cultured astrocytes: immunocytochemical, molecular, and electrophysiological analysis. *J Neurosci,* 11*,* 1421-32.

DONG, P., XIE, T., ZHOU, X., HU, W., CHEN, Y., DUAN, Y., LI, X. & HAN, J. 2011. Induction of macrophage scavenger receptor type BI expression by tamoxifen and 4-hydroxytamoxifen. *Atherosclerosis,* 218*,* 435-42.

DOUGLAS, K. L. 2008. Toward development of artificial viruses for gene therapy: a comparative evaluation of viral and non-viral transfection. *Biotechnol Prog,* 24*,* 871-83.

DRINGEN, R., GUTTERER, J. M. & HIRRLINGER, J. 2000. Glutathione metabolism in brain metabolic interaction between astrocytes and neurons in the defense against reactive oxygen species. *Eur J Biochem,* 267*,* 4912-6.

DUAN, Y., ZHENG, J., HAN, S., WU, Y., WANG, Y., LI, D., KONG, D. & YU, Y. 2008. A tumor targeted gene vector modified with G250 monoclonal antibody for gene therapy. *J Control Release,* 127*,* 173-9.

EGUCHI, A., FURUSAWA, H., YAMAMOTO, A., AKUTA, T., HASEGAWA, M., OKAHATA, Y. & NAKANISHI, M. 2005. Optimization of nuclear localization signal for nuclear transport of DNA-encapsulating particles. *J Control Release,* 104*,* 507-19.

EMERY, B. 2010. Regulation of oligodendrocyte differentiation and myelination. *Science,* 330*,* 779-82.

ENDOH, T. & OHTSUKI, T. 2009. Cellular siRNA delivery using cell-penetrating peptides modified for endosomal escape. *Adv Drug Deliv Rev,* 61*,* 704-9.

ENG, L. F., VANDERHAEGHEN, J. J., BIGNAMI, A. & GERSTL, B. 1971. An acidic protein isolated from fibrous astrocytes. *Brain Res,* 28*,* 351-4.

ESCRIOU, V., CARRIERE, M., BUSSONE, F., WILS, P. & SCHERMAN, D. 2001. Critical assessment of the nuclear import of plasmid during cationic lipid-mediated gene transfer. *J Gene Med,* 3*,* 179-87.

FABRE, J. W. & COLLINS, L. 2006. Synthetic peptides as non-viral DNA vectors. *Current Gene Therapy,* 6*,* 459-480.

FARRELL, L. L., PEPIN, J., KUCHARSKI, C., LIN, X., XU, Z. & ULUDAG, H. 2007. A comparison of the effectiveness of cationic polymers poly-L-lysine (PLL) and polyethylenimine (PEI) for non-viral delivery of plasmid DNA to bone marrow stromal cells (BMSC). *Eur J Pharm Biopharm,* 65*,* 388-97.

FENG, L., GUO, M., ZHANG, S., CHU, J. & ZHUANG, Y. 2008. Improvement in the suspension-culture production of recombinant adeno-associated virus-LacZ in HEK-293 cells using polyethyleneimine-DNA complexes in combination with hypothermic treatment. *Biotechnol Appl Biochem,* 50*,* 121-32.

FENG, M., LEE, D. & LI, P. 2006. Intracellular uptake and release of poly(ethyleneimine)-co-poly(methyl methacrylate) nanoparticle/pDNA complexes for gene delivery. *Int J Pharm,* 311*,* 209-14.

FENG, Y., VAN ECK, M., VAN CRAEYVELD, E., JACOBS, F., CARLIER, V., VAN LINTHOUT, S., ERDEL, M., TJWA, M. & DE GEEST, B. 2009. Critical role of scavenger receptor-BI-expressing bone marrow-derived endothelial progenitor cells in the attenuation of allograft vasculopathy after human apo A-I transfer. *Blood,* 113*,* 755-64.

FERRARI, C. C. & TARELLI, R. 2011. Parkinson's disease and systemic inflammation. *Parkinsons Dis,* 2011*,* 436813.

FERRER, I., BERNET, E., SORIANO, E., DEL RIO, T. & FONSECA, M. 1990. Naturally occurring cell death in the cerebral cortex of the rat and removal of dead cells by transitory phagocytes. *Neuroscience,* 39*,* 451-8.

FISHMAN, D. M. & PATTERSON, G. D. 1996. Light scattering studies of supercoiled and nicked DNA. *Biopolymers,* 38*,* 535-52.

FLARIS, N. A., DENSMORE, T. L., MOLLESTON, M. C. & HICKEY, W. F. 1993. Characterization of microglia and macrophages in the central nervous system of rats: definition of the differential expression of molecules using standard and novel monoclonal antibodies in normal CNS and in four models of parenchymal reaction. *Glia,* 7*,* 34-40.

FLODEN, A. M., LI, S. & COMBS, C. K. 2005. Beta-amyloid-stimulated microglia induce neuron death via synergistic stimulation of tumor necrosis factor alpha and NMDA receptors. *J Neurosci,* 25*,* 2566-75.

FLOYD, C. L., RZIGALINSKI, B. A., SITTERDING, H. A., WILLOUGHBY, K. A. & ELLIS, E. F. 2004. Antagonism of group I metabotropic glutamate receptors and PLC attenuates increases in inositol trisphosphate and reduces reactive gliosis in strain-injured astrocytes. *Journal of Neurotrauma,* 21*,* 205-216.

FLUITER, K., VAN DER WESTHUIJZEN, D. R. & VAN BERKEL, T. J. 1998. In vivo regulation of scavenger receptor BI and the selective uptake of high density lipoprotein cholesteryl esters in rat liver parenchymal and Kupffer cells. *J Biol Chem,* 273*,* 8434-8.

FORD, A. L., FOULCHER, E., LEMCKERT, F. A. & SEDGWICK, J. D. 1996. Microglia induce CD4 T lymphocyte final effector function and death. *J Exp Med,* 184*,* 1737-45.

FORREST, M. L. & PACK, D. W. 2002. On the kinetics of polyplex endocytic trafficking: implications for gene delivery vector design. *Mol Ther,* 6*,* 57-66.

FRADE, J. M. & BARDE, Y. A. 1998. Microglia-derived nerve growth factor causes cell death in the developing retina. *Neuron,* 20*,* 35-41.

FRANCO, L., BODRATO, N., MORESCHI, I., USAI, C., BRUZZONE, S., SCARF I, S., ZOCCHI, E. & DE FLORA, A. 2006. Cyclic ADP-ribose is a second messenger in the lipopolysaccharide-stimulated activation of murine N9 microglial cell line. *J Neurochem,* 99*,* 165-76.

FRANK, M. G., BARRIENTOS, R. M., BIEDENKAPP, J. C., RUDY, J. W., WATKINS, L. R. & MAIER, S. F. 2006. mRNA up-regulation of MHC II and pivotal pro-inflammatory genes in normal brain aging. *Neurobiol Aging,* 27*,* 717-22.

FRANKE, W. W., SCHEER, U., KROHNE, G. & JARASCH, E. D. 1981. The nuclear envelope and the architecture of the nuclear periphery. *J Cell Biol,* 91*,* 39s-50s.

FRAU, L., BORSINI, F., WARDAS, J., KHAIRNAR, A. S., SCHINTU, N. & MORELLI, M. 2011. Neuroprotective and anti-inflammatory effects of the adenosine A(2A) receptor antagonist ST1535 in a MPTP mouse model of Parkinson's disease. *Synapse,* 65*,* 181-8.

FRICK, M., BRIGHT, N. A., RIENTO, K., BRAY, A., MERRIFIED, C. & NICHOLS, B. J. 2007. Coassembly of flotillins induces formation of membrane microdomains, membrane curvature, and vesicle budding. *Curr Biol,* 17*,* 1151-6.

FURUYA, T., TANAKA, R., URABE, T., HAYAKAWA, J., MIGITA, M., SHIMADA, T., MIZUNO, Y. & MOCHIZUKI, H. 2003. Establishment of modified chimeric mice using GFP bone marrow as a model for neurological disorders. *Neuroreport,* 14*,* 629-31.

GAMO, K., KIRYU-SEO, S., KONISHI, H., AOKI, S., MATSUSHIMA, K., WADA, K. & KIYAMA, H. 2008. G-protein-coupled receptor screen reveals a role for chemokine receptor CCR5 in suppressing microglial neurotoxicity. *J Neurosci,* 28*,* 11980-8.

GARMAN, R. H. 2011. Histology of the central nervous system. *Toxicol Pathol,* 39*,* 22-35.

GASPAR, H. B., PARSLEY, K. L., HOWE, S., KING, D., GILMOUR, K. C., SINCLAIR, J., BROUNS, G., SCHMIDT, M., VON KALLE, C., BARINGTON, T., JAKOBSEN, M. A., CHRISTENSEN, H. O., AL GHONAIUM, A., WHITE, H. N., SMITH, J. L., LEVINSKY, R. J., ALI, R. R., KINNON, C. & THRASHER, A. J. 2004. Gene therapy of X-linked severe combined immunodeficiency by use of a pseudotyped gammaretroviral vector. *Lancet,* 364*,* 2181-7.

GEISSMANN, F., MANZ, M. G., JUNG, S., SIEWEKE, M. H., MERAD, M. & LEY, K. 2010. Development of monocytes, macrophages, and dendritic cells. *Science,* 327*,* 656-61.

GELLERT, M., MIZUUCHI, K., O'DEA, M. H. & NASH, H. A. 1976. DNA gyrase: an enzyme that introduces superhelical turns into DNA. *Proc Natl Acad Sci U S A,* 73*,* 3872-6.

GERACE, L. 1992. Molecular trafficking across the nuclear pore complex. *Curr Opin Cell Biol,* 4*,* 637-45.

GERMERSHAUS, O., MERDAN, T., BAKOWSKY, U., BEHE, M. & KISSEL, T. 2006. Trastuzumab-polyethylenimine-polyethylene glycol conjugates for targeting Her2-expressing tumors. *Bioconjug Chem,* 17*,* 1190-9.

GILLOTTE-TAYLOR, K., BOULLIER, A., WITZTUM, J. L., STEINBERG, D. & QUEHENBERGER, O. 2001. Scavenger receptor class B type I as a receptor for oxidized low density lipoprotein. *J Lipid Res,* 42*,* 1474-82.

GINHOUX, F., GRETER, M., LEBOEUF, M., NANDI, S., SEE, P., GOKHAN, S., MEHLER, M. F., CONWAY, S. J., NG, L. G., STANLEY, E. R., SAMOKHVALOV, I. M. & MERAD, M. 2010. Fate mapping analysis reveals that adult microglia derive from primitive macrophages. *Science,* 330*,* 841-5.

GIULIAN, D. & BAKER, T. J. 1986. Characterization of ameboid microglia isolated from developing mammalian brain. *J Neurosci,* 6*,* 2163-78.

GLENN, J. A., WARD, S. A., STONE, C. R., BOOTH, P. L. & THOMAS, W. E. 1992. Characterisation of ramified microglial cells: detailed morphology, morphological plasticity and proliferative capability. *J Anat,* 180 (Pt 1)*,* 109-18.

GLOMSET, J. A. 1968. The plasma lecithins:cholesterol acyltransferase reaction. *J Lipid Res,* 9*,* 155-67.

GLOVER, D. J., LIPPS, H. J. & JANS, D. A. 2005. Towards safe, non-viral therapeutic gene expression in humans. *Nature Reviews Genetics,* 6*,* 299-U29.

GLOVER, D. M. & HAMES, B. D. 1995. *DNA Cloning - Volume 4 - Mammalian Systems*.

GOLDSTEIN, J. L., HO, Y. K., BASU, S. K. & BROWN, M. S. 1979a. Binding site on macrophages that mediates uptake and degradation of acetylated low density lipoprotein, producing massive cholesterol deposition. *Proc Natl Acad Sci U S A,* 76*,* 333-7.

GOLDSTEIN, J. L., HO, Y. K., BASU, S. K. & BROWN, M. S. 1979b. Binding site on macrophages that mediates uptake and degradation of acetylated low density lipoprotein, producing massive cholesterol deposition. *Proceedings of the National Academy of Sciences,* 76*,* 333-337.

GORDON, S. 2003. Alternative activation of macrophages. *Nat Rev Immunol,* 3*,* 23-35.

GORLICH, D. & MATTAJ, I. W. 1996. Nucleocytoplasmic transport. *Science,* 271*,* 1513-8.

GOSSELIN, M. A., GUO, W. & LEE, R. J. 2002. Incorporation of reversibly cross-linked polyplexes into LPDII vectors for gene delivery. *Bioconjug Chem,* 13*,* 1044-53.

GOULA, D., REMY, J. S., ERBACHER, P., WASOWICZ, M., LEVI, G., ABDALLAH, B. & DEMENEIX, B. A. 1998. Size, diffusibility and transfection performance of linear PEI/DNA complexes in the mouse central nervous system. *Gene Ther,* 5*,* 712-7.

GRAEBER, M. B. & STREIT, W. J. 2010. Microglia: biology and pathology. *Acta Neuropathol,* 119*,* 89-105.

GRAEBER, M. B., TETZLAFF, W., STREIT, W. J. & KREUTZBERG, G. W. 1988. Microglial cells but not astrocytes undergo mitosis following rat facial nerve axotomy. *Neurosci Lett,* 85*,* 317-21.

GRESCH, O., ENGEL, F. B., NESIC, D., TRAN, T. T., ENGLAND, H. M., HICKMAN, E. S., KORNER, I., GAN, L., CHEN, S., CASTRO-OBREGON, S., HAMMERMANN, R., WOLF, J., MULLER-HARTMANN, H., NIX, M., SIEBENKOTTEN, G., KRAUS, G. & LUN, K. 2004. New non-viral method for gene transfer into primary cells. *Methods,* 33*,* 151-63.

GROPPO, R., BROWN, B. A. & PALMENBERG, A. C. 2011. Mutational analysis of the EMCV 2A protein identifies a nuclear localization signal and an eIF4E binding site. *Virology,* 410*,* 257-67.

GU, Z., TOLIVER-KINSKY, T., GLASGOW, J., WERRBACH-PEREZ, K. & PEREZ-POLO, J. R. 2000. NGF-mediated alteration of NF-kappaB binding activity after partial immunolesions to rat cholinergic basal forebrain neurons. *Int J Dev Neurosci,* 18*,* 455-68.

GUAN, C., YE, C., YANG, X. & GAO, J. 2010. A review of current large-scale mouse knockout efforts. *Genesis,* 48*,* 73-85.

GUO, Z., IYUN, T., FU, W., ZHANG, P. & MATTSON, M. P. 2004. Bone marrow transplantation reveals roles for brain macrophage/microglia TNF signaling and nitric oxide production in excitotoxic neuronal death. *Neuromolecular Med,* 5*,* 219-34.

HACKER, G., REDECKE, V. & HACKER, H. 2002. Activation of the immune system by bacterial CpG-DNA. *Immunology,* 105*,* 245-51.

HAGSTROM, J. E., LUDTKE, J. J., BASSIK, M. C., SEBESTYEN, M. G., ADAM, S. A. & WOLFF, J. A. 1997. Nuclear import of DNA in digitonin-permeabilized cells. *J Cell Sci,* 110 (Pt 18)*,* 2323-31.

HANISCH, U. K. 2002. Microglia as a source and target of cytokines. *Glia,* 40*,* 140-55.

HANISCH, U. K. & KETTENMANN, H. 2007. Microglia: active sensor and versatile effector cells in the normal and pathologic brain. *Nat Neurosci,* 10*,* 1387-94.

HANSSON, E. 1988. Astroglia from defined brain regions as studied with primary cultures. *Prog Neurobiol,* 30*,* 369-97.

HARADA, A., KAWAMURA, M., MATSUO, T., TAKAHASHI, T. & KONO, K. 2006. Synthesis and characterization of a head-tail type polycation block copolymer as a nonviral gene vector. *Bioconjugate Chemistry,* 17*,* 3-5.

HARDING, C. V. & FELDHERR, C. 1959. Semipermeability of the nuclear membrane in the intact cell. *J Gen Physiol,* 42*,* 1155-65.

HASELKORN, M. L., SHELLINGTON, D. K., JACKSON, E. K., VAGNI, V. A., JANESKO-FELDMAN, K., DUBEY, R. K., GILLESPIE, D. G., CHENG, D., BELL, M. J., JENKINS, L. W., HOMANICS, G. E., SCHNERMANN, J. & KOCHANEK, P. M. 2010. Adenosine A1 receptor activation as a brake on the microglial response after experimental traumatic brain injury in mice. *J Neurotrauma,* 27*,* 901-10.

HAYNES, S. E., HOLLOPETER, G., YANG, G., KURPIUS, D., DAILEY, M. E., GAN, W. B. & JULIUS, D. 2006. The P2Y12 receptor regulates microglial activation by extracellular nucleotides. *Nat Neurosci,* 9*,* 1512-9.

HAZAMA, G. I., YASUHARA, O., MORITA, H., AIMI, Y., TOOYAMA, I. & KIMURA, H. 2005. Mouse brain IgG-like immunoreactivity: strain-specific occurrence

in microglia and biochemical identification of IgG. *J Comp Neurol,* 492*,* 234-49.

HENEKA, M. T. & O'BANION, M. K. 2007. Inflammatory processes in Alzheimer's disease. *J Neuroimmunol,* 184*,* 69-91.

HICKEY, W. F. & KIMURA, H. 1988. Perivascular microglial cells of the CNS are bone marrow-derived and present antigen in vivo. *Science,* 239*,* 290-2.

HIRANO, K., YAMASHITA, S., NAKAGAWA, Y., OHYA, T., MATSUURA, F., TSUKAMOTO, K., OKAMOTO, Y., MATSUYAMA, A., MATSUMOTO, K., MIYAGAWA, J. & MATSUZAWA, Y. 1999. Expression of human scavenger receptor class B type I in cultured human monocyte-derived macrophages and atherosclerotic lesions. *Circulation Research,* 85*,* 108-116.

HOEK, R. M., RUULS, S. R., MURPHY, C. A., WRIGHT, G. J., GODDARD, R., ZURAWSKI, S. M., BLOM, B., HOMOLA, M. E., STREIT, W. J., BROWN, M. H., BARCLAY, A. N. & SEDGWICK, J. D. 2000. Down-regulation of the macrophage lineage through interaction with OX2 (CD200). *Science,* 290*,* 1768-71.

HOEKSTRA, D., REJMAN, J., WASUNGU, L., SHI, F. & ZUHORN, I. 2007. Gene delivery by cationic lipids: in and out of an endosome. *Biochem Soc Trans,* 35*,* 68-71.

HOLM, T. M., BRAUN, A., TRIGATTI, B. L., BRUGNARA, C., SAKAMOTO, M., KRIEGER, M. & ANDREWS, N. C. 2002. Failure of red blood cell maturation in mice with defects in the high-density lipoprotein receptor SR-BI. *Blood,* 99*,* 1817-24.

HOLTHOFF, K. & WITTE, O. W. 2000. Directed spatial potassium redistribution in rat neocortex. *Glia,* 29*,* 288-92.

HOOPER, C., SAINZ-FUERTES, R., LYNHAM, S., HYE, A., KILLICK, R., WARLEY, A., BOLONDI, C., POCOCK, J. & LOVESTONE, S. 2012. Wnt3a induces exosome secretion from primary cultured rat microglia. *BMC neuroscience,* 13*,* 144.

HOOPER, C., TAYLOR, D. L. & POCOCK, J. M. 2005. Pure albumin is a potent trigger of calcium signalling and proliferation in microglia but not macrophages or astrocytes. *Journal of neurochemistry,* 92*,* 1363-76.

HORVATH, R. J., NUTILE-MCMENEMY, N., ALKAITIS, M. S. & DELEO, J. A. 2008. Differential migration, LPS-induced cytokine, chemokine, and NO expression in immortalized BV-2 and HAPI cell lines and primary microglial cultures. *J Neurochem,* 107*,* 557-69.

HOWARD, K. A. 2009. Delivery of RNA interference therapeutics using polycation-based nanoparticles. *Adv Drug Deliv Rev,* 61*,* 710-20.

HSU, C. Y. & ULUDAG, H. 2008. Effects of size and topology of DNA molecules on intracellular delivery with non-viral gene carriers. *BMC Biotechnol,* 8*,* 23.

HU, J., ZHANG, Z., SHEN, W. J. & AZHAR, S. 2010. Cellular cholesterol delivery, intracellular processing and utilization for biosynthesis of steroid hormones. *Nutr Metab (Lond),* 7*,* 47.

HUANG, S., ENDO, R. I. & NEMEROW, G. R. 1995. Upregulation of integrins alpha v beta 3 and alpha v beta 5 on human monocytes and T lymphocytes facilitates adenovirus-mediated gene delivery. *J Virol,* 69*,* 2257-63.

HUSEMANN, J., LOIKE, J. D., ANANKOV, R., FEBBRAIO, M. & SILVERSTEIN, S. C. 2002. Scavenger receptors in neurobiology and neuropathology: Their role on microglia and other cells of the nervous system. *Glia,* 40*,* 195-205.

HUSEMANN, J., LOIKE, J. D., KODAMA, T. & SILVERSTEIN, S. C. 2001. Scavenger receptor class B type I (SR-BI) mediates adhesion of neonatal murine microglia to fibrillar beta-amyloid. *J Neuroimmunol,* 114*,* 142-50.

HUSEMANN, J. & SILVERSTEIN, S. C. 2001. Expression of scavenger receptor class B, type I, by astrocytes and vascular smooth muscle cells in normal adult mouse and human brain and in Alzheimer's disease brain. *American Journal of Pathology,* 158*,* 825-832.

HUTSON, T. H., VERHAAGEN, J., YANEZ-MUNOZ, R. J. & MOON, L. D. 2011. Corticospinal tract transduction: a comparison of seven adeno-associated viral vector serotypes and a non-integrating lentiviral vector. *Gene Ther*.

IADECOLA, C. & NEDERGAARD, M. 2007. Glial regulation of the cerebral microvasculature. *Nat Neurosci,* 10*,* 1369-76.

IMAI, Y., IBATA, I., ITO, D., OHSAWA, K. & KOHSAKA, S. 1996. A novel gene iba1 in the major histocompatibility complex class III region encoding an EF hand protein expressed in a monocytic lineage. *Biochem Biophys Res Commun,* 224*,* 855-62.

IMAI, Y. & KOHSAKA, S. 2002. Intracellular signaling in M-CSF-induced microglia activation: role of Iba1. *Glia,* 40*,* 164-74.

ISHII, N., MINAMI, N., CHEN, E. Y., MEDINA, A. L., CHICO, M. M. & KASAMATSU, H. 1996. Analysis of a nuclear localization signal of simian virus 40 major capsid protein Vp1. *Journal of Virology,* 70*,* 1317-1322.

ITO, D., IMAI, Y., OHSAWA, K., NAKAJIMA, K., FUKUUCHI, Y. & KOHSAKA, S. 1998. Microglia-specific localisation of a novel calcium binding protein, Iba1. *Brain Res Mol Brain Res,* 57*,* 1-9.

JANA, M., LIU, X., KOKA, S., GHOSH, S., PETRO, T. M. & PAHAN, K. 2001. Ligation of CD40 stimulates the induction of nitric-oxide synthase in microglial cells. *J Biol Chem,* 276*,* 44527-33.

JI, A., MEYER, J. M., CAI, L., AKINMUSIRE, A., DE BEER, M. C., WEBB, N. R. & VAN DER WESTHUYZEN, D. R. 2011. Scavenger receptor SR-BI in macrophage lipid metabolism. *Atherosclerosis,* 217*,* 106-12.

JULIANO, R. L. 2006. Intracellular delivery of oligonucleotide conjugates and dendrimer complexes. *Ann N Y Acad Sci,* 1082*,* 18-26.

JULVE, J., LLAVERIAS, G., BLANCO-VACA, F. & ESCOLA-GIL, J. C. 2011. Seeking novel targets for improving in vivo macrophage-specific reverse cholesterol transport: translating basic science into new therapies for the prevention and treatment of atherosclerosis. *Curr Vasc Pharmacol,* 9*,* 220-37.

KALDERON, D., ROBERTS, B. L., RICHARDSON, W. D. & SMITH, A. E. 1984. A short amino acid sequence able to specify nuclear location. *Cell,* 39*,* 499-509.

KALKBRENNER, T., ARNOLD, A. & TANS, S. J. 2009. Internal dynamics of supercoiled DNA molecules. *Biophys J,* 96*,* 4951-5.

KALLA, R., BOHATSCHEK, M., KLOSS, C. U., KROL, J., VON MALTZAN, X. & RAIVICH, G. 2003. Loss of microglial ramification in microglia-astrocyte

cocultures: involvement of adenylate cyclase, calcium, phosphatase, and Gi-protein systems. *Glia,* 41*,* 50-63.

KATZ-LEVY, Y., NEVILLE, K. L., PADILLA, J., RAHBE, S., BEGOLKA, W. S., GIRVIN, A. M., OLSON, J. K., VANDERLUGT, C. L. & MILLER, S. D. 2000. Temporal development of autoreactive Th1 responses and endogenous presentation of self myelin epitopes by central nervous system-resident APCs in Theiler's virus-infected mice. *J Immunol,* 165*,* 5304-14.

KAUPPINEN, T. M., HIGASHI, Y., SUH, S. W., ESCARTIN, C., NAGASAWA, K. & SWANSON, R. A. 2008. Zinc triggers microglial activation. *J Neurosci,* 28*,* 5827-35.

KAUR, P., ASCHNER, M. & SYVERSEN, T. 2007. Role of glutathione in determining the differential sensitivity between the cortical and cerebellar regions towards mercury-induced oxidative stress. *Toxicology,* 230*,* 164-77.

KAUSHAL, V. & SCHLICHTER, L. C. 2008. Mechanisms of microglia-mediated neurotoxicity in a new model of the stroke penumbra. *J Neurosci,* 28*,* 2221-30.

KESSLER, C. & MANTA, V. 1990. Specificity of restriction endonucleases and DNA modification methyltransferases a review (Edition 3). *Gene,* 92*,* 1-248.

KETTENMANN, H., HANISCH, U. K., NODA, M. & VERKHRATSKY, A. 2011. Physiology of microglia. *Physiol Rev,* 91*,* 461-553.

KETTENMANN, H., KIRCHHOFF, F. & VERKHRATSKY, A. 2013. Microglia: new roles for the synaptic stripper. *Neuron,* 77*,* 10-8.

KIDA, S., STEART, P. V., ZHANG, E. T. & WELLER, R. O. 1993. Perivascular cells act as scavengers in the cerebral perivascular spaces and remain distinct from pericytes, microglia and macrophages. *Acta Neuropathol,* 85*,* 646-52.

KIM, J., KIM, S. W. & KIM, W. J. 2011. PEI-g-PEG-RGD/small interference RNA polyplex-mediated silencing of vascular endothelial growth factor receptor and its potential as an anti-angiogenic tumor therapeutic strategy. *Oligonucleotides,* 21*,* 101-7.

KIM, J. B., CHOI, J. S., NAM, K., LEE, M., PARK, J. S. & LEE, J. K. 2006. Enhanced transfection of primary cortical cultures using arginine-grafted PAMAM dendrimer, PAMAM-Arg. *J Control Release,* 114*,* 110-7.

KIMELBERG, H. K. & NEDERGAARD, M. 2010. Functions of astrocytes and their potential as therapeutic targets. *Neurotherapeutics,* 7*,* 338-53.

KINGHAM, P. J., CUZNER, M. L. & POCOCK, J. M. 1999. Apoptotic pathways mobilized in microglia and neurones as a consequence of chromogranin A-induced microglial activation. *Journal of neurochemistry,* 73*,* 538-47.

KINGHAM, P. J. & POCOCK, J. M. 2001. Microglial secreted cathepsin B induces neuronal apoptosis. *J Neurochem,* 76*,* 1475-84.

KIRCHEIS, R., KICHLER, A., WALLNER, G., KURSA, M., OGRIS, M., FELZMANN, T., BUCHBERGER, M. & WAGNER, E. 1997. Coupling of cell-binding ligands to polyethylenimine for targeted gene delivery. *Gene Therapy,* 4*,* 409-418.

KIRCHEIS, R., WIGHTMAN, L., SCHREIBER, A., ROBITZA, B., ROSSLER, V., KURSA, M. & WAGNER, E. 2001. Polyethylenimine/DNA complexes shielded by transferrin target gene expression to tumors after systemic application. *Gene Therapy,* 8*,* 28-40.

KISS, A. L. 2012. Caveolae and the regulation of endocytosis. *Adv Exp Med Biol,* 729*,* 14-28.

KLEIN, R. L., MEYER, E. M., PEEL, A. L., ZOLOTUKHIN, S., MEYERS, C., MUZYCZKA, N. & KING, M. A. 1998. Neuron-specific transduction in the rat septohippocampal or nigrostriatal pathway by recombinant adeno-associated virus vectors. *Exp Neurol,* 150*,* 183-94.

KOCHER, O., YESILALTAY, A., CIROVIC, C., PAL, R., RIGOTTI, A. & KRIEGER, M. 2003. Targeted disruption of the PDZK1 gene in mice causes tissue-specific depletion of the high density lipoprotein receptor scavenger receptor class B type I and altered lipoprotein metabolism. *J Biol Chem,* 278*,* 52820-5.

KODAMA, K., KATAYAMA, Y., SHOJI, Y. & NAKASHIMA, H. 2006. The features and shortcomings for gene delivery of current non-viral carriers. *Current Medicinal Chemistry,* 13*,* 2155-2161.

KOFLER, J. & WILEY, C. A. 2011. Microglia: key innate immune cells of the brain. *Toxicol Pathol,* 39*,* 103-14.

KOIZUMI, S., SHIGEMOTO-MOGAMI, Y., NASU-TADA, K., SHINOZAKI, Y., OHSAWA, K., TSUDA, M., JOSHI, B. V., JACOBSON, K. A., KOHSAKA, S. & INOUE, K. 2007. UDP acting at P2Y6 receptors is a mediator of microglial phagocytosis. *Nature,* 446*,* 1091-5.

KOPATZ, I., REMY, J. S. & BEHR, J. P. 2004. A model for non-viral gene delivery: through syndecan adhesion molecules and powered by actin. *J Gene Med,* 6*,* 769-76.

KRANGEL, M. S. 1987. Endocytosis and recycling of the T3-T cell receptor complex. The role of T3 phosphorylation. *J Exp Med,* 165*,* 1141-59.

KREUTZBERG, G. W. 1996. Microglia: a sensor for pathological events in the CNS. *Trends Neurosci,* 19*,* 312-8.

KRIEGER, M. 1999. Charting the fate of the "good cholesterol": Identification and characterization of the high-density lipoprotein receptor SR-BI. *Annual Review of Biochemistry,* 68*,* 523-558.

KRIEGER, M. 2001. Scavenger receptor class B type I is a multiligand HDL receptor that influences diverse physiologic systems. *J Clin Invest,* 108*,* 793-7.

KRIEGER, M. & HERZ, J. 1994. Structures and functions of multiligand lipoprotein receptors: macrophage scavenger receptors and LDL receptor-related protein (LRP). *Annu Rev Biochem,* 63*,* 601-37.

KUMAR, P., WU, H., MCBRIDE, J. L., JUNG, K. E., KIM, M. H., DAVIDSON, B. L., LEE, S. K., SHANKAR, P. & MANJUNATH, N. 2007. Transvascular delivery of small interfering RNA to the central nervous system. *Nature,* 448*,* 39-43.

KURSA, M., WALKER, G. F., ROESSLER, V., OGRIS, M., ROEDL, W., KIRCHEIS, R. & WAGNER, E. 2003. Novel shielded transferrin-polyethylene glycol-polyethylenimine/DNA complexes for systemic tumor-targeted gene transfer. *Bioconjugate Chemistry,* 14*,* 222-231.

KWON, E. J., BERGEN, J. M., PARK, I. K. & PUN, S. H. 2008a. Peptide-modified vectors for nucleic acid delivery to neurons. *J Control Release,* 132*,* 230-5.

KWON, E. J., BERGEN, J. M. & PUN, S. H. 2008b. Application of an HIV gp41-derived peptide for enhanced intracellular trafficking of synthetic gene and siRNA delivery vehicles. *Bioconjug Chem,* 19*,* 920-7.

LABUZEK, K., LIBER, S., GABRYEL, B. & OKOPIEN, B. 2010. Metformin has adenosine-monophosphate activated protein kinase (AMPK)-independent effects on LPS-stimulated rat primary microglial cultures. *Pharmacol Rep,* 62*,* 827-48.

LAJOIE, P. & NABI, I. R. 2010. Lipid rafts, caveolae, and their endocytosis. *Int Rev Cell Mol Biol,* 282*,* 135-63.

LAM, A. P. & DEAN, D. A. 2010. Progress and prospects: nuclear import of nonviral vectors. *Gene Ther,* 17*,* 439-47.

LAMBERT, R. C., MAULET, Y., DUPONT, J. L., MYKITA, S., CRAIG, P., VOLSEN, S. & FELTZ, A. 1996. Polyethylenimine-mediated DNA transfection of peripheral and central neurons in primary culture: probing Ca2+ channel structure and function with antisense oligonucleotides. *Mol Cell Neurosci,* 7*,* 239-46.

LAMBERTSEN, K. L., CLAUSEN, B. H., BABCOCK, A. A., GREGERSEN, R., FENGER, C., NIELSEN, H. H., HAUGAARD, L. S., WIRENFELDT, M., NIELSEN, M., DAGNAES-HANSEN, F., BLUETHMANN, H., FAERGEMAN, N. J., MELDGAARD, M., DEIERBORG, T. & FINSEN, B. 2009. Microglia protect neurons against ischemia by synthesis of tumor necrosis factor. *J Neurosci,* 29*,* 1319-30.

LAMBERTSEN, K. L., DEIERBORG, T., GREGERSEN, R., CLAUSEN, B. H., WIRENFELDT, M., NIELSEN, H. H., DALMAU, I., DIEMER, N. H., DAGNAES-HANSEN, F., JOHANSEN, F. F., KEATING, A. & FINSEN, B. 2011. Differences in origin of reactive microglia in bone marrow chimeric mouse and rat after transient global ischemia. *J Neuropathol Exp Neurol,* 70*,* 481-94.

LANDSCHULZ, K. T., PATHAK, R. K., RIGOTTI, A., KRIEGER, M. & HOBBS, H. H. 1996. Regulation of scavenger receptor, class B, type I, a high density lipoprotein receptor, in liver and steroidogenic tissues of the rat. *J Clin Invest,* 98*,* 984-95.

LANE, D., PRENTKI, P. & CHANDLER, M. 1992. Use of Gel Retardation to Analyze Protein-Nucleic Acid Interactions. *Microbiological Reviews,* 56*,* 509-528.

LAUBER, K., BOHN, E., KROBER, S. M., XIAO, Y. J., BLUMENTHAL, S. G., LINDEMANN, R. K., MARINI, P., WIEDIG, C., ZOBYWALSKI, A., BAKSH, S., XU, Y., AUTENRIETH, I. B., SCHULZE-OSTHOFF, K., BELKA, C., STUHLER, G. & WESSELBORG, S. 2003. Apoptotic cells induce migration of phagocytes via caspase-3-mediated release of a lipid attraction signal. *Cell,* 113*,* 717-30.

LAUDE, A. J. & PRIOR, I. A. 2004. Plasma membrane microdomains: organization, function and trafficking. *Mol Membr Biol,* 21*,* 193-205.

LAUGHTON, J. D., BITTAR, P., CHARNAY, Y., PELLERIN, L., KOVARI, E., MAGISTRETTI, P. J. & BOURAS, C. 2007. Metabolic compartmentalization in the human cortex and hippocampus: evidence for a cell- and region-specific localization of lactate dehydrogenase 5 and pyruvate dehydrogenase. *BMC Neurosci,* 8*,* 35.

LAWSON, L. J., PERRY, V. H., DRI, P. & GORDON, S. 1990. Heterogeneity in the distribution and morphology of microglia in the normal adult mouse brain. *Neuroscience,* 39*,* 151-70.

LAWSON, L. J., PERRY, V. H. & GORDON, S. 1992. Turnover of resident microglia in the normal adult mouse brain. *Neuroscience,* 48*,* 405-15.

LE, Y., YAZAWA, H., GONG, W., YU, Z., FERRANS, V. J., MURPHY, P. M. & WANG, J. M. 2001. The neurotoxic prion peptide fragment PrP(106-126) is a chemotactic agonist for the G protein-coupled receptor formyl peptide receptor-like 1. *J Immunol,* 166*,* 1448-51.

LEE, S. H., CHOI, S. H., KIM, S. H. & PARK, T. G. 2008. Thermally sensitive cationic polymer nanocapsules for specific cytosolic delivery and efficient gene silencing of siRNA: swelling induced physical disruption of endosome by cold shock. *J Control Release,* 125*,* 25-32.

LEE, Y., SU, M., MESSING, A. & BRENNER, M. 2006. Astrocyte heterogeneity revealed by expression of a GFAP-LacZ transgene. *Glia,* 53*,* 677-687.

LEE, Y. J., HAN, S. B., NAM, S. Y., OH, K. W. & HONG, J. T. 2010. Inflammation and Alzheimer's disease. *Arch Pharm Res,* 33*,* 1539-56.

LEE, Y. J., JOHNSON, G., PELTIER, G. C. & PELLOIS, J. P. 2011. A HA2-Fusion tag limits the endosomal release of its protein cargo despite causing endosomal lysis. *Biochim Biophys Acta,* 1810*,* 752-8.

LEHMENKÜHLER, A., SYKOVA, E., SVOBODA, J., ZILLES, K. & NICHOLSON, C. 1993. Extracellular space parameters in the rat neocortex and subcortical white matter during postnatal development determined by diffusion analysis. *Neuroscience,* 55*,* 339-51.

LEWIS, G. F. & RADER, D. J. 2005. New insights into the regulation of HDL metabolism and reverse cholesterol transport. *Circ Res,* 96*,* 1221-32.

LI, H., GANG, Z., YULING, H., LUOKUN, X., JIE, X., HAO, L., LI, W., CHUNSONG, H., JUNYAN, L., MINGSHEN, J., YOUXIN, J., FEILI, G., BOQUAN, J. & JINQUAN, T. 2006. Different neurotropic pathogens elicit neurotoxic CCR9- or neurosupportive CXCR3-expressing microglia. *J Immunol,* 177*,* 3644-56.

LI, L., LUNDKVIST, A., ANDERSSON, D., WILHELMSSON, U., NAGAI, N., PARDO, A. C., NODIN, C., STAHLBERG, A., APRICO, K., LARSSON, K., YABE, T., MOONS, L., FOTHERINGHAM, A., DAVIES, I., CARMELIET, P., SCHWARTZ, J. P., PEKNA, M., KUBISTA, M., BLOMSTRAND, F., MARAGAKIS, N., NILSSON, M. & PEKNY, M. 2008. Protective role of reactive astrocytes in brain ischemia. *J Cereb Blood Flow Metab,* 28*,* 468-81.

LIM, S. T., AIRAVAARA, M. & HARVEY, B. K. 2010. Viral vectors for neurotrophic factor delivery: a gene therapy approach for neurodegenerative diseases of the CNS. *Pharmacol Res,* 61*,* 14-26.

LINDSTEN, T., GOLDEN, J. A., ZONG, W. X., MINARCIK, J., HARRIS, M. H. & THOMPSON, C. B. 2003. The proapoptotic activities of Bax and Bak limit the size of the neural stem cell pool. *J Neurosci,* 23*,* 11112-9.

LIOU, J. S., LIU, B. R., MARTIN, A. L., HUANG, Y. W., CHIANG, H. J. & LEE, H. J. 2012. Protein transduction in human cells is enhanced by cell-penetrating peptides fused with an endosomolytic HA2 sequence. *Peptides*.

LIU, B., WANG, K., GAO, H. M., MANDAVILLI, B., WANG, J. Y. & HONG, J. S. 2001. Molecular consequences of activated microglia in the brain: overactivation induces apoptosis. *J Neurochem,* 77*,* 182-9.

LÖSER, P., JENNINGS, G. S., STRAUSS, M. & SANDIG, V. 1998. Reactivation of the previously silenced cytomegalovirus major immediate-early promoter in the mouse liver: involvement of NFkappaB. *J Virol,* 72*,* 180-90.

LUCIN, K. M. & WYSS-CORAY, T. 2009. Immune activation in brain aging and neurodegeneration: too much or too little? *Neuron,* 64*,* 110-22.

LUKACS, G. L., HAGGIE, P., SEKSEK, O., LECHARDEUR, D., FREEDMAN, N. & VERKMAN, A. S. 2000. Size-dependent DNA mobility in cytoplasm and nucleus. *J Biol Chem,* 275*,* 1625-9.

LUTHMAN, H. & MAGNUSSON, G. 1983. High efficiency polyoma DNA transfection of chloroquine treated cells. *Nucleic Acids Res,* 11*,* 1295-308.

LV, H., ZHANG, S., WANG, B., CUI, S. & YAN, J. 2006. Toxicity of cationic lipids and cationic polymers in gene delivery. *J Control Release,* 114*,* 100-9.

MACHADO, A., HERRERA, A. J., VENERO, J. L., SANTIAGO, M., DE PABLOS, R. M., VILLARAN, R. F., ESPINOSA-OLIVA, A. M., ARGUELLES, S., SARMIENTO, M., DELGADO-CORTES, M. J., MAURINO, R. & CANO, J. 2011. Peripheral inflammation increases the damage in animal models of nigrostriatal dopaminergic neurodegeneration: possible implication in Parkinson's disease incidence. *Parkinsons Dis,* 2011*,* 393769.

MAHMUTEFENDIC, H., BLAGOJEVIC, G., KUCIC, N. & LUCIN, P. 2007. Constitutive internalization of murine MHC class I molecules. *J Cell Physiol,* 210*,* 445-55.

MANFREDSSON, F. P. & MANDEL, R. J. 2010. Development of gene therapy for neurological disorders. *Discov Med,* 9*,* 204-11.

MANZANO-LEON, N., DELGADO-COELLO, B., GUADERRAMA-DIAZ, M. & MAS-OLIVA, J. 2006. Beta-adaptin: key molecule for microglial scavenger receptor function under oxidative stress. *Biochem Biophys Res Commun,* 351*,* 588-94.

MAREK, R., CARUSO, M., ROSTAMI, A., GRINSPAN, J. B. & DAS SARMA, J. 2008. Magnetic cell sorting: a fast and effective method of concurrent isolation of high purity viable astrocytes and microglia from neonatal mouse brain tissue. *J Neurosci Methods,* 175*,* 108-18.

MARIN-TEVA, J. L., DUSART, I., COLIN, C., GERVAIS, A., VAN ROOIJEN, N. & MALLAT, M. 2004. Microglia promote the death of developing Purkinje cells. *Neuron,* 41*,* 535-47.

MARSDEN, H. R., TOMATSU, I. & KROS, A. 2011. Model systems for membrane fusion. *Chem Soc Rev,* 40*,* 1572-85.

MARTINEZ-FONG, D., NAVARRO-QUIROGA, I., OCHOA, I., ALVAREZ-MAYA, I., MERAZ, M. A., LUNA, J. & ARIAS-MONTANO, J. A. 1999. Neurotensin-SPDP-poly-L-lysine conjugate: a nonviral vector for targeted gene delivery to neural cells. *Molecular Brain Research,* 69*,* 249-262.

MARZOLO, M. P., VON BERNHARDI, R., BU, G. & INESTROSA, N. C. 2000. Expression of alpha(2)-macroglobulin receptor/low density lipoprotein receptor-related protein (LRP) in rat microglial cells. *J Neurosci Res,* 60*,* 401-11.

MATSUMOTO, H., KUMON, Y., WATANABE, H., OHNISHI, T., SHUDOU, M., II, C., TAKAHASHI, H., IMAI, Y. & TANAKA, J. 2007. Antibodies to CD11b, CD68, and lectin label neutrophils rather than microglia in traumatic and ischemic brain lesions. *J Neurosci Res,* 85*,* 994-1009.

MATTSON, G., CONKLIN, E., DESAI, S., NIELANDER, G., SAVAGE, D. & MORGENSEN, S. 1993. A practical approach to crosslinking. *Molecular Biology Reports,* 17 167-183.

MCCLUSKEY, L. P. & LAMPSON, L. A. 2000. Local neurochemicals and site-specific immune regulation in the CNS. *J Neuropathol Exp Neurol,* 59*,* 177-87.

MCCLUSKEY, L. P. & LAMPSON, L. A. 2001. Local immune regulation in the central nervous system by substance P vs. glutamate. *J Neuroimmunol,* 116*,* 136-46.

MCCOWN, T. J., XIAO, X., LI, J., BREESE, G. R. & SAMULSKI, R. J. 1996. Differential and persistent expression patterns of CNS gene transfer by an adeno-associated virus (AAV) vector. *Brain Res,* 713*,* 99-107.

MCMAHON, E. J., SUZUKI, K. & MATSUSHIMA, G. K. 2002. Peripheral macrophage recruitment in cuprizone-induced CNS demyelination despite an intact blood-brain barrier. *J Neuroimmunol,* 130*,* 32-45.

MELLMAN, I. 1996. Endocytosis and molecular sorting. *Annu Rev Cell Dev Biol,* 12*,* 575-625.

MERDAN, T., CALLAHAN, J., PETERSEN, H., KUNATH, K., BAKOWSKY, U., KOPECKOVA, P., KISSEL, T. & KOPECEK, J. 2003. Pegylated polyethylenimine-Fab' antibody fragment conjugates for targeted gene delivery to human ovarian carcinoma cells. *Bioconjug Chem,* 14*,* 989-96.

MICHALSKI, D., GROSCHE, J., PELZ, J., SCHNEIDER, D., WEISE, C., BAUER, U., KACZA, J., GARTNER, U., HOBOHM, C. & HARTIG, W. 2010. A novel quantification of blood-brain barrier damage and histochemical typing after embolic stroke in rats. *Brain Res,* 1359*,* 186-200.

MIDOUX, P., MENDES, C., LEGRAND, A., RAIMOND, J., MAYER, R., MONSIGNY, M. & ROCHE, A. C. 1993. Specific gene transfer mediated by lactosylated poly-L-lysine into hepatoma cells. *Nucleic Acids Res,* 21*,* 871-8.

MILDNER, A., SCHMIDT, H., NITSCHE, M., MERKLER, D., HANISCH, U. K., MACK, M., HEIKENWALDER, M., BRUCK, W., PRILLER, J. & PRINZ, M. 2007. Microglia in the adult brain arise from Ly-6ChiCCR2+ monocytes only under defined host conditions. *Nat Neurosci,* 10*,* 1544-53.

MILLER, A. M. & DEAN, D. A. 2008. Cell-specific nuclear import of plasmid DNA in smooth muscle requires tissue-specific transcription factors and DNA sequences. *Gene Ther,* 15*,* 1107-15.

MILLER, R. H. & RAFF, M. C. 1984. Fibrous and protoplasmic astrocytes are biochemically and developmentally distinct. *Journal of Neuroscience,* 4*,* 585-592.

MINGHETTI, L. & LEVI, G. 1998. Microglia as effector cells in brain damage and repair: focus on prostanoids and nitric oxide. *Progress in neurobiology,* 54*,* 99-125.

MITRASINOVIC, O. M., PEREZ, G. V., ZHAO, F., LEE, Y. L., POON, C. & MURPHY, G. M., JR. 2001. Overexpression of macrophage colony-stimulating factor

receptor on microglial cells induces an inflammatory response. *J Biol Chem,* 276*,* 30142-9.

MITTELBRONN, M., DIETZ, K., SCHLUESENER, H. J. & MEYERMANN, R. 2001. Local distribution of microglia in the normal adult human central nervous system differs by up to one order of magnitude. *Acta Neuropathol,* 101*,* 249-55.

MONIER, A., EVRARD, P., GRESSENS, P. & VERNEY, C. 2006. Distribution and differentiation of microglia in the human encephalon during the first two trimesters of gestation. *J Comp Neurol,* 499*,* 565-82.

MONIF, M., REID, C. A., POWELL, K. L., SMART, M. L. & WILLIAMS, D. A. 2009. The P2X7 receptor drives microglial activation and proliferation: a trophic role for P2X7R pore. *J Neurosci,* 29*,* 3781-91.

MOODY, D. M. 2006. The Blood-Brain Barrier and Blood-Cerebral Spinal Fluid Barrier. *Seminars in Cardiothoractic Vascular Anesthetics,* 10*,* 128-131.

MORGAN, S. C., TAYLOR, D. L. & POCOCK, J. M. 2004. Microglia release activators of neuronal proliferation mediated by activation of mitogen-activated protein kinase, phosphatidylinositol-3-kinase/Akt and delta-Notch signalling cascades. *J Neurochem,* 90*,* 89-101.

MORIOKA, T., KALEHUA, A. N. & STREIT, W. J. 1991. The microglial reaction in the rat dorsal hippocampus following transient forebrain ischemia. *J Cereb Blood Flow Metab,* 11*,* 966-73.

MURAMATSU, T., MIZUTANI, Y., OHMORI, Y. & OKUMURA, J. 1997. Comparison of three nonviral transfection methods for foreign gene expression in early chicken embryos in ovo. *Biochem Biophys Res Commun,* 230*,* 376-80.

MURAO, K., TERPSTRA, V., GREEN, S. R., KONDRATENKO, N., STEINBERG, D. & QUEHENBERGER, O. 1997. Characterization of CLA-1, a human homologue of rodent scavenger receptor BI, as a receptor for high density lipoprotein and apoptotic thymocytes. *Journal of Biological Chemistry,* 272*,* 17551-17557.

MUYDERMAN, H., YEW, W. P., HOMKAJORN, B. & SIMS, N. R. 2010. Astrocytic responses to DNA delivery using nucleofection. *Neurochem Res,* 35*,* 1771-9.

NAG, S. 2011. Morphology and properties of astrocytes. *Methods Mol Biol,* 686*,* 69-100.

NAGY, A., MAR, L. & WATTS, G. 2009. Creation and use of a cre recombinase transgenic database. *Methods Mol Biol,* 530*,* 365-78.

NAGY, A. & ROSSANT, J. 1996. Targeted mutagenesis: analysis of phenotype without germ line transmission. *J Clin Invest,* 97*,* 1360-5.

NAKAGAWA, A., NAGAOSA, K., HIROSE, T., TSUDA, K., HASEGAWA, K., SHIRATSUCHI, A. & NAKANISHI, Y. 2004. Expression and function of class B scavenger receptor type I on both apical and basolateral sides of the plasma membrane of polarized testicular Sertoli cells of the rat. *Dev Growth Differ,* 46*,* 283-98.

NAKAMURA, Y., WAKIMOTO, H., ABE, J., KANEGAE, Y., SAITO, I., AOYAGI, M., HIRAKAWA, K. & HAMADA, H. 1994. Adoptive immunotherapy with

murine tumor-specific T lymphocytes engineered to secrete interleukin 2. *Cancer Res,* 54*,* 5757-60.

NAPOLI, I. & NEUMANN, H. 2009. Microglial clearance function in health and disease. *Neuroscience,* 158*,* 1030-8.

NAVARRO-QUIROGA, I., GONZALEZ-BARRIOS, J. A., BARRON-MORENO, F., GONZALEZ-BERNAL, V., MARTINEZ-ARGUELLES, D. B. & MARTINEZ-FONG, D. 2002. Improved neurotensin-vector-mediated gene transfer by the coupling of hemagglutinin HA2 fusogenic peptide and Vp1 SV40 nuclear localization signal. *Molecular Brain Research,* 105*,* 86-97.

NEDERGAARD, M., RANSOM, B. & GOLDMAN, S. A. 2003. New roles for astrocytes: redefining the functional architecture of the brain. *Trends Neurosci,* 26*,* 523-30.

NEUMANN, H., KOTTER, M. R. & FRANKLIN, R. J. 2009. Debris clearance by microglia: an essential link between degeneration and regeneration. *Brain,* 132*,* 288-95.

NICHOLS, B. 2003. Caveosomes and endocytosis of lipid rafts. *J Cell Sci,* 116*,* 4707-14.

NILSSON, M., HANSSON, E. & RONNBACK, L. 1991. Adrenergic and 5-HT2 receptors on the same astroglial cell. A microspectrofluorimetric study on cytosolic Ca2+ responses in single cells in primary culture. *Brain Res Dev Brain Res,* 63*,* 33-41.

NIMMERJAHN, A., KIRCHHOFF, F. & HELMCHEN, F. 2005. Resting microglial cells are highly dynamic surveillants of brain parenchyma in vivo. *Science,* 308*,* 1314-8.

NONNENMACHER, C., DALPKE, A., ZIMMERMANN, S., FLORES-DE-JACOBY, L., MUTTERS, R. & HEEG, K. 2003. DNA from periodontopathogenic bacteria is immunostimulatory for mouse and human immune cells. *Infect Immun,* 71*,* 850-6.

NORATA, G. D., PIRILLO, A. & CATAPANO, A. L. 2011. HDLs, immunity, and atherosclerosis. *Curr Opin Lipidol,* 22*,* 410-6.

NORDIN, C., NILSSON, M. & BLOMSTRAND, F. 2005. Gap junction blockage limits intercellular spreading of astrocytic apoptosis induced by metabolic depression. *Journal of Neurochemistry,* 94*,* 1111-1123.

OBERHEIM, N. A., GOLDMAN, S. A. & NEDERGAARD, M. 2012. Heterogeneity of astrocytic form and function. *Methods Mol Biol,* 814*,* 23-45.

OBERHEIM, N. A., TAKANO, T., HAN, X., HE, W., LIN, J. H., WANG, F., XU, Q., WYATT, J. D., PILCHER, W., OJEMANN, J. G., RANSOM, B. R., GOLDMAN, S. A. & NEDERGAARD, M. 2009. Uniquely hominid features of adult human astrocytes. *J Neurosci,* 29*,* 3276-87.

OGRIS, M., BRUNNER, S., SCHULLER, S., KIRCHEIS, R. & WAGNER, E. 1999. PEGylated DNA/transferrin-PEI complexes: reduced interaction with blood components, extended circulation in blood and potential for systemic gene delivery. *Gene Therapy,* 6*,* 595-605.

OGRIS, M., CARLISLE, R. C., BETTINGER, T. & SEYMOUR, L. W. 2001. Melittin enables efficient vesicular escape and enhanced nuclear access of nonviral gene delivery vectors. *J Biol Chem,* 276*,* 47550-5.

OGRIS, M., STEINLEIN, P., KURSA, M., MECHTLER, K., KIRCHEIS, R. & WAGNER, E. 1998. The size of DNA/transferrin-PEI complexes is an important factor for gene expression in cultured cells. *Gene Therapy,* 5*,* 1425-1433.

OHGAMI, N., NAGAI, R., MIYAZAKI, A., IKEMOTO, M., ARAI, H., HORIUCHI, S. & NAKAYAMA, H. 2001. Scavenger receptor class B type I-mediated reverse cholesterol transport is inhibited by advanced glycation end products. *J Biol Chem,* 276*,* 13348-55.

OHNISHI, S., ITO, H., SUZUKI, Y., ADACHI, Y., WATE, R., ZHANG, J., NAKANO, S., KUSAKA, H. & IKEHARA, S. 2009. Intra-bone marrow-bone marrow transplantation slows disease progression and prolongs survival in G93A mutant SOD1 transgenic mice, an animal model mouse for amyotrophic lateral sclerosis. *Brain Res,* 1296*,* 216-24.

OHNO, M., FORNEROD, M. & MATTAJ, I. W. 1998. Nucleocytoplasmic transport: the last 200 nanometers. *Cell,* 92*,* 327-36.

OKUN, E., MATTSON, M. P. & ARUMUGAM, T. V. 2010. Involvement of Fc receptors in disorders of the central nervous system. *Neuromolecular Med,* 12*,* 164-78.

OLSON, J. K., ZAMVIL, S. S. & MILLER, S. D. 2003. Efficient technique for immortalization of murine microglial cells relevant for studies in murine models of multiple sclerosis. *J Neurosci Methods,* 128*,* 33-43.

OMELYANENKO, V., KOPECKOVA, P., GENTRY, C., SHIAH, J. G. & KOPECEK, J. 2003. HPMA copolymer-anticancer drug-OV-TL-TL16 antibody conjugates. 1. Influence of the method of synthesis on the biding affinity to OVCAR-3 ovarian carcinoma cells in vitro. *Journal of Drug Targeting,* 11*,* 295-309.

OPPENHEIM, R. W. 1991. Cell death during development of the nervous system. *Annu Rev Neurosci,* 14*,* 453-501.

ORTHMANN-MURPHY, J. L., ABRAMS, C. K. & SCHERER, S. S. 2008. Gap junctions couple astrocytes and oligodendrocytes. *J Mol Neurosci,* 35*,* 101-16.

OSADA, Y., SHIRATSUCHI, A. & NAKANISHI, Y. 2006. Involvement of mitogen-activated protein kinases in class B scavenger receptor type I-induced phagocytosis of apoptotic cells. *Exp Cell Res,* 312*,* 1820-30.

PAINE, P. L. & FELDHERR, C. M. 1972. Nucleocytoplasmic exchange of macromolecules. *Exp Cell Res,* 74*,* 81-98.

PARATHATH, S., CONNELLY, M. A., RIEGER, R. A., KLEIN, S. M., ABUMRAD, N. A., DE LA LLERA-MOYA, M., IDEN, C. R., ROTHBLAT, G. H. & WILLIAMS, D. L. 2004. Changes in plasma membrane properties and phosphatidylcholine subspecies of insect Sf9 cells due to expression of scavenger receptor class B, type I, and CD36. *J Biol Chem,* 279*,* 41310-8.

PARK, J. W., HONG, K., CARTER, P., ASGARI, H., GUO, L. Y., KELLER, G. A., WIRTH, C., SHALABY, R., KOTTS, C., WOOD, W. I. & ET AL. 1995. Development of anti-p185HER2 immunoliposomes for cancer therapy. *Proc Natl Acad Sci U S A,* 92*,* 1327-31.

PARKER, A. L., COLLINS, L., ZHANG, X. & FABRE, J. W. 2005. Exploration of peptide motifs for potent non-viral gene delivery highly selective for dividing cells. *J Gene Med,* 7*,* 1545-54.

PARPURA, V., HENEKA, M. T., MONTANA, V., OLIET, S. H., SCHOUSBOE, A., HAYDON, P. G., STOUT, R. F., JR., SPRAY, D. C., REICHENBACH, A., PANNICKE, T., PEKNY, M., PEKNA, M., ZOREC, R. & VERKHRATSKY, A. 2012. Glial cells in (patho)physiology. *Journal of neurochemistry,* 121*,* 4-27.

PASLEAU, F., TOCCI, M. J., LEUNG, F. & KOPCHICK, J. J. 1985. Growth hormone gene expression in eukaryotic cells directed by the Rous sarcoma virus long terminal repeat or cytomegalovirus immediate-early promoter. *Gene,* 38*,* 227-32.

PATERNA, J. C., MOCCETTI, T., MURA, A., FELDON, J. & BUELER, H. 2000. Influence of promoter and WHV post-transcriptional regulatory element on AAV-mediated transgene expression in the rat brain. *Gene Ther,* 7*,* 1304-11.

PELLERIN, L. & MAGISTRETTI, P. J. 1994. Glutamate uptake into astrocytes stimulates aerobic glycolysis: a mechanism coupling neuronal activity to glucose utilization. *Proc Natl Acad Sci U S A,* 91*,* 10625-9.

PENG, L., ARYSTARKHOVA, E. & SWEADNER, K. J. 1998. Plasticity of Na,K-ATPase isoform expression in cultures of flat astrocytes: species differences in gene expression. *Glia,* 24*,* 257-71.

PERALES, J. C., FERKOL, T., BEEGEN, H., RATNOFF, O. D. & HANSON, R. W. 1994. Gene transfer in vivo: sustained expression and regulation of genes introduced into the liver by receptor-targeted uptake. *Proc Natl Acad Sci U S A,* 91*,* 4086-90.

PEREA, G., NAVARRETE, M. & ARAQUE, A. 2009. Tripartite synapses: astrocytes process and control synaptic information. *Trends Neurosci,* 32*,* 421-31.

PERSSON, M., BRANTEFJORD, M., HANSSON, E. & RONNBACK, L. 2005. Lipopolysaccharide increases microglial GLT-1 expression and glutamate uptake capacity in vitro by a mechanism dependent on TNF-alpha. *Glia,* 51*,* 111-20.

PETITO, C. K., MORGELLO, S., FELIX, J. C. & LESSER, M. L. 1990. The two patterns of reactive astrocytosis in postischemic rat brain. *J Cereb Blood Flow Metab,* 10*,* 850-9.

PIANI, D., FREI, K., DO, K. Q., CUENOD, M. & FONTANA, A. 1991. Murine brain macrophages induced NMDA receptor mediated neurotoxicity in vitro by secreting glutamate. *Neurosci Lett,* 133*,* 159-62.

PICHON, C., BILLIET, L. & MIDOUX, P. 2010. Chemical vectors for gene delivery: uptake and intracellular trafficking. *Curr Opin Biotechnol,* 21*,* 640-5.

PIKE, L. J. 2006. Rafts defined: a report on the Keystone Symposium on Lipid Rafts and Cell Function. *J Lipid Res,* 47*,* 1597-8.

PLANK, C., ZATLOUKAL, K., COTTEN, M., MECHTLER, K. & WAGNER, E. 1992. Gene transfer into hepatocytes using asialoglycoprotein receptor mediated endocytosis of DNA complexed with an artificial tetra-antennary galactose ligand. *Bioconjug Chem,* 3*,* 533-9.

PLUDDEMANN, A., MUKHOPADHYAY, S. & GORDON, S. 2006. The interaction of macrophage receptors with bacterial ligands. *Expert Rev Mol Med,* 8*,* 1-25.

POCOCK, J. M. & KETTENMANN, H. 2007. Neurotransmitter receptors on microglia. *Trends in neurosciences,* 30*,* 527-35.

POLAZZI, E. & CONTESTABILE, A. 2006. Overactivation of LPS-stimulated microglial cells by co-cultured neurons or neuron-conditioned medium. *J Neuroimmunol,* 172*,* 104-11.

POLAZZI, E. & MONTI, B. 2010. Microglia and neuroprotection: from in vitro studies to therapeutic applications. *Prog Neurobiol,* 92*,* 293-315.

POLLARD, H., TOUMANIANTZ, G., AMOS, J. L., AVET-LOISEAU, H., GUIHARD, G., BEHR, J. P. & ESCANDE, D. 2001. Ca2+-sensitive cytosolic nucleases prevent efficient delivery to the nucleus of injected plasmids. *J Gene Med,* 3*,* 153-64.

POLLOCK, S., ANTROBUS, R., NEWTON, L., KAMPA, B., ROSSA, J., LATHAM, S., NICHITA, N. B., DWEK, R. A. & ZITZMANN, N. 2010. Uptake and trafficking of liposomes to the endoplasmic reticulum. *FASEB J,* 24*,* 1866-78.

PORTO-PAZOS, A. B., VEIGUELA, N., MESEJO, P., NAVARRETE, M., ALVARELLOS, A., IBANEZ, O., PAZOS, A. & ARAQUE, A. 2011. Artificial astrocytes improve neural network performance. *PLoS One,* 6*,* e19109.

POSADAS, I., GUERRA, F. J. & CENA, V. 2010. Nonviral vectors for the delivery of small interfering RNAs to the CNS. *Nanomedicine (Lond),* 5*,* 1219-36.

PRAT, A., BIERNACKI, K., WOSIK, K. & ANTEL, J. P. 2001. Glial cell influence on the human blood-brain barrier. *Glia,* 36*,* 145-55.

PRINZ, M., SCHMIDT, H., MILDNER, A., KNOBELOCH, K. P., HANISCH, U. K., RAASCH, J., MERKLER, D., DETJE, C., GUTCHER, I., MAGES, J., LANG, R., MARTIN, R., GOLD, R., BECHER, B., BRUCK, W. & KALINKE, U. 2008. Distinct and nonredundant in vivo functions of IFNAR on myeloid cells limit autoimmunity in the central nervous system. *Immunity,* 28*,* 675-86.

PUSCHMANN, T. B., DIXON, K. J. & TURNLEY, A. M. 2010. Species differences in reactivity of mouse and rat astrocytes in vitro. *Neurosignals,* 18*,* 152-63.

QASBA, P. K. & APOSHIAN, H. V. 1971. DNA and gene therapy: transfer of mouse DNA to human and mouse embryonic cells by polyoma pseudovirions. *Proc Natl Acad Sci U S A,* 68*,* 2345-9.

QUINTANA, A., GIRALT, M., ROJAS, S., PENKOWA, M., CAMPBELL, I. L., HIDALGO, J. & MOLINERO, A. 2005. Differential role of tumor necrosis factor receptors in mouse brain inflammatory responses in cryolesion brain injury. *J Neurosci Res,* 82*,* 701-16.

RAHIM, A. A., WONG, A. M., HOEFER, K., BUCKLEY, S. M., MATTAR, C. N., CHENG, S. H., CHAN, J. K., COOPER, J. D. & WADDINGTON, S. N. 2011a. Intravenous administration of AAV2/9 to the fetal and neonatal mouse leads to differential targeting of CNS cell types and extensive transduction of the nervous system. *FASEB J,* 25*,* 3505-18.

RAHIM, A. A., WONG, A. M., HOEFER, K., BUCKLEY, S. M., MATTAR, C. N., CHENG, S. H., CHAN, J. K., COOPER, J. D. & WADDINGTON, S. N. 2011b. Intravenous administration of AAV2/9 to the fetal and neonatal mouse leads to differential targeting of CNS cell types and extensive transduction of the nervous system. *FASEB J*.

RAIVICH, G., BOHATSCHEK, M., KLOSS, C. U., WERNER, A., JONES, L. L. & KREUTZBERG, G. W. 1999. Neuroglial activation repertoire in the injured

brain: graded response, molecular mechanisms and cues to physiological function. *Brain Res Brain Res Rev,* 30*,* 77-105.

RAMIREZ, G., TORO, R., DOBELI, H. & VON BERNHARDI, R. 2005. Protection of rat primary hippocampal cultures from A beta cytotoxicity by pro-inflammatory molecules is mediated by astrocytes. *Neurobiol Dis,* 19*,* 243-54.

RANSOHOFF, R. M. & BROWN, M. A. 2012. Innate immunity in the central nervous system. *The Journal of clinical investigation,* 122*,* 1164-71.

RANSOHOFF, R. M. & PERRY, V. H. 2009. Microglial physiology: unique stimuli, specialized responses. *Annu Rev Immunol,* 27*,* 119-45.

RAPER, S. E., CHIRMULE, N., LEE, F. S., WIVEL, N. A., BAGG, A., GAO, G. P., WILSON, J. M. & BATSHAW, M. L. 2003. Fatal systemic inflammatory response syndrome in a ornithine transcarbamylase deficient patient following adenoviral gene transfer. *Mol Genet Metab,* 80*,* 148-58.

REJMAN, J., OBERLE, V., ZUHORN, I. S. & HOEKSTRA, D. 2004. Size-dependent internalization of particles via the pathways of clathrin- and caveolae-mediated endocytosis. *Biochem J,* 377*,* 159-69.

REN, L., LUBRICH, B., BIBER, K. & GEBICKE-HAERTER, P. J. 1999. Differential expression of inflammatory mediators in rat microglia cultured from different brain regions. *Brain Res Mol Brain Res,* 65*,* 198-205.

RHAINDS, D., BOURGEOIS, P., BOURRET, G., HUARD, K., FALSTRAULT, L. & BRISSETTE, L. 2004. Localization and regulation of SR-BI in membrane rafts of HepG2 cells. *J Cell Sci,* 117*,* 3095-105.

RHAINDS, D. & BRISSETTE, L. 2004. The role of scavenger receptor class B type I (SR-BI) in lipid trafficking. defining the rules for lipid traders. *Int J Biochem Cell Biol,* 36*,* 39-77.

RHAINDS, D., FALSTRAULT, L., TREMBLAY, C. & BRISSETTE, L. 1999. Uptake and fate of class B scavenger receptor ligands in HepG2 cells. *Eur J Biochem,* 261*,* 227-35.

RIGOTTI, A., EDELMAN, E. R., SEIFERT, P., IQBAL, S. N., DEMATTOS, R. B., TEMEL, R. E., KRIEGER, M. & WILLIAMS, D. L. 1996. Regulation by adrenocorticotropic hormone of the in vivo expression of scavenger receptor class B type I (SR-BI), a high density lipoprotein receptor, in steroidogenic cells of the murine adrenal gland. *J Biol Chem,* 271*,* 33545-9.

RIGOTTI, A., TRIGATTI, B., BABITT, J., PENMAN, M., XU, S. & KRIEGER, M. 1997a. Scavenger receptor BI--a cell surface receptor for high density lipoprotein. *Curr Opin Lipidol,* 8*,* 181-8.

RIGOTTI, A., TRIGATTI, B. L., PENMAN, M., RAYBURN, H., HERZ, J. & KRIEGER, M. 1997b. A targeted mutation in the murine gene encoding the high density lipoprotein (HDL) receptor scavenger receptor class B type I reveals its key role in HDL metabolism. *Proc Natl Acad Sci U S A,* 94*,* 12610-5.

ROBERTSON, R. M., LAIB, S. & SMITH, D. E. 2006. Diffusion of isolated DNA molecules: dependence on length and topology. *Proc Natl Acad Sci U S A,* 103*,* 7310-4.

ROBINSON, A. P., WHITE, T. M. & MASON, D. W. 1986. Macrophage heterogeneity in the rat as delineated by two monoclonal antibodies

MRC OX-41 and MRC OX-42, the latter recognizing complement receptor type 3. *Immunology,* 57*,* 239-47.

ROGERS, M. L. & RUSH, R. A. 2012. Non-viral gene therapy for neurological diseases, with an emphasis on targeted gene delivery. *J Control Release,* 157*,* 183-9.

ROSENSTIEL, P., LUCIUS, R., DEUSCHL, G., SIEVERS, J. & WILMS, H. 2001. From theory to therapy: implications from an in vitro model of ramified microglia. *Microsc Res Tech,* 54*,* 18-25.

ROSOCHACKI, S. J. & MATEJCZYK, M. 2002. Green fluorescent protein as a molecular marker in microbiology. *Acta Microbiol Pol,* 51*,* 205-16.

SAIJO, K. & GLASS, C. K. 2011. Microglial cell origin and phenotypes in health and disease. *Nature reviews. Immunology,* 11*,* 775-87.

SAITO, G., SWANSON, J. A. & LEE, K. D. 2003. Drug delivery strategy utilizing conjugation via reversible disulfide linkages: role and site of cellular reducing activities. *Adv Drug Deliv Rev,* 55*,* 199-215.

SAN JOSE, E. & ALARCON, B. 1999. Receptor engagement transiently diverts the T cell receptor heterodimer from a constitutive degradation pathway. *J Biol Chem,* 274*,* 33740-6.

SAUER, B. & HENDERSON, N. 1988. Site-specific DNA recombination in mammalian cells by the Cre recombinase of bacteriophage P1. *Proc Natl Acad Sci U S A,* 85*,* 5166-70.

SAURA, J. 2007. Microglial cells in astroglial cultures: a cautionary note. *J Neuroinflammation,* 4*,* 26.

SAURA, J., TUSELL, J. M. & SERRATOSA, J. 2003. High-yield isolation of murine microglia by mild trypsinization. *Glia,* 44*,* 183-9.

SCHAFFERT, D. & WAGNER, E. 2008. Gene therapy progress and prospects: synthetic polymer-based systems. *Gene Ther,* 15*,* 1131-8.

SCHILLING, T., NITSCH, R., HEINEMANN, U., HAAS, D. & EDER, C. 2001. Astrocyte-released cytokines induce ramification and outward K+ channel expression in microglia via distinct signalling pathways. *Eur J Neurosci,* 14*,* 463-73.

SCHLEGELMILCH, T., HENKE, K. & PERI, F. 2011. Microglia in the developing brain: from immunity to behaviour. *Curr Opin Neurobiol,* 21*,* 5-10.

SCHMIDT, J. A., MARSHALL, J., HAYMAN, M. J., PONKA, P. & BEUG, H. 1986. Control of erythroid differentiation: possible role of the transferrin cycle. *Cell,* 46*,* 41-51.

SCHMIDTMAYER, J., JACOBSEN, C., MIKSCH, G. & SIEVERS, J. 1994. Blood monocytes and spleen macrophages differentiate into microglia-like cells on monolayers of astrocytes: membrane currents. *Glia,* 12*,* 259-67.

SCHNEIDER, S. D., RUSCONI, S., SEGER, R. A. & HOSSLE, J. P. 1997. Adenovirus-mediated gene transfer into monocyte-derived macrophages of patients with X-linked chronic granulomatous disease: ex vivo correction of deficient respiratory burst. *Gene Ther,* 4*,* 524-32.

SCHNOOR, M., BUERS, I., SIETMANN, A., BRODDE, M. F., HOFNAGEL, O., ROBENEK, H. & LORKOWSKI, S. 2009. Efficient non-viral transfection of THP-1 cells. *J Immunol Methods,* 344*,* 109-15.

SCHROETER, M. L., MERTSCH, K., GIESE, H., MULLER, S., SPORBERT, A., HICKEL, B. & BLASIG, I. E. 1999. Astrocytes enhance radical defence in capillary endothelial cells constituting the blood-brain barrier. *FEBS Lett,* 449*,* 241-4.

SCHULTE-HERBRUGGEN, O., HORTNAGL, H., PONATH, G., ROTHERMUNDT, M. & HELLWEG, R. 2008. Distinct regulation of brain-derived neurotrophic factor and noradrenaline in S100B knockout mice. *Neurosci Lett,* 442*,* 100-3.

SEBESTYEN, M. G., LUDTKE, J. J., BASSIK, M. C., ZHANG, G., BUDKER, V., LUKHTANOV, E. A., HAGSTROM, J. E. & WOLFF, J. A. 1998. DNA vector chemistry: the covalent attachment of signal peptides to plasmid DNA. *Nat Biotechnol,* 16*,* 80-5.

SEETHARAM, D., MINEO, C., GORMLEY, A. K., GIBSON, L. L., VONGPATANASIN, W., CHAMBLISS, K. L., HAHNER, L. D., CUMMINGS, M. L., KITCHENS, R. L., MARCEL, Y. L., RADER, D. J. & SHAUL, P. W. 2006. High-density lipoprotein promotes endothelial cell migration and reendothelialization via scavenger receptor-B type I. *Circ Res,* 98*,* 63-72.

SELKIRK, S. M., GREENBERG, S. J., PLUNKETT, R. J., BARONE, T. A., LIS, A. & SPENCE, P. O. 2002. Syngeneic central nervous system transplantation of genetically transduced mature, adult astrocytes. *Gene Therapy,* 9*,* 432-443.

SEO, T., VELEZ-CARRASCO, W., QI, K., HALL, M., WORGALL, T. S., JOHNSON, R. A. & DECKELBAUM, R. J. 2002. Selective uptake from LDL is stimulated by unsaturated fatty acids and modulated by cholesterol content in the plasma membrane: role of plasma membrane composition in regulating non-SR-BI-mediated selective lipid transfer. *Biochemistry,* 41*,* 7885-94.

SETERNES, T., SORENSEN, K. & SMEDSROD, B. 2002. Scavenger endothelial cells of vertebrates: a nonperipheral leukocyte system for high-capacity elimination of waste macromolecules. *Proc Natl Acad Sci U S A,* 99*,* 7594-7.

SHANNON, C., SALTER, M. & FERN, R. 2007. GFP imaging of live astrocytes: regional differences in the effects of ischaemia upon astrocytes. *J Anat,* 210*,* 684-92.

SHARMA, D. K., CHOUDHURY, A., SINGH, R. D., WHEATLEY, C. L., MARKS, D. L. & PAGANO, R. E. 2003. Glycosphingolipids internalized via caveolar-related endocytosis rapidly merge with the clathrin pathway in early endosomes and form microdomains for recycling. *J Biol Chem,* 278*,* 7564-72.

SHERWOOD, C. C., STIMPSON, C. D., RAGHANTI, M. A., WILDMAN, D. E., UDDIN, M., GROSSMAN, L. I., GOODMAN, M., REDMOND, J. C., BONAR, C. J., ERWIN, J. M. & HOF, P. R. 2006. Evolution of increased glia-neuron ratios in the human frontal cortex. *Proc Natl Acad Sci U S A,* 103*,* 13606-11.

SHIMIZU, E., KAWAHARA, K., KAJIZONO, M., SAWADA, M. & NAKAYAMA, H. 2008. IL-4-induced selective clearance of oligomeric beta-amyloid peptide(1-42) by rat primary type 2 microglia. *J Immunol,* 181*,* 6503-13.

SHIMIZU, N., CHEN, J. B., GAMOU, S. & TAKAYANAGI, A. 1996. Immunogene approach toward cancer therapy using erythrocyte growth factor receptor-mediated gene delivery. *Cancer gene therapy,* 3*,* 113-120.

SIEVERS, J., PARWARESCH, R. & WOTTGE, H. U. 1994. Blood monocytes and spleen macrophages differentiate into microglia-like cells on monolayers of astrocytes: morphology. *Glia,* 12*,* 245-58.

SILVER, D. L., WANG, N., XIAO, X. & TALL, A. R. 2001. High density lipoprotein (HDL) particle uptake mediated by scavenger receptor class B type 1 results in selective sorting of HDL cholesterol from protein and polarized cholesterol secretion. *J Biol Chem,* 276*,* 25287-93.

SILVER, J. & MILLER, J. H. 2004. Regeneration beyond the glial scar. *Nat Rev Neurosci,* 5*,* 146-56.

SIMARD, A. R., SOULET, D., GOWING, G., JULIEN, J. P. & RIVEST, S. 2006. Bone marrow-derived microglia play a critical role in restricting senile plaque formation in Alzheimer's disease. *Neuron,* 49*,* 489-502.

SKEHEL, J. J. & WATERFIELD, M. D. 1975. Studies on the primary structure of the influenza virus hemagglutinin. *Proc Natl Acad Sci U S A,* 72*,* 93-7.

SKULJEC, J., SUN, H., PUL, R., BENARDAIS, K., RAGANCOKOVA, D., MOHARREGH-KHIABANI, D., KOTSIARI, A., TREBST, C. & STANGEL, M. 2011. CCL5 induces a pro-inflammatory profile in microglia in vitro. *Cell Immunol*.

SLOANE, E., LANGER, S., JEKICH, B., MAHONEY, J., HUGHES, T., FRANK, M., SEIBERT, W., HUBERTY, G., COATS, B., HARRISON, J., KLINMAN, D., POOLE, S., MAIER, S., JOHNSON, K., CHAVEZ, R., WATKINS, L. R., LEINWAND, L. & MILLIGAN, E. 2009. Immunological priming potentiates non-viral anti-inflammatory gene therapy treatment of neuropathic pain. *Gene Ther,* 16*,* 1210-22.

SOFRONIEW, M. V. 2009. Molecular dissection of reactive astrogliosis and glial scar formation. *Trends Neurosci,* 32*,* 638-47.

SOFRONIEW, M. V. & VINTERS, H. V. 2010. Astrocytes: biology and pathology. *Acta Neuropathol,* 119*,* 7-35.

SOLOMON, J. N., LEWIS, C. A., AJAMI, B., CORBEL, S. Y., ROSSI, F. M. & KRIEGER, C. 2006. Origin and distribution of bone marrow-derived cells in the central nervous system in a mouse model of amyotrophic lateral sclerosis. *Glia,* 53*,* 744-53.

SONAWANE, N. D., SZOKA, F. C. & VERKMAN, A. S. 2003. Chloride accumulation and swelling in endosomes enhances DNA transfer by polyamine-DNA polyplexes. *Journal of Biological Chemistry,* 278*,* 44826-44831.

SOULET, D. & RIVEST, S. 2008. Bone-marrow-derived microglia: myth or reality? *Curr Opin Pharmacol,* 8*,* 508-18.

STACEY, K. J., SWEET, M. J. & HUME, D. A. 1996. Macrophages ingest and are activated by bacterial DNA. *J Immunol,* 157*,* 2116-22.

STEINER, J., BOGERTS, B., SCHROETER, M. L. & BERNSTEIN, H. G. 2011. S100B protein in neurodegenerative disorders. *Clin Chem Lab Med,* 49*,* 409-24.

STENCE, N., WAITE, M. & DAILEY, M. E. 2001. Dynamics of microglial activation: a confocal time-lapse analysis in hippocampal slices. *Glia,* 33*,* 256-66.

STEPHEN, S. L., FREESTONE, K., DUNN, S., TWIGG, M. W., HOMER-VANNIASINKAM, S., WALKER, J. H., WHEATCROFT, S. B. & PONNAMBALAM, S. 2010. Scavenger receptors and their potential as therapeutic targets in the treatment of cardiovascular disease. *Int J Hypertens,* 2010*,* 646929.

STEVENS, B., ALLEN, N. J., VAZQUEZ, L. E., HOWELL, G. R., CHRISTOPHERSON, K. S., NOURI, N., MICHEVA, K. D., MEHALOW, A. K., HUBERMAN, A. D., STAFFORD, B., SHER, A., LITKE, A. M., LAMBRIS, J. D., SMITH, S. J., JOHN, S. W. & BARRES, B. A. 2007. The classical complement cascade mediates CNS synapse elimination. *Cell,* 131*,* 1164-78.

STEWART, M. 1992. Nuclear pore structure and function. *Semin Cell Biol,* 3*,* 267-77.

STICHEL, C. C., MULLER, C. M. & ZILLES, K. 1991. Distribution of glial fibrillary acidic protein and vimentin immunoreactivity during rat visual cortex development. *J Neurocytol,* 20*,* 97-108.

STREHBLOW, C., SCHUSTER, M., MORITZ, T., KIRCH, H. C., OPALKA, B. & PETRI, J. B. 2005. Monoclonal antibody-polyethyleneimine conjugates targeting Her-2/neu or CD90 allow cell type-specific nonviral gene delivery. *J Control Release,* 102*,* 737-47.

STREIT, W. J. 2002. Microglia as neuroprotective, immunocompetent cells of the CNS. *Glia,* 40*,* 133-9.

SU, M., HU, H. M., LEE, Y. J., D'AZZO, A., MESSING, A. & BRENNER, M. 2004. Expression specificity of GFAP transgenes. *Neurochemical Research,* 29*,* 2075-2093.

SUGAMA, S., FUJITA, M., HASHIMOTO, M. & CONTI, B. 2007. Stress induced morphological microglial activation in the rodent brain: involvement of interleukin-18. *Neuroscience,* 146*,* 1388-99.

SUH, W. H., CHUNG, J. K., PARK, S. H. & KIM, S. W. 2001. Anti-JL1 antibody-conjugated poly (L-lysine) for targeted gene delivery to leukemia T cells. *Journal of Controlled Release,* 72*,* 171-178.

SULSTON, J. E., SCHIERENBERG, E., WHITE, J. G. & THOMSON, J. N. 1983. The embryonic cell lineage of the nematode Caenorhabditis elegans. *Dev Biol,* 100*,* 64-119.

SUN, B., ECKHARDT, E. R., SHETTY, S., VAN DER WESTHUYZEN, D. R. & WEBB, N. R. 2006. Quantitative analysis of SR-BI-dependent HDL retroendocytosis in hepatocytes and fibroblasts. *J Lipid Res,* 47*,* 1700-13.

SYED, M. M., PHULWANI, N. K. & KIELIAN, T. 2007. Tumor necrosis factor-alpha (TNF-alpha) regulates Toll-like receptor 2 (TLR2) expression in microglia. *J Neurochem,* 103*,* 1461-71.

SZABO, M. & GULYA, K. 2013. Development of the microglial phenotype in culture. *Neuroscience,* 241*,* 280-95.

TABATA, H. & NAKAJIMA, K. 2001. Efficient in utero gene transfer system to the developing mouse brain using electroporation: visualization of neuronal migration in the developing cortex. *Neuroscience,* 103*,* 865-72.

TALSMA, S. S., BABENSEE, J. E., MURTHY, N. & WILLIAMS, I. R. 2006. Development and in vitro validation of a targeted delivery vehicle for DNA vaccines. *J Control Release,* 112*,* 271-9.

TANAKA, J., TOKU, K., SAKANAKA, M. & MAEDA, N. 1999. Morphological differentiation of microglial cells in culture: involvement of insoluble factors derived from astrocytes. *Neurosci Res,* 34*,* 207-15.

TANAKA, R., KOMINE-KOBAYASHI, M., MOCHIZUKI, H., YAMADA, M., FURUYA, T., MIGITA, M., SHIMADA, T., MIZUNO, Y. & URABE, T. 2003. Migration of

enhanced green fluorescent protein expressing bone marrow-derived microglia/macrophage into the mouse brain following permanent focal ischemia. *Neuroscience,* 117*,* 531-9.

TANAKA, S., UEHARA, T. & NOMURA, Y. 2000. Up-regulation of protein-disulfide isomerase in response to hypoxia/brain ischemia and its protective effect against apoptotic cell death. *J Biol Chem,* 275*,* 10388-93.

TAYLOR, D. L., DIEMEL, L. T., CUZNER, M. L. & POCOCK, J. M. 2002. Activation of group II metabotropic glutamate receptors underlies microglial reactivity and neurotoxicity following stimulation with chromogranin A, a peptide up-regulated in Alzheimer's disease. *Journal of neurochemistry,* 82*,* 1179-91.

THACI, B., ULASOV, I. V., WAINWRIGHT, D. A. & LESNIAK, M. S. 2011. The challenge for gene therapy: innate immune response to adenoviruses. *Oncotarget,* 2*,* 113-21.

THOMSEN, D. R., STENBERG, R. M., GOINS, W. F. & STINSKI, M. F. 1984. Promoter-regulatory region of the major immediate early gene of human cytomegalovirus. *Proc Natl Acad Sci U S A,* 81*,* 659-63.

THOMSEN, P., ROEPSTORFF, K., STAHLHUT, M. & VAN DEURS, B. 2002. Caveolae are highly immobile plasma membrane microdomains, which are not involved in constitutive endocytic trafficking. *Mol Biol Cell,* 13*,* 238-50.

THORPE, P. E., WALLACE, P. M., KNOWLES, P. P., RELF, M. G., BROWN, A. N. F., WATSON, G. J., KNYBA, R. E., WAWRZYNCZAK, E. J. & BLAKEY, D. C. 1987. New Coupling Agents for the Synthesis of Immunotoxins Containing A Hindered Disulfide Bond with Improved Stability Invivo. *Cancer Research,* 47*,* 5924-5931.

TINSLEY, R. B., VESEY, M. J., BARATI, S., RUSH, R. A. & FERGUSON, I. A. 2004. Improved non-viral transfection of glial and adult neural stem cell lines and of primary astrocytes by combining agents with complementary modes of action. *J Gene Med,* 6*,* 1023-32.

TOMITA, M. & TSUMOTO, K. 2011. Hybridoma technologies for antibody production. *Immunotherapy,* 3*,* 371-80.

TOZAKI-SAITOH, H., TSUDA, M., MIYATA, H., UEDA, K., KOHSAKA, S. & INOUE, K. 2008. P2Y12 receptors in spinal microglia are required for neuropathic pain after peripheral nerve injury. *J Neurosci,* 28*,* 4949-56.

TSAI, F. Y., KELLER, G., KUO, F. C., WEISS, M., CHEN, J., ROSENBLATT, M., ALT, F. W. & ORKIN, S. H. 1994. An early haematopoietic defect in mice lacking the transcription factor GATA-2. *Nature,* 371*,* 221-6.

TSAI, H. C. & IMAE, T. 2011. Fabrication of dendrimers toward biological application. *Prog Mol Biol Transl Sci,* 104*,* 101-40.

TSIEN, J. Z., HUERTA, P. T. & TONEGAWA, S. 1996. The essential role of hippocampal CA1 NMDA receptor-dependent synaptic plasticity in spatial memory. *Cell,* 87*,* 1327-38.

TYNAN, R. J., NAICKER, S., HINWOOD, M., NALIVAIKO, E., BULLER, K. M., POW, D. V., DAY, T. A. & WALKER, F. R. 2010. Chronic stress alters the density and morphology of microglia in a subset of stress-responsive brain regions. *Brain Behav Immun,* 24*,* 1058-68.

UHEREK, C., FOMINAYA, J. & WELS, W. 1998. A modular DNA carrier protein based on the structure of diphtheria toxin mediates target cell-specific gene delivery. *J Biol Chem,* 273*,* 8835-41.

UITTENBOGAARD, A., EVERSON, W. V., MATVEEV, S. V. & SMART, E. J. 2002. Cholesteryl ester is transported from caveolae to internal membranes as part of a caveolin-annexin II lipid-protein complex. *J Biol Chem,* 277*,* 4925-31.

VALACCHI, G., STICOZZI, C., LIM, Y. & PECORELLI, A. 2011. Scavenger receptor class B type I: a multifunctional receptor. *Ann N Y Acad Sci,* 1229*,* E1-7.

VAN DER AA, M. A., KONING, G. A., D'OLIVEIRA, C., OOSTING, R. S., WILSCHUT, K. J., HENNINK, W. E. & CROMMELIN, D. J. 2005. An NLS peptide covalently linked to linear DNA does not enhance transfection efficiency of cationic polymer based gene delivery systems. *J Gene Med,* 7*,* 208-17.

VAN FURTH, R. & COHN, Z. A. 1968. The origin and kinetics of mononuclear phagocytes. *J Exp Med,* 128*,* 415-35.

VANDENBERGHE, L. H., WILSON, J. M. & GAO, G. 2009. Tailoring the AAV vector capsid for gene therapy. *Gene Ther,* 16*,* 311-9.

VANDENBROUCKE, R. E., LUCAS, B., DEMEESTER, J., DE SMEDT, S. C. & SANDERS, N. N. 2007. Nuclear accumulation of plasmid DNA can be enhanced by non-selective gating of the nuclear pore. *Nucleic Acids Res,* 35*,* e86.

VEDELER, C., ULVESTAD, E., GRUNDT, I., CONTI, G., NYLAND, H., MATRE, R. & PLEASURE, D. 1994. Fc receptor for IgG (FcR) on rat microglia. *J Neuroimmunol,* 49*,* 19-24.

VIRCHOW, R. L. K. 1858. *Die cellularpathologie in ihrer begründung auf physiologische und pathologische gewebelehre,* Berlin.

VIRCHOW, R. L. K. 1860. *Cellular pathology (English ed.),* London.

VOLTERRA, A. & MELDOLESI, J. 2005. Astrocytes, from brain glue to communication elements: the revolution continues. *Nat Rev Neurosci,* 6*,* 626-40.

VOSKUHL, R. R., PETERSON, R. S., SONG, B., AO, Y., MORALES, L. B., TIWARI-WOODRUFF, S. & SOFRONIEW, M. V. 2009. Reactive astrocytes form scar-like perivascular barriers to leukocytes during adaptive immune inflammation of the CNS. *J Neurosci,* 29*,* 11511-22.

VRY, J. D., MARTINEZ-MARTINEZ, P., LOSEN, M., BODE, G. H., TEMEL, Y., STECKLER, T., STEINBUSCH, H. W., BAETS, M. D. & PRICKAERTS, J. 2010. Low Current-driven Micro-electroporation Allows Efficient In Vivo Delivery of Nonviral DNA into the Adult Mouse Brain. *Mol Ther*.

WAGNER, E. 2004. Strategies to Improve DNA Polyplexes for in Vivo Gene Transfer: Will "Artificial Viruses" Be the Answer? . *Pharmaceutical research,* 21 8-13.

WAGNER, E. & KLOECKNER, J. 2006. Gene delivery using polymer therapeutics. *Polymer Therapeutics I: Polymers As Drugs, Conjugates and Gene Delivery Systems,* 192*,* 135-173.

WAHEED, A. A., RAO, K. S. & GUPTA, P. D. 2000. Mechanism of dye binding in the protein assay using eosin dyes. *Analytical Biochemistry,* 287*,* 73-79.

WALZ, W. & WUTTKE, W. A. 1999. Independent mechanisms of potassium clearance by astrocytes in gliotic tissue. *J Neurosci Res,* 56*,* 595-603.

WANG, H., KO, C. H., KOLETAR, M. M., RALPH, M. R. & YEOMANS, J. 2007a. Casein kinase I epsilon gene transfer into the suprachiasmatic nucleus via electroporation lengthens circadian periods of tau mutant hamsters. *Eur J Neurosci,* 25*,* 3359-66.

WANG, N., WENG, W., BRESLOW, J. L. & TALL, A. R. 1996. Scavenger receptor BI (SR-BI) is up-regulated in adrenal gland in apolipoprotein A-I and hepatic lipase knock-out mice as a response to depletion of cholesterol stores. In vivo evidence that SR-BI is a functional high density lipoprotein receptor under feedback control. *J Biol Chem,* 271*,* 21001-4.

WANG, X. J., YE, M., ZHANG, Y. H. & CHEN, S. D. 2007b. CD200-CD200R regulation of microglia activation in the pathogenesis of Parkinson's disease. *J Neuroimmune Pharmacol,* 2*,* 259-64.

WEBB, M. & BARCLAY, A. N. 1984. Localisation of the MRC OX-2 glycoprotein on the surfaces of neurones. *J Neurochem,* 43*,* 1061-7.

WELSER-ALVES, J. V., CROCKER, S. J. & MILNER, R. 2011. A dual role for microglia in promoting tissue inhibitor of metalloproteinase (TIMP) expression in glial cells in response to neuroinflammatory stimuli. *J Neuroinflammation,* 8*,* 61.

WHARTON, S. A., MARTIN, S. R., RUIGROK, R. W., SKEHEL, J. J. & WILEY, D. C. 1988. Membrane fusion by peptide analogues of influenza virus haemagglutinin. *J Gen Virol,* 69 (Pt 8)*,* 1847-57.

WHITE, E., BIENEMANN, A., MEGRAW, L., BUNNUN, C. & GILL, S. 2011. Evaluation and optimization of the administration of a selectively replicating herpes simplex viral vector to the brain by convection-enhanced delivery. *Cancer Gene Ther,* 18*,* 358-69.

WIESENHOFER, B. & HUMPEL, C. 2000. Lipid-mediated gene transfer into primary neurons using FuGene: comparison to C6 glioma cells and primary glia. *Exp Neurol,* 164*,* 38-44.

WILCOCK, D. M., ROJIANI, A., ROSENTHAL, A., LEVKOWITZ, G., SUBBARAO, S., ALAMED, J., WILSON, D., WILSON, N., FREEMAN, M. J., GORDON, M. N. & MORGAN, D. 2004. Passive amyloid immunotherapy clears amyloid and transiently activates microglia in a transgenic mouse model of amyloid deposition. *J Neurosci,* 24*,* 6144-51.

WISHART, R. & MACKINNON, M. 1990. Uptake and metabolism of high-density lipoproteins by cultured rabbit hepatocytes. *Biochim Biophys Acta,* 1044*,* 375-81.

WOLFERT, M. A., DASH, P. R., NAZAROVA, O., OUPICKY, D., SEYMOUR, L. W., SMART, S., STROHALM, J. & ULBRICH, K. 1999. Polyelectrolyte vectors for gene delivery: influence of cationic polymer on biophysical properties of complexes formed with DNA. *Bioconjug Chem,* 10*,* 993-1004.

WOLFF, J. A., MALONE, R. W., WILLIAMS, P., CHONG, W., ACSADI, G., JANI, A. & FELGNER, P. L. 1990. Direct gene transfer into mouse muscle in vivo. *Science,* 247*,* 1465-8.

WOLLMER, M. A., LUCIUS, R., WILMS, H., HELD-FEINDT, J., SIEVERS, J. & MENTLEIN, R. 2001. ATP and adenosine induce ramification of microglia in vitro. *J Neuroimmunol,* 115*,* 19-27.

WU, B. Y., LIU, R. Y., SO, K. L. & YU, A. C. 2000. Multi-lipofection efficiently transfected genes into astrocytes in primary culture. *J Neurosci Methods,* 102*,* 133-41.

WU, G. Y. & WU, C. H. 1987. Receptor-mediated in vitro gene transformation by a soluble DNA carrier system. *J Biol Chem,* 262*,* 4429-32.

WU, Z., ASOKAN, A. & SAMULSKI, R. J. 2006. Adeno-associated virus serotypes: vector toolkit for human gene therapy. *Mol Ther,* 14*,* 316-27.

WURST, W., AUERBACH, A. B. & JOYNER, A. L. 1994. Multiple developmental defects in Engrailed-1 mutant mice: an early mid-hindbrain deletion and patterning defects in forelimbs and sternum. *Development,* 120*,* 2065-75.

WYSS-CORAY, T., LOIKE, J. D., BRIONNE, T. C., LU, E., ANANKOV, R., YAN, F., SILVERSTEIN, S. C. & HUSEMANN, J. 2003. Adult mouse astrocytes degrade amyloid-beta in vitro and in situ. *Nat Med,* 9*,* 453-7.

XIONG, M. P., FORREST, M. L., TON, G., ZHAO, A., DAVIES, N. M. & KWON, G. S. 2007. Poly(aspartate-g-PEI800), a polyethylenimine analogue of low toxicity and high transfection efficiency for gene delivery. *Biomaterials,* 28*,* 4889-900.

XU, L., EMERY, J. F., OUYANG, Y. B., VOLOBOUEVA, L. A. & GIFFARD, R. G. 2010. Astrocyte targeted overexpression of Hsp72 or SOD2 reduces neuronal vulnerability to forebrain ischemia. *Glia,* 58*,* 1042-9.

YASUDA, K., KAWANO, H., YAMANE, I., OGAWA, Y., YOSHINAGA, T., NISHIKAWA, M. & TAKAKURA, Y. 2004. Restricted cytokine production from mouse peritoneal macrophages in culture in spite of extensive uptake of plasmid DNA. *Immunology,* 111*,* 282-90.

YI, Y., NOH, M. J. & LEE, K. H. 2011. Current advances in retroviral gene therapy. *Curr Gene Ther,* 11*,* 218-28.

YIP, W. L., WEYERGANG, A., BERG, K., TONNESEN, H. H. & SELBO, P. K. 2007. Targeted delivery and enhanced cytotoxicity of cetuximab-saporin by photochemical internalization in EGFR-positive cancer cells. *Molecular Pharmaceutics,* 4*,* 241-251.

YOUNG, J. L., BENOIT, J. N. & DEAN, D. A. 2003. Effect of a DNA nuclear targeting sequence on gene transfer and expression of plasmids in the intact vasculature. *Gene Ther,* 10*,* 1465-70.

YU, A., OLOSZ, F., CHOI, C. Y. & MALEK, T. R. 2000. Efficient internalization of IL-2 depends on the distal portion of the cytoplasmic tail of the IL-2R common gamma-chain and a lymphoid cell environment. *J Immunol,* 165*,* 2556-62.

YU, H. J., CHEN, X. S., LU, T. C., SUN, J., TIAN, H. Y., HU, J., WANG, Y., ZHANG, P. B. & JING, X. B. 2007. Poly(L-lysine)-graft-chitosan copolymers: Synthesis, characterization, and gene transfection effect. *Biomacromolecules,* 8*,* 1425-1435.

ZABNER, J., FASBENDER, A. J., MONINGER, T., POELLINGER, K. A. & WELSH, M. J. 1995. Cellular and molecular barriers to gene transfer by a cationic lipid. *J Biol Chem,* 270*,* 18997-9007.

ZAISS, A. K., LIU, Q., BOWEN, G. P., WONG, N. C., BARTLETT, J. S. & MURUVE, D. A. 2002. Differential activation of innate immune responses by adenovirus and adeno-associated virus vectors. *J Virol,* 76*,* 4580-90.

ZANTA, M. A., BELGUISE-VALLADIER, P. & BEHR, J. P. 1999. Gene delivery: A single nuclear localization signal peptide is sufficient to carry DNA to the cell nucleus. *Proceedings of the National Academy of Sciences of the United States of America,* 96*,* 91-96.

ZAUNER, W., OGRIS, M. & WAGNER, E. 1998. Polylysine-based transfection systems utilizing receptor-mediated delivery. *Advanced drug delivery reviews,* 30 97-113.

ZENG, J., WANG, X. & WANG, S. 2007. Self-assembled ternary complexes of plasmid DNA, low molecular weight polyethylenimine and targeting peptide for nonviral gene delivery into neurons. *Biomaterials,* 28*,* 1443-51.

ZHANG, H. & VINOGRADOV, S. V. 2010. Short biodegradable polyamines for gene delivery and transfection of brain capillary endothelial cells. *J Control Release,* 143*,* 359-66.

ZHANG, J., FUJII, S., WU, Z., HASHIOKA, S., TANAKA, Y., SHIRATSUCHI, A., NAKANISHI, Y. & NAKANISHI, H. 2006. Involvement of COX-1 and up-regulated prostaglandin E synthases in phosphatidylserine liposome-induced prostaglandin E2 production by microglia. *J Neuroimmunol,* 172*,* 112-20.

ZHANG, J., SHI, X. Q., ECHEVERRY, S., MOGIL, J. S., DE KONINCK, Y. & RIVEST, S. 2007a. Expression of CCR2 in both resident and bone marrow-derived microglia plays a critical role in neuropathic pain. *J Neurosci,* 27*,* 12396-406.

ZHANG, Y., AHMED, A. M., MCFARLANE, N., CAPONE, C., BOREHAM, D. R., TRUANT, R., IGDOURA, S. A. & TRIGATTI, B. L. 2007b. Regulation of SR-BI-mediated selective lipid uptake in Chinese hamster ovary-derived cells by protein kinase signaling pathways. *J Lipid Res,* 48*,* 405-16.

ZHANG, Y., SCHLACHETZKI, F., ZHANG, Y. F., BOADO, R. J. & PARDRIDGE, W. M. 2004. Normalization of striatal tyrosine hydroxylase and reversal of motor impairment in experimental parkinsonism with intravenous nonviral gene therapy and a brain-specific promoter. *Human Gene Therapy,* 15*,* 339-350.

ZHAO, F., ZHANG, J., LIU, Y. S., LI, L. & HE, Y. L. 2011. Research advances on flotillins. *Virol J,* 8*,* 479.

ZHAO, P., WAXMAN, S. G. & HAINS, B. C. 2007. Modulation of thalamic nociceptive processing after spinal cord injury through remote activation of thalamic microglia by cysteine cysteine chemokine ligand 21. *J Neurosci,* 27*,* 8893-902.

ZHOU, Y. X., CHEN, S. S., WU, T. F., DING, D. D., CHEN, X. H., CHEN, J. M., SU, Z. P., LI, B., CHEN, G. L., XIE, X. S., DAI, Y. F., WEI, Y. X. & DU, Z. W. 2011. A novel gene RNF138 expressed in human gliomas and its function in the glioma cell line U251. *Anal Cell Pathol (Amst)*.

ZIADY, A. G., FERKOL, T., DAWSON, D. V., PERLMUTTER, D. H. & DAVIS, P. B. 1999. Chain length of the polylysine in receptor-targeted gene transfer complexes affects duration of reporter gene expression both in vitro and in vivo. *Journal of Biological Chemistry,* 274*,* 4908-4916.

ZIELLO, J. E., HUANG, Y. & JOVIN, I. S. 2010. Cellular endocytosis and gene delivery. *Mol Med,* 16*,* 222-9.

ZONTA, M., ANGULO, M. C., GOBBO, S., ROSENGARTEN, B., HOSSMANN, K. A., POZZAN, T. & CARMIGNOTO, G. 2003. Neuron-to-astrocyte signaling is central to the dynamic control of brain microcirculation. *Nat Neurosci,* 6*,* 43-50.

ZOU, S., SCARFO, K., NANTZ, M. H. & HECKER, J. G. 2010. Lipid-mediated delivery of RNA is more efficient than delivery of DNA in non-dividing cells. *Int J Pharm,* 389*,* 232-43.